Antiviral therapy can reverse the development of immune senescence in elderly mice with latent cytomegalovirus infection

by

Mark Beswick

A thesis submitted to

The University of Birmingham

for the degree of

DOCTOR OF PHILOSOPHY

School of Medical and Dental Science

College of Medical and Dental School

The University of Birmingham

August 2012

ABSTRACT

Immune responses towards Cytomegalovirus (CMV) often increase in magnitude with age; a phenomenon termed 'memory inflation'. Elevated CMV-specific immunity is correlated with an increased mortality rate in elderly individuals and there is considerable interest in therapeutic approaches that may reverse this. Latent CMV infection is characterised by intermittent episodes of subclinical viral reactivation which may play a role in boosting CMV-specific immunity however, the relative importance of reactivation in the development of 'memory inflation' is currently uncertain. In order to investigate these questions valaciclovir was administered as to aged mice with established murine CMV (MCMV) infection to block stochastic lytic reactivation from latency. Following 12 months of treatment there were highly significant reductions in the frequency of the MCMV-specific $CD8^+$ T-lymphocytes and the residual MCMV-tetramer specific response exhibited a less differentiated phenotype. The accumulation of memory cells associated with untreated MCMV infection suppressed the proportion of naïve $CD8^+$ T-cells by 60%, whereas antiviral treatment was able to completely restore this effect. Furthermore, valaciclovir treatment of MCMV reduced the elevated viral load that followed influenza virus challenge demonstrating that anti-MCMV treatment can lead to improved immunity to other pathogens in old age.

ACKNOWLEDGMENTS

I would first like to thank Professor Paul Moss and Dr Clive Sweet for giving me the opportunity to study towards my PhD.

I am also very grateful for the help offered by Dr Annette Pachnio who assisted in the development of many of the assays used throughout this study. I am indebted to Dr Sarah Lauder who kindly offered guidance and help in all things related to Influenza (even after returning to the University of Cardiff) and Dr Abdulaziz Al-Ali who ensured that I never ran out of viruses.

I am also very thankful to the staff of the Biomedical Services Unit at the University of Birmingham, especially Ian Ricketts and Karin Sweryda, who always readily offered their time and experience.

PUBLICATIONS ARISING FROM THIS THESIS

Beswick M, Pachnio A, Lauder SN, Sweet C, Moss PA.

Antiviral therapy can reverse the development of immune senescence in elderly mice with latent cytomegalovirus infection.

The Journal of Virology. 2012 Oct 31. [1]

Solana R, Tarazona R, Aiello AE, Akbar AN, Appay V, Beswick M, Bosch JA, Campos C, Cantisán S, Cicin-Sain L, Derhovanessian E, Ferrando-Martínez S, Frasca D, Fulöp T, Govind S, Grubeck-Loebenstein B, Hill A, Hurme M, Kern F, Larbi A, López-Botet M, Maier AB, McElhaney JE, Moss P, Naumova E, Nikolich-Zugich J, Pera A, Rector JL, Riddell N, Sanchez-Correa B, Sansoni P, Sauce D, van Lier R, Wang GC, Wills MR, Zielinski M, Pawelec G.

CMV and Immunosenescence: from basics to clinics.

Immunity and Ageing. 2012 Oct 31; 9(1):23. [2]

TABLE OF CONTENTS

LIST OF FIGURES

CHAPTER 1

CHAPTER 2

CHAPTER 3

CHAPTER 4

CHAPTER 5

CHAPTER 6

LIST OF TABLES

TABLE 1

TABLE 2

TABLE 3

TABLE 4

TABLE 5

LIST OF ABBREVIATIONS

ACV	Aciclovir
AIDS	Acquired immune deficiency syndrome
ANOVA	Analysis of variance
APC	Antigen presenting cell
ATCC	American type culture collection
BAL	Bronchoalveolar lavage
B-cell	B-lymphocyte
BCR	B-cell receptor
CD	Cluster of differentiation cDC
	Conventional dendritic cell
CMLN	Caudal mediastinal lymph node
CMMG	9-[(carboxymethoxy)methyl]guanine
CMV	Cytomegalovirus
CPE	Cytopathic effect
DC	Dendritic cell
E	Early (gene)
EBV	Epstein Barr virus
EID	Egg infectious dose
ELISPOT	Enzyme-linked immunosorbent spot assay
ELISA	Enzyme-linked immunosorbent assay
ER	Endoplasmic reticulum

DB	Dense bodies
DNA	Deoxyribonucleic acid
EGFR	Epidermal growth factor
FPLC	Fast-protein liquid chromatography
FSC	Forward scatter
GAPDH	Glyceraldehyde 3-phosphate dehydrogenase
gB	Glycoprotein B
GF	Germ free
GFP	Green-fluorescent protein
GM	Growth media
HCMV	Human cytomegalovirus
HEV	High endothelium venule
HPLC	High-performance liquid chromatography
IAV	Influenza A virus
IC	Inhibitory concentration
ICS	Intracellular cytokine staining
IE	Immediate early (gene)
IL	Interleukin
IFNγ	Interferon gamma
Ig	Immunoglobulin
i.p	Intraperitoneal
i.n	Intranasal
IRP	Immune risk profile

HA	Haemagglutinin
HHV-6	Herpes lymphotropic virus 6
HHV-7	Roseolovirus
HIV	Human immunodeficiency virus
HLA	Human leukocyte antigen
HSV-1	Herpes-simplex virus 1
HSV-2	Herpes-simplex virus 2
KIR	Killer cell Ig-like receptor
KLRG1	Killer cell lectin-like receptor subfamily G member
KSHV	Kaposi's sarcoma herpes virus
L	Late (gene)
LCMV	Lymphocytic choriomeningitis virus
MCMV	Murine cytomegalovirus
MDCK	Madin Darby canine kidney
MICA	Major histocompatability polypeptide related sequence A
MEF	Mouse embryo fibroblast
MHC	Major histocompatability antigens
MIEP	Major Immediate Early promoter
MM	Maintenance media
mRNA	Messenger ribonucleic acid
MFI	Mean fluorescence intensity
MHC	Major histocompatability antigen
NA	Neuraminidase

NFAT	Nuclear factor activated T-cells
NF-κB	Nuclear factor kappa-light-chain-enhancer of activated B cells
NK	Natural Killer cell
OD	Optical density
ORF	Open reading frame
PBMC	Peripheral blood mononuclear cells
PD-1	Programmed death ligand receptor
PFU	Plaque forming units
p.i	Post-infection
PD-1	Programmed cell death 1
PK	Protein kinase
PMA	Phorbol myristate acetate
pMHC	Peptide-MHC
PNP	Purine nucleoside phosphorylase
PV	Pichinde virus
Q-PCR	Quantitative polymerase chain reaction
RhCMV	Rhesus macaque cytomegalovirus
RNA	Ribonucleic acid
RPMI	Roswell Park Memorial Institue medium
SA	Sialic acid
SDS	Sodium Dodecyl Sulphate
SSC	Side scatter
SPF	Specific pathogen free

STAT	Signal transducer and activator of transcription
TAP	Transporter associated with antigen processing
T_{CM}	Central memory T-cell
TCR	T-cell receptor
T_{DN}	Double negative T-cell
T_{EM}	Effector memory T-cell
TEMRA	T-effector memory revertant CD45RA
Tet	Tetramer
TK	Thymidine kinase
TMB	3,3′,5,5′-Tetramethylbenzidine
T_{reg}	Regulatory T-cell
T_N	Naïve T-cell
TNFα	Tumour necrosis factor alpha
tsm5	Temperature sensitive mutant 5
VV	Vaccinia virus
VZV	Varicella zoster virus
wt	Wild type
8-OH-ACV	8-hydoxy-aciclovir
β2M	β-2-microglobulin

1. AN INTRODUCTION TO: *ANTIVIRAL THERAPY CAN REVERSE THE DEVELOPMENT OF IMMUNE SENESCENCE IN ELDERLY MICE WITH LATENT CYTOMEGALOVIRUS INFECTION*

1.1. INTRODUCTION TO HERPESVIRIDAE

The order Herpesvirales is divided into 3 subfamilies, 17 genera and over 90 species of herpes viruses [3, 4].

The Alphaherpesvirinae subfamily includes three human pathogens: Herpes-simplex virus 1 (HSV-1), Herpes-simplex virus 2 (HSV-2) and Varicella zoster virus (VZV). The alphaherpes-viruses primarily have tropism directed towards sites of mucosal epithelium and are associated with establishing latency in neurones [5]. *In vitro*, the alphaherpesvirinae spread rapidly and have a relatively short replicative cycle.

The Betaherpesvirinae subfamily includes the genus Cytomegalovirus (CMV), Herpes lymphotropic virus 6 (HHV-6) [6] and Roseolovirus (HHV-7) [7]. CMVs are found in many mammalian species. This introduction will mainly concern human (HCMV) and murine cytomegalovirus (MCMV). HCMV infection is normally asymptomatic in an immunocompetent individual due to robust innate and adaptive immune responses however, severe disease manifestations may occur in immunocompromised patients [8-10]. Unlike the alphaherpesvirinae, CMVs have a slower replicative cycle and cause infected cells to become enlarged (cytomegaly) prior to cell death (cytopathic effect or CPE). CMVs can infect many cell types and are believed to persist in primarily a latent form in cells of the myeloid lineage [11]. The HHV-6 and HHV-7 viruses are the aetiological agents of *roseola infantum* [12].

The subfamily Gammaherpesvirinae includes the two human pathogens Epstein-Barr virus (EBV) and Kaposi sarcoma-associated herpesvirus (KSHV). EBV infection is usually asymptomatic during childhood infection although primary EBV infection during adolescence is the most common cause of infectious mononucleosis. Moreover, EBV is the causative agent for a number of malignancies, e.g. nasopharyngeal carcinoma, Burkitt lymphoma and post-transplant lymphoproliferative disorder. Like EBV the KSHV is also oncogenic and can cause a sarcoma in immune-suppressed individuals [13].

Of the eight Herpesveridae that infect humans, each has its own unique profile of pathogenicity, tropism and sequelae. Acute infections with Herpesveridae are usually self-limiting due to successful immunological control by both the innate and adaptive immune systems. Herpesveridae viruses are never eradicated persisting for the lifetime of the host. To reduce the exposure to the immune system many of the Herpesveridae enter a state of latency and employ immune evasion mechanisms. Herpes viruses do undergo lytic reactivation from latency and deleterious changes to the immune system such as immunosuppression or the aging process are implicated in increased viral reactivation [14].

1.2. CYTOMEGALOVIRUS

1.2.1. STRAINS OF HCMV

The cytomegaly of cells attributed to HCMV was first recognised in the mid-part of the twentieth century, since then several “wild-type” (*wt*) strains of HCMV have been isolated from clinical tissue [15]. Estimates suggest that up to 95% of the human population may be carriers of HCMV [16].

Toledo and *Merlin* are two common *wt* isolates of HCMV. The *Toledo* viral strain remains at a low passage however, it has acquired a number of mutations and up to 19 new open reading frames (ORFs) [17]. Polymorphisms among *wt* isolates can subtly alter the viral genome having an advantageous effect in regards to the viruses' fitness [18]. Larger alterations and genetic variability of *wt* HCMV isolates may facilitate superinfection and be responsible for the viruses high prevalence [19].

In addition to HCMV of *wt* origin, there are a larger number of laboratory-adapted viruses and mutant virus strains of HCMV [20]. For example the laboratory strain *Towne* and *AD169* have been routinely passaged in cell culture and as a result are considered less virulent due mutations they have acquired that restrict their tissue tropism. Comparisons between the genome of the isolate *Towne* and the laboratory strain *AD169* highlighted a number of large genomic rearrangements in *AD169* [21]. As a consequence the *AD169* virus is missing very large sections of the genome including the ORFs RL5A [22], RL13 [23]and UL131A [24] which therefore makes immune studies of this particular virus non-representative of *wt* strains.

1.2.2. STRAINS OF MCMV

CMVs are highly species specific and in small animal models, the most frequently used strains of CMV used are those capable of infecting mice (MCMV). Like HCMV, there are multiple MCMV strains and variants. Two of the most widely used MCMV strains are the widely laboratory passaged serotype *Smith* and the less frequently passaged isolate of *K181*.

In contrast to studies of HCMV, the MCMV genome is more stable. The MCMV genome has lower rates of mutation in both *in vitro* or *in vivo* passaged isolates and therefore genome size is better conserved, with fewer major genomic rearrangements, large insertions or deletions [25, 26]. Akin to HCMV, the process of propagation of MCMV *in vitro* does reduce the virulence of the virus; however, MCMV can be isolated from the salivary gland during acute infection to prevent the loss of virulence.

1.2.3. STRUCTURE OF CMV

Cytomegaloviruses have a classical herpesvirus structure. At its core is its large linear double stranded DNA genome contained within an icosahedral capsid. The capsid is in turn located within a mesh of matrix proteins and a tegument layer. An outer envelope and membrane encompasses the complete virion.

The HCMV genome is approximately 236,000 bp in length. This is much larger than many viruses including other members of the Herpesviridae (e.g. EBV ≈170,000 bp). The HCMV genome usually encodes for approximately 170 ORFs, with rare isolates that encode up to 250 ORFs [27, 28].

Sequence analysis of the MCMV genome of the *Smith* isolate was published in 1996 [29]. The *Smith* genome measures 230,278 bp. Encoded within this large genome are 170 ORFs, of which 78 share significant sequence homologies to the HCMV isolate *AD169*. MCMV genes denoted “M” e.g. M45, share direct homology to HCMV whereas non-homologous genes are denoted “m” e.g. m139.

1.3. THE TROPISM OF CMV

Exposure to CMV in bodily secretions, such as saliva and breast milk, means that often the primary cell type to which the virus will be first exposed to is the mucosal epithelium [30]. CMV disseminates from the mucosal epithelium into the circulatory systems where it can infect multiple cell types.

Lytic HCMV has been extracted from both pulmonary tissue and monocytes from the lungs [31-34]; and the sinusoidal [35] and hepatocytes of the liver [36]. CMVs have been detected in many large organs and for this reason during solid organ transplantation, an attempt is made to match the donor's HCMV status to that of the patient to reduce the risk of primary infection post-transplant [37]. In addition, HCMV can infect the arteriole endothelium and the presence of HCMV in atherosclerotic plaques contributes to vascular disease [38, 39]. Latent HCMV is believed to primarily resides in very low copy numbers within cells of the myeloid origin including monocytes [40], macrophages [41] and dendritic cells (DCs) [40, 42].

In the wild MCMV is most likely spread through biting, scratching and the shedding of the virus is bodily secretions. In the laboratory, recombinant MCMV, designed to express green fluorescent protein (GFP), was used to track the dissemination of viral infection following intraperitoneal (i.p) inoculation. MCMV is carried from the site of inoculation into the mediastinal lymphatic system and from there into the bloodstream [43]. Six hours post-infection (p.i.) MCMV disseminates to the spleen where initially the marginal zones are targeted before the virus transmits into the red pulp (17 hours p.i.). Within 48 hours, MCMV has infected the spleen and liver causing cytomegaly. Lytic MCMV then becomes detectable

in many others organs during the primary infection but upon establishing a latent infection the virus resides in the fewer anatomical sites. The reservoirs of latent MCMV are the liver sinusoidal endothelial cells (LSECs) [35, 44] the lungs [34] and also within the non-haematopoietic cells of the lymph node [45].

1.4. OVERVIEW OF THE CMV LIFE CYCLE

The tethering of the CMV envelope to cell surface receptors is the most likely mechanism through which CMV attaches and gains entry to infect a cell [46]. An initial interaction between cell surface heparin sulphate and the HCMV glycoprotein complex gC-II stabilises the virus and the cell membrane [47-49]. In addition, cellular integrins, e.g. the β1 and αvβ3 integrins, can also mediate adherence and function as entry receptors for HCMV, through binding of viral glycoproteins and mediating endocytosis of the viral particle [50-52]. The most often cited cellular receptor for HCMV entry is the epidermal growth factor receptor (EGFR) [53]. For infection of monocytes, the EGFR mediates HCMV entry [54] and post-entry into the cell HCMV migrates to the nucleus and inhibits downstream epidermal growth factor signalling to prevent further viral entry into the same cell [55]. MCMV infection also uses the EGFR to gain entry into cells as small molecule inhibitors of this receptor are effective in preventing MCMV establishing infection *in vivo* [56]. HCMV entry via membrane fusion is typically pH-independent [57] although pH maybe significant for infection of cells of epithelial and endothelial origin [58].

1.4.1. REPLICATION OF CMV

Transcription of the CMV genome occurs within the nucleus of an infected cell. Transcription is segmented into three kinetic phases; firstly, Immediate Early (IE or α) gene expression, followed by Early (E or β) gene expression, and finally Late (L or γ) genes are expressed.

The IE genes are the first set of viral genes expressed. Transcription of IE genes is prior to *de novo* viral protein synthesis and requires host transcription factors. The IE gene products are transactivators that provide the necessary stimuli to induce E and L viral gene expression. For example, the HCMV IE viral tegument protein pp71 is one of the first gene products produced from latently infected cells. The pp71 ORF encodes a protein that functions to remove a cellular DAXX protein (anti-apoptotic) enabling cell cycle progression and viral replication [59-63]. Other IE gene products that induce E and L stages of replication are the gene products IE72 [64, 65] and IE19 [64]. These two products work as transcriptional co-activators alongside IE86 [66] to promote viral DNA replication [11, 67-70].

Post-IE gene synthesis and within the first 24 hours of HCMV infection of primary human foreskin fibroblasts, the E gene products are understood to be expressed. The E genes are primarily non-structural proteins that are involved in viral-DNA replication and maintenance of the genome e.g. DNA-polymerase (UL54) [71, 72] and the helicase-primase complex (UL70) [72, 73]. Without E gene expression further CMV replication could not occur.

Subsequent to E gene expression, the L genes are synthesised. The L genes require the manifestation of E gene products i.e. the DNA-replication machinery, to enable their transcription. The L gene products tend to be structural proteins, and are involved in assembly of the complete virion [74].

Following gene synthesis and CMV genome replication within the nucleus of the infected cell the virus is processed into virions. Firstly, the viral genome inserts itself within the capsid.

The CMV capsid is an icosahedral protein structure organized into capsomeres, hexamers, pentamers and triplexes approximately 110 nm in diameter [75, 76].

The capsid translocates from the inner nuclear membrane into the perinuclear space and acquires a primary envelope, which fuses during budding into the outer nuclear membrane releasing the capsid into the cytoplasm. A final envelope is acquired through fusion with Golgi derived vesicles. The viral envelope encompasses the tegument that contains numerous proteins, glycoproteins, phospholipids, polyamines, and small RNAs [77, 78]. The CMV viral tegument region is approximately 50 nm thick. The tegument layer contains multiple viral proteins including immunogenic targets e.g. pp65 [79-81]. Egress of the virus particle occurs through the fusion between the cell membrane and the virion [82]. A single CMV infected cell has the potential to generate many viral progeny including two non-virion forms of CMV: the non-infectious enveloped particles (NIEPs) and dense bodies (DBs) [83, 84]. NIEP lack the dsDNA whereas DBs lack a capsid. Both are more abundant than complete virions (produced in a ratio exceeding 20:1) [85].

1.4.2. CMV DURING LATENCY

The lytic phase of CMV's life cycle sees the production of *de novo* viral progeny whereas the period(s) of latency is defined as the persistence of the viral genome in the absence of lytic replication or evidence of gene expression. Under specific conditions, the latent CMV is capable of re-entering lytic replication. The pattern of lytic replication, latent infection and sporadic viral reactivation is likely to repeat a number of times throughout the lifetime of the host.

HCMV has the potential to infect many cell types however the exact sites of viral latency and the mechanisms from which the virus is able to reactivate is a source of contention. Latent HCMV does reside within undifferentiated myeloid cells and the reactivation of the virus and the progression of myeloid cell maturation are interconnected. In a recent study, by Chan *et al* (2012), it was shown that initiation of viral reactivation occurred prior to the differentiation of the myeloid progenitor cell and this process caused the simultaneous production of virions and the differentiation of the monocyte [86]. Whereas, Reeves *et al* (2005) concludes that reactivation of infectious virus results from cellular chromatin remodelling during DC differentiation [87, 88]. Therefore, as HCMV resides in myeloid progenitor cells it is also likely that upon differentiation latent virus will be present in the daughter cells of the progenitors.

1.5. TRANSMISSION OF CMVS

The definition of CMV seropositivity is the presence of anti-HCMV IgG or IgM immunoglobulins in the serum [89, 90]. HCMV seroprevalence is often described as ubiquitous [32, 91], with seroprevalence fluctuating between 40-95% of the global population being serologically positive [92]. The high prevalence rate is partly due to multiple routes of dissemination that include both vertical and horizontal transmission. Studies that have analysed the prevalence of MCMV isolates among wild house mice (*Mus domesticus*) [93] and wild mice (*Mus musculus*) [94] both confirmed almost universal MCMV seroprevalence.

Vertical transmission of HCMV from mother to foetus via the placenta occurs in humans. MCMV does not transmit between a mouse and its offspring due to the structural differences in the placenta [95]. Animal models of vertical CMV transmission rely on the guinea pig model [96-98]. Contraction of maternal primary HCMV infection during pregnancy is a major concern due to the vertical transmission of the virus to the developing foetus. It is estimated that in excess of 5500 children in the USA are born each year with defects caused by congenital HCMV [16]. *In utero* HCMV can induce a variety of neurological complications including sensorineural and bilateral hearing loss [99], later development of speech and a reduced IQ [100], macrocephaly, seizures and premature death. Interestingly the transmission of latent virus to the foetus is less associated with congenital disease as a result only primary HCMV infection is screened for routinely during pregnancy [101].

Horizontal transmission of CMV is typically associated with the shedding of virus in bodily fluids. Neonates may contract HCMV during breast-feeding as HCMV DNA is transmitted in both the cellular and whey component of breast milk [102-109]. In addition, HCMV has been isolated from over 60% of saliva and 37% of urine samples from healthy individuals [110]. As a direct consequence, the risk of HCMV exposure is elevated in areas of poor sanitation or in professions where exposure to bodily secretions is high, e.g. child-care workers [111].

1.6. CMV PATHOGENESIS

HCMV infection is not a serious pathogen in healthy individuals; this is because the immune system has adapted to suppress lytic replication. Primary HCMV infection is usually asymptomatic and therefore records of acute infection inevitably go unreported. Case reports of more severe HCMV disease in immunocompetent individuals do inevitably exist [112], however cases of symptomatic HCMV infections usually result in a self-limiting infectious mononucleosis [113, 114]. The immune response that limits HCMV infection is required to control viral reactivation and loss of immunological control can result in viraemia that affects multiple organs and systems. The most common clinical manifestations of HCMV disease seen in immune suppressed patients are pneumonitis, retinitis, enteritis and colonitis and disease of the gastroenteric tract which all have the potential to be fatal [115].

1.7. CMV THERAPEUTIC OPTIONS

1.7.1. ACYCLOGUANOSINE PRODRUGS

Antiviral treatment of herpes infection was revolutionised in the 1970s with the introduction of Acycloguanosine prodrug compounds. Aciclovir was the first anti-herpes drug to be introduced that inhibited herpes-viral DNA replication. Acycloguanosines are used clinically to treat a broad range of infections, e.g. cold sores, shingles and HCMV reactivation. Acycloguanosine prodrugs may also have benefit in other conditions where Herpesviridae have been implicated, e.g. Bell's palsy [116], schizophrenia [117] and in delaying the onset of *Human immunodeficiency virus* (HIV) acquired immunodeficiency disease (AIDS) [118].

Figure 1.1. The chemical structures of the purine base guanine ($C_5H_5N_5O$) and the prodrug aciclovir ($C_8H_{11}N_5O_3$). Aciclovir resembles a nucleoside and once activated more closely resembles a guanine nucleotide that is selectively incorporated into the viral genome during transcription.

Acycloguanosine prodrugs exert an antiviral function due to their resemblance to the purine base guanine (Figure 1.1). The activation from the prodrug into an active form requires a series of three phosphorylation events to convert the guanine nucleoside analogue into a tri-phosphate molecule that mimics a guanine nucleotide (Figure 1.2).

The first phosphorylation reaction is performed by a viral phosphatase thus creating a mono-phosphate acycloguanosine. Most Herpesviridae encode a thymidine kinase (TK) enzyme that provides the initial phosphorylation reaction to convert aciclovir into a mono-phosphate form. CMVs are an exception and do not encode a TK, but HCMV and MCMV remain sensitive to acycloguanosine antivirals because of a protein kinase (PK) enzyme with a homologous function to the TK. The phosphotransferase enzyme UL97 of HCMV and M97 of MCMV is capable of performing the same necessary primary phosphorylation as the HSV-TK [119].

The cellular kinase(s), (d)GMP and (d)NDP kinase, provides two further phosphorylation reactions to generate a guanine nucleotide analogue. The herpes virus' DNA polymerase (M57 ORF of MCMV) then incorporates this analogue into the genome (Figure 1.2). Consequently, this leads to chain termination of the viral DNA due to the lack of a 3'-OH group on the sugar residue and a failure of viral genome replication. The antiviral does not kill virally infected cells it only prevents further viral replication.

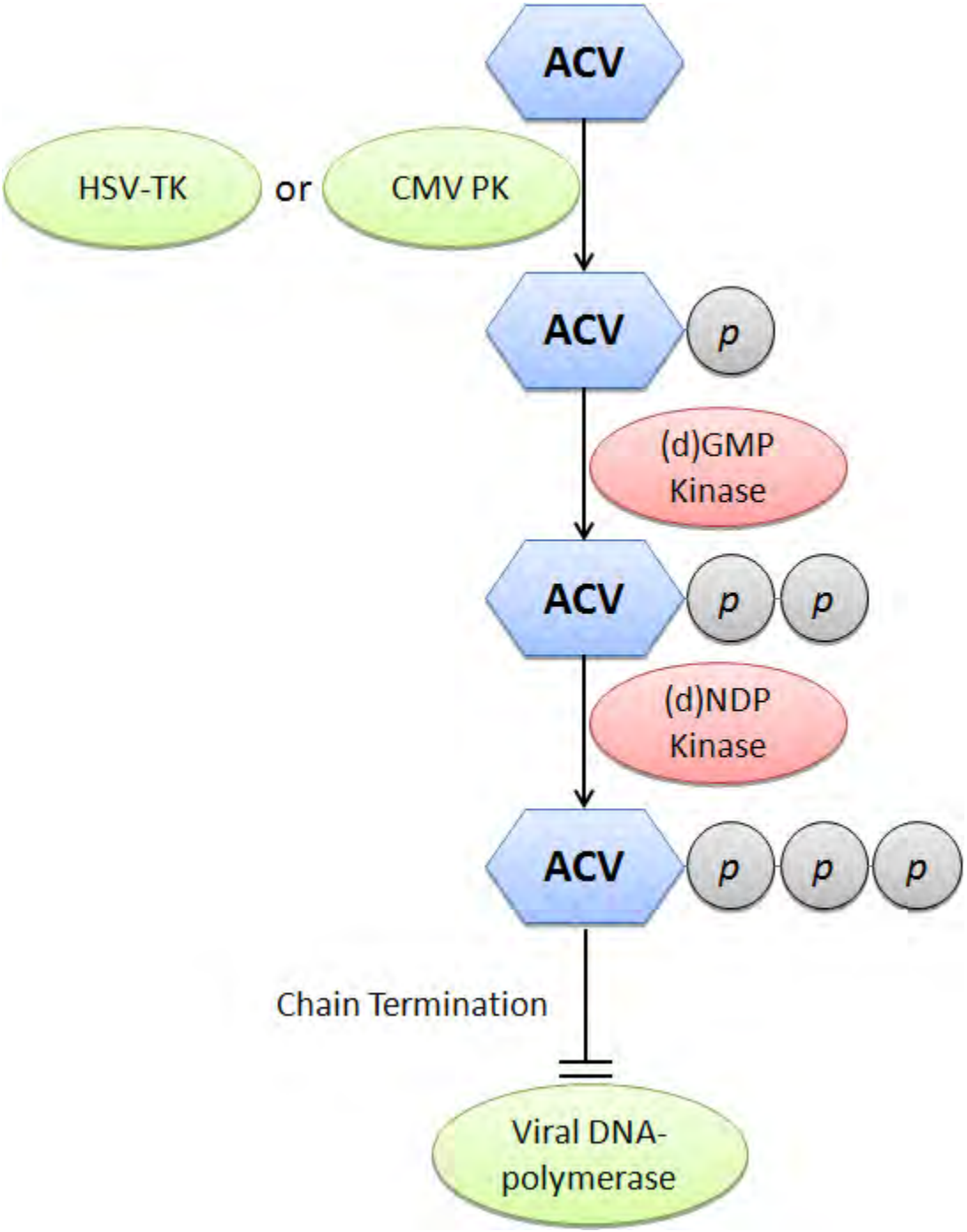

Figure 1.2. Activation of the aciclovir (ACV) prodrug requires an initial phosphorylation event by a herpes virus encoded thymidine kinase (HSV-TK) or a CMV protein kinase (CMV-PK). Aciclovir-monophosphate is phosphorylated by cellular (d)GMP and (d)NDP kinase(s) creating aciclovir-triphosphate that selectively inhibits herpes virus DNA-polymerase.

Early acycloguanosine nucleoside prodrugs such as aciclovir have a short half-life in the body and a poor bioavailability. Therefore, aciclovir(s) are administered at a high dose. For example, doses exceeding 10 mg/kg daily of valaciclovir is given for the prevention and treatment of HCMV-disease post-allogeneic hematopoietic stem cell transplantation [120]. Valaciclovir ($C_{13}H_{20}N_6O_4$) is an esterified form of aciclovir converted into an active prodrug by a cellular valaciclovirase(s) (Figure 1.3) [121-124]. Newer acycloguanosine compounds such as ganciclovir are more potent derivatives acycloguanosines however; this class of antiviral has serious side effects in approximately 1% of patients. For example, ganciclovir is listed as being toxic, a mutagen and a carcinogen. Haematological side effects seen with ganciclovir treatment include neutropenia and thrombocytopenia [125]. Due to the toxicity associated with acycloguanosine prodrugs there has been a recent focus on developing new drugs to treat HCMV disease. These newer drugs e.g. Foscarnet, Cidofovir, Formivirsen [126] and Maribavir [127] are designed primarily to be administered for relatively short periods until the immune system is capable of controlling HCMV independently.

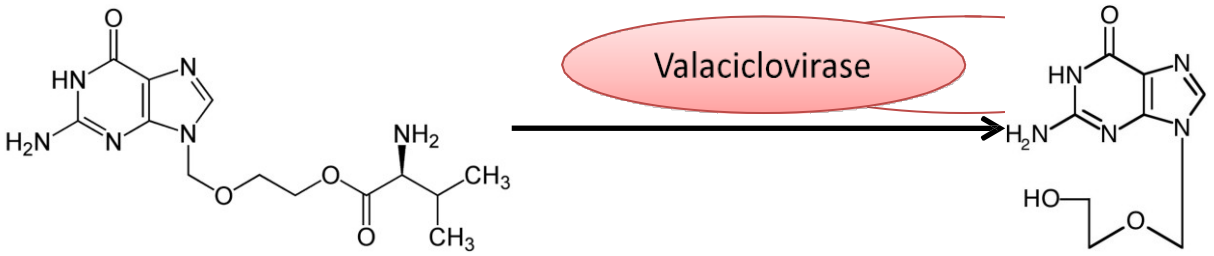

Figure 1.3. Conversion of valaciclovir into aciclovir. Valaciclovir has an improved bioavailability due to carrier-mediated intestinal absorption. Enzymatic conversion by a valaciclovirase is required for the conversion/activation *in vivo* [121].

In vitro propagation of HCMV in the presence of antiviral compounds has led to the emergence of antiviral resistant mutant strains [128]. Similarly, long-term antiviral therapy can lead to the emergence of drug resistant HCMV strains *in vivo* [129, 130]. In the pre-HAART (highly active antiretroviral therapies) era it was estimated that approximately 8% of AIDS patients would develop resistance to ganciclovir and become susceptible to HCMV disease after three months [131]; by six months estimates suggest 11% of patients and in excess of 25% will have a recrudescence of herpesvirus infection [132]. The clinical significance of antiviral resistance is that for successful long-term suppression of HCMV, a continuous dose of antiviral is required and cessation of therapy may result in disease. The selective pressure applied to HCMV during antiviral therapy may select for advantageous mutations to the phosphotransferase gene, UL97 [133]. These mutations often confer cross-resistance to other acycloguanosine antivirals [134, 135].

1.7.2. HCMV VACCINE DEVELOPMENT

HCMV infection is asymptomatic in immunocompetent individuals; however, a vaccine that generates protective immunity to the virus would be beneficial in preventing HCMV disease manifestations during pregnancy and immunosuppression. Anti-HCMV vaccines have entered clinical trials with moderate success. A particle vaccine expressing either the glycoprotein (gB) protein or a pp65/IE1 fusion protein was tested in a randomised, double-blind Phase-1 clinical trial in HCMV seronegative adults. The vaccine elicited T-lymphocyte responses (measured by IFNγ ELISPOT assays) and neutralising antibodies [136, 137]. A separate Phase-1 trial conducted in HCMV-seronegative toddlers administered the gB antigen with the MF59 adjuvant was highly immunogenic with higher immunoglobulin titres achieved than those who acquire HCMV naturally [138]. A different gB vaccine, again given with the MF59 adjuvant, was tested in a randomised placebo controlled trial of patients awaiting kidney/liver transplantation elicited strong humoral immunity and immunoglobulin titres that inversely correlated with the duration of viraemia [139]. These promising trials suggest that it may be possible to vaccinate and protect against HCMV.

1.8. THE IMMUNE RESPONSE TO CMV

Acquisition of CMV infection becomes a life-long challenge to the immune system, as the virus is not eradicated from the host. To avoid detection by the immune system CMVs are able to revert from a lytic into latent states and employ a series of immune evasion mechanisms. Importantly prior CMV exposure does not provide protective immunity to secondary infection [140].

Loss of immunity can give rise to an increase in opportunistic HCMV infection [141, 142]. Cells of the innate system are usually the first to respond to infection and are not reliant upon prior sensitisation to non-self-antigens. The haematopoietic stem cells of the bone marrow are multipotent and differentiate to form the myeloid and lymphoid lineages of the immune system. The myeloid professional antigen-presenting cells (APCs), such as DCs and macrophages, provide the necessary stimuli to prime and maintain lymphoid immunity [143]. The adaptive immune response is initially less rapid, however upon resolution of acute infection a quiescent form of immunological memory is formed that rapidly responds to antigen re-exposure by proliferation and effector functioning [144].

The establishment of latent CMV infection, although asymptomatic, may be best phrased as a chronic infection due to dramatic changes seen in the T-lymphocytes populations of seropositive donors/animals [145-147]. A series of longitudinal epidemiological studies compared changes in immune parameters in relation to HCMV seropositivity in octogenarians and nonagenarians. They concluded HCMV seropositive individuals had oligoclonal expansions of HCMV-specific $CD8^+$ T-lymphocytes, an inverted CD4:CD8 T-cell

ratio, restricted T-cell receptor (TCR) usage and a low number of B-lymphocytes. The collective term for these changes was the Immune Risk Profile (IRP). Individuals with an IRP were characterised as being at an elevated risk of mortality at two, four and six years follow-up [148, 149]. Similarly, in a cross-sectional analysis of 70^{+} year old females in Baltimore USA, HCMV seropositivity directly impact upon mortality and in addition was found to accelerate the onset of frailty [150].

1.8.1. $CD8^{+}$ T-LYMPHOCYTE RESPONSE TO CMV

The $CD8^{+}$ T-lymphocytes are form part of the adaptive immune response. They are cytotoxic and kill virally infected cells. The $CD8^{+}$ T-cell response is initiated by a number of signals within the immunological synapse. First, direct antigenic stimulation is provided by engagement of the $CD8^{+}$ T-cells own TCR binding to the APC presenting a cognate viral peptide loaded onto a major histocompatability complex (pMHC) (Figure 1.4). The antigenic peptides are prepared via proteasomal processing of viral proteins into shorter sequences that are loaded onto the MHC via the transporter for antigen presentation (TAP). The pMHC complex translocates from the ER to the outer membrane of the APC for detection by $CD8^{+}$ T-cells with cognate TCR. TCR-binding of the pMHC causes the CD8 complex within the lymphocytes outer membrane to cluster around the TCR bringing the *src* family kinases e.g. Lck or Fyn, into close proximity of the CD3 ζ-side chain of the lymphocyte. The recruitment of Lck phosphorylates immuno-receptor tyrosine-based activation motifs (ITAMs) on the CD3 ζ-side chain. This induces a cascade of events including recruitment and activation of ZAP-70 to the phosphorylated ITAM, and induction of downstream pathways such as upregulation

of transcription factors e.g. nuclear factor of activated T-cells (NFAT) and nuclear factor kappa-light-chain-enhancer of activated B cells (NF-κB) which results in T-lymphocyte activation/proliferation [151, 152]. To augment the $CD8^+$ T-cell proliferation a second co-stimulatory signal is provided; such as CD28 on the T-cell surface (constitutively expressed on naïve T cells) binding the B7-ligands (CD80 and CD86) on activated APCs which aids T-cell mitosis [153]. A third signal within the immunological synapses is provided by inflammatory cytokines e.g. interleukin-2 (IL-2), binding to its receptor (CD25) on the lymphocyte. These signals are required for the initiation of proliferation and cytotoxic function of the $CD8^+$ T-cells (Figure 1.4).

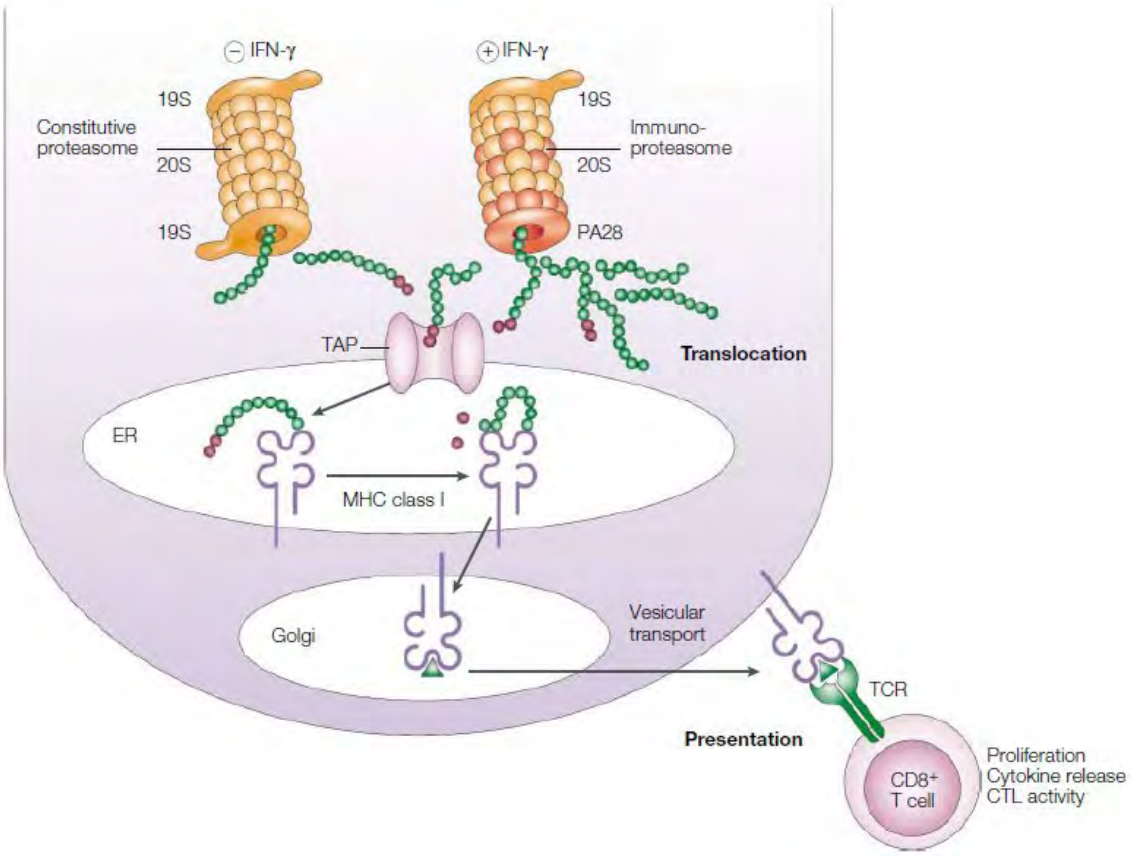

Figure 1.4. CMV viral proteins are processed into short antigenic peptides by the constitutive proteasome or IFNγ inducible immunoproteasome. The peptide is then transloacted from the endoplasmic reticulum (ER) by the transporter for antigen processing (TAP) and presented by MHC-I on the cell surface to interact with $CD8^+$ T-cells with a complementary TCR. Also within the immunological synapse, co-stimulation from CD28, OX40 and 41-BBL interactions and addition stimuli from proinflammatory cytokines aid $CD8^+$ T-cell proliferation, cytokine release and cytotoxic activity. Nature Reviews in Immunology [154]. Licence number 2864720728549.

The entire HCMV proteome was previously screened for immunogenic MHC-I and MHC-II T-lymphocyte epitopes using 15mer overlapping peptides. Sylwester *et al* (2005) demonstrated that 60.9% of the 213 HCMV ORFs were immunogenic, with 38% of ORFs eliciting both $CD4^+$ and $CD8^+$ T-lymphocyte responses (measured by $CD69^+$ and IFNγ production) and 12.2% of ORFs elicited only HCMV-specific memory $CD8^+$ T-cell responses [155]. On average the $CD8^+$ T-cell repertoire of an HCMV seropositive individual responds to 21 ORFs with the five most frequently recognised by $CD8^+$ T-cells being UL48, pp65, IE1, IE2 and US32. The immunogenic ORFs spanned the entire kinetic profile of gene expression (IE, E, E-L or L), function (capsid, matrix, glycoprotein, DNA and immune evasions) localisation (virions and DBs), and was irrespective of major histocompatability complex (MHC) haplotype [156]. Furthermore, in the Sylwester *et al* (2005) study the average peripheral blood HCMV-specific immune response, per individual, was approximately 4.5% of the entire $CD8^+$ T-cell pool in adults and 10% of the $CD8^+$ T-cell memory compartment in older donors [155].

Staining of the peripheral blood mononuclear cells (PBMC) with MHC-I tetramer reagents showed that in elderly donors up to 40% of the entire lymphocyte pool may be directed against a single HCMV-epitope [145-147]. The expansion in HCMV-specific memory T-lymphocytes seen in the elderly reduces the heterogeneity of the overall cytotoxic $CD8^+$ T-cell repertoire which has been demonstrated to be highly clonal [145, 147, 157, 158].

Ex vivo analysis of PBMC from elderly HCMV, seropositive donors display a skewed distribution of $CD8^+$ T-lymphocyte memory populations. The phenotype can exist almost

exclusively of T-effector memory revertant CD45RA $CD8^+$ T-cells ($CD45RA^+$ $CCR7^-$) with very few naïve ($CD45RA^+$ $CCR7^+$) $CD8^+$ T-cells. Within the HCMV seropositive donor a large proportion of the TEMRA cells are HCMV-specific and under the correct experimental conditioning stimuli e.g. 4-1BBL or peptide stimulation the cells are able to proliferate and/or produce multiple pro-inflammatory cytokines [146, 159].

Reactivation of HCMV-antigen could provide the necessary stimulus to generate the large peripheral HCMV-clonal expansions of $CD8^+$ T-lymphocytes detected in the elderly. The high frequency of these cells and the corresponding decline in the naïve $CD8^+$ T-cell repertoire could be detrimental to health. In HCMV seropositive donors, the accumulation of HCMV-specific $CD8^+$ T cells is associated with six fold fewer EBV-specific $CD8^+$ T-cells in the peripheral blood compared with seronegative donors [146]. It was proposed that HCMV is potentially detrimental in an immunocompetent host, through suppressing heterologous virus-specific immunity during aging and consequently, a HCMV seropositive individual maybe more susceptible to infection(s) and may be predisposed to earlier mortality [148, 149, 160].

There are many parallels between HCMV and MCMV infection including the high prevalence, dissemination, persistence and shedding from the host. Likewise, immunological models of HCMV infection have been developed in a number of laboratories that mimicked the large expansions of HCMV-specific $CD8^+$ T-lymphocytes. The model of MCMV induced memory inflation was first developed in MCMV susceptible mice strains. Intravenous inoculation of BALB/c mice with the MCMV strain *Smith* resulted in an accumulation of pp89 and m164-

specific $CD8^+$ T-cells that peaked at day 100 p.i. and were maintained at high frequencies [161]. For example, pp89 specific $CD8^+$ T-cells have been estimated to contribute to 8% of the $CD8^+$ T-cells from the spleen, 16% from the lungs, 16% from the liver and 24% from the salivary gland. Latent MCMV has been shown to reside within the spleen [162], lung [34], liver [35] and salivary gland [163] therefore it is unsurprising that a high frequency of MCMV-specific CTLs are found in these organs. In contrast, the percentage of pp89-specific cells was not enriched in the mesenteric lymph nodes or the salivary gland associated lymph nodes. Consequently, it appears that memory inflation is tissue specific and the homing or proliferation of these cells is independent of lymphoid organs and more closely associated with the sites of MCMV latency.

Snyder *et al* (2008) further refined the MCMV model. They were amongst the first to show memory inflationary in the C57BL/6 mouse and detected diverse memory responses to over twenty viral proteins [164]. Immunogenic epitopes contained within the proteins encoded by the M45 and M57 ORFs elicit robust $CD8^+$ T-cell proliferation during the acute phase of infection which later contracts to form a stable resting long-lived memory population [165]. Immunity towards the M38 and m139 epitopes displays kinetics that is atypical to the understanding of normal memory T-cell development. Initially proliferation of M38 and m139-specific $CD8^+$ T-cells occurs during the primary infection, followed by a short contraction phase, however, there is then a gradual accumulation of virus-specific cytotoxic T-lymphocytes (CTLs) termed “memory inflation”. The lymphocytes that undergo memory inflation also present a highly differentiated membrane phenotype equivalent to the TEMRA phenotype. A third epitope that also develops memory inflation is processed from the

IE3/M122 ORF. $CD8^+$ T-cell responses towards IE3 are not usually detected during the acute phase of infection but expanded to very high frequencies (>16% $CD8^+$ T-cells) by 100 days p.i. [164]. These inflationary immune responses seen in the mouse [161, 165] are analogous to those immune responses seen in humans as they are detected in older age and have a distinctive highly differentiated membrane phenotype [146, 147].

The MCMV $CD8^+$ T-lymphocytes which undergo memory inflation display lower levels of CD62L (L-selectin) than the non-inflationary M45 and M57 antigen-specific cells [165]. CD62L interacts with its receptor on the high endothelium venule (HEV) binding molecule CD62L (L-selectin) and expression on a lymphocyte ensures that the cell is preferentially retained within the lymph node at the correct anatomical site for antigen presentation. In addition the M38, m139 and IE3-specific CTLS have reduced expression of the cytokine receptors CD127 (IL-7Rα) and CD122 (IL-15Rβ) [165]. Surface expression of these receptors is down regulated upon chronic stimulation and antigen exposure to prevent the cells from being exhausted and unable to proliferate [166-170]. Similarly, the inflationary subsets of cells have reduced levels of CD27 compared to the M45 and M57 subsets [165], expression of the CD27 molecule is regulated its interaction with CD70 on the APC and during chronic infection is believed to represent a transition of an effector cell into a long-lived memory cell [171, 172]. CD28 expression is also modulated via interactions with its ligands (CD80/86) on the APC and successful activation promotes T-cell proliferation, the loss of this molecule occurs on the more highly differentiated lymphocyte subsets [173] and is unsurprisingly CD28 expression is low on the M38, m139 and IE3 specific T-cells [165]. The inflationary cells were further characterised as having low expression of killer cell lectin-like receptor subfamily G

member (KLRG1) and programmed cell death (PD-1) [165]. KLRG1 is a receptor than binds E-cadherin and is located on the surface of both NK and T-lymphocytes. Elevated KLRG1 expression can lead to inhibition of T-cell proliferation (inhibition of Akt signalling) and is more prominent with age and T-cell differentiation and therefore the high levels of KLRG1 on inflationary T-cells show the cells as less capable of proliferation [174-176]. PD-1 is an inhibitory receptor expressed on T-cells. Levels of PD-1 are partially modulated by T-bet (transcription repressor) and loss of PD-1 is believed to help sustain virus-specific $CD8^+$ T-cells from becoming exhausted therefore it is likely that the accumulating cells also have some functional impairment [177].

The inflationary MCMV-specific $CD8^+$ T-cells proliferate rapidly during acute infection with the Ki67 (molecule expressed during mitosis) expressed on 100% of pp89-specific cells at day 7 which was seen to fall to 22% by day 30, and as low as 7.5% by day 150 [161]. The M38, m139 or IE3-specific $CD8^+$ T-cells when adoptively transferred, (from donor CD45.1 mice into immunologically naïve CD45.2 recipient mice) did not proliferate independently of latent MCMV infection and were almost completely lost from the recipient mice within 90 days [165]. When Snyder *et al* (2008) repeated the transfer of the same inflationary subset of T-cells, into MCMV infected mice the antigen-specific memory pool was maintained by the repopulation of cells with the same specificity from the recipient and not the donor [165]. In contrast, transfer of M45 or M57 (non-inflationary) specific $CD8^+$ T-cells into MCMV immune mice were maintained at the same relative frequency in naïve mice, however upon transfer into MCMV immune mice the M45/M57 T-cell frequency decayed and was almost absent at

day 119 after adoptive transfer illustrating that the CTL populations are maintained via an additional signal(s) [165].

The work of Tanaka *et al* (2007) showed memory inflation (IE1-specific $CD8^+$ T-cells) did not occur at 12 months following MCMV-infection in germ-free mice (GF). In addition, Tanaka did not detect an elevation in viral load or proinflammatory cytokines levels (IL-2, IL-7, IL-15, and IFNγ) within the lungs of GF mice compared to SPF mice. Re-colonisation of the GF gut with indigenous microbiota then enabled memory inflation of MCMV-specific $CD8^+$ T-cells to occur [178]. From this the authors remarked that the wide variety of antigenic peptides derived from the microbiota were a likely source of cross-reactive epitopes of MCMV highlighting a role of antigen(s) and their presentation which influences whether memory inflation occurs.

There are multiple lineages of $CD4^+$ T-cells and in addition to directly suppressing MCMV replication [179] $CD4^+$ T-cells can help to initiate cross-presentation of MHC-I antigens by professional APC such as conventional DCs (cDC) [180, 181]. Snyder *et al* (2009) investigated whether the mechanism of memory inflation would occur during the latent-phase of infection in the absence of $CD4^{-/-}$ or MHC-$II^{-/-}$. They showed that the loss of $CD4^+$ T-cells impaired the generation and accumulation of IE3-specific $CD8^+$ T-cells within the blood, spleen and lung [182]. It was also reported that the absence of $CD4^+$ T-cells did not influence memory inflation of the m139 and M38-specific $CD8^+$ T-cell response. Contrasting data from Walton *et al* (2011) showed that MHC-$II^{-/-}$ knock-out mice do not generate the normal frequencies of M45 and M57 T-cells (non-inflating) and memory inflation of the M38, m139

and IE3-specific $CD8^+$ T-cells does not occur [183]. The additional role that $CD4^+$ T-cells provide was not IL-21 mediated and is most probably mediated by CD40L interaction with infected APCs as $CD40L^{-/-}$ mice also have reduced frequencies of IE3-specific T-cells in the blood (24 weeks p.i.) [182, 183].

Similar observations of impaired IE3-specific $CD8^+$ T-cell responses were seen in $Batf3^{-/-}$ (basic leucine zipper transcriptional factor ATF-like 3) knockout mice. Batf3 is a transcription factor required for cDC development, knockout mice have severe defects in the cross-presenting of viral and tumour antigens [184]. MCMV infection of $Batf3^{-/-}$ mice have approximately 30% fewer IE3-specific $CD8^+$ T-cells in comparison to mice with *wt* infection in both the lungs and spleen at 110 days post-MCMV infection [185]. In addition, the frequencies of M38 and m139-specific T-cells display "early" inflation kinetics, accumulating post-acute infection, and retaining an effector phenotype ($CD127^{lo}$ $CD62L^-$ $KLRG1^{hi}$); however, three months post-MCMV infection there was a partial reduction in the frequency of M38 and m139-specific $CD8^+$ cells in $Batf3^{-/-}$ mice. Therefore, $CD4^+$ T-cells may facilitate an interaction between virally infected cells that cross-present the IE3-antigen that initiates the expansion of IE3-specific $CD8^+$ T-cells during latent infection.

Presentation of pMHC to $CD8^+$ T-cells requires the processing of viral proteins into shorter antigenic peptides by either the constitutive proteasome or the immunoproteasome. The presence of pro-inflammatory IFNγ is associated with an upregulation of MHC-I expression and the construction of the immunoproteasome in non-professional APCs [186]. Professional APCs express the immunoproteasome constitutively so it is unsurprising that MCMV is able

to modulate the immunoproteasome through inhibiting phosphorylation of STAT-2 and consequently inhibiting IFNγ-receptor signalling [187, 188]. The presence of the LMP7 (IFNγ inducible subunit of the immunoproteasome) is required for memory inflation as the frequency of M38 and m139-specific $CD8^+$ T-cells is approximately double in *wt* compared to $LMP7^{-/-}$ mice at 100 days post-MCMV infection [189]. Memory inflation of the IE3-specific cells was not examined in relation to a functional immunoproteasome however as the accumulation of cells of this specificity is reliant on cross-presentation [190] and presentation from non-haematopoietic cells [45] IE3-presentation is also likely to utilise processing by the immunoproteasome. It was shown for IE1-specific T-cells to inflate in a BALB/c infected mouse that expression of the epitope is required from host MHC class-I molecules on non-professional infected cells presenting antigen as inflation did not occur in mice with mismatched MHC-I on the professional APCs [191].

Investigations that sought to inhibit lytic MCMV replication with acycloguanosine treatment have solely focused on treatment of a mutant MCMV strain (MCMV-Δm157-TK). There are a number of issues that arise through the using the MCMV-Δm157-TK mutant virus. The deletion of the m157 gene enables the virus to escape from NK-cell Ly49h-mediated cytotoxicity, which results in elevated acute MCMV titres in the lung and spleen. Consequently, the adaptive immune system responds to the higher viral loads with a larger $CD8^+$ T-cell response (M45, M57 and m139 epitopes) and significantly elevated levels of proinflammatory cytokines (IFNγ, IFNα, IL12, IL-6 and IL-15) in the serum and in addition reduced numbers of circulatory DCs [192]. Therefore, the MCMV-Δm157 viruses do not elicit memory inflation to the same magnitude or kinetics as a *wt* MCMV. Furthermore, the

addition of the HSV-I TK to the MCMV-Δm157 mutant is believed to increase the virus' sensitivity to acycloguanosines [193]. However, the insertion of the TK into the MCMV genome is unnecessary as *Smith* MCMV is highly susceptible to doses of antiviral as low as 1 μM [194]. Consequently, the MCMV-Δm157-TK mutant virus is so far removed from the original that the immune response generated (+/- antiviral treatment) is not representative of MCMV infection.

Both Walton *et al* (2011) and Snyder *et al* (2011) exposed MCMV-Δm157-TK infected mice to famciclovir treatment (2 mg/ml) and measured the corresponding $CD8^+$ T-cell frequencies [183, 193]. Neither study reported any direct immunotoxicity towards the T-cells [195]. Snyder *et al* (2011) illustrated that antiviral treatment given seven days prior to MCMV-Δm157-TK infection resulted in the almost complete attrition of the IE3-specific immune response after 12 weeks of treatment [193]. Similarly, Walton *et al* (2011) demonstrated that famciclovir treatment of MHC-$II^{-/-}$ deficient mice infected with MCMV further reduced the frequency of IE-specific CTLs [183]. In addition, famciclovir treatment resulted in a larger proportion of both M45 and M38-tetramer specific cells to display a less differentiated surface phenotype ($CD62L^+$ $CD27^+$) [183]. Unfortunately, the phonotype of IE3 and m139-tetramer specific cells was not included in their analysis.

In addition to antigen, cytokines directly modulate memory inflation. MCMV infection of IL-$10^{-/-}$ knockout mice have amplified numbers of MCMV-specific $CD8^+$ T-cells due to the removal of the suppressive effect of this anti-inflammatory cytokine [196]. Likewise, co-stimulation via the TNF superfamily of receptors is required for T-cell responses. The

absence of an interaction between 4-1BB and its receptor has two independent effects upon the MCMV-specific T-cell response in 4-1BB$^{-/-}$ mice. The 4-1BB$^{-/-}$ mice develop exaggerated acute MCMV-specific CD8^{+} T-cell responses however memory inflation does not occur for the M38 and m139-specific CD8^{+} T-cells (IE3-specific cells not tested) [197]. OX40 is transiently expressed by activated T-cells and functions to bypass the inhibitory signals provided by CTLA-4. Loss of OX40$^{-/-}$ interactions with its ligand OX40L (expressed on the APC) was shown to impair memory inflation of M38 by approximately 50% at day 90 p.i. suggesting memory inflation may require periodic costimulation from an infected cell [198]. In contrast loss of the costimulatory B7 ligands, CD80 and CD86, in B7.1/2$^{-/-}$ mice, was shown not to result in reduced numbers of M38, m139 and IE3-specific CD8^{+} T-cells [199].

Typically CMV-specific immune responses modelled *in vivo* have focused upon infections in immunologically naïve specific-pathogen free (SPF) animals to avoid cofounding effects on the experimental data. However, in the natural environment all animals become exposed to a large variety of pathogens throughout their lifetime and as a result would develop multiple immune responses. Having a history of pathogen exposure modulates the ability to mount *de novo* immune responses. For example, successive infection of C57BL/6 mice with *Lymphocytic choriomeningitis virus* (LCMV), *Pichinde virus* (PV), *Vaccinia virus* (VV), MCMV, and *Vesicular stomatitis virus* (VSV), caused the attrition of the pre-existing LCMV-specific CD8^{+} T-cells with each subsequent infection [200]. The decline in memory CD8^{+} T-cell frequencies was attributed to the exposure of “heterologous antigen” and the attempts made by the immune system to accommodate the proliferation of the new lymphocyte response within a finite lymphoid population. The series of heterologous viral infections was

illustrated to cause the attrition of the absolute numbers and not just percentages of pre-existing memory T cells [201]. The mechanism through which this attrition may occur is through an increased sensitivity to type I interferons in memory T-cells. In experimental models interferon cytokines can selectively activate caspase-3 and caspase-8 and initiate apoptosis in sensitive memory T-cells but not antigen inexperienced lymphocytes [202-204]. Therefore, frequent viral (CMV) reactivation and the pro-inflammatory environment generated could both contribute to the loss of T-lymphocytes of other specificities and memory inflation of CMV-specific CTLs.

1.8.2. $CD4^+$ T-LYMPHOCYTE RESPONSE TO CMV

Ageing and lifelong HCMV infection sculpts both the naïve and memory $CD8^+$ T-lymphocyte repertoires in older people. In contrast, age has been shown to be the strongest factor in the depletion of naïve ($CD45RA^+$ $CD27^+$) $CD4^+$ T-lymphocytes from the peripheral blood of older donors [205]. However, healthy HCMV-seropositive individuals also develop an age-dependent decrease in naïve $CD4^+$ T-lymphocytes and accumulation of memory $CD4^+$ T-lymphocytes which is likely to start immediately p.i. as changes to $CD4^+$ T-cell profile become evident in PBMC samples taken from children [9, 206]. Pourgheysari *et al* (2007) demonstrated memory inflation of $CD4^+$ T-cells; as the frequency of HCMV-specific $CD4^+$ T-cells more than doubled from on average 2.2% in younger donors (<50 years old) to 4.7% in older donors (>65 years old) [207].

In the study of Sylwester *et al* (2005) overlapping peptides were used to screen for HCMV immune responses; 44 ORFs generated HCMV-specific $CD4^+$ T-lymphocyte responses [208]. The two most dominant $CD4^+$ T-cell specificities were directed towards epitopes from the gB and pp65 proteins that were present in over 25% of the individuals they assayed. HCMV-specific immune responses constituted on average 4% of the entire $CD4^+$ T-cell pool and over 9% of the memory $CD4^+$ T-cell compartment [208]. In another small study of memory $CD4^+$ T-cell response to HCMV, the $CD4^+$ specific T-cell response was dominated by small number of clonotypes [209]. Similarly, in rhesus macaque models of CMV infection the developing virus-specific $CD4^+$ T-cells are clonal if the macaques are re-challenged with the same pathogen [210].

Aging alone is thought to be the strongest factor for the decrease in the naïve ($CD45RA^+$ $CD27^+$) $CD4^+$ T-lymphocyte population observed in older donors [205]. However, HCMV causes a paradoxical increase in the $CD4^+$ $CD45RA^+$ $CD27^+$ T-cell populations. The majority of these cells are HCMV-specific and are at an elevated frequency in the bone marrow compared with the blood [205]. In healthy aged donors the phenotype of the overall $CD4^+$ T-lymphocyte alters displaying elevated $CD57^+$ expression, decreased levels of the co-stimulatory CD28 [205] and CD27 molecules [207], and disproportionately high levels of CD69 [211]. The $CD4^+$ T-cell memory subset of cells from elderly donors produces less IL-2 [207] but are not anergic as the cells can proliferate with IL-15 stimuli [212].

Animal models of $CD4^+$ T-lymphocyte responses to MCMV have shown the cells to be essential in controlling acute infection. A number of MHC-II restricted $CD4^+$ T-cell responses specific to MCMV have been mapped across the MCMV genome [213]. During the acute phase of infection, the MCMV-specific $CD4^+$ T-cells proliferate and accumulate in the spleen and lungs. The MCMV-specific $CD4^+$ T-cells were found to be polyfunctional producing proinflammatory cytokines such as IFNγ, TNFα and IL-2 [213] and regulatory cytokines such as IL-10 [214]. Furthermore, loss of the co-stimulatory ligands $B7.1^{-/-}$ and $B7.2^{-/-}$ impairs the expansion of MCMV-specific $CD4^+$ T lymphocytes implies a role strong role of the APC in priming MCMV specific $CD4^+$ responses [215].

The HCMV-specific $CD4^+$ T-lymphocyte response has been characterised with an accumulation of memory $CD4^+$ T-cells and the decline in naïve $CD4^+$ T-cells observed in the peripheral blood [214]. Moreover, in the C57BL/6 system a single MHC-II restricted $CD4^+$ T-

cell epitope encoded by the m09 ORF was undetectable during the first 20 days p.i. but accumulates to 0.2% of the entire $CD4^+$ T-cell response by day 50 and is maintained at that same relatively high frequency to day 100 during the latent infection [213]. The m09 ORF encodes for a non-essential glycoprotein and the inflationary $CD4^+$ T-cell kinetics most closely resembles those observed by $CD8^+$ T-cells towards the IE3 epitope in C57BL/6 mice.

1.8.3. B-LYMPHOCYTE RESPONSE

CMV infection creates a number of immunogenic antigens that B-lymphocytes target. From an early stage of lymphocyte development through to plasma cell maturation B-cells express the surface molecule CD19. Activation of the B-cell receptor (BCR) and CD19 by CMV antigen leads to the proliferation of the cell and the generation of highly specific immunoglobulins.

A number of epidemiological studies have highlighted a detrimental relationship between the magnitude of the HCMV-specific humoral response and survival in older populations [160, 216-219]. Data from the USA highlighted in an elderly population of Latino men those with the highest quartile of HCMV-specific IgG antibody titres had significantly elevated all-cause mortality (>1.4 times) over a 9-year period compared to those with lower three quartile titres of anti-HCMV IgG [218]. The IgG immunoglobulins have a short half-life ($t_{1/2}$ of 7-23 days) [220, 221] therefore, like the inflationary T-cell response, elevated antibody titres found in elderly HCMV seropositive individuals are most probably maintained by antigen re-exposure and subsequent B-cell proliferation (some studies have indicated a larger higher number of B-cells in PBMCs from elderly HCMV seropositive donors) [222].

The humoral immune response is best studied in animal models where B-cell deficient mice strains and adoptive therapy experiments have indicated the role of immunoglobulins in immune control of CMV. The transfer of hyper-immune serum, containing MCMV-specific immunoglobulins, into MCMV naïve C3H mice were found to be protective in over 90% of mice subsequently challenged with MCMV *Smith*. The hyper-immune serum resulted in low or absent viral titres during acute infection, but did not prevent MCMV establishing latent

infection as lytic virus was detected upon administration of anti-lymphocyte serum [223]. Likewise, the immunisation of newborn mice with immune serum reduced the immune pathology caused by MCMV infection [224]. Subsequently, immunoglobulins were confirmed to reduce virus titres in both the salivary glands and blood of infected C57BL/6 mice, whereas the serum of B-cell deficient mice was not protective [225, 226]. The higher the affinity of the anti-MCMV IgG the greater the degree of protection against MCMV challenge [227]. Adoptive transfer of MCMV-experienced B-lymphocytes into $RAG^{-/-}$ mice lead to efficient control of MCMV in the absence of T-cell mediated immunity [8].

1.8.1. NK-CELL MEDIATED RESPONSE

Natural killer cells (NK-cells) are a principal component of the innate immune system. The NK-cell primary function is to recognise and kill virally infected cells. The NK-cell lineage is derived from a common lymphoid progenitor and in humans expresses the molecules CD16 and CD56, and in C57BL/6 mice are identified by the expression of either the NK1.1 or NK1.2 antigens on the cells surface. NK-cells seek out virally infected cells by sensing a reduction in MHC-I molecules ("missing-self") and the upregulation of stress ligands, e.g. MHC class I polypeptide-related sequence A (MICA), on the surface of infected cells. A NK-cell deficiency [141, 228] or loss in NK-cell function [229, 230] has been associated with the increased incidence in HCMV disease.

MCMV models have highlighted a balance between the virus and the corresponding NK-cell response. A number of experiments have screened multiple mouse strains to determine their genetic susceptibility to a lethal dose of MCMV [231]. Beige mice are the most vulnerable to MCMV doses whereas the same dose delivered via the same route of infection into a C57BL/6 mouse was shown to be asymptomatic [232]. The genetic difference between strains of mice susceptibility towards lethal doses of MCMV was mapped to the *Cmv1* locus on chromosome 6. The *Cmv1* gene encodes for the NK-cell gene complex, an MHC-I like molecule, called the Ly49h activating receptor. Insertion of the Ly49h encoding gene into susceptible beige mice - which lack this gene - confers resistance to MCMV [10, 233, 234]. The Ly49h receptor is bound to the outer membrane of the NK-cell, however it lacks an intracellular signalling domain, therefore, it requires the recruitment of the ITAMs DAP12 and/or DAP10 [235-237]. The Ly49h-receptor on the NK-cell binds to the viral m157 protein,

an MHC-I like molecule, which activates and leads to the degranulation and release of cytotoxic granules such as perforin and granzyme, which work in combination to perforate the infected cell membrane and induce apoptosis (Figure 1.5). The Ly49h interaction with m157 occurs only in the mouse; however, interactions between Killer-cell Ig-like receptors (KIRs) on the NK-cells and HLA-C molecules have a similar effect with HCMV infection [238]. *Wt* isolates of MCMV often have acquired deletions or mutations in the m157 ORF causing the virus to evade the hosts NK-cell response [239]. The m157 gene has been retained by MCMV because of a secondary function: binding to the Ly49i receptor provides an inhibitory signal to the NK-cell [240].

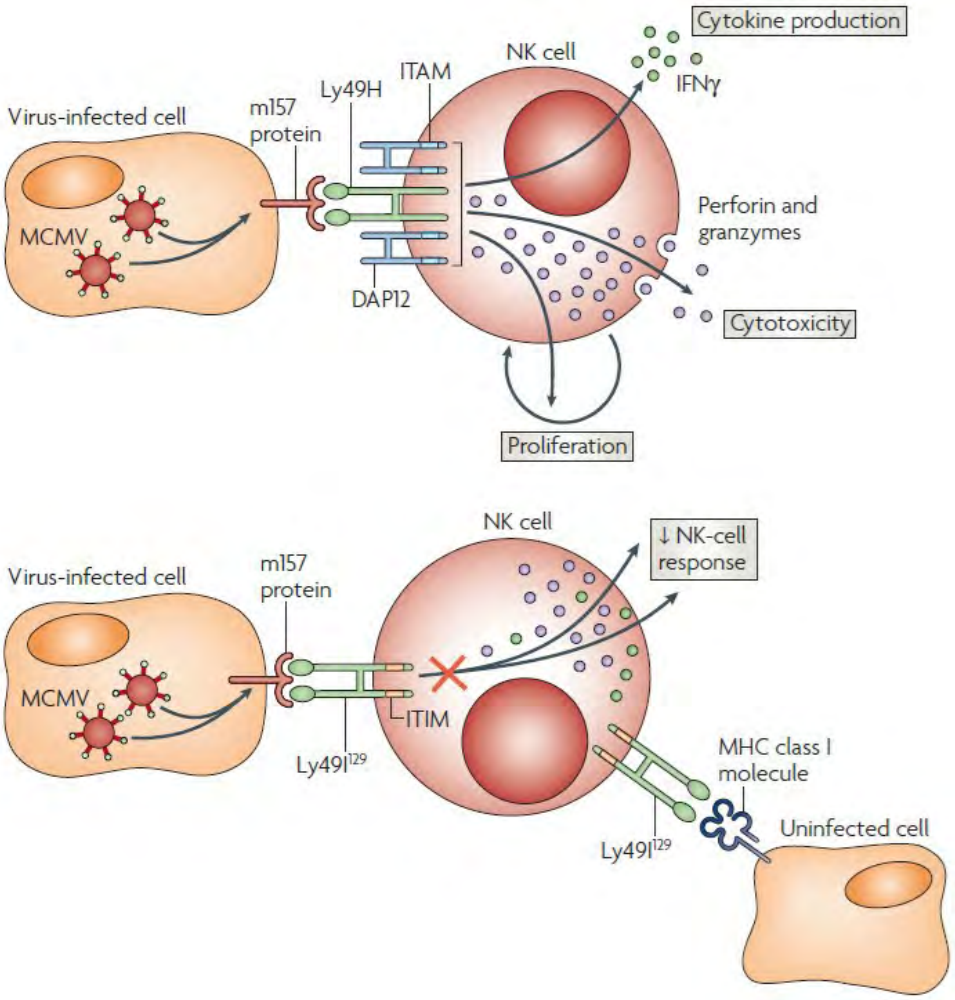

Figure 1.5 MCMV activation of NK-cells. Top) NK-cells from C57BL/6 mice express the DAP12-associated activating Ly49H receptor, which upon binding of the m157 protein initiates proliferation and cell-mediated cytotoxicity (perforin, granzyme and IFNγ) release from the NK-cells. Bottom) BALB/c mice do not express Ly49H and can express the inhibitory receptor (Ly49I) which upon binding m157 can impede the cytotoxic NK-cell response. Nature Reviews in Immunology [241]. Licence number 2864711358726.

1.9. IMMUNE EVASION MECHANISMS OF CMV

Viruses employ mechanisms to evade detection by the immune system. CMVs, due to their co-evolution alongside their host, have developed numerous mechanisms to avoid detection by the innate and adaptive immune system. The immune evasion molecules of CMV are primarily expressed during the E-phase of replication. The evasion molecules are described most frequently as “immunoevasins” [154], “viral proteins interfering with antigen presentation” [242], or “viral regulators of antigen presentation” [243].

During both MCMV and HCMV infection the APCs are a key target of both acute infection and latent HCMV can reside in myeloid cells [244, 245]. For CMVs to survive within an APC or any infected cell the virus makes use of techniques to reduce its exposure to both the innate and adaptive immune system (Table 1.1) [44, 243, 246].

Table 1.1. Adapted from Lemmermann *et al* (2011) [247]: Table includes a list of HCMV and MCMV immunoevasins genes and the mechanism that aids immune evasion.

Human Cytomegalovirus			
ORF	**Protein**	**Phase**	**Function**
US2	gp24	E	Targets MHC-I ER-associated degradation in the proteasome
US3	gp23	IE	Binds to tapasin preventing peptide loading – retains MHC I complexes in the ER
US6	gp21	E	Inhibits peptide translocation into the ER – blocking of TAP-mediated peptide transport into the ER
US10	gp21	E	Induces degradation of HLA-G
US11	gp33	E	Targets MHC-I for proteosomal degradation
UL82	pp71	L	Retains MHC-I in a pre-Golgi compartment
UL18	gpUL18	L	MHC class I homolog ***(NK-cell immunoevasin)***
UL142	gpUL142	L	Sequesters MICA ligands in Golgi ***(NK-cell immunoevasin)***
Murine Cytomegalovirus			
ORF	**Protein**	**Phase**	**Function**
m04	gp34	E	Blocks pMHC expression on the cells surface
m06	gp48	E	Redirects pMHC to lysosomes for degradation
m152	gp40	E	Retains pMHC in the ER–Golgi intermediate compartment

The m04 immunoevasin protein encoded by MCMV is abundant in the ER and binds to the pMHC-I complex whilst it is still located in the ER. The m04 evasin remains bound to the pMHC and translocates with the pMHC-I complex from the ER to the infected cells surface where it remains attached and preventing complementary TCR interactions and impedes T-cell activation [248, 249]. The m04 protein has a dual function in allowing the pMHC complex to translocate to the cell surface prevents NK-cell activation via the "missing-self" mechanism whilst also blocking pMHC presentation to the TCR.

The m06 immunoevasin protein binds to newly synthesised pMHC-I in the Golgi and combines with two cellular adapter proteins (AP-1A and AP-3A) before redirecting the complex for lysosomal degradation and hence the virally infected cell cannot be detected by the lymphocytes [250].

The m152 viral protein also strongly binds to the pMHC-I in the ER-Golgi compartment and prevents translocation of the complex to the cell surface [251]. More recently the m152 protein has also been shown to down-regulate the surface expression of the NK-cell activating ligand RAE-1 making this evasin help the virus to evade both $CD8^+$ T-cell and NK-cell mediated cytotoxicity [252].

HCMV also synthesises a number of its own MHC-I immunoevasin proteins. The US3 ORF encodes for a protein that binds to tapasin and prevents loading of peptide onto the MHC-I molecule [253]. Likewise US6 also functions through inhibiting peptide loading onto the MHC-I through preventing the translocation of peptide into the ER via inhibition of TAP [254-

256]. The UL82 evasin retains the MHC-I molecule within the pre-Golgi compartment thus preventing peptide loading [257]. Two HCMV evasion proteins target the MHC-I molecule for degradation. The US11 ORF encodes for gp33 protein that targets MHC-I for degradation in the ER [258]. The ORFs US2 and gp24 also target degradation of MHC-I [259].The US10 immunoevasin has a slightly different function in that regulates cell expression of the non-classical MHC molecule HLA-G [260].

The m155 ORF gene product of MCMV leads to evasion of Th1 $CD4^+$ T-cell responses through mediating expression of CD40 on APCs thus preventing $CD4^+$ T-cell activation/co-stimulation [261]. The UL18 and UL142 ORFs perform evasion of NK-mediated immunity. UL18 is a viral MHC-I homologue. The UL18 glycoprotein has α1 and α2 domains but lacks the α3 domain [262]; however this is sufficient to prevent NK-cell activation [263-266]. UL142 sequesters NK-cell activating ligands e.g. MICA and ULBP3 in the Golgi [155, 267-269].

1.10. INFLUENZA A AND IMMUNOSENESCENCE

1.10.1. INFLUENZA A PATHOGEN

Influenza A viruses (IAV) belong to the family of Orthomyxoviridae viruses and are broadly characterised into subtypes according to their haemagglutinin (HA) and neuraminidase (NA) components. There are currently 16 known serotypes of HA and nine NA serotypes [270]. Individual strains of influenza virus are first designated according to their antigenic type (A or B) based on the nucleoprotein antigen (NP), the host of origin (if not human), geographic origin, strain number, year of isolation and for IAV their HA and NA subtype, e.g. A/Beijing/262/95 (H1N1).

All IAV have a single stranded, segmented, negative sense RNA genome. The genome consists of eight segments and shares significant homology to Influenza B viruses whereas Influenza C viruses only have seven segments. The negative sense genome of IAV provides the template for the viruses own RNA-dependent RNA-polymerase to synthesise new messenger RNA (mRNA) and proteins.

1.10.2. EXPERIMENTAL MODELS OF INFLUENZA A

The IAV infection requires adsorption of the virus into the cell via attachment of the virus to specific cell surface receptors [271]. It has been known since the 1940s that the viral HA binds to sialic acid (SA) on the cell surface to mediate viral entry [272, 273]. SA is a negatively charged 9-carbon sugar that forms glycosidic bonds with galactose and is involved in normal cellular adhesion events but is exploited by IAV to gain entry into cells [274]. IAV discriminately bind to SA as they require specific sugar chains e.g. human IAV prefer to bind α2,6 residues whereas avian IAV adhere with α2,3 linkages on SA [275, 276]. Although the IAV have a preference, the viruses are capable of crossing species barriers and have therefore been modelled in many animal systems.

Apes are rarely used to model human IAV infection because many primate species do not share the same α2,6 SA linkages [274]. In contrast, pigs are more prone to Influenza infection and are a natural vehicle of genetic re-assortment of human pandemic IAV [277]. Pigs express both the α2,6 and α2,3 SA residues making them susceptible to human and avian Influenza viruses [278]. Ferrets are an excellent experimental model of infection because they are susceptible to human IAV strains, exhibit “flu-like” symptoms and transmit the virus via aerosol [279-281]. Mice are also routinely challenged with Influenza viruses [282]. The BALB/c mouse has α2,6 and α2,3 SA receptors on cells of the lung and trachea making them suitable models for studies of Influenza pathogenesis [283, 284]. The C57BL/6 mouse is also used to model IAV infection and many immune parameters of infection well documented [285, 286].

1.10.3. IMMUNE RESPONSES TO INFLUENZA A

IAVs are highly immunogenic pathogens and seasonal outbreaks contribute to ~500,000 deaths annually [287]. The 1918 Spanish IAV pandemic arose due to antigen shift and recent estimates suggests the outbreak resulted in 50 million deaths worldwide [288]. The more recent 2009 outbreak of Swine flu (H1N1) occurred due to triple re-assortment of avian, swine and human viruses and was fatal in almost 3% of individuals infected with the virus [289].

IAV infection primes the entire immune system. The immediate primary response which limits viral dissemination within the first 48 hours, is attributed to neutrophils [290], macrophages [291] and NK-cells [292] that occur prior to the development of the CTL response [293]. C57BL/6 mice generate a diverse number of IAV-specific $CD8^+$ T-cells to multiple IAV antigens, e.g. the nucleoprotein (H2-D^b restricted: $NP_{366–374}$) [294], viral polymerase (H2-D^b: $PA_{224–233}$) [295] and the polymerase subunit 1 (H2-K^b: $PB1_{703–711}$,) [296] which are well studied targets in murine models. The $CD8^+$ T-cell response to the $NP_{366–374}$ epitope can dominate the acute infection and can constitute up to 80% of the IAV-specific T-cells yet contract to form smaller memory pools that persist to provide rapid responses to antigen re-exposure/challenge [297, 298].

$CD4^+$ T-cells have both cytotoxic and regulatory roles during acute IAV infection. Upon Swine flu infection, $CD4^+$ T-cells induce production of a wide variety of cytokines [299]. *In vitro* re-stimulation of IAV-specific Th1 $CD4^+$ T-cells produce IL-2 that augments a more proficient cytotoxic response towards A/PR/8/34 (H1N1) infected cells. In contrast, co-culture of CTLs

with IL-4 secreting Th2 $CD4^+$ T-helper cells was shown to have an antagonistic effect on $CD8^+$ T-cell expansion [300]. *In vivo*, lymphocytes isolated from the mediastinal lymph node of C57BL/6 mice, inoculated with a nonfatal form of IAV, secreted IL-2, IL-10, and/or IFNγ. Peak cytotoxic $CD4^+$ T-cells levels can be observed around 7 days p.i. whereas levels of the regulatory IL-10 secreting cells remain more constant during the first week of infection [301].

The transfer of hyper-immune serum provides protection in naïve mice from IAV challenge [302]. Immunoglobulins directed towards the HA antigen appear within the first week of illness and continue to increase for a number of weeks. Anti-HA antibodies neutralise IAV infection by preventing the virus adhering to SA. Anti-HA immunoglobulin titres tend to correlate with protection of illness therefore IAV vaccine strategies attempt to generate robust antibody titres and cellular responses.

1.11. HCMV AS A FACTOR OF IMMUNOSENESCENCE

The term “Immunosenescence” refers to the decreased ability to mount an effective adaptive immune response to pathogens and vaccinations that occurs with an increase in age. This process occurs naturally because of thymic involution and exhaustion of existing immunity [303-305] (Figure 1.6). For example influenza vaccination is highly effective in younger adults with protective antibody responses are generated in 70–90% of individuals; however, the same vaccine may only be effective in 17–53% of the elderly [306]. Currently attempts to restore immune function in the elderly with sex steroid ablation, growth factor treatment and cytokine replenishment have had only limited success [307].

Epidemiological data has correlated with immunological parameters to show that the presence of HCMV infection exacerbates immune senescence in the elderly [148]. The OCTO (>80 years old) and NONA (>90 years old) studies concluded that a HCMV seropositivity results in an accumulation of high differentiated $CD8^+$ $CD27^-$ $CD28^-$ $CD56^+$ $CD57^+$ $CD45RA^+$ T-cells, an inversion of the CD4:CD8 T-cell ratio [216, 217]. The presence of underlying HCMV seropositivity has been estimated to equate to an additional 'ageing effect' of 35 years on the $CD8^+$ T-cell repertoire [308]. As a separate study the presence of HCMV-specific oligoclonal expansions was seen to result in reduced numbers of EBV-specific $CD8^+$ T-cells in the blood of healthy adults [146]. Therefore, HCMV seropositive individuals maybe more susceptible to infections caused by other pathogens as a result of reduced numbers of $CD8^+$ T-cells to infections other than HCMV. Consequently this may contribute to the significantly increased rates of mortality seen in epidemiological studies. Models of murine immune senescence showed pre-existing memory $CD8^+$ T-cells are susceptible to attrition following a

series of heterologous infections [201, 309] and therefore trying to accommodate the accumulation of MCMV-specific cells may come at the expense of generating heterologous memory populations.

The perception that the immune system is of a finite size and that the history of pathogen exposure can erode the ability to respond to infection is controversial because experimental evidence has also shown the adaptive immune system is capable of growing in size in response to repeated immunological challenge. Vezys *et al* (2009) utilised a prime-boost vaccination strategy to generate "enormous numbers of memory CD8 T cells specific for a single antigen" and subsequently monitored the number of pre-existing memory T-cells [310]. They noted an increased proliferation of $CD8^+$ T-cells, in particular the non-lymphoid T_{EM} subset within the lung, which did not develop at the expense of the initial memory pool.

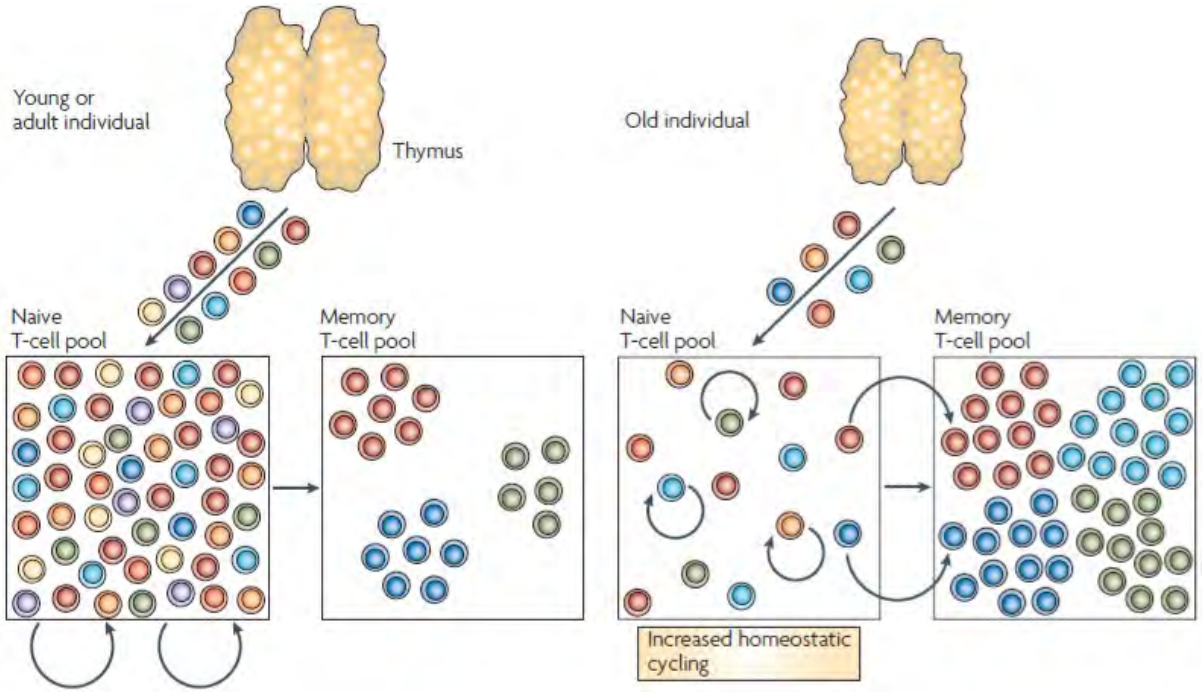

Figure 1.6. Image represents naïve lymphocyte synthesis from the thymus from young and older individuals. Each coloured cell represents a unique TCR and therefore antigen specificity. During advancing age, the thymic medulla is gradually replaced by adipose tissue and the shrinkage of the thymus contributes to fewer naïve T-cell precursors in older individuals. Homeostatic proliferation can partially maintain naïve T-cell frequencies however; this leads to a restricted TCR-diversity. Consequently, older individuals are less well equipped to mount an immune response to a new pathogen. Nature Reviews in Immunology [311]. Licence number 2864710364858.

1.12. HYPOTHESIS AND AIMS: MCMV REACTIVATION IS A LIKELY CAUSE OF MEMORY INFLATION; THEREFORE, ANTIVIRAL INTERVENTION MAY PROVIDE AN OPPORTUNITY TO IMPROVE IMMUNE FUNCTION.

Oligoclonal HCMV-specific $CD8^+$ T-lymphocyte expansions towards immunodominant viral epitopes are readily detectable in the peripheral blood and accumulate with age [146, 147]. Likewise, memory inflation is characterised following MCMV infection [161, 165]. Both the inflationary HCMV [312] and MCMV [165] subsets of virus-specific $CD8^+$ T-lymphocytes are relatively short-lived therefore their ability to accumulate is paradoxical. The accumulation of CMV-specific $CD8^+$ T-lymphocytes occurs when viral titres are undetectable and therefore the large immune response is contrary to our understanding of how memory T-cells are maintained during a latent infection.

The first aim of this thesis is to establish an MCMV model of memory inflation. Once this system is verified I will go on to determine the extent at which MCMV reactivation, during the latent phase of infection, has in maintaining the high frequency of virus-specific $CD8^+$ T-cells. In order to examine if lytic replication is required for memory inflation MCMV infected mice will be administered the antiviral valaciclovir (for up to one year) to block stochastic lytic reactivation. Then the magnitude of the $CD8^+$ T-cell response will be compared to untreated mice using a combination of peptide stimulation followed by measurement of intracellular IFN-γ production and also MHC-I tetramer staining. In addition, mice will be

infected with a mutant MCMV strain to examine whether a replication defective virus is capable of causing memory inflation.

The second aim of this thesis is to examine whether a prior history of MCMV exposure affects the generation of a primary immune response to IAV challenge in an elderly population of animals. Furthermore, mice with latent MCMV infection will be administered valaciclovir and again challenged with IAV to asses if antiviral treatment can improve immune function compared mice with untreated memory inflation.

2. MATERIALS & METHODS

2.1. LIST OF MATERIALS

- 10% SDS solution, BIORAD
- 2-(*N*-morpholino)ethanesulfonic acid (MES), Sigma
- 3,3,5,5-tetramethylbenzidine substrate (TMB), Sigma
- 39% formaldehyde, Sigma
- 3-Amino-9-ethylcarbazole (AEC) tablet, Sigma
- Acetic acid, Sigma
- Acrylamide, Sigma
- Aciclovir, Sigma
- Adenosine-5'-triphosphate (ATP), Sigma),
- Ammonium persulphate (APS), Sigma
- Ampicillin, Invitrogen
- Atipamezole, Tocris Bioscience
- Bovine serum albumin (BSA), Sigma
- Brefeldin A, Invitrogen
- Calcium chloride, Sigma
- Carboxymethylcellulose (CMC), Sigma
- Chloramphenicol, Sigma
- Coomassie brilliant blue, Sigma
- Crystal violet, Sigma
- d-Biotin Sigma

- Dimethyl sulfoxide (DMSO), Sigma

- Dithiothreitol (DTT), Sigma
- Dulbecco's modified essential media (DMEM), Sigma
- Ethylenediaminetetraacetic acid (EDTA), Sigma
- Extravidin peroxidise, Sigma
- Foetal calf serum (FCS), Sigma
- Gelatine, Sigma
- Glucose, Sigma
- Glycerol, Sigma
- Heparin sodium (1000 I.U/ml), Wockhardt,
- Hydrochloric acid, Sigma
- Hydrogen peroxide, Sigma
- Insulin-transferring-selenium, Sigma
- Ionomycin calcium salt, Sigma
- Iscove's modified Dulbecco's medium (IMDM), Sigma
- Isopropyl-beta-D-thiogalactoside (IPTG), Invitrogen
- Ketamine hydrochloride, Tocris Bioscience
- L-arginine, Sigma
- LB agar, Sigma •

LB broth, Sigma •

Leupeptin, Sigma

- L-glutamine, Sigma
- Manganese chloride, Sigma

- Medetomidine hydrochloride, Tocris Bioscience
- Methanol, Sigma
- Mouse serum, Sigma
- N,N-dimethylformamide (DMF), Sigma
- Nucleoprotein monoclonal antibody (MCA400), Serotec
- Oxidised glutathione, Sigma
- Paraformaldehyde, Sigma
- Penicillin-streptomycin, Sigma
- Pepstatin , Sigma
- Phenol red, Sigma
- Phenylmethanesulfonylfluoride (PMSF), Sigma
- Phorbol 12-myristate 13 acetate (PMA), Sigma
- Phosphate buffered saline (PBS)
- Potassium acetate, Sigma
- Potassium bicarbonate
- Potassium chloride, Sigma
- Primatone, Sigma
- Reduced glutathione, Sigma
- RMPI-1640 media, Sigma
- Saline, Invitrogen
- Saponin, Sigma

- S.O.C. medium, Invitrogen

- Secondary anti-mouse IgG (H+L) HRP conjugated antibody, Promega
- Sodium acetate, Sigma
- Sodium azide, Sigma
- Sodium bicarbonate, Sigma
- Sodium carbonate, Sigma
- Sodium chloride, Sigma
- Sodium dodecyl sulphate (SDS), Sigma
- Sodium MOPS, Sigma
- Streptavidin-APC, Invitrogen
- Tetramethylethylenediamine (TEMED), Sigma
- Tris, Sigma
- Triton X-100, Sigma
- Trypan blue, Sigma
- Tween, Sigma
- Urea, Sigma
- Valacyclovir hydrochloride, GlaxoSmithKline
- β-meracaptoethanol, Sigma

2.2. LIST OF BUFFERS

- 0.3% crystal violet solution: 0.3% (w/v) crystal violet dissolved in 10% (v/v) methanol in H_2O
- 0.5% (w/v) saponin: diluted in PBS
- 15% running gel: 115 ml H_2O, 125 ml 1 M Tris pH 8.8, 5 ml 10% SDS; mixed with 5 ml of 30% acrylamide, 160 µl of 10% APS and 6 µl of TEMED
- 4% (v/v) formaldehyde: 39% formaldehyde diluted in PBS
- 4% (w/v) paraformaldehyde: diluted in PBS
- Antisedan: 2 ml atipamezole, 8 ml saline
- BIORAD solution: 1 part 10% SDS solution to 4 parts H_2O
- Bir A buffer: 100 mM Tris, 20 mM sodium chloride, 5 mM magnesium chloride, 0.1 mM PMSF
- Carboxymethylcellulose overlay (CMC overlay): one part 5% CMC, two parts MM
- Coomassie brilliant blue stain
- D10 media (500 ml DMEM, 10% (v/v) FCS, 1% v/v penicillin-streptomycin, 1% v/v L-glutamine, 1% v/v sodium pyruvate, 1% v/v sodium bicarbonate
- Destain buffer: 10% acetic acid, 50% methanol
- ELISA coating buffer: 0.2 M sodium bicarbonate, 0.2 M sodium carbonate
- ELISA dilution buffer: 1% (w/v) BSA, 0.05% (v/v) Tween20, PBS
- ELISA wash buffer: 0.05% (v/v) Tween20, PBS
- F-media: 140 mM sodium chloride, 8 mM potassium chloride, 7 mM calcium chloride, 0.5 mM magnesium chloride, 1.7 mM glucose, 0.3 mM chloramphenicol, 0.25 mM

phenol red and 2 g gelatine

- Growth media (GM): DMEM, penicillin-streptomycin, L-glutamine, 10% (v/v) FCS
- IMDM media: 500ml Iscove's modified Dulbecco's medium, 1.5 ml 10% (w/v) primatone. 2.5 ml FCS, 0.5 ml insulin-transferring-selenium, 5 ml penicillin-streptomycin, 0.5 ml 25 µM β-meracaptoethanol
- Lavage buffer: 50 ml PBS and 50 µl EDTA
- LB agar: 1.5% (w/v) in distilled H_2O
- LB media: 2% LB broth (w/v) in distilled H_2O
- MACS buffer: PBS and 1% BSA
- Maintenance media (MM): DMEM, penicillin-streptomycin, L-glutamine, 2% (v/v) FCS
- MonoQ buffer A: 20 mM Tris
- MonoQ buffer B: 20 mM Tris, 500 mM sodium chloride
- Red-cell lysis buffer: 800 ml H_20, 89.9 g ammonium chloride, 10.0 g potassium bicarbonate, 370.0 mg tetrasodium EDTA, pH 7.3
- Refolding buffer: 100 mM Tris, 400 mM L-arginine, 2 mM EDTA, 5 mM reduced glutathione, 0.5 mM oxidised glutathione, 0.1 mM PMSF
- Resuspension buffer: 50 mM Tris, 100 mM sodium chloride, 1 mM EDTA, 1 mM DTT
- Sedative solution:0.5 ml medetomidine, 0.38 ml ketamine 4.12 ml H_2O
- S75 buffer: 20 mM Tris and 50 mM sodium chloride
- Stacking gel: 136 ml H_2O, 23 ml 1 M Tris pH 6.8, 2 ml SDS was mixed with 670 µl of 30% acrylamide and 60 µl of 10% APS and 6 µl of TEMED
- TFB1 buffer: 30 mM potassium acetate, 100 mM potassium chloride, 10 mM calcium

chloride, 50 mM manganese chloride, 15% v/v glycerol, pH 5.8

- TFB2 buffer: 10 mM sodium MOPS, 25 mM calcium chloride, 10 mM potassium chloride, 15% v/v glycerol, pH 6.5
- Triton wash: 50 mM Tris, 100 mM sodium chloride, 0.5% Triton X-100, 1 mM EDTA, 1 mM DTT, 0.1% sodium azide
- Tween buffer: 0.05% v/v Tween in H_2O
- Urea solubilisation buffer: 8 M Urea, 50 mM MES, 0.1 mM EDTA, 0.1 mM DTT
- Valacyclovir antiviral: 500 mg valaciclovir tablet crushed and diluted in 500 ml distilled H_2O

Table 2.1. List of the fluorescent conjugated anti-mouse antibodies used in subsequent tetramer and ICS staining experiments.

Anti-mouse lymphocyte surface antibodies			
Target Antigen	**Clone**	**Fluorochrome**	**Company**
CD3	500A2	FITC	eBioscience
CD4	GK1.5, L3T4	AF-700	eBioscience
CD4	GK1.5, L3T4	PE	eBioscience
CD8	Ly-2, 53-6.7	Pacific Blue	eBioscience
CD8	Ly-2, 53-6.7	APC	eBioscience
CD27	LG.3A10	PerCp/Cy5.5	BioLegend
CD44	IM7, Ly-24	APC-Cy7	eBioscience
CD62L	Ly-22, MEL-14	PE-Cy7	eBioscience
CD122	TM-b1	FITC	eBioscience
CD127	A7R34	PE	eBioscience
Anti-mouse intracellular antibodies			
Target Cytokine	**Clone**	**Fluorochrome**	**Company**
IFNγ	XMG1.2	FITC	eBioscience
TNFα	MP6-XT22	PE	eBioscience

2.3. MCMV CULTURE

2.3.1. MOUSE EMBRYO FIBROBLASTS

Mouse embryo fibroblasts (MEFs) are the most widely used permissive cell type for propagating MCMV and for accurate titration of the number of lytic virus particles in a given volume. To generate MEFs female BALB/c mice were mated to generate pregnancy. At embryonic day 14, the pregnant mice were euthanised by cervical dislocation, pinned onto a dissection board and sprayed with 70% ethanol. Under aseptic conditions, within a laminar flow cabinet, an incision was made dissecting the lower abdomen exposing the uterine horn and embryos. The embryonic sacs were removed and placed into a Petri dish containing sterile PBS. Any placental or uterine horn tissue was discarded and the embryos transferred into a second Petri dish containing fresh PBS.

The embryos were placed into the barrel of a 20 ml syringe, and homogenised by returning the plunger, dissociating the embryo into 10 ml TE. The homogenate was then incubated at 37 °C, 95% air/5% CO_2 for a maximum of 10 minutes.

The homogenate was then passed through a fine metal sieve into a Petri dish containing 2 ml of FCS. The sieving removes large cellular debris but ensures the passage of fibroblast cells.

The MEF homogenate was transferred into a falcon tube containing 10 ml of GM and centrifuged at 720 g for 10 minutes at room temperature (RT). The supernatant was

aspirated; the pellet resuspended in 10 ml of GM and used to seed 150 cm^2 tissue culture flasks with, on average, one embryo seeding up to three 150 cm^2 flasks.

The MEF suspension was then incubated (37 °C, 95% air/ 5% CO_2) until a confluent monolayer of cells was formed (approximately one week). At which point it is essential to passage the cells to prevent cell death, maintain cell viability and increase MEF cell numbers for further assays.

2.3.2. PASSAGE OF MEF CELLS

Upon the MEFs reaching confluence the spent growth medium was discarded, and the monolayer was washed with 10 ml of sterile PBS to remove trypsin inhibitors in the serum. The PBS rinse was then discarded and 3 ml of TE added to the flask. After approximately three minutes, the cells start to detach from the flask and at this point serum-containing GM was added to inhibit the trypsin-reaction. The medium was then agitated to dislodge the monolayer and create a MEF suspension.

The MEF suspension was spun at 700 g for 10 minutes at RT to create a cell pellet and the supernatant removed. The MEF cell pellet was then resuspended in MM and transferred to the appropriate sized culture flask or enumerated.

2.3.3. TRYPAN BLUE CELL COUNTING

To check cell viability and enumerate the numbers MEFs/lymphocytes, 20 µl of cell suspension was diluted 1:1 with 0.4% trypan blue stain and loaded onto a counting chamber of a Neubauer haemocytometer (FastRead Counting Slides, Immune Systems). The number of viable cells (the intact membrane excludes the blue dye whereas dead cells are stained blue) were counted in four 1 mm^2 squares; this was repeated a further four times and an average calculated. To determine the concentration of the cells per ml the following formula was used:

$$c = [(n/4)*2]*10^4$$

Where c = concentration (cells/ml)

n = average number of cells per 1 mm^2

2.4. MCMV VIRUS STRAINS

2.4.1. MCMV *SMITH*

The *Smith* strain of MCMV (ATCC) was obtained from Dr C. Sweet (School of Biosciences, University of Birmingham, UK). A working stock of *Smith* was propagated using MEFs and an infectious stock of less frequently cultured virus was used for *in vivo* inoculations.

2.4.2. MCMV *tsm5*

The temperature-sensitive mutant virus 5 (*tsm5*) was generated in the laboratory of Dr C. Sweet by N-methyl-N'-nitro-N-nitrosoguanidine mutagenesis of the *K181-Birmingham* strain. The *tsm5* virus has restricted growth at temperatures exceeding 39 °C in MEFs and at 37 °C in macrophages and does not produce detectable infectious virus *in vivo* [313-315]. Working stocks of *tsm5* were propagated *in vitro* using MEF cells.

2.4.3. MCMV PROPAGATION AND HARVESTING

MEFs were seeded into 150 cm^2 tissue culture flasks, containing 25 ml of GM, and incubated (37 °C, 95% air/ 5% CO_2) until 80-90% confluent. The GM was then replaced and 200 µl of working stock virus (either *Smith* or *tsm5*) was added along with 5 ml of MM. The flasks were returned to the incubator for one hour, before a further 15 ml of MM was added. The flasks were then incubated (37 °C, 95% air/ 5% CO_2) until the MEF monolayer showed 100% CPE. The supernatant from the MCMV infected flasks was harvested and transferred to a

centrifuge tube. This was centrifuged at 850 g for 10 minutes at RT to sediment the MEF debris.

The supernatant was aspirated, transferred into a sterile high-speed centrifuge tube (NALGENE) for ultracentrifugation at 29,000 g for 30 minutes (4 °C) to sediment the virus. The supernatant was discarded and the viral pellet resuspended in 8 ml of MM. The viral stock was then divided into 1 ml aliquots and immediately frozen at -80 °C.

2.4.1. MCMV TITRATION BY PLAQUE ASSAY

MCMV infected MEFs are killed by the replicating virus, the dead cells detach from the monolayer leaving behind a visible plaque. The addition of the CMC overlay provides an impermeable barrier that traps and prevents the released viruses killing non-adjacent cells.

MEF cells from the second passage of cell culture were enumerated using the trypan blue method. The concentration of cells was adjusted with GM to $1x10^6$ cells/ml. A volume of 0.5 ml MEF suspension was seeded into individual wells of flat-bottomed 24-well plates (Corning), for 24 hours (37 °C, 95% air/ 5% CO_2) until approximately 80-90% confluent.

Titration of MCMV stocks was performed in triplicate using separate aliquots of virus. Viral stocks were serially diluted in MM (1:10) across a dilution range ($x10^{-1}$ to $x10^{-5}$) (Figure 2.1).

The media in the wells was replaced with 200 µl of the appropriate viral dilution and the plates returned to the incubator for one hour. After one hour 1 ml of semi-solid CMC overlay was added to each well and the plates returned to the incubator for five days.

To visualise the MCMV plaques 0.5 ml of 4% formaldehyde fixative was added to each well for 10 minutes. The overlay fixative was then removed and replaced with a further 0.5 ml of 4% fixative for 30 minutes, followed by 0.5 ml of 0.3% crystal violet staining solution. The stain was left for one hour before gently washing the wells with running tap water. Plates were allowed to air dry and plaques counted using a light microscope.

	1	**2**	**3**	**4**	**5**	**6**
A	Uninfected	1×10^{-1}	1×10^{-2}	1×10^{-3}	1×10^{-4}	1×10^{-5}
B	Uninfected	1×10^{-1}	1×10^{-2}	1×10^{-3}	1×10^{-4}	1×10^{-5}
C	Uninfected	1×10^{-1}	1×10^{-2}	1×10^{-3}	1×10^{-4}	1×10^{-5}
D	Uninfected	1×10^{-1}	1×10^{-2}	1×10^{-3}	1×10^{-4}	1×10^{-5}
E	Uninfected	1×10^{-1}	1×10^{-2}	1×10^{-3}	1×10^{-4}	1×10^{-5}
F	Uninfected	1×10^{-1}	1×10^{-2}	1×10^{-3}	1×10^{-4}	1×10^{-5}

Figure 2.1. Plate scheme showing the titration of MCMV on MEF. Row 1 uninfected fibroblasts. Row 2 virus dilution of 1×10^{-1}. Row 3: 1×10^{-2}. Row 4: 1×10^{-3}. Row 5: 1×10^{-4}. Row 6: 1×10^{-5}.

To calculate the number of average plaque forming units (PFU) the number of plaques per well was counted from a suitable dilution range. The average number of plaques was corrected for the dilution factor to quantify the MCMV titre as $\log_{10}$ PFU/ml.

2.5. INFLUENZA A VIRUS

2.5.1. INFLUENZA A VIRUS

The IAV strain A/PuertoRico/8/34-A/England/939/69 (H3N2) clone 7a was previously generated in the laboratory of Dr C. Sweet through re-assortment of A/Puerto Rico/8/34 (H1N1) and the A/England/939/69 (H3N2) strains.

2.5.2. INFLUENZA A VIRUS CULTURE

Twenty-four fertilised white hens' eggs were placed into a specialised Marshall Egg incubator (37 °C) in a humid atmosphere.

After 10 days, a light source was used to "torch" the eggs making visible the position of the air sac, embryo and its vasculature. Marks were made indicating the air sac and a suitable position over the allantoic cavity. Using a blunted needle the shell was weakened at the marks before two punctures were made in the shell, first over the air sac followed by one over the allantoic cavity.

An aliquot containing the IAV clone 7a was removed from -80 °C and diluted in approximately 10 ml RMPI-1640.

200 µl of the dilute virus was injected into the allantoic cavity of each egg. The needle was placed parallel to the shell to prevent piercing the yolk sac. The holes in the shell were then repaired using melted wax to make an airtight repair.

The influenza-infected eggs were then returned to incubator for a further three days to encourage IAV replication. On the fourth day, the eggs were placed at 4 °C overnight as a humane method of killing the embryo.

The following day the shell over the air sac was carefully removed using scissors ensuring the chorioallantoic membrane remained intact. Then using sterilised pipettes, the chorioallantoic membrane was broken and the allantoic fluid was removed from each egg (approximately 5-8 ml/egg) and pooled. The IAV stock was then divided into 1 ml aliquots and frozen at -80 °C.

One aliquot was immediately used to confirm that IAV was successfully propagated in the eggs by haemagglutination assay.

2.5.3. HAEMAGGLUTINATION ASSAY

Whole blood (6 ml) was isolated from a healthy human donor and centrifuged at 700 g for 10 minutes at RT. The supernatant and white cell layers were removed and discarded using a Pasteur pipette and the erythrocytes washed in dilute F-media. The centrifugation and wash step was repeated until the supernatant appeared clear. The red blood cells were then diluted in F medium to create a 1% w/v suspension.

Into each well of a W.H.O plate 200 µl of F-media was added. A serial two-fold dilution series of IAV stock was performed in F-media by adding 200 µl of virus to the first well, mixing and transferring 200 µl to the next well. This was repeated along the row. 200 µl of the red blood suspension was then added to each well. Plates were incubated for 30-45 minutes at RT. The presence of the IAV binds to the SA on the erythrocytes, causes haemagglutination, and prevents the cells from sedimenting in the well.

2.5.4. TITRATION OF INFLUENZA A VIRAL STOCKS

To calculate the IAV titre 78 fertilised white hens' eggs were placed into the Marshall Egg incubator for 10 days at 37 °C. As before, the eggs were "torched" and the shell pierced in the air sac and allantoic cavity.

Two aliquots of the IAV were defrosted from -80 °C and diluted (1:10) to the highest dilution factor of 1 $x10^{-9}$ in RMPI-1640 containing antibiotics. Three series of viral dilutions were created, two from aliquot A (A_1 and A_2) to compare the variability within the same aliquot and one from aliquot B to compare the difference in titre between individual aliquots of IAV.

As before 200 µl of each virus dilution was injected into the allantoic cavity of each of four eggs per dilution and the holes were sealed with melted wax. The infected eggs were then returned to the incubator and after three days incubation the eggs were placed at 4 °C overnight.

To determine the IAV dose needed to infect 50% of eggs (EID_{50}), 200 µl of the allantoic fluid from each egg was placed into an individual well of a WHO plate. 200 µl of red blood cell suspension was added and incubated for 30 minutes at RT. Each well was scored for the presence or absence of haemagglutination. This score was then applied to Weil's Table to determine the IAV titre.

2.5.5. MOVING AVERAGES AND WEIL'S TABLES

To calculate the EID_{50}/ml of clone 7a the following formula was used:

$Log_{10}\ EID_{50}$ = log *do + log R ** (f+1)

* do = highest dilution used for the derivation of "f" in Weil's Tables

**R = dilution factor

Table 2.2. The R and f-values for each aliquot taken from Weil's Tables.

Ampoule	Highest Dilution	R-values	f-value
A_1	$x10^{-8}$	0, 1, 3, 4	0.500
A_2	$x10^{-9}$	0, 0, 2, 4	1.000
B	$x10^{-8}$	0, 1, 2, 4	0.750

Where **R = dilution factor, therefore log R is 1

Ampoule A_1

Log_{10} EID_{50} = log *do + log R ** (f+1)

Log_{10} EID_{50} = -8 + 1 (0.500+1)

Log_{10} EID_{50} = -8 + 1.5

Log_{10} EID_{50} = -6.5

This is an estimate of the dilution of virus needed to infect 50% of the eggs. The reciprocal of this number is the infectious dose per unit volume.

Infectious dose = 1 $x10^{6.5}$ EID_{50}/ 0.2ml

Infectious dose = **$\underline{1x\ 10^{7.2}}$** EID_{50}/ml

Ampoule A_2

Log_{10} EID_{50} = -9 + 1 (1.000+1)

Log_{10} EID_{50} = -9 + 2

Log_{10} EID_{50} = -7

Infectious dose = 1 $x10^{7}$ EID_{50}/ 0.2ml

Infectious dose = **$\underline{1\ x10^{7.7}}$** EID_{50}/ml

Ampoule B

Log_{10} EID_{50} = -8 + 1 (0.750+1)

Log_{10} EID_{50} = -8 + 1.75

Log_{10} EID_{50} = -6.25

Infectious dose EID_{50} = 1 $x10^{6.25}$ EID_{50}/ 0.2ml

Infectious dose EID_{50} = **$\underline{1\ x10^{6.95}}$** EID_{50}/ml

The geometric mean titre was then calculated to allow a calculation for the amount required to infect the mice.

Mean Titre = (EID_{50} A_1 + EID_{50} A_2 + EID_{50} B) / n

Mean Titre = (7.199 + 7.699 + 6.949) / 3

Geometric Mean Titre = **$\underline{1\ x10^{7.28}}$** EID_{50}/ml

The antilog (7.282) is $1.92x10^7$

Therefore, **$1x10^6$** EID_{50} is present in **52.2µl**

2.6. MICRO-PLAQUE REDUCTION ASSAY

The method for the micro-plaque reduction assay (µPRA) was modified from a similar method used previously by Pavic *et al* (1997) [316] and Kruppenbacher *et al* (2001) [317]. In those assays, the degree of CPE, caused by HSV-1 in the presence of acycloguanosine prodrugs, was scored subjectively to estimate the percentage viability/CPE. This µPRA determined the actual number of plaques formed in the presence/absence of drug and is therefore quantitative.

Aciclovir was dissolved in DMSO at 7 mg/ml. Valaciclovir hydrochloride was prepared by grinding a 500 mg tablet in a pestle and mortar with PBS and filter sterilised through a 0.2 µm syringe filter (Millipore).

Primary MEFs were isolated from 14 day pregnant BALB/c mice, cultured, and enumerated as described previously. MEF cells from a second passage were adjusted to $5x10^5$ cells/ml and 100 µl added per well (flat bottomed 96 well plates) to create a cell density of $5x10^4$ cells per well.

50 µl of the appropriate concentration of aciclovir (plate 1) or valaciclovir (plate 2) was added to create a dilution series with final antiviral concentrations ranging from 0 to 125 µM. Finally, 50 µl of MCMV *Smith* was added to all wells at an MOI≈0.01. Also included were a DMSO control and uninfected wells.

Plates were incubated for four days (37 °C, 95% air/ 5% CO_2) during which infected cells die to form plaques.

Following the four day incubation, the plates were removed from the incubator and 50 µl of 4% fixative was added to each well. The plate was incubated for 10 minutes at RT to fix the cell membrane. The fixative and media was then flicked off into bleach. A further 100 µl of fixative added for 30 minutes prior to staining. 0.5 ml of 0.3% crystal violet staining solution was then applied for one hour before gently washing under running water. Plates were allowed to air dry.

The number of plaques was then counted at x10 magnification using a light microscope. The mean number of plaques per well was then calculated (n=8). This figure was then normalised to the highest number of plaques observed in the absence of aciclovir or valaciclovir.

2.7. TETRAMER SYNTHESIS

2.7.1. GENERATION OF COMPETENT *E. COLI*

A stock of *Escherichia coli* (*E. coli*) strain BL21 (DE3)pLys was briefly thawed from -80 °C. Using a wire loop a small volume was streaked onto an agar plate (2% LB broth and 1.5% LB agar). This plate was incubated at 37 °C overnight and a single colony was used to inoculate 5 ml of LB media that was placed into a 37 °C shaking incubator and monitored until the bacterial culture had grown to the optical density ($OD_{550\ nm}$) of 0.5. The 5 ml culture was then centrifuged at 2,000 g for 15 minutes at 4 °C. The supernatant was decanted and the pellet resuspended in 80 ml of cold TFB1 buffer. The TFB1 culture was then centrifuged at 4000 g for 10 minutes at 4 °C and the pellet resuspended in 8 ml of cold TFB2 buffer. The *E. coli* culture was then divided into pre-chilled eppendorfs and snap frozen in liquid nitrogen. These BL21 are now artificially competent and are able to take up extracellular DNA from the environment.

2.7.2. MHC-I AND B2M PLASMIDS

The pET-24a plasmid encodes an antibiotic resistance gene in addition to a *Lac* operon sequence. The *Lac* operon can be selectively activated to induce protein expression with the addition of IPTG (Invitrogen). In three separate plasmids, the murine MHC-I proteins H2-D^b and H2-K^b and human β2-microglobulin (β2M) were cloned downstream of the IPTG response element. The H2-D^b and H2-K^b plasmids were obtained as a gift from Prof P. Klenerman and Dr A. Gallimore.

2.7.3. TRANSFORMATION OF BL21 WITH PLASMID DNA

An aliquot of competent BL21 *E. coli* was defrosted on ice. 2 µl of the appropriate plasmid DNA (H2-D^b, H2-K^b or β2M) was added to the BL21 cells and incubated on ice for one hour, after which the BL21 cells were subjected to heat shock: 42 °C for 45 seconds followed by 4 °C for one minute. The process of subjecting the bacteria to the cycling of temperatures between hot and cold encourages the uptake of the plasmid DNA into the bacteria. In addition, 200 µl of S.O.C. medium was then added. The transformed BL21 were then placed into the orbital shaker, and incubated at 37 °C for one hour, to expand the cultures. The culture was then spread evenly onto an agar plate containing the antibiotic ampicillin. Only successfully transformed bacteria that express the gene for antibiotic resistance would grow when incubated overnight at 37 °C.

2.7.4. EXPRESSION OF MHC-I/B2M

The growth of bacterial colonies in the presence of the antibiotic agar is evidence of a successful transformation procedure. A single transformed BL21 colony was then selected using a wire loop to inoculate 25 ml LB media containing 1 mg/ml ampicillin and incubated overnight at 37 °C in the orbital shaker to generate a small subculture.

The following day 5 ml of the overnight subculture was used to inoculate a larger one litre conical flask containing LB media and ampicillin. The large culture was then incubated in an orbital shaker at 37 °C until the $OD_{600\ nm}$ reached 0.4-0.5; at this point protein expression was induced by adding 0.5 ml of 1 M IPTG and incubated for a further four hours. The addition of

IPTG activates the *Lac* operon, enabling transcription of the cloned MHC-I/β2M genes and subsequent translation into the required protein. The cultures were then divided into plastic containers designed to be centrifuged at high-speeds. The cells were then harvested by ultra-centrifugation at 18,000 g for 15 minutes at 4 °C. The supernatant was discarded and the transformed bacteria resuspended in 40 ml cold PBS. The MHC-I heavy chain or β2M proteins remain suspended in inclusion bodies within the *E. coli*.

2.7.5. PURIFICATION FROM INCLUSION BODIES

Sonication is required to isolate and purify the inclusion bodies from bacteria. The bacterial suspension was transferred into a glass beaker and placed on ice. The cold suspension is placed under the flat probe of the sonicator (Qsonica Q500) and pulsed five times for 45 seconds, with a 15 second gap in between pulses to prevent the solution overheating.

The solution was transferred to an ultracentrifugation tube and spun at 18,000 g for 15 minutes at 4 °C. The supernatant was discarded and the pellet resuspended in 6 ml of Triton wash. The suspension was transferred into a mechanical glass homogeniser and used to break open the bacterial membrane. The suspension was transferred back into an ultracentrifugation tube and spun again at 18,000 g for 15 minutes at 4 °C The homogenisation process was repeated two more times with Triton wash and twice with 4 ml of resuspension buffer.

The protein suspension was pelleted, the resuspension buffer discarded and the pellet resuspended into 10 ml of Urea solubilisation buffer. The protein was incubated at 4 °C overnight on an orbital shaker to encourage solubilisation. The following morning the solution was again pelleted using the ultracentrifuge, spun for 15 minutes at 18,000 g at 4 °C, to sediment the insoluble material. The supernatant contains the solubilised MHC-I/β2M that was then transferred into aliquots and frozen at -80 °C.

To check for successful protein expression and the purity of the expressed proteins an SDS-page was performed (Figure 2.2).

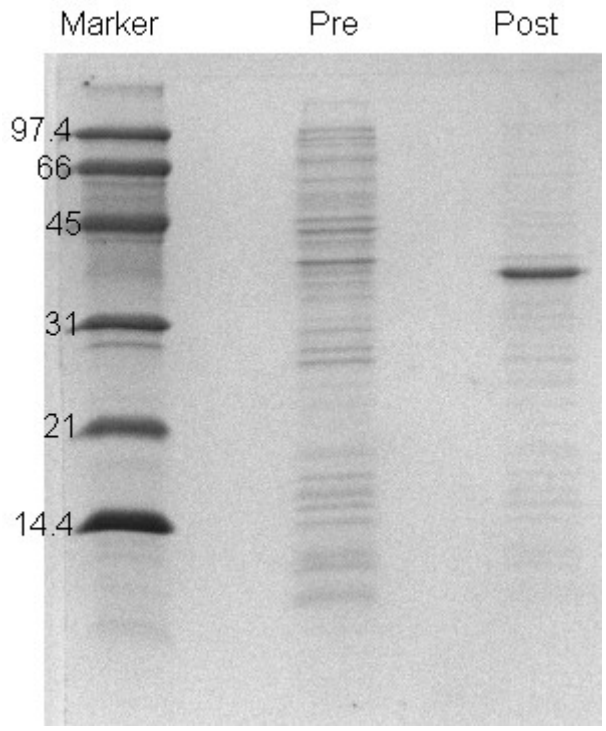

Figure 2.2. SDS page expression of H2-K^{b} protein from *E. coli* inclusion bodies. Synthesised by *E. coli* pre-IPTG induction (middle lane), post-IPTG induction, and urea solubilisation (right lane).

2.7.6. REFOLDING OF MHC-I WITH MCMV CD8$^+$ T-CELL PEPTIDES

To create a refolded MHC-I monomer, 500 ml refolding buffer was chilled to 4-8 °C and stirred constantly with a magnetic stirrer. Into each individual refolding buffer, 1 mg of MCMV peptide was added (Table 2.3).

Table 2.3. Immunogenic MCMV viral epitopes used for tetramer synthesis.

Protein	Epitope	Sequence	MHC-I
M38	316-323	SSPPMFRV	H2-K^b
m139	419-426	TVYGFCLL	H2-K^b
IE3	416-423	RALEYKNL	H2-K^b
M57	816-824	SCLEFWQRV	H2-K^b
M45	985-993	HGIRNASFI	H2-D^b

A 10 mg stock of human β_2M protein was thawed and transferred into 5 ml of 5 M urea, into which 20 ml of the refold buffer was added very slowly using a Pasteur pipette. The dilute β_2M was then transferred back into the larger 500 ml refolding buffer very slowly to avoid the protein precipitating.

Approximately 5 mg of MHC-I heavy chain (either H2-K^b or H2-D^b) was then used to pulse the refold buffer using the same technique as for β_2M. Pulsing was typically performed four times allowing a minimum of eight hours between the additions of the heavy chain.

2.7.7. BUFFER EXCHANGING OF MONOMER

The 500 ml of refold buffer in addition to containing the successfully refolded monomer molecule contained a combination of unbound viral peptide, β2M, MHC-I heavy chain and aggregated proteins. To isolate the refolded monomer the refold buffer was transferred into an ultrafiltration Amicon stirred cell (Millipore) containing a nitrocellulose membrane (pore size 25 nm). The buffer was concentrated to approximately 4 ml as per manufacturer instructions.

At this stage, the monomer is in a buffer that contains high concentrations of salt and urea that are removed prior to biotinylation and purification by liquid chromatography.

To buffer exchange the monomer suspension, PD10 desalting columns (GE Healthcare) were used as per manufacturer instructions with cold Bir A buffer and the monomer solution adjusted to 7 ml using an Amicon centricon filter device (Millipore).

To the 7 ml sample, 35 µl of 100 mM d-Biotin, 350 µl of 100 mM ATP, 7 µl of 1 mg/ml leupeptin and pepstatin and 3 µl of the Bir A enzyme were added. This was incubated overnight at RT in the dark.

2.7.8. PURIFICATION OF MONOMER BY FPLC AND HPLC

Refolds were judged successful if the monomers purified at the correct size using liquid chromatography. The refolded monomer contains the murine MHC-I bound with the viral

peptide, human β2M and a biotin tag. The refolded molecule has a molecular weight of approximately 35 kDa.

Initial purification is performed by size exclusion chromatography. The biotinylated monomers were loaded onto an Äkta purifier (GE health care) for purification by fast-protein liquid chromatography (FPLC) using a Superdex™ 75 column (S75) and the S75 buffer (Figure 2.3). This fraction was then further purified by anion exchange chromatography. The monomer was loaded onto the MonoQ™ column of the Äkta purifier. Buffer A is first added to equilibrate the column followed by increasing volumes of Buffer B that contains salt to elute the monomer (Figure 2.4).

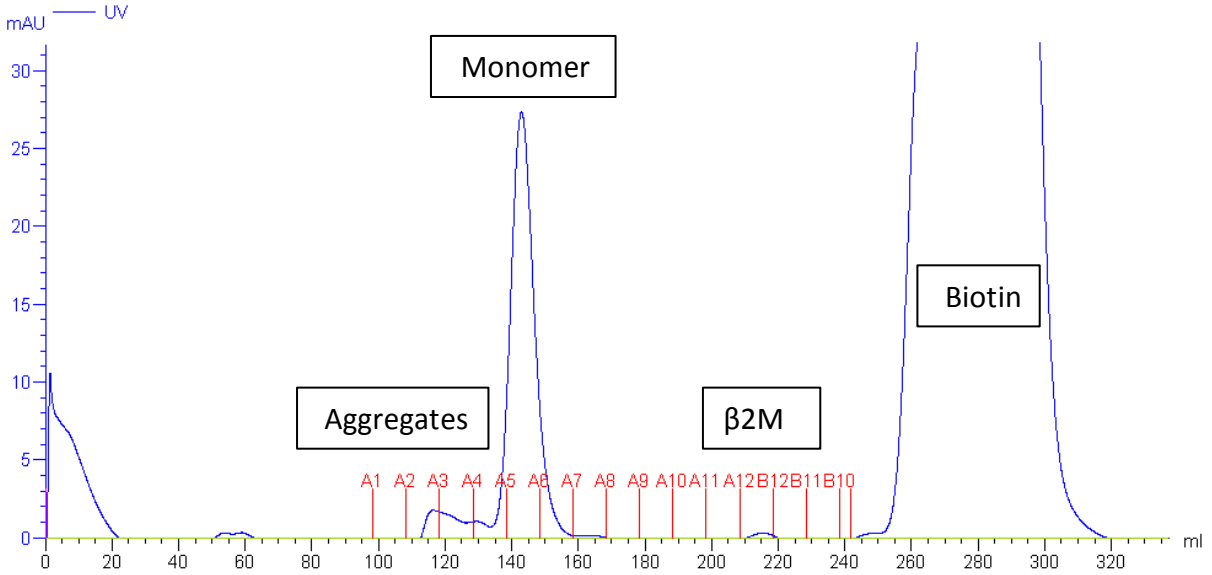

Figure 2.3. Size exclusion of m139-monomer. Protein aggregates elute in fractions A2-A5, followed by the refolded pMHC-I β2M monomer complex in A5-A7. Finally, free β2M and biotin are removed from the column (Fraction A11+).

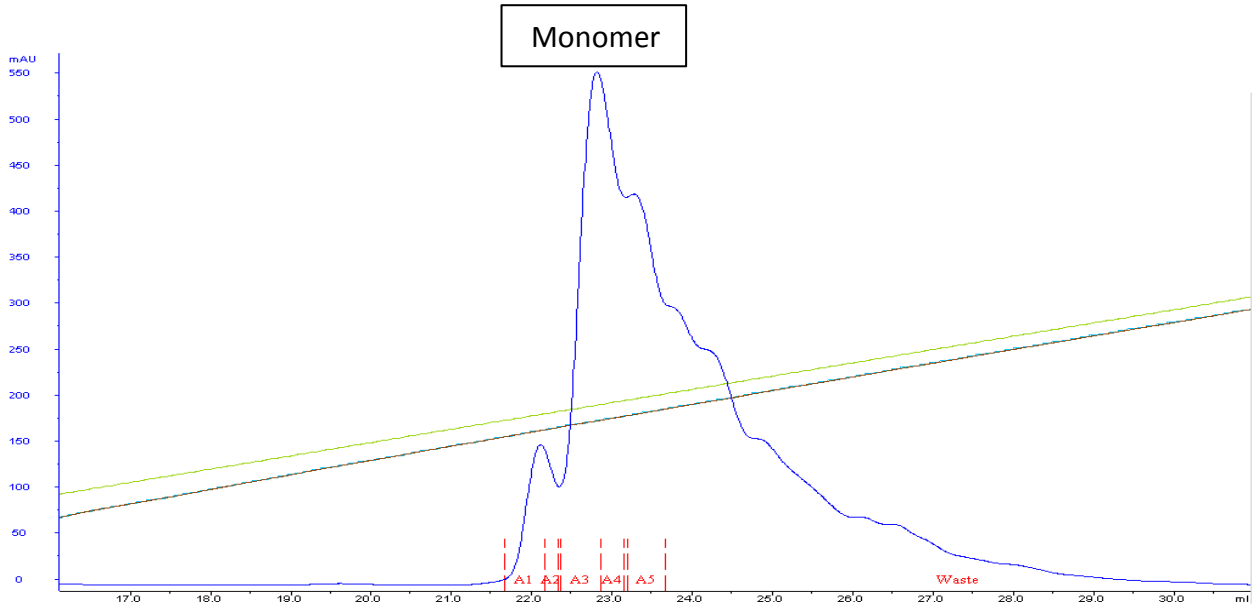

Figure 2.4. Anion exchange of m139-monomer. The green line shows increasing NaCl concentration with the highly pure monomer eluted into fraction A3.

2.7.9. MONOMER CONJUGATION

The biotinylated monomers were conjugated into tetramers using Streptavidin-APC. The biotin molecule on the α3 chain of the H2-K^b/H2-D^b acts as an acceptor for avadin binding. To achieve equimolar ratios of Streptavidin-APC and monomer, the protein concentrations of the monomers were calculated using either a Biuret or Bradford assay. Monomer stocks were kept in 20-100 µl aliquots and the protein concentration recorded (mg/ml).

For every 1 mg of monomer 87 µg of Streptavidin-APC was added. The Streptavidin-APC was added over 10 intervals. Adding the Streptavidin-APC gradually maximises monomer conjugation and tetramer formation. The conjugated monomers were kept at 4 °C in the dark until use.

2.8. SDS PAGE

To analyse the purity of inclusion body preparations or proteins following HPLC purification samples were run on a non-reducing sodium dodecyl sulphate (SDS) page.

A stock of polyacrylamide running gel was loaded into the 75 mm glass plates of a BIORAD specialised gel caster. A stacking gel was added to the top of the polyacrylamide running gel and a loading comb was added. The SDS gel was allowed to set and then placed into the BIORAD electrophoresis module and filled with SDS buffer.

Small volumes of samples were denatured on a heating block for 10 minutes at 95 °C. Samples were loaded into the wells of the gel and 90 volts applied across the gel. Gels were stained with Coomassie dye and incubated overnight at RT and excess stain removed using the destain buffer.

2.9. BRADFORD ASSAY

To determine the protein concentration of the inclusion body preparations and the purified monomers a standard Bradford assay was used.

BSA was diluted two-fold in PBS from 1 mg/ml to 0.03 mg/ml to generate a standard curve. 5 µl of the known BSA standards were added in duplicate into a flat-bottomed 96-well plate (IWAKI) and into each well 200 µl of dilute BIORAD solution was added. The plates were read using a microplate reader (Model 680, BIORAD) at $OD_{595\ nm}$ to produce the standard curve of optical density against protein concentration. Samples were analysed in duplicate as were PBS blanks.

Protein concentrations were calculated according to the absorbance from the known standard curve (linear regression) and the following equation:

$$y = ax - b$$

Where y = protein concentration (mg/ml)

a = sample $OD_{595\ nm}$

x = gradient of standard curve

b = y-axis intercept of standard curve

2.10. BIOTINYLATION ELISA

To asses if the HPLC purified monomer has been successfully biotinylated an enzyme-linked immunosorbent assay (ELISA) was performed.

Into a flat-bottomed 96-well PolySorp™ ELISA plate (NUNC) 10 µl of the appropriate sample was added to the corresponding well, into which 90 µl of PBS was added. A minimum of two negative controls were included for each assay, 100 µl of PBS.

The plate was then incubated for one hour at 37 °C. 200 µl of dilute Tween buffer was added to each well, flicked off, and the plate patted dry on tissue. This wash step was repeated a further two times.

Extravidin peroxidase was diluted 1:1100, of which 100 µl was added to each well and the plate incubated at RT in the dark for 15 minutes. The ELISA plate washed three times as before with dilute Tween buffer. Finally, 100 µl of TMB substrate was added to each well. This assay is not quantitative and only requires the biotinylated fractions to become blue.

2.11. MOUSE MODEL

2.11.1. MICE

SPF immunocompetent female C57BL/6 mice were obtained from Harlan and kept at the Biomedical Services Unit at the University of Birmingham. Food and water was available *ad libitum*. All experiments were carried out in accordance with Home Office project licence PPL 40/2998 and personal licence PIL 40/9427.

2.11.2. MCMV INOCULATIONS

A dose of $1x10^6$ PFU of MCMV strain *Smith* was administered via intraperitoneal injection (i.p).

Mutant MCMV strain temperature sensitive mutant 5 (*tsm5*) was administered i.p at a dose of $1x10^4$ PFU.

All infected animals were housed in negative pressure film isolators to prevent the spread of MCMV infection to other experimental colonies.

2.11.3. INFLUENZA A INOCULATIONS

Mice were anaesthetised with 0.1 ml of Sedative solution. $1x10^6$ EID_{50} of IAV strain A/Puerto Rico/8/34-A/England/939/69 clone 7a (H3N2) was administered drop wise by intranasal inoculation (i.n.). To reverse the sedative, mice were given a subcutaneous recovery injection of 0.2 ml Antisedan solution.

2.11.4. ANTIVIRAL TREATMENT

The antiviral valaciclovir was administered orally. To prepare the antiviral 500 mg Valaciclovir hydrochloride (GSK) tablets were crushed using a pestle and mortar and resuspended in 500 ml of distilled H_2O. The valaciclovir suspension at 1 mg/ml was placed into the drinking bottles and replaced up to twice weekly.

2.12. ANIMAL DISSECTIONS

2.12.1. ASEPTIC ISOLATION OF MAJOR ORGANS

Mice were sacrificed by approved Schedule 1 methods and dissected immediately. The spleen, kidneys, liver, lungs and salivary glands were taken from all animals, washed in cold 2 ml sterile PBS, frozen immediately and stored at -80 °C.

2.12.2. SPLENIC LYMPHOCYTES

Spleens were placed into a Petri dish containing 10 ml of RPMI-1640 medium. The spleen was macerated between two frosted microscope slides. The homogenate was then transferred into a 15 ml tube, the debris allowed to settle, and the supernatant transferred into another 15 ml tube and centrifuged at 700 g for 10 minutes to generate a cell pellet.

The supernatant was removed and pellet resuspended in 4 ml of cold red-cell lysis buffer and incubated for five minutes at RT. 10 ml of RPMI-1640 was added to dilute the lysis buffer and the cell suspension was spun at 700 g for 10 minutes at RT to generate a lymphocyte pellet.

The lymphocytes were then resuspended in 10 ml of RPMI-1640 and counted using the Trypan blue method. The lymphocyte suspension was adjusted to a working concentration of $5x10^6$ splenocytes per ml.

2.12.3. ISOLATING LYMPHOCYTES FROM CAUDAL MEDIASTINAL LYMPH-NODES

Caudal mediastinal lymph nodes (CMLN) were placed into 5 ml of sterile PBS. The membrane of the lymph node was mechanically disrupted using a 1 ml syringe. The lymph node suspension was transferred into a 15 ml tube and centrifuged at 700 g for 10 minutes at RT. The numbers of lymphocytes were counted using the Trypan blue method and resuspended in 200 µl of MACS buffer.

2.12.4. BRONCHIOLAR LAVAGE OF PULMONARY LYMPHOCYTES

Two incisions were made in the dissected mice to enable bronchiolar lavage. The first incision was made in the diaphragm and a second at the top of the trachea. 1 ml of lavage buffer was drawn up into the barrel of 2 ml syringe through a 23 gauge needle (25 mm) fitted with 23 gauge tubing (80 mm). The tube was then placed into the trachea of the mouse and the 1 ml of lavage fluid flushed into the lungs and drawn back up into the syringe. The lavage fluid containing lymphocytes was then centrifuged at 700 g for 10 minutes at RT and the lymphocyte pellet resuspended in 200 µl of MACS buffer.

2.13. FLOW CYTOMETRY: DETECTION OF VIRUS-SPECIFIC $CD8^+$ T-LYMPHOCYTES

2.13.1. TETRAMER STAINING

To detect virus-specific $CD8^+$ T-lymphocytes by flow cytometry MHC-I tetramers were used To standardise the tetramer staining procedure, where possible $1x10^6$ splenocytes were used per staining reaction. Splenocytes were first washed, centrifuged (700 g for 10 minutes at 4 °C) and resuspended in 200 µl of MACS buffer. 1-2 µl of the appropriate APC-conjugated tetramer was added and incubated for 30 minutes at 37 °C in the dark. The unbound tetramer was then removed by adding 4 ml of MACS buffer and the cells were centrifuged as before and resuspended in 200 µl of MACS buffer.

To provide detailed information on the cell's phenotype, surface molecules on the lymphocytes were stained with antibodies to CD4, CD8a, CD27, CD44, CD62L, CD122 and CD127 (See Table 2.1). Antibodies were incubated with the cells for 15-30 minutes at 4 °C in the dark. Again, any unbound antibody was removed and the splenocytes resuspended in a final volume of 200 µl MACS buffer. Lymphocytes were then ready for flow cytometric analysis, events were acquired on a LSR-II and data analysed using FACSDiva software.

2.13.2. INTRACELLULAR CYTOKINE STAINING (ICS)

Splenocytes were rested overnight in RPMI (37 °C, 95% air/5% CO_2) and the following morning $1x10^6$ lymphocytes were placed into the wells of a 96-well plate in a volume of 200

µl. The corresponding MCMV peptide was added at 1 µg/ml. The splenocytes were then returned to the incubator for one hour prior to the addition of 5 µM brefeldin A (prevents cytokine secretion from the Golgi). Following the addition of brefeldin A the cells were incubated for a further five hours. A negative unstimulated control and a positive PMA-ionomycin stimulated control were also included in each experiment.

Following stimulation lymphocytes were washed, centrifuged (700 g for 10 minutes at 4 °C), resuspended in 200 µl of MACS buffer. The splenocytes were then labelled on their surface with the anti-CD4 and anti-CD8 monoclonal antibodies for 15-30 minutes at 4 °C. The unbound antibody was removed with MACS buffer and the cells fixed with 100 µl of 4% paraformaldehyde. The cells were then incubated for 30 minutes in the dark before washing off the fixative. The membranes of the splenocytes were then permeabilised with the addition of 0.5% saponin. Intracellular cytokines were fluorescently labelled with IFNγ and TNFα antibodies. The intracellular antibodies were incubated for 30 minutes at RT in the dark. Unbound antibodies were removed; the cells resuspended in 200 µl MACS and transferred into FACS tubes. Samples acquired on a LSR-II and data analysed using FACSDiva software.

2.14. TITRATION OF LYTIC MCMV *EX VIVO* BY EXPLANT CULTURE

MCMV infects multiple sites and cell types within an animal thus the liver, lungs, kidney, heart and salivary glands of infected mice were harvested to detect lytic MCMV within these tissues.

MEFs were adjusted to $1x10^5$ cells/ml in D10 media. 1 ml of cells was added to each well of a 24-well plate and incubated at overnight (37 °C, 95% air/5% CO_2) whereby cells reached approximately 70% confluency.

Tissue samples were homogenised in 1 ml D10 media in 5 ml FALCON tubes. In between each sample, the probe was cleaned by submerging it into bleach once, 70% ethanol three times and PBS three times, and any fibrous tissue was removed with tweezers. Samples were serially diluted (1:10) across a dilution range ($1x10^{-1}$ to $1x10^{-3}$) and kept on ice.

The D10 media was aspirated from each well and washed immediately with 1 ml of PBS (warmed to 37 °C). The PBS was removed and 200 µl of homogenate dilution added to the cells (duplicate). The plates incubated for one hour (or for centrifugal enhancement spun at 1,000 g for 30 minutes at 37 °C). The homogenate was removed and 1 ml of CMC overlay was added and the plates incubated further for six days (37 °C, 95% air/ 5% CO_2).

The plates were removed from the incubator and the overlay was flicked off the wells into bleach. 1 ml of 4% fixative solution was added to each well and the plates were left overnight at RT. The following day fixative was flicked off and the plates rinsed gently under running water from the tap. Wells were stained for 10 minutes with 500 µl of 0.3% crystal violet solution. The stain was then flicked off and the plates rinsed under water and allowed to air dry.

The number of PFU per organ was calculated by multiplying the mean number of plaques per organ by the dilution factor and correcting for volume (PFU/organ).

2.15. DETERMINING MCMV TITRE BY REAL-TIME QUANTITATIVE PCR

Tissue was removed and washed in 2 ml of sterile PBS and immediately frozen at -80 °C. Samples were thawed at room temperature and whole organ or 0.268 g (+/- 0.016 g) of liver was homogenised using a mechanical probe (Pro 200, Monroe, USA) in 2 ml of sterile RPMI. The homogenate was then centrifuged at 720 g for 10 min at 4 °C. The supernatant was then harvested and then spun as before to remove residual cellular debris. The supernatant was then divided into three 700 µl aliquots and stored at -80 °C.

An individual aliquot was thawed and spun at 13k g for 10 minutes to generate a pellet. The supernatant was discarded and the DNA extracted from the cells was performed as per manufactures instructions (QIAgen: Blood and Tissue Kit).

Primers were designed to amplify sections of the m29.1 gene:

Fwd: 3'- GAAATGCACACGGAAAAAAAGC

Rev: 3'- ATCGTATGAGTAGTGGGCGTTTCT

The reference gene used was for the murine GAPDH:

Fwd: 3'- AAGAGAGGCCCTATCCCAACTC

Rev: 3'- TAGGCCCCTCCTGTTATTATGG

The corresponding TaqMan probes were:

m29.1: FAM-TACCCGAATGGCTTTATGCCATTGCC-TAMRA

GAPDH: GAPDH: YY-TCTCCCTCACAATTTCCATCCCAGACC-BHQ1

The assay was designed to run in multiplex on the ABI Prism 7500 FAST series. Each reaction was performed in duplicate and contained 3 µl of DNA, 450 nM of m29.1 primers, 25 nM of GAPDH primers, 187.5 nM of probes and 10 µl of Universal Master Mix II (Applied Biosciences).

The thermo-cycle conditions were as follows: 50 °C for 2 minutes, 95 °C for 10 minutes, and 40 cycles of 95 °C for 15 seconds and 60 °C for 1 minute. Data was analysed on the 7500 ABI Prism Fast software and the relative number of MCMV genomes to GAPDH was calculated using the $2^{-\Delta Ct}$ method.

Where$2^{-\Delta Ct}$ = Ct(m29.1) – [Ct(GAPDH)+1]

2.16. SEMI-QUANTITATIVE MCMV IgG ELISA

To obtain plasma, cardiac bleeds were required. First mice were administered 0.2 ml Sedative solution by i.p. injection to anaesthetise the animal. Cardiac bleeds were then performed before the mice recovered using a 26 gauge needle (25 mm) attached to a 1ml syringe. The blood obtained was placed into sterile Eppendorf tubes containing 5 µl of heparin sodium. Plasma was separated from whole blood by centrifugation, 1500 g for five minutes at RT.

Plasma from a minimum of five MCMV infected mice was pooled and a standard curve generated in the ELISA dilution buffer (1:100, 1:200, 1:400, 1:800 and 1:1600).

MCMV lysate was produced by harvesting MCMV from the culture media of MCMV-infected MEFs. The culture media was transferred from the flask to a centrifuge tube and centrifuged at 850 g for 10 minutes at RT. The supernatant was then sonicated five times in a sonicating water bath. A mock lysate was produced by sonicating uninfected MEFs. The protein concentration of the MCMV lysate and mock lysate was confirmed by Bradford assay.

The MCMV lysate was diluted in ELISA coating buffer 1:600 whereas the mock lysate was diluted 1:800 to achieve a final protein concentration of 3 µg/ml. 50 µl of the appropriate lysate was added to the corresponding well of a 96-well ELISA plate. This plate was then covered and incubated at 4 °C overnight.

The following day the serum samples were diluted 1:600 in the ELISA dilution buffer and the plated was washed three times with 200 µl of ELISA wash buffer. Each time the wash buffer was flicked off into bleach and any remaining fluid was removed by tapping the plate onto tissue.

100 µl of the appropriate standard dilution was added to the wells of the 96-well plate. Two 100 µl PBS blanks were also included on the plate. 100 µl of the appropriate serum sample dilution was added in duplicate to the plate. The plate was incubated for one hour at RT, and then washed three times (as above) with ELISA wash buffer.

The secondary anti-mouse IgG (H+L) HRP conjugated antibody was diluted 1:2500 and 100 µl added to each well. The plate was again incubated for one hour at RT and washed three times (as above) with ELISA wash buffer.

100 µl of TMB solution was then added directly to the wells and the plate incubated for 10 minutes at RT in the dark. Immediately, 100 µl of 1 M hydrochloric acid was then added to stop the reaction. The plates were read using a microplate reader at $OD_{450\ nm}$.

2.17. DETERMINING INFLUENZA A VIRAL TITRES

Madin Darby canine kidney (MDCK) cells were grown to confluency in 150 cm^2 tissue culture flasks in 20 ml of IMDM. Once confluent MDCKs were washed in PBS, trypsinised and resuspended at $7x10^5$ cells per ml.

Lungs from IAV infected mice were homogenised in 1 ml of IMDM and centrifuged at 700 g for 10 minutes at RT. The supernatant was collected and diluted two fold over the, range 1:2-1:32. The IAV stock virus was also diluted in IMDM (1:2000, 1:6000 and 1:18000).

200 µl of MDCK cells and 200 µl of lung homogenate or IAV stock virus were added immediately to the appropriate wells of a 24-well plate. The plates were incubated (37 °C, 95% air/5% CO_2) for five hours after which 300 µl of 2% w/v CMC was added to each well and the plates returned to the incubator for a further 48 hours.

The existing media was removed and the wells washed with 600 µl of PBS. The cells were fixed with 400 µl of 4% formaldehyde for 30 minutes. 250 µl of 0.5% TritionX-100 was then added for 30 minutes to permeabilise the cells.

Cells were washed twice with 200 µl of PBS. Into each well 200 µl of 10% FCS/PBS was then added for 90 minutes. The buffer was then removed and the cells washed again with PBS. Then 200 µl of primary mouse anti-Influenza A nucleoprotein monoclonal antibody (MCA400) was added to each well and incubated for 90 minutes.

The supernatant was then discarded and the wells washed five times with PBS. 200 µl of the secondary antibody (anti-mouse IgG HRP diluted 1:2500 in 10% FCS/PBS) was then added. Plates were then incubated for 90 minutes in the dark.

One AEC tablet was dissolved in DMF. Once dissolved 47.5 ml of acetate buffer was added slowly to the DMF with constant stirring. Once mixed 25 µl of 30% hydrogen peroxide was also added to create a developing solution.

The supernatant from the plates was then discarded and the wells washed five times with PBS. Then 300 µl of the developing solution was added to each well and the plates incubated in the dark for 30 minutes to one hour. IAV infected cells turned a reddish-pinkish colour. Each well was then washed in 200 µl of sterile water, before the numbers of plaques were counted.

3. RESULT 1: PROLONGED (12 MONTHS) VALACICLOVIR TREATMENT REDUCES THE MCMV-SPECIFIC IMMUNE RESPONSE COMPARED TO UNTREATED MCMV-INFECTED MICE

3.1. DETERMINING THE IMPACT MCMV INFECTION HAS ON CD8$^+$ T-CELL PHENOTYPE

MCMV causes memory inflation within the murine immune system and those lymphocytes display a highly differentiated T-cell phenotype [165].

Murine T-lymphocytes express a combination of molecules on their cell surface to aid adhesion including: CD62L [318] and CD44 (hyaluronan receptor) [319]. The CD62L molecule mediates lymphocyte rolling on inflamed endothelium and enables lymphocytes to attachment to the lymphatic high endothelium venule [320-322]. In contrast CD44 interaction with its ligand causes adherence of the T-cell at an inflammatory site [323, 324] and, furthermore, loss of CD44 facilitates lymph node homing [325, 326]. The antigen-inexperienced subset of lymphocytes, i.e. naïve CD8$^+$ T-cells, express the combination of CD44$^-$ CD62L$^+$ (T_N) (Figure 3.1 F). Naïve lymphocytes preferentially migrate and remain within the T-cell zones of the lymph node awaiting presentation of foreign antigens by professional APCs. The central memory (T_{CM}) subset expresses both CD44$^+$ and CD62L$^+$ molecules on its cell membrane. The central memory population of lymphocytes forms following resolution of acute infection and relocate to the lymph node in anticipation of re-exposure to antigen. The third main subset distinguished by CD44 and CD62L co-expression are the effector memory (T_{EM}) populations of lymphocytes. T_{EM} lymphocytes express CD44 but not CD62L on their surface. The lack of CD62L indicates these cells are not located in the lymph node, and high expression of CD44 shows the cells to be attracted to sites of inflammation/activity.

Those lymphocytes which do not express both CD44 and CD62L were classified as double-negatives (T_{DN}) and are the least frequent T-cell subset found in the spleen [327].

In prior experimental models of MCMV infection the inflationary memory MCMV-specific $CD8^+$ T-cells exclusively have a T_{EM} phenotype [165]. In addition to low level CD62L and high CD44 expression the M38, m139 and IE3 antigen-specific T-cells have a highly differentiated phenotype. This is characterised by low levels of expression of CD27 and low levels of the cytokine receptors CD122 and CD127. In addition, the inflationary T-cells have high levels of NKG2D and KLRG1 with reduced expression of PD-1 [165] which were not measured in this study.

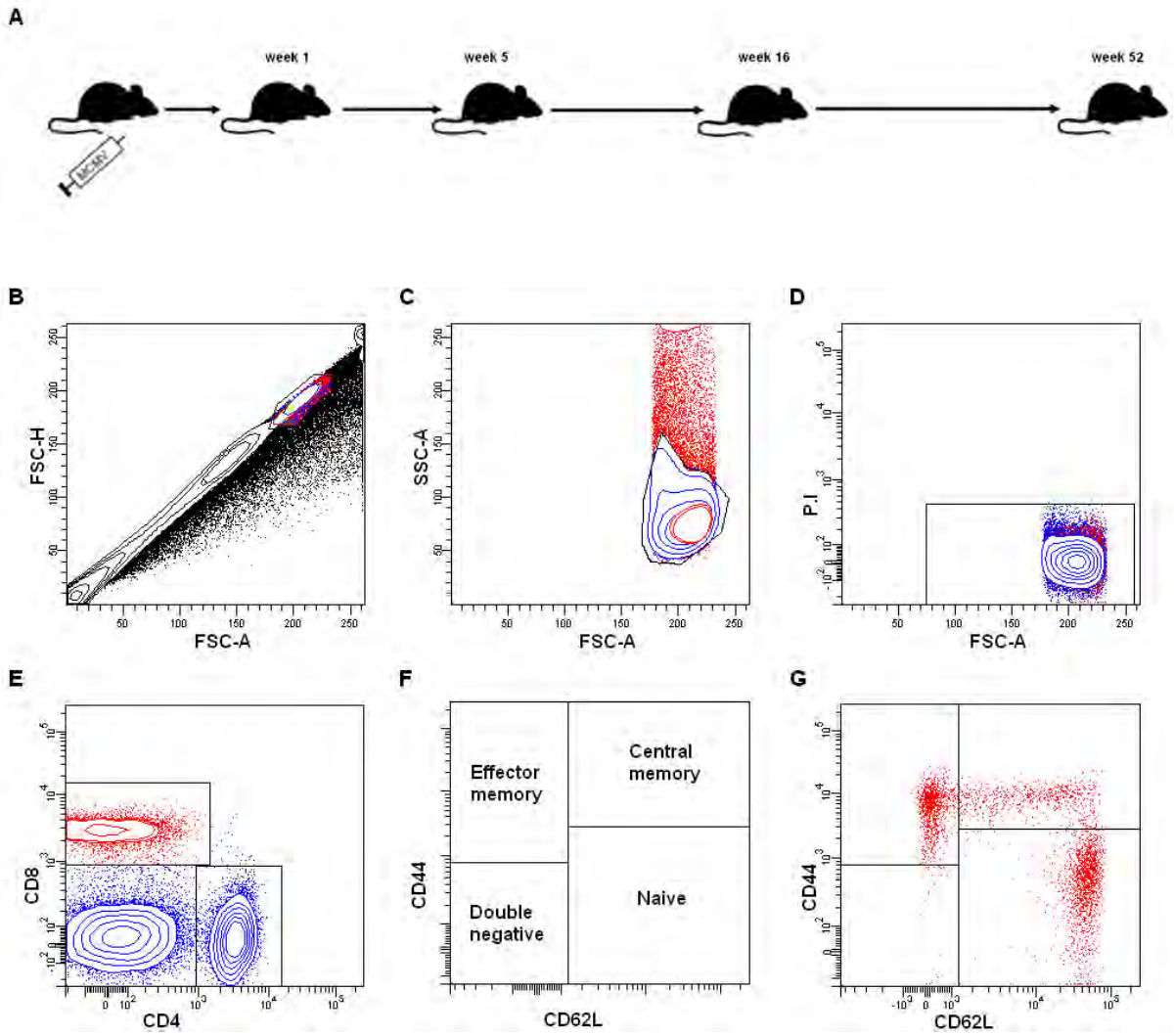

Figure 3.1. Phenotype of $CD8^+$ T-cells based on CD44 and CD62L co expression. A) C57BL/6 mice infected with 1 $x10^6$ PFU MCMV *Smith* and mice periodically sacrificed at one, five, 16 and 52 weeks p.i. B-G) FACS plots demonstrating the gating set of memory $CD8^+$ T-cells. Single cells (B), lymphocytes (C), live lymphocytes (D), $CD8^+$ T-cells (E). Co-expression CD44 and CD62L (F-G) naïve (T_N: $CD8^+$ $CD44^-$ $CD62L^+$), central memory (T_{CM}: $CD8^+$ $CD44^+$ $CD62L^+$), effector memory (T_{EM}: $CD8^+$ $CD44^+$ $CD62L^-$) and double negative (T_{DN}: $CD8^+$ $CD44^-$ $CD62L^-$) phenotype.

A group of six to eight week old female C57BL/6 mice were inoculated i.p with $1x10^6$ PFU *Smith* strain of MCMV and the spleens removed at weeks one, five, 16 and 52 p.i. (Figure 3.1 A). The lymphocytes were stained with antibodies for CD8, CD44 and CD62L. The cells were analysed and the $CD8^+$ T-cell population classified into the four memory subsets based on the cell surface distribution of CD44 and CD62L (Figure 3.1 B-G).

Prior to MCMV infection (week 0) the most prominent $CD8^+$ subset in the SPF animals were T_N $CD8^+$ T-cells contributing towards 82% of the $CD8^+$ T-cell pool. In addition, only 15% of the $CD8^+$ T-lymphocytes displayed a memory phenotype (T_{CM} + T_{EM}). The remaining 2.5% of $CD8^+$ T-cells were double negative for CD44 and CD62L (Figure 3.2, Table 3.1).

Immediately following inoculation the hierarchy of the memory subsets changed because of the proliferation of lymphocytes needed to control the MCMV infection. One week post-inoculation saw the primary expansion of T_{EM} $CD8^+$ T-cells from 5% to over 30% of $CD8^+$ T-lymphocytes. A corresponding decline in naïve $CD8^+$ T-cells was observed (82% to 54%) during the first week of infection. Subsequent to controlling primary infection, the proportion of T_{EM} contracted to 15% of the $CD8^+$ T-cell pool at week five. In contrast, the proportion of T_N $CD8^+$ T-cells rebounded, between week one and five p.i., to almost pre-inoculation levels. At this stage the mice were approximately only 11-13 weeks old therefore the recovery in T_N can be still attributed to thymopoiesis [328].

Memory inflation of the T_{EM} population occurs at a rapid rate between week 16 and 52 post *Smith* infection. The T_{EM} cells at week 52 accumulated within the spleen and the population

exceeded 50% of the entire $CD8^+$ T-cell population. Corresponding to the increase in $T_{EM,}$ the frequency of T_N $CD8^+$ T-cells declined to 25% causing an inversion of the T_N to T_{EM} ratio (Figure 3.2, Table 3.1). Loss of naïve T-cells either through aging or through infection is implicated in senescence of the adaptive immune response [329-331].

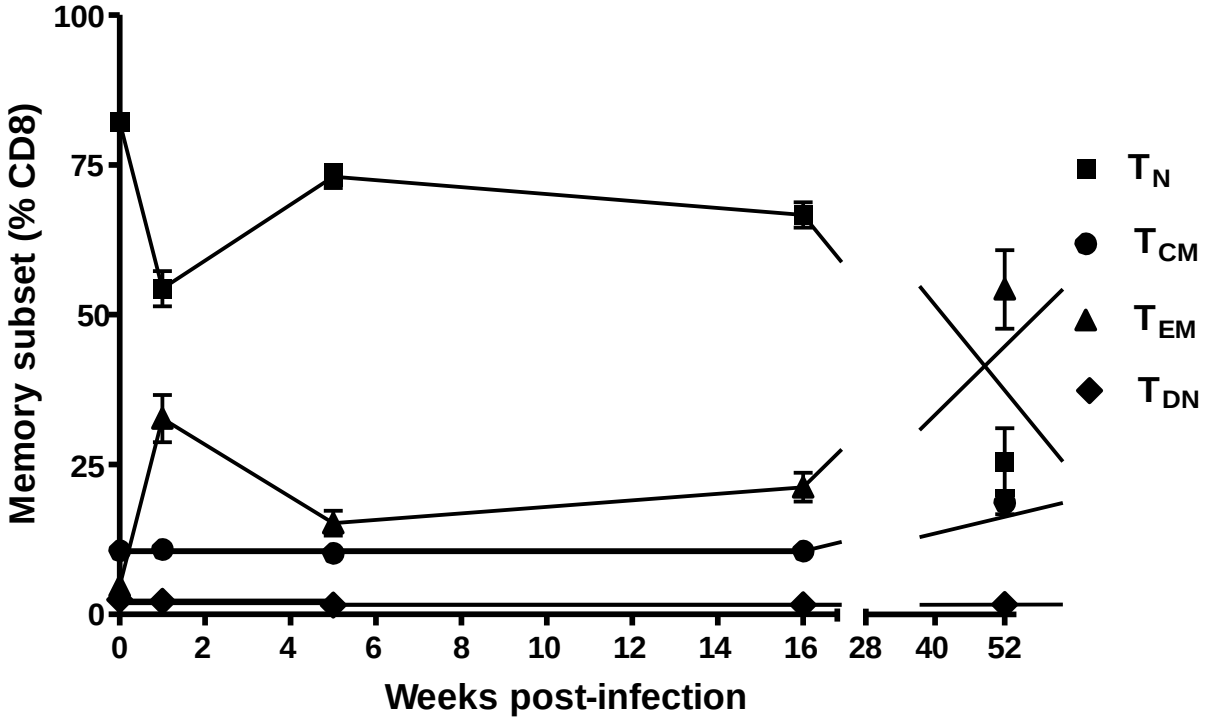

Figure 3.2. MCMV infection drives the expansion of T_{EM} $CD8^+$ T-cells. Frequency of T_N, T_{CM}, T_{EM} and T_{DN} $CD8^+$ T-cells sampled from the spleen of *Smith* infected mice at zero, one, five, 16 and 52 weeks p.i. Mean +/- SEM (n=4).

Table 3.1. Proportion of T_N, T_{CM}, T_{EM} and T_{DN} $CD8^+$ T-cells pre and post-MCMV infection. Mean +/- SEM.

	Memory Subset (% CD8) (n=4)				
Week	**0**	**1**	**5**	**16**	**52**
T_N	82.1 +/- 1.7	54.3 +/- 6.0	73.0 +/- 3.8	66.6 +/- 4.2	25.5 +/- 11.1
T_{CM}	10.7 +/- 0.8	10.8 +/- 1.7	10.2 +/- 1.2	10.6 +/- 0.7	18.6 +/- 3.9
T_{EM}	4.8 +/- 0.9	32.7 +/- 7.9	15.2 +/- 4.1	21.2 +/- 4.8	54.2 +/- 13.1
T_{DN}	2.5 +/- 0.3	02.2 +/- 1.5	1.6 +/- 0.2	1.6 +/- 0.3	1.6 +/- 0.31

Having shown the expansion of T_{EM} in MCMV infected mice it was important to compare the frequency of each memory subset to that seen in an aged-matched MCMV uninfected mouse due to the spontaneous generation of clonal T-cells [332, 333]. Here the frequency of T_N $CD8^+$ T-cells at 12 months old in the uninfected animals was 53% of the entire $CD8^+$ T-cell pool (Figure 3.3, Table 3.2). In MCMV infected animals the proportion of T_N $CD8^+$ T-cells is halved to approximately 25% (***$p<0.001$). The proportion of T_{CM} T-cells did not vary between MCMV infected and uninfected animals. MCMV infection causes the selective accumulation of the T_{EM} population of $CD8^+$ T-cells (from 27% to 54% ***$p<0.001$). The proportions of T_{CM} and T_{DN} phenotype $CD8^+$ T-cells did not vary between MCMV infected and uninfected animals.

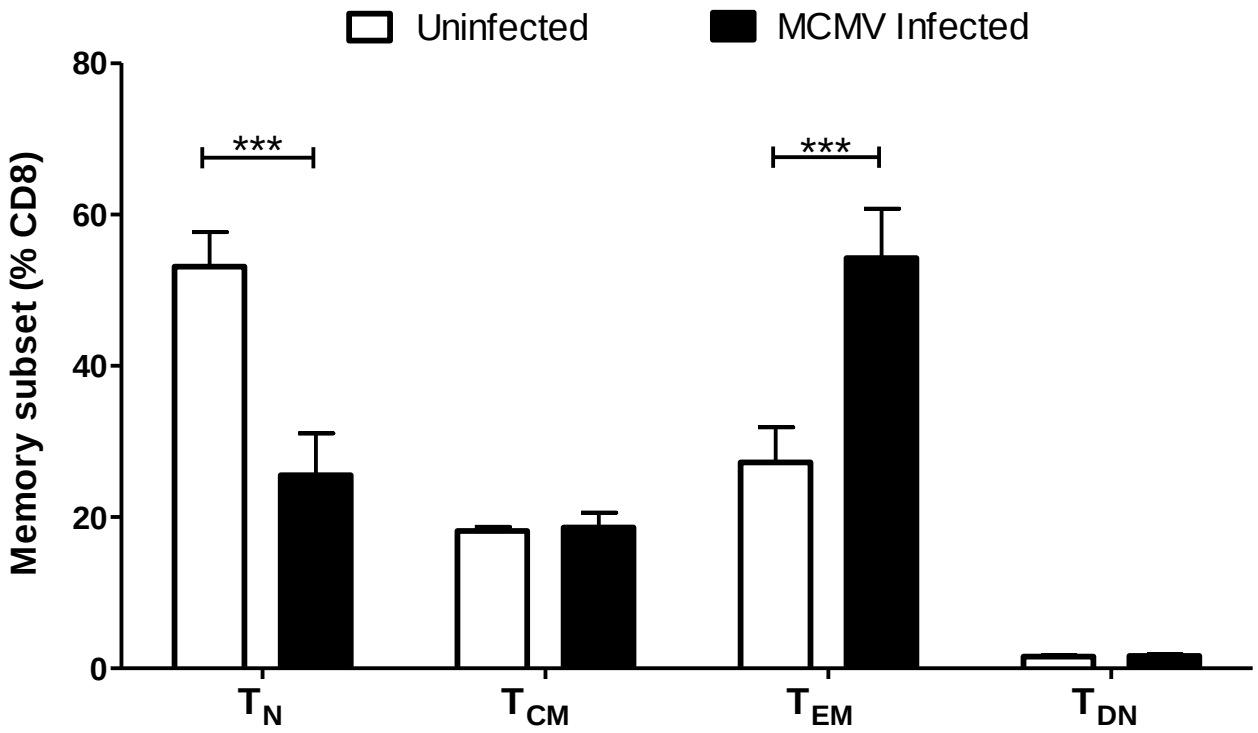

Figure 3.3. MCMV infection expands the T_{EM} $CD8^+$ T-cell pool. Frequency of memory $CD8^+$ T-cells in the spleen 52 weeks p.i. compared to uninfected aged matched litter mates. Mean +/- SEM (n=4). Data analysed by 2way-ANOVA plus Bonferroni post-test (*p<0.001).**

Table 3.2. Memory $CD8^+$ T-cells in uninfected mice and MCMV infected 52 weeks p.i. Mean +/- SEM.

	Memory Subset (% CD8)	
	Uninfected (n=4)	**MCMV Infected (n=4)**
T_N	53.10 +/- 4.56	25.52 +/- 5.53
T_{CM}	18.13 +/- 0.57	18.62 +/- 1.94
T_{EM}	27.22 +/- 4.66	54.21 +/- 6.54
T_{DN}	1.55 +/- 0.16	1.65 +/- 0.18

3.1.1. MCMV BECOMES UNDETECTABLE IN CHRONICALLY INFECTED MICE

Herpesvirus infections are synonymous with establishing latent infection and intermittent lytic reactivation from latency [164, 165]. My hypothesis suggested that the well-documented expansion of MCMV-specific $CD8^+$ T-cells is due to intermittent lytic reactivation and antigen stimulation of the naïve lymphocyte pool during the latent-phase of infection. The accumulation of T_{EM} $CD8^+$ T-cells proved to be a good surrogate marker of the accumulation of virus-specific CTLs (Figure 3.2 & 3.3). Therefore, the MCMV viral titre was assessed by quantitative PCR (qPCR) over the course of infection in the salivary gland. Primers were designed to amplify a short sequence of the viral gene m29.1 and the cellular GAPDH gene to determine a relative quantification of viral genomes per cell [334].

The presence of MCMV gene m29.1 relative to GAPDH was calculated from DNA extracted from salivary gland tissue at weeks one, five, 16 and 52 p.i. Viral titres were highest at week one p.i. (ΔCt 10) (Figure 3.4). At week five p.i., MCMV DNA was present in only 75% of salivary glands sampled and by week 16 latent MCMV genomes was only evident in one animal. At week 52 p.i., the virus was completely undetectable by qPCR in the salivary gland in all mice. The absence of detectable virus in the salivary gland does not exclude that viral reactivation and possible T-cell priming is occurring at other anatomical sites within the animal.

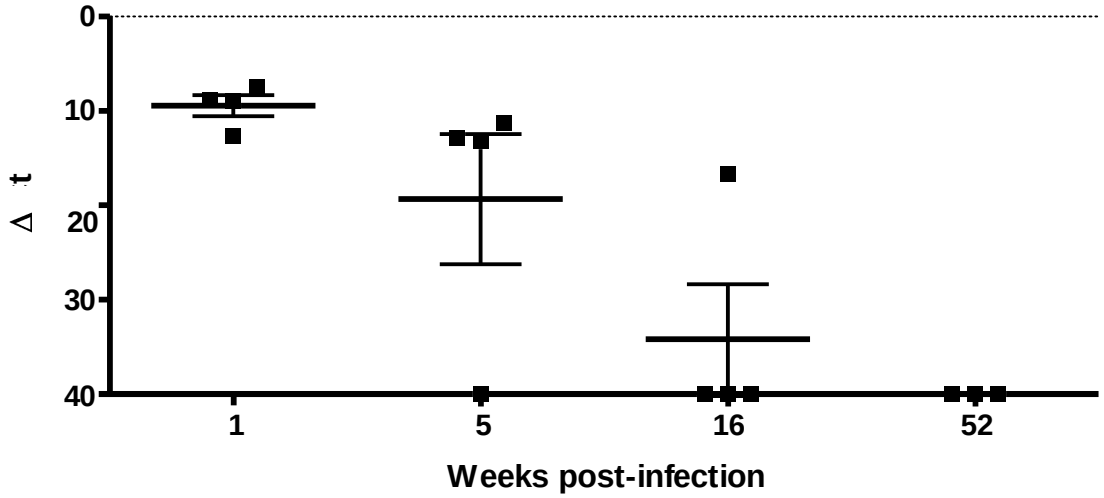

Figure 3.4. MCMV infection becomes undetectable during latent infection. MCMV viral loads in salivary glands as determined by qPCR at one, five, 16 and 52 weeks p.i. Data presented as delta Ct (ΔCt) comparing signal for the m29.1 gene vs. GAPDH.

DETECTION OF MCMV-SPECIFIC CD8$^+$ T-CELL RESPONSES BY ICS

In a second experiment, six-eight week old female C57BL/6 mice were inoculated i.p with 1x10^6 PFU *Smith* strain of MCMV. The infected mice were periodically sacrificed by cervical dislocation. Lymphocytes were isolated from the spleens and the proportion of virus-specific cells measured by peptide stimulation and ICS. Samples were made during the acute phases of infection at seven (n=2) and 14 days (n=2) p.i. and again at the later stages of infection at 36 (n=2) and 116 (n=3) days post-MCMV infection by which time memory inflation would occur (Figure 3.5 A).

The gating was designed to determine the percentage of MCMV-specific CD8$^+$ T-lymphocytes in the spleen. Splenocytes were stained using a combination of monoclonal antibodies directed to cell surface antigens such as CD8 and the intracellular cytokines. Lymphocyte populations selected from the other cell types within the spleen using a combination of inclusive gates. The CD8$^+$ T-cells were selected and the cytotoxic lymphocytes producing IFNγ were determined in response to peptide stimulation (Figure 3.5 B).

3.1.2. MONITORING ACUTE AND LATENT MCMV-SPECIFIC CD8$^+$ T-CELL RESPONSES BY ICS

Antigen-experienced memory CD8$^+$ T-lymphocytes can be detected by the synthesis of pro-inflammatory cytokines such as IFNγ or TNFα following *ex vivo* peptide stimulation and ICS. Here ICS for IFNγ-specific CD8$^+$ T-lymphocytes proved to be a highly sensitive method of detecting the antigen-specific CTLs without the need for MHC-I tetramers.

After i.p inoculation, MCMV disseminates from the peritoneal cavity, through professional APCs to the mediastinal lymphatics and is then widely disseminated throughout the body [43]. The hierarchy of CD8$^+$ T-cell immunity has previously been determined for immunodominant T-cell epitopes from the M38, M45, M57, m139 and IE3 viral proteins in both acute and latent phases of MCMV infection in C57BL/6 mice [164, 165]. For example, seven days p.i. Munks *et al* (2006) observed large frequencies (5-14%) of CD8$^+$ T-cells synthesising IFNγ in response to each of the M38, M45, M57 and m139 viral peptide antigens [164]. In contrast Snyder *et al* (2008) identified fewer than 1% of M45-specific CD8$^+$ T-cells at the same time following MCMV (*MW97.01*) infection [165]. It has been calculated that the growth rate of MCMV-specific CD8$^+$ T-cells in the spleen has an average doubling time of 12 hours and corresponds to the peak immune response between days six and seven p.i. [335].

In the present study, following i.p MCMV *Smith* infection, the M38 epitope was initially the most immunogenic with 4.8% of the entire CD8$^+$ T-cell pool specific for this epitope at day 7

p.i. In addition to robust immune responses to M38 approximately 3% of the $CD8^+$ T-cells produced IFNγ in response to m139 or M45 stimulation whereas 2% of $CD8^+$ T-cells were directed towards IE3 and M57 (Figure 3.5 C). The differences in initial immunodominance between this model and those observed by Munks *et al* (2006) and Snyder *et al* (2008) are most likely a reflection of the strain differences: both Munks and Snyder infected mice i.p with *MW97.01* (BAC derived virus) whereas here the non-manipulated *Smith* strain was used [164, 165].

Both Munks *et al* (2006) and Snyder *et al* (2008) observed a very low frequency of IE3-specific $CD8^+$ T-cells (<1%) during acute infection and saw memory inflation of the T-cell response towards this epitope during the chronic phase of infection [164, 165]. Here, unexpectedly CTLs with specificity for the IE3 antigen (2.4%) detected at day 7 and this finding was consistent in all future experiments (Figure 3.5 C). An explanation why IE3-specific lymphocytes were detected so early in the course of infection may be due to slight genetic variations between viral strains or the cross-presentation of similar antigens [336].

It is widely accepted that between days seven and 14 post-MCMV infection there is a contraction in frequency of virus-specific $CD8^+$ T-cells. This contraction is thought to occur at a near constant rate to form a small pool of cytotoxic memory T-cells. The proportion of M38, M45 and m139-specific $CD8^+$ T-cells demonstrated a rapid rate of decay from the peak immune response between day seven and 14, e.g. m139-specific $CD8^+$ T-cells decreased by over 50% (contracting from 3.4% to 1.5%). The rapid decay of $CD8^+$ T-cells observed between day seven and 14 fits an exponential model whereby initially the frequency of lymphocytes

decreases at a constant rate (approximately every 16 hours) until it reaches a plateau phase which becomes the central memory pool [335]. In slight contrast to this exponential model the frequency of M57 and IE3 CTLs increased slightly between day seven and 14, e.g. M57-specific $CD8^+$ T-cells increased from 2.2% to 2.8%. However, these increases were not statistically significant and at day 14 the M57 and IE3 CTLs did undergo their own contraction phase. The frequency of virus-specific T-cells was again determined for the five viral antigens at day 36 p.i. where further contraction in the T-cell frequency was observed. At day 36, the acute infection would be expected to be resolved and therefore an attrition of the primary cytotoxic immune response was expected (Figure 5.3 C).

Memory inflation was observed for all five epitopes assayed at day 116 p.i. The viral epitope that raised the greatest inflation from day 36 was IE3 (Figure 3.5 C). The IE3 CTLs accumulated in frequency from 1.2% to 5.0% of the entire $CD8^+$ T-cell pool at day 116. The IE3 protein is homologous to IE1 of HCMV and also a common target for $CD8^+$ T-cell responses in HCMV infected individuals [145]. The immunodominant immune response directed towards the m139 viral antigen also contributed to 5% of the CTL pool. The m139 gene product belongs to the US22 family, which is conserved in HCMV strains. The m139 forms part of a complex with m140 and m141 and co-localises in the cis-Golgi within the infected cell's cytoplasm [337]. The US22 complex is an early gene product and is essential for viral replication in macrophages [338]. The frequency of M38-specific cells inflated to almost the same magnitude as the acute immune response [165]. M38 and its family member m38.5 are possible immune evasion genes therefore, the immune response to this particular antigen is potentially very important in preventing viral escape.

Memory inflation was previously described as a unique characteristic to some but not all of the known immunodominant MCMV $CD8^+$ T-cell epitopes [164, 165]. For example, Snyder *et al* (2008) detailed that the frequency of M45 and M57 specific CTLs remained below 1% for the course of MCMV infection forming long-lived stable central memory populations [165] whereas here there was an accumulation of those cells with the same antigen specificity. In addition to this experiment, all subsequent experiments detected relatively high frequencies (≈5%) of M45 and M57 MCMV-specific $CD8^+$ T-cells during the latent phase of infection (Figure 3.5 C).

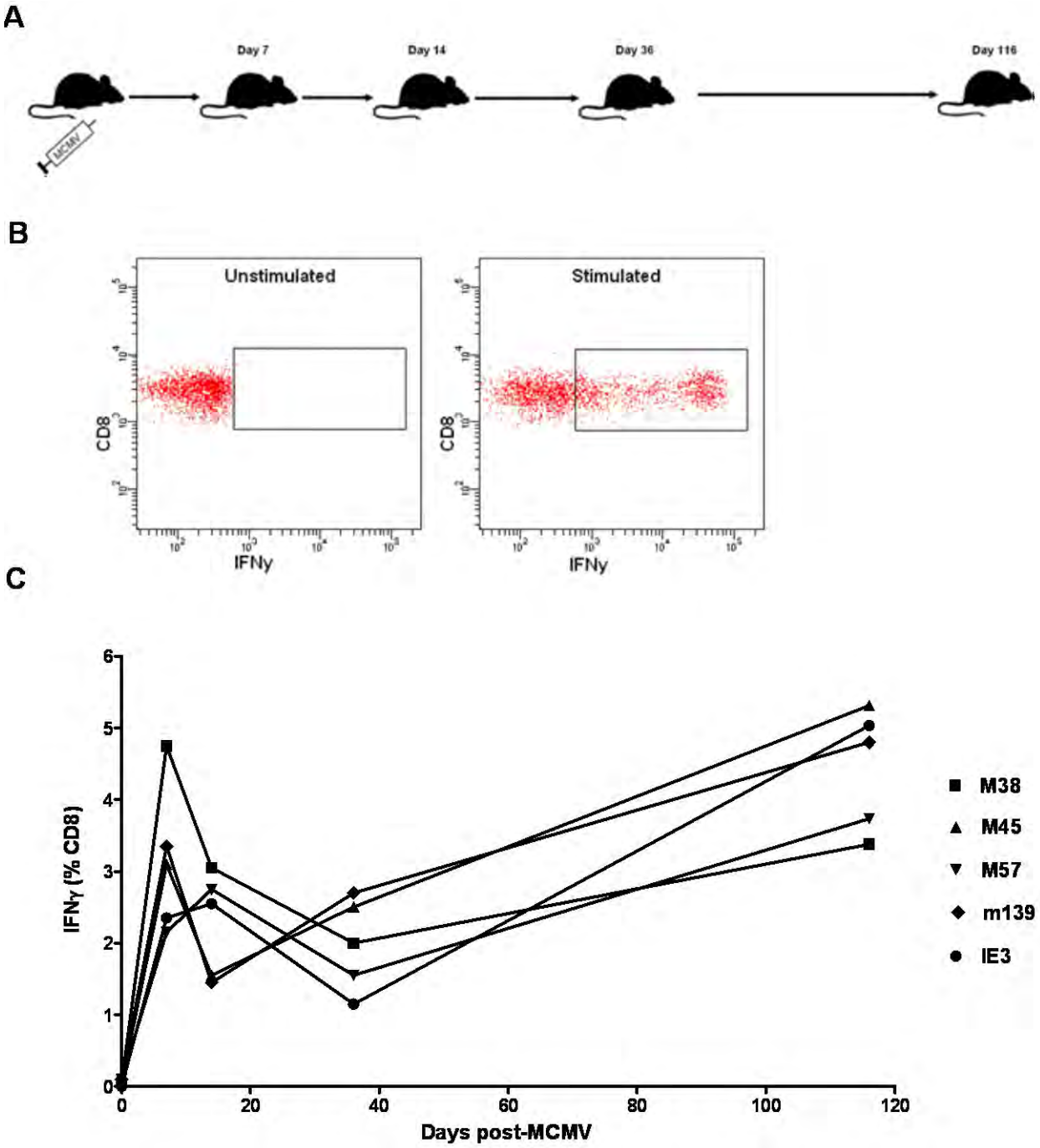

Figure 3.5. Memory inflation: an accumulation of MCMV-specific $CD8^+$ T-cells. A) C57BL/6 mice infected with $1x10^6$ PFU MCMV *Smith*. Mice sampled at seven, 14, 36 and 116 days p.i. B) Representative gating of IFNγ producing $CD8^+$ T-cells. C) Average frequency of IFNγ producing $CD8^+$ T-cells as a percentage of $CD8^+$ T-cells (n=2-3 mice per time point).

INHIBITION OF MCMV REPLICATION BY NUCLEOSIDE ANALOGUES IN AN *IN VITRO* SYSTEM

The acycloguanosine antivirals are nucleoside analogues designed to inhibit the replication of herpes viruses. *In vitro* procedures by Pavic *et al* (1997) [316] and Kruppenbacher *et al* (1994) [317] determined the effectiveness of acycloguanosine drugs at inhibiting CPE caused by HSV-1 *in vitro*. In the present study, the method of micro-plaque reduction assay (µPRA) was modified to compare the capacity of aciclovir and valaciclovir, two similar nucleoside analogues, in preventing MCMV replication in permissive MEF primary cells following four-days of co-culture.

		Antiviral Concentration (µM)			
Antiviral	**Uninfected MEF**	**0.00**	**0.13**	**0.50**	**1.25**
Aciclovir	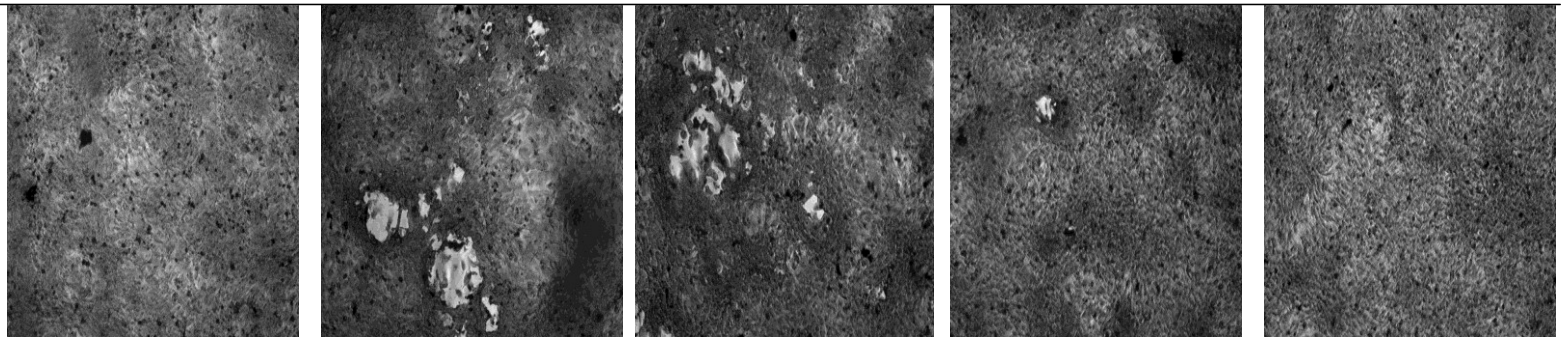				
Valaciclovir	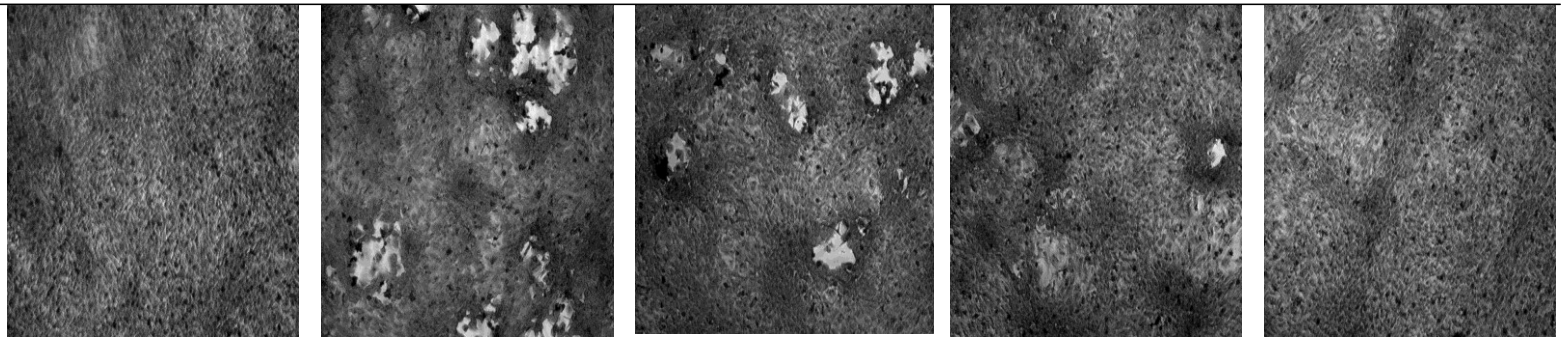				

Figure 3.6. Micro-plaque reduction assay: MEFs were co-cultured in media containing either aciclovir or valaciclovir (0-125µM) and infected with the *Smith* strain of MCMV (MOI≈0.01). The mean number of PFU was determined after four days. Representative images taken at x100 magnification.

The *Smith* virus proved capable of infecting and replicating within MEFs causing CPE and viral plaque formation (Figure 3.6). The average number of plaques per well was plotted against the range of antiviral concentrations (Figure 3.7 A). In the absence of aciclovir or valaciclovir the virus created an average of 25 or 30 viral PFU per well respectively. Increasing the concentration of antiviral produced an almost linear decrease in the mean number of PFU/well.

At high concentrations of antiviral, e.g. 125 µM, both aciclovir and valaciclovir totally inhibited the CPE of the MEF monolayer. As a result, zero plaques were detected within any of the eight replicate wells. Further dilution of aciclovir concentration from 125 µM to 2.50 µM also completely abrogated plague formation. It was not until 1.25 µM that viral plaques were detected in the monolayer cultured with aciclovir. Furthermore, valaciclovir was equal to, if not slightly superior to aciclovir; in inhibiting MCMV replication within MEF as plaque formation did not occur until 0.50 µM (Figure 3.7).

The average number of plaques per well was normalised to the highest number of plaques observed at 0 µM concentration of antiviral(s) (Figure 3.7 B). Normalisation of the mean PFU/well reduced the variability between the two assays. Both aciclovir and valaciclovir were equally efficacious and showed similar kinetics in their inhibition of plaque formation within the MEF monolayer.

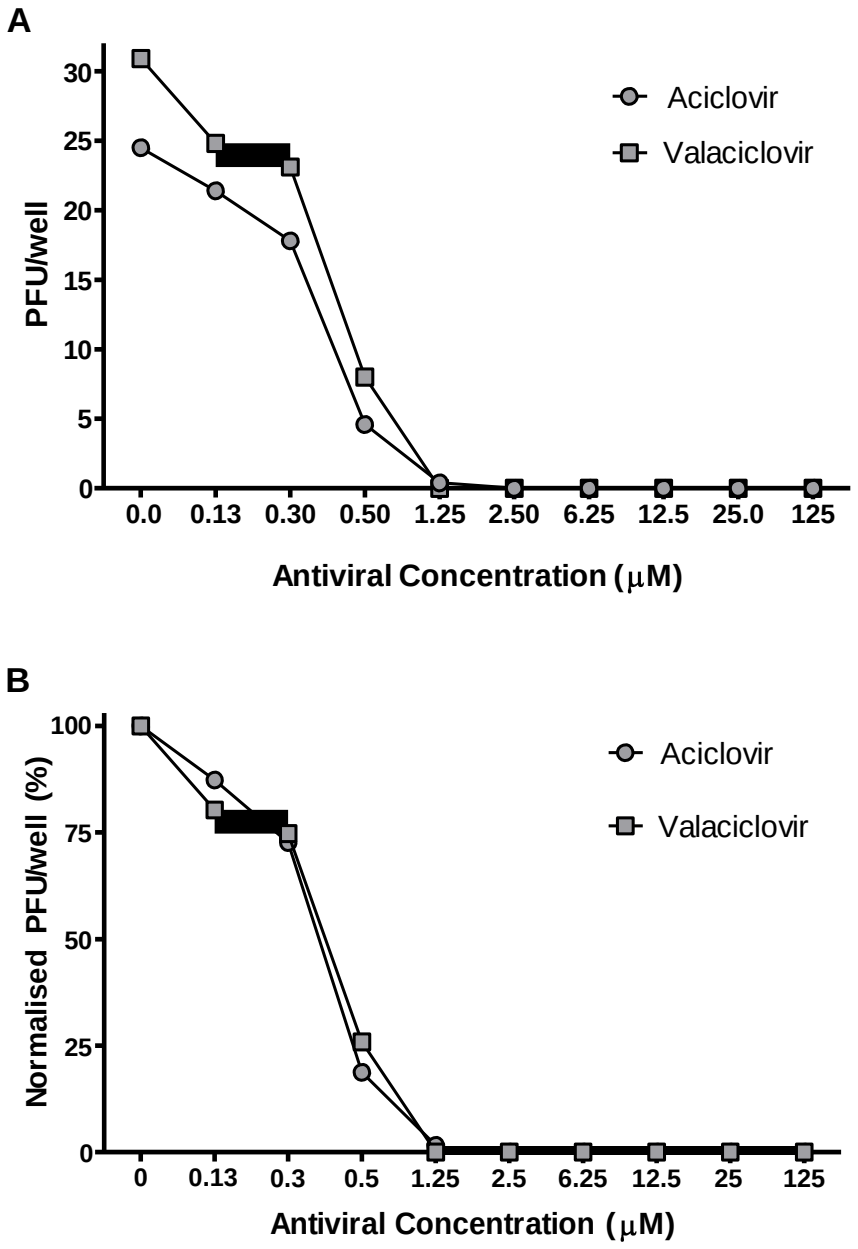

Figure 3.7. Nucleoside analogues inhibit plaque formation in MCMV infected fibroblasts. Micro-plaque reduction assay: MEFs were co-cultured in media containing aciclovir or valaciclovir (zero to 125 μM) and infected with the MCMV *Smith* strain at an MOI≈0.01. The mean number of PFU was determined at each antiviral concentration following four days incubation. X-axis antiviral concentration (μM), Y-axis shows mean PFU/well (A), y-axis shows normalised PFU/well (%) (B).

3.1.3. ESTIMATION OF THE EC_{50} OF ACICLOVIR AND VALACICLOVIR *IN VITRO*

The *Smith* strain of MCMV displayed a similar level of sensitivity to both acycloguanosines in the micro-plaque reduction assay (μPRA). To calculate half the maximal inhibitory concentration (EC_{50}), dose response curves for aciclovir and valaciclovir were generated (Figure 3.8). The EC_{50} of aciclovir was estimated to be 0.52 μM and similarly valaciclovir 0.51 μM.

EC_{50} Aciclovir	EC_{50} Valaciclovir
y = mx + c	y = mx + c
y = 80.17x + 8.96	y = 79.13x + 9.32
x = **0.52 μM**	x = **0.51 μM**

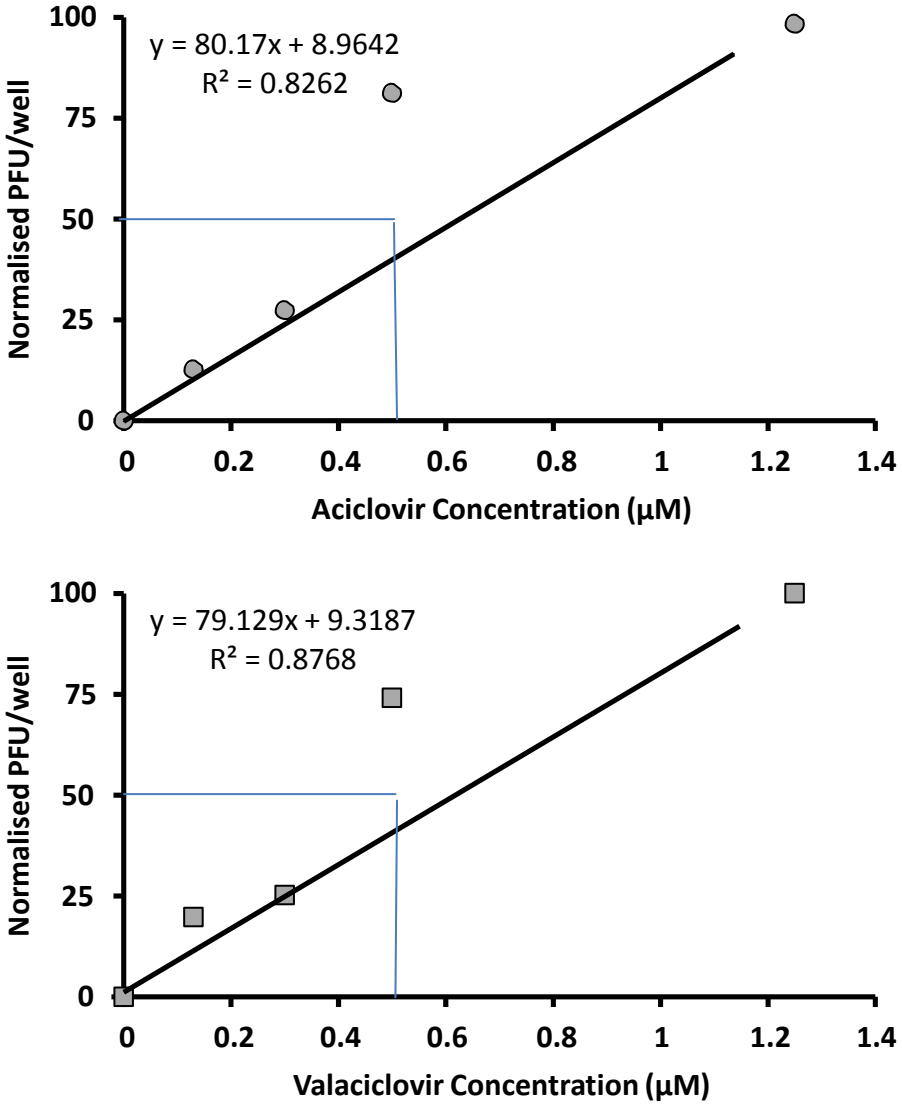

Figure 3.8. Nucleoside-analogue dose-response. Top: aciclovir and Bottom: valaciclovir dose-response curves. X-axis antiviral concentration (µM) vs. Y-axis normalised PFU/well. Linear line of best applied, line equation and R^2 also shown.

3.2. SHORT TERM VALACICLOVIR TREATMENT PARTIALLY REDUCES THE MCMV-SPECIFIC IMMUNE RESPONSE

I hypothesised that to reduce the MCMV-specific immune response valaciclovir treatment given for a period that extends beyond the half-life of the inflationary T-cells would inhibit any stochastic DNA-replication and prevent the repopulation of the virus-specific/effector memory $CD8^+$ T-cells. Therefore, six-eight week old female C57BL/6 mice were inoculated with 1 $x10^6$ PFU of MCMV *Smith* (n=20). Mice were examined at one year p.i. to determine MCMV-specific memory inflation (n=4). Subsequently half of the mice were given valaciclovir for three months (90 days, n=4) or six months (180 days, n=4) and the frequency of MCMV-specific $CD8^+$ T-cells compared to untreated mice (Figure 3.9 A).

The valaciclovir treatment consisted of the antiviral being orally available *ad libitum* in the drinking water. The antiviral suspension was changed up to twice weekly. The average volume of drinking water consumed by the cage of animals was recorded and the average fluid intake consumed by each mouse per day was determined; this figure was then converted into an equivalent dose for a 75 kg individual (Figure 3.9 B). The average daily volume of drinking water consumed per day per mouse was 3.66 ml. The drinking water contained 1 mg/ml valaciclovir in suspension. Therefore, each mouse consumed on average 3.66 mg of valaciclovir per day. The average mass of a one year old mouse was measured to be 30 g therefore the equivalent dose in a 75 kg human would be 9.10 g/day equivalent to doses used in transplant patients [339, 340]. The dose of antivirals given to the mice was estimated to excessive of that needed to supress MCMV infection *in vivo*.

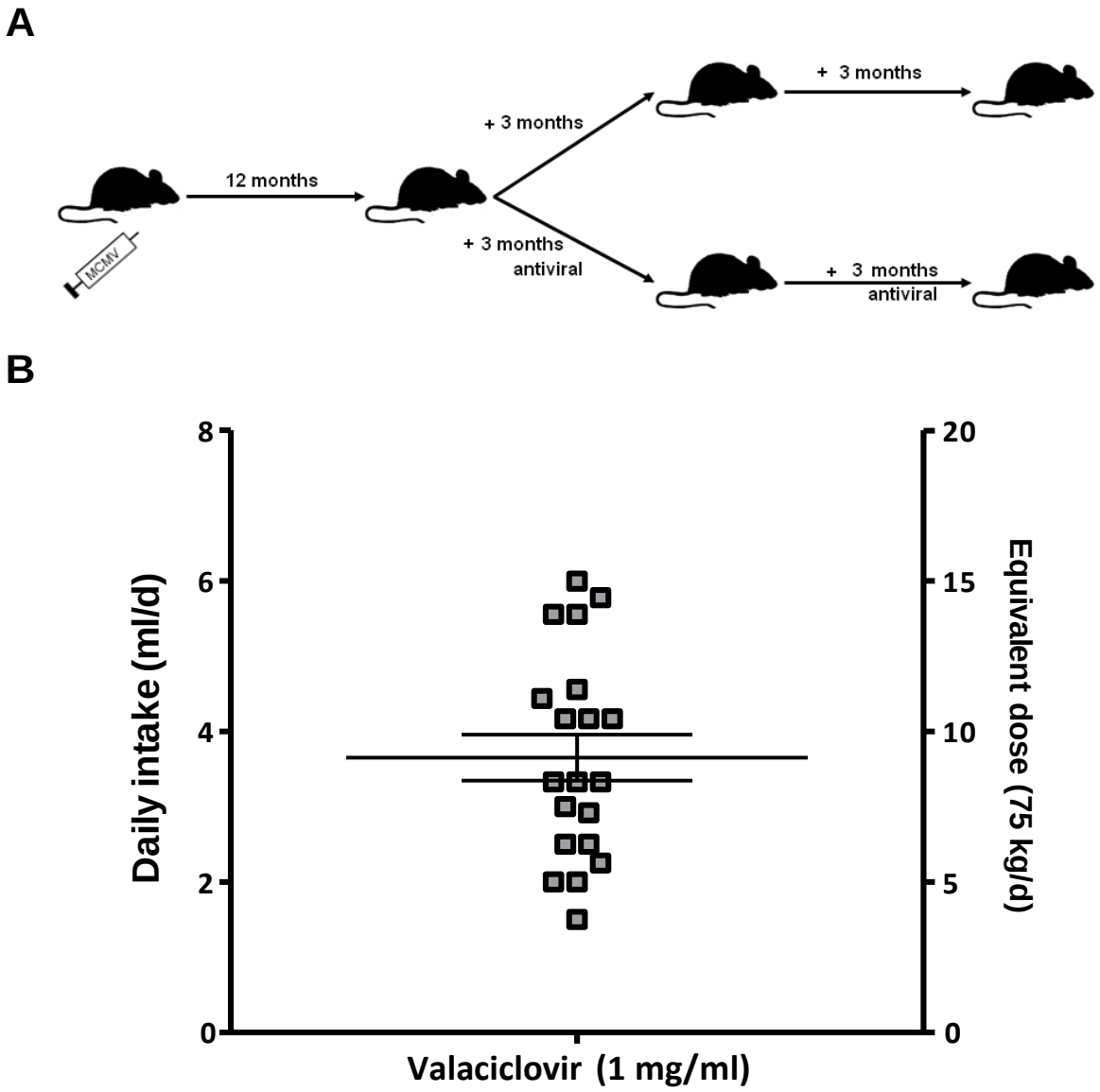

Figure 3.9. Valaciclovir treatment of MCMV infection in elderly mice. A) C57BL/6 mice were infected i.p with 1 x10^6 PFU MCMV *Smith*. After 12 months the mice were divided into either the untreated arm or the oral valaciclovir (1 mg/ml) treated arm for a total of three or six months. The MCMV-specific $CD8^+$ T-cell response was determined at 12, 15 and 18 months p.i. B) Left axis average daily fluid intake by the mice fed oral valaciclovir in their drinking water (ml/d). Right axis equivalent valaciclovir dose for an adult (75 kg/d).

3.2.1. MEASURING THE EFFECT OF 3 AND 6 MONTHS ANTIVIRAL LONGITUDINAL MCMV-SPECIFIC IMMUNE RESPONSE

The inflationary MCMV-specific $CD8^+$ T-lymphocytes (M38, m139 and IE3) were shown via adoptive transfer into SPF animals to have a half-life of approximately 45-60 days [165]. Therefore, to repopulate the inflationary memory pool lymphocytes from the T_N and T_{CM} $CD8^+$ T-cell reserves are believed to be activated through MCMV reactivation and antigen presentation [341]. To inhibit the formation of new antigen-dependent inflationary $CD8^+$ T-cells valaciclovir was initially administered one year p.i. for three or six months (double-to-four times the expected half-life of the short-lived effector cells). Initially antiviral treatment only caused small fluctuations in the frequency of MCMV-specific cells (determined by ICS); however, six months of valaciclovir did cause partial attrition of all MCMV-specific $CD8^+$ T-cell responses measured.

Taking the frequency of M38-specific CTLs as an example, at 12 months p.i. 3.71% of $CD8^+$ T-cells produced IFNγ in response to *ex vivo* stimulation. M38-specific memory inflation continued to occur, rising to 5.51% (at 15 months p.i.) and 8.07% (18 months) in the untreated mice. Whereas, with the addition of antiviral therapy memory inflation was lessened; at 15 months to 3.57% and only 4.92% by 18 months p.i. (Figure 3.10 C, Table 3.3). In summary, following six months of antiviral treatment the M38-specific immune response was 40% smaller compared with animals that did not receive any treatment.

The proportions of the m139-specific CTLs showed similar, although not identical, kinetics to M38-specific cells. Short-term (three months) treatment was ineffective at reducing the

MCMV-specific response. For example, memory inflation continued for m139-IFNy specific cells between more than doubled between 15 (6.64%) and 18 months (14.13%) p.i. Comparing this frequency to the mice that received 6 months of valaciclovir, fewer than 9% of $CD8^+$ T-cells were m139-specific at 18 months p.i. (Figure 3.10 D, Table 3.3).

In the spleens of valaciclovir treated mice IE3-specific $CD8^+$ T-cells accumulated to become the most immunodominant T-cell population reaching 10.48% of $CD8^+$ T-cells at 18 months p.i. (Figure 3.10 E, Table 3.3). The IE3-response in MCMV untreated mice was approximately 10% higher than that in the valaciclovir treated mice (Figure 3.10 E, Table 3.3). It was surprising that the three inflationary T-cell populations all responded differently to the same period of treatment. Without further investigation the reason(s) why the IE3-response was least affected by six months antiviral treatment may correspond to the delayed kinetics in which these cells accumulate compared to the M38 and m139 antigen-specific T-cells [165]. The IE3 antigen is thought not to generate T-cell proliferation during the acute immune response and consequently may be expressed at higher levels during latency. The IE3 gene has been characterised as being an immediate-early viral product essential in reactivation from latency, therefore antigens expressed prior to DNA-replication such as the IE ORFs may be least affected by treatment due to the presence of pre-existing translated products made prior to the antiviral exerting an effect.

The frequency of M45 and M57-specific $CD8^+$ T-cells fluctuated less than m139 and IE3-specific T-cells (Figure 3.10 A+B). The M45 and M57-specific $CD8^+$ T-cells were previously demonstrated to have higher expression of CD27, CD122 and CD127 on their cell surface

than the inflationary subsets of MCMV-specific cells [165]. The CD27 co-stimulatory receptor is usually down-regulated on the CTL surface upon its interaction with its CD70 ligand on the APC and likewise the presence of cell surface cytokine receptors suggests the cell is still very capable of replicating via homeostatic proliferation; they were also shown to have a half-life of approximately 120 days following adoptive transfer into naïve animals [165]. Therefore, antiviral treatment administered for greater than three months could reduce the proportion of the most highly differentiated M45 and M57-specific $CD8^+$ T-cells which are maintained by sporadic TCR stimulation and not self-proliferation [165]. Following six months of valaciclovir treatment, the frequency of M45 CTLs was reduced from 8.5% to 5.2% and M57 CTLs from 7.9% to 4.7% of $CD8^+$ T-cells suggesting the "non-inflationary" T-cells require viral reactivation (Figure 3.10 A+B, Table 3.3).

Although none of the reductions in CTL frequencies was statistically significant by non-parametric analysis, the data is suggestive that the maintenance of high frequencies of MCMV-specific $CD8^+$ T-cells is sensitive to current pharmacological therapies. The magnitude of the MCMV-specific $CD8^+$ T-cells was not ablated by treatment, which suggests either homeostatic mechanisms are partially compensating or the virus is able to survive in niches in the presence of the antiviral.

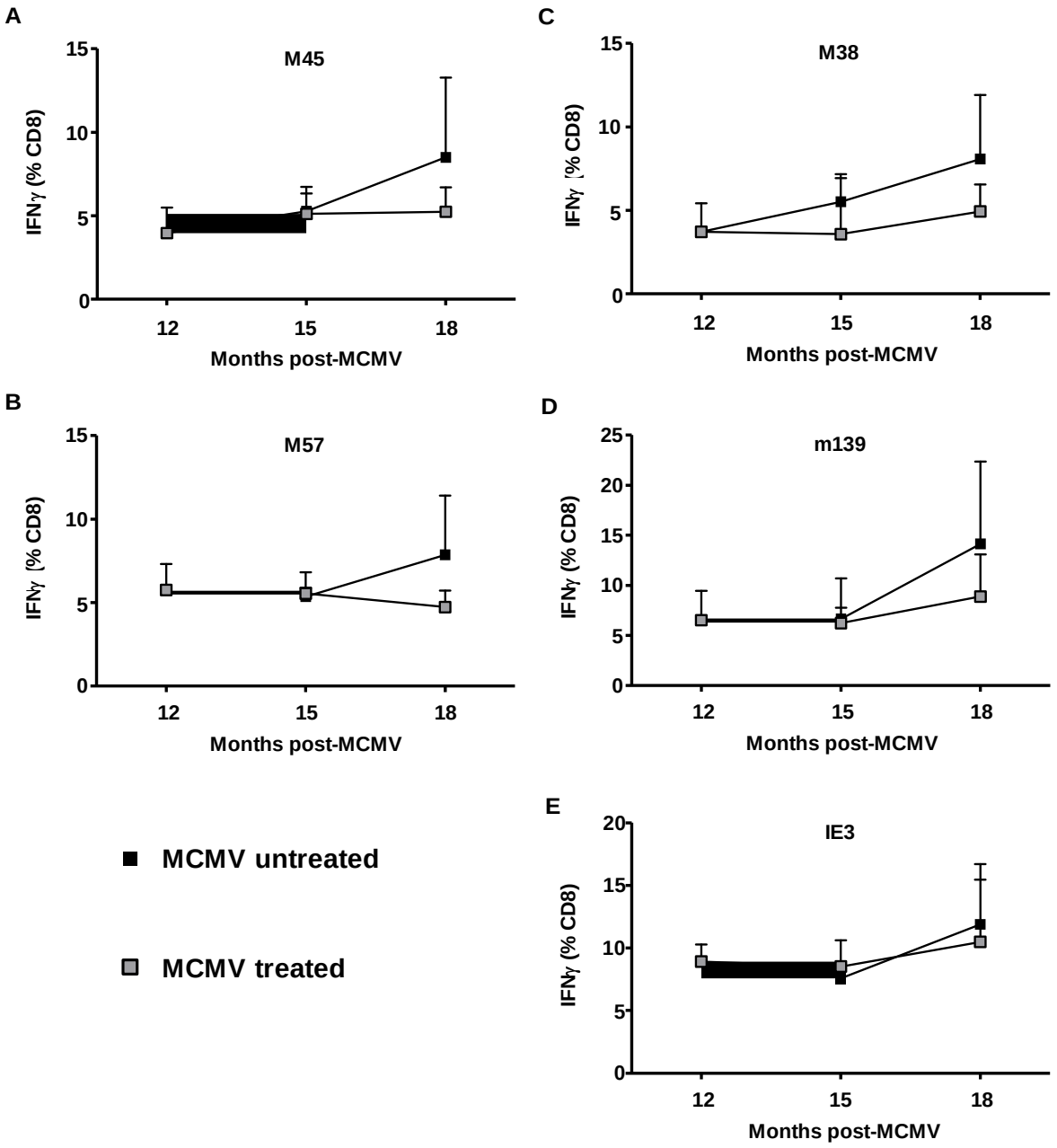

Figure 3.10. Valaciclovir treated mice have reduced frequencies of MCMV-specific $CD8^+$ $IFN\gamma^+$ T-cells. Frequency of M45 (A), M57 (B), M38 (C), m139 (D) and IE3-specific (E) $CD8^+$ T-cells in MCMV untreated (black squares) and antiviral treated (grey squares) mice. Mean +/- SEM (n=3-4).

Table 3.3. Frequency of *MCMV*-specific CTLs determined by ICS at 12, 15 and 18 months post-infection +/- three or six months valaciclovir treatment. Mean +/- SEM.

			IFNγ (% CD8)		
		MCMV untreated		MCMV treated	
Epitopes	**12 months**	**15 months**	**18 months**	**15 months**	**18 months**
M38	3.71 +/- 0.99	5.51 +/- 0.95	8.07 +/- 1.92	3.57 +/- 1.93	4.92 +/- 0.82
M45	3.96 +/- 0.89	5.27 +/- 0.61	8.50 +/- 2.39	5.11 +/- 0.94	5.24 +/- 0.73
M57	5.74 +/- 0.91	5.36 +/- 0.31	7.86 +/- 1.78	5.55 +/- 0.73	4.72 +/- 0.50
m139	6.51 +/- 1.70	6.64 +/- 0.65	14.13 +/- 4.11	6.24 +/- 2.57	8.89 +/- 2.10
IE3	8.90 +/- 0.79	7.57 +/- 0.21	11.88 +/- 2.40	8.51 +/- 1.21	10.48 +/- 2.49

3.2.2. MCMV TREATED MICE HAVE FEWER $CD8^+$ $CD62L^-$ T-CELLS

MCMV infection and the associated memory inflation causes the massive expansion of T_{EM} which do not express CD62L [165]. Using CD62L as an indirect marker of T-cell activation three subsets of $CD8^+$ T-cells can be determined: they are the $CD62L^-$, $CD62L^{lo}$ and $CD62L^{hi}$ T-cells (Figure 3.11 A + B).

18 months post-MCMV infection, untreated MCMV infection resulted in an accumulation of over 70% of $CD8^+$ T-cells having no expression of CD62L on the cell surface whereas six months treatment the frequency of $CD8^+$ $CD62L^-$T-cells was reduced to below 40% (*P<0.05) (Figure 3.11 B). There was no difference in the frequency of $CD62L^{lo}$ expressing $CD8^+$ T-cells between the MCMV untreated (8.2%) and MCMV treated (7.5%) groups of mice (Figure 3.11 B). Corresponding to the accumulation of $CD62L^-$ cells in untreated mice the $CD62L^{hi}$ population constituted only 15% of $CD8^+$ T-cells in untreated mice whereas over 52% of $CD8^+$ T-cells in the treated group were $CD62L^{hi}$ (*p<0.05) (Figure 3.11 B). These data demonstrate that MCMV causes a high-level of T-cell stimulation in latently infected mice that is reversible through antiviral treatment. Importantly, the $CD62L^{hi}$ subset is the least differentiated subset of $CD8^+$ T-cells that includes the naïve lymphocytes that are partly responsible for *de novo* immunity.

To assess if valaciclovir treatment was directly responsible for the increased CD62L expression on $CD8^+$ T-cells was determined the effect of high doses of antiviral directly upon splenocytes *ex vivo* (Figure 3.11 C). Lymphocytes were isolated from the spleen of a single MCMV infected mouse. The cells were cultured for 24 hours in media containing valaciclovir

exceeding the EC_{50} required to suppress MCMV replication in MEFs (Figure 3.6 + 3.7). The percentage of $CD8^+$ $CD62L^-$ T-cells was determined in the absence of antiviral where only 10.5% of cells retained the expression of CD62L. Those splenocytes cultured with valaciclovir (0-100 μM) did not gain further expression of CD62L (Figure 3.11 C). The antiviral is unlikely to indirectly raise CD62L expression however to confirm this antiviral treatment should also have been administered to uninfected mice *in vivo*.

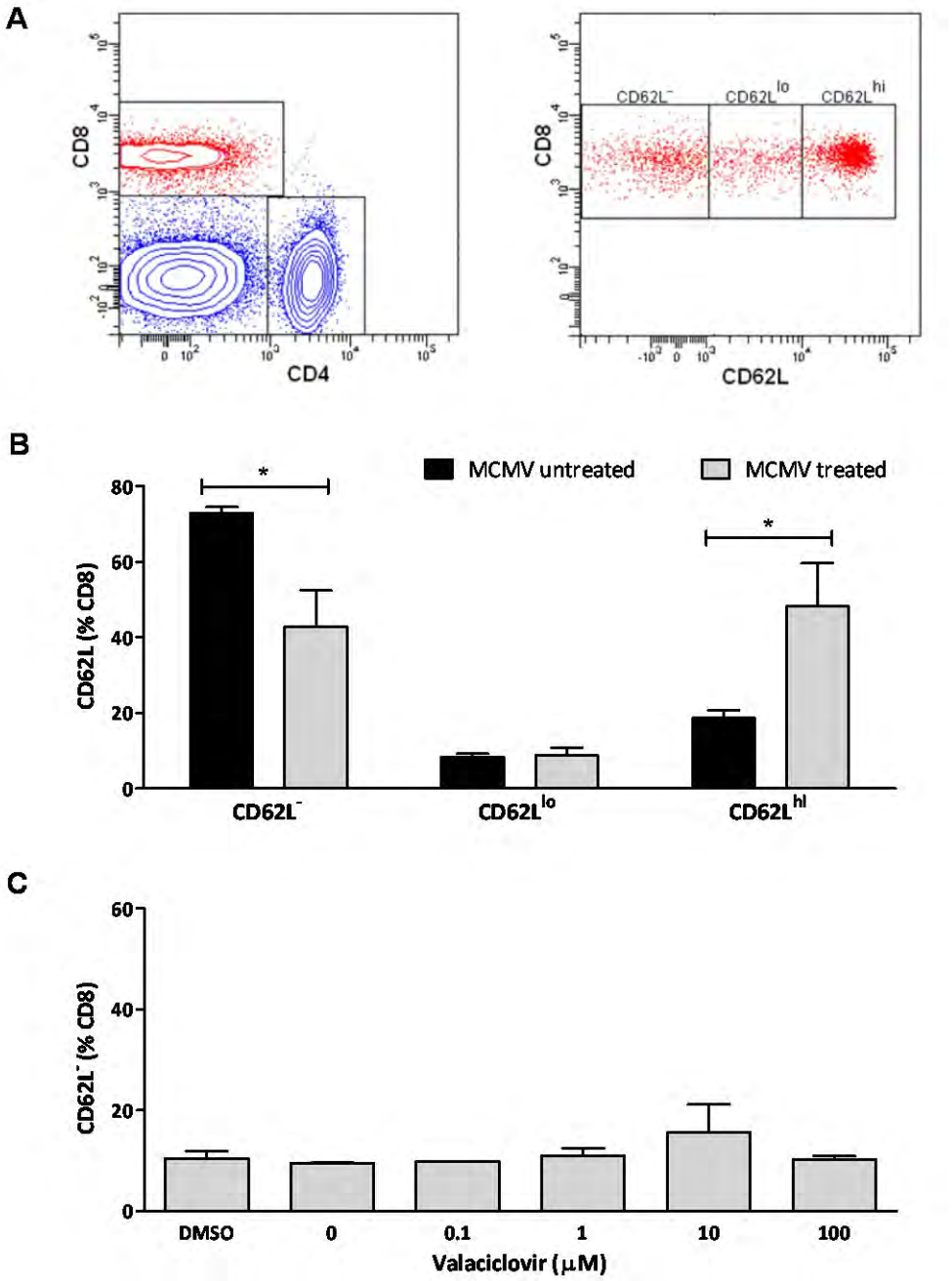

Figure 3.11. MCMV untreated mice have elevated frequencies of $CD8^+$ $CD62L^-$ T-cells. A) Gating of $CD62L^-$, $CD62L^{lo}$ and $CD62L^{hi}$ $CD8^+$ T-cells. B) Frequency of $CD62L^-$, $CD62L^{lo}$ and $CD62L^{hi}$ $CD8^+$ T-cells six months post-antiviral treatment. Mean +/- SEM (n=3-4). Data analysed by 2way-ANOVA (*p<0.05). C) Mean $CD62L^+$ $CD8^+$ T-cells isolated from the spleen. Splenocytes (1 x10^6) were cultured for 24 hours in media containing valaciclovir (0-100μM) and percentage of $CD62L^-$ cells recorded.

3.3. MONTHS VALACICLOVIR TREATMENT DOES NOT REDUCE MCMV-SPECIFIC IgG

Elevated anti-HCMV-specific IgG titres have been correlated to increased rates of vaccine failure and mortality in elderly individuals. Therefore, it was sought to determine if prolonged valaciclovir treatment would suppress the generation of anti-MCMV-specific IgG.

ELISA determined humoral immunity for anti-MCMV-specific IgG. The standard curve generated to show non-specific binding of pooled serum from uninfected mice and MCMV infected mice to a mock-infected lysate. Anti-MCMV-specific IgG binding was determined by showing the $OD_{450\ nm}$ of pooled MCMV-infected sera binding to an MCMV-infected lysate (Figure 3.12 A). Antiviral treatment did not significantly reduce the anti-MCMV-specific IgG titre at either three or six months of antiviral treatment in comparison to untreated mice (Figure 3.12 B).

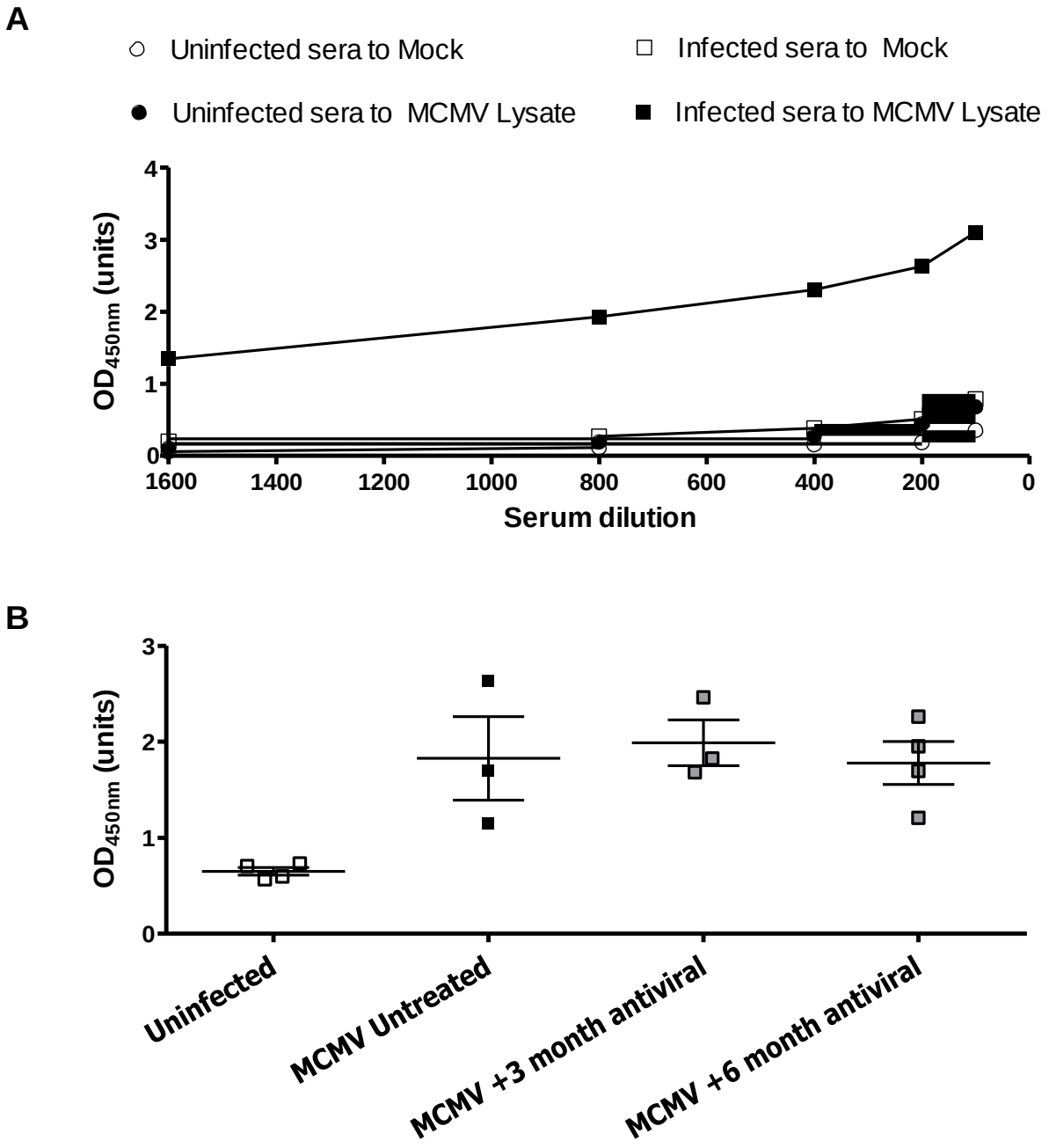

Figure 3.12. Valaciclovir treatment does not reduce the anti-MCMV specific IgG titre. A) Binding of uninfected sera to mock (open circles) and MCMV lysate (black circles) and binding of MCMV-infected sera to mock (open squares) and MCMV lysate (black squares). B) MCMV-specific IgG titre from uninfected animals, MCMV infected mice and following three and six months treatment. Mean +/- SEM (n=3-4).

3.4. PROLONGED TREATMENT (12 MONTHS) CAN SIGNIFICANTLY REDUCE THE MCMV-SPECIFIC CD8$^+$ T-CELL RESPONSE

In a third experimental setting, animals were infected with MCMV and six months p.i. the mice were separated into untreated (MCMV untreated) or the antiviral therapy (MCMV treated) groups. Treatment was administered for 12 months and the magnitude of the MCMV-specific CD8$^+$ T-cell response was recorded 18 months after the initial inoculation (Figure 3.13 A).

12 months of antiviral treatment did not affect the cellularity of the spleen. The average number of cells was determined between the MCMV untreated and Valaciclovir treated groups of animals 18 months post infection. The data shows a relatively small increase in the number of lymphocytes that is not statistically significant. On average the spleens from the MCMV untreated mice contained 16.9x10^6 cells compared to 21.4x10^6 in the MCMV treated group (Figure 3.13 B). This concludes that antiviral treatment does not affect the cellularity of the spleen.

The frequency of MCMV-specific CD8$^+$ T-cells was determined by ICS and compared between the two groups at 18-month p.i. (+/- 12 months treatment). In all instances, the frequency of antigen-specific lymphocytes was lower in the treated than the untreated mice. The M38 and M45 IFNγ$^+$ producing CD8$^+$ T-cells comprised around 5% of CD8$^+$ T-cells in the untreated mice and by comparison were reduced to approximately 1% in the treated mice (a relative

reduction of 80%) (Figure 3.13 C). The most significant reductions were observed in relation to the frequency of IE3 CTLs. In untreated mice 8.4% of $CD8^+$ T-cells were IE3-specific compared to only 2% in the valaciclovir treated mice (a relative reduction of 83%) (Figure 3.13 C).

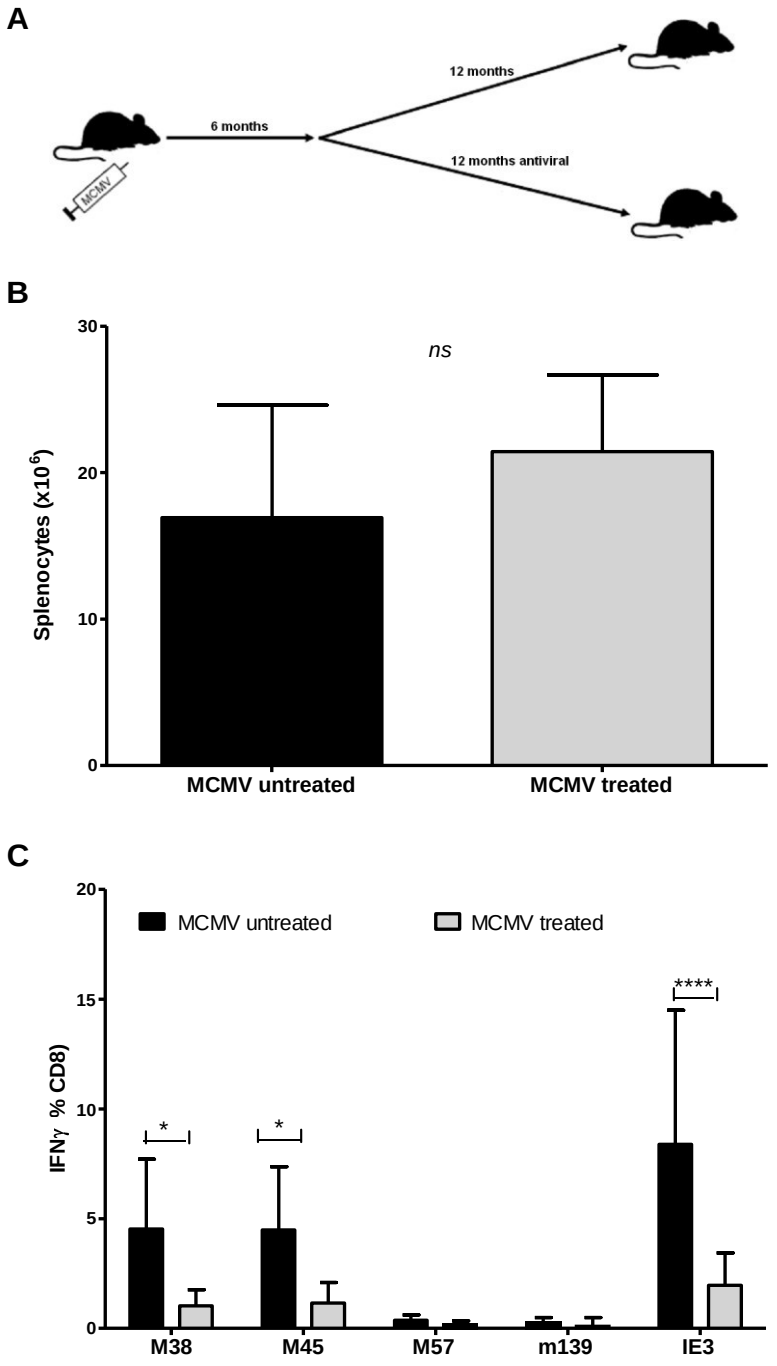

Figure 3.13. Prolonged valaciclovir treatment does not affect cellularity and leads to large reductions in MCMV-specific CTLs. A) Mice infected i.p. 1x10^6 PFU *Smith*. After six months animals divided into untreated (MCMV untreated n=7) or received valaciclovir (MCMV treated n=8). B) Number of splenocytes 18 months p.i. Mean +/- SEM. Data analysed by

Mann-Whitney U test. C) Frequency $CD8^+$ $IFN\gamma^+$ splenocytes 18 months p.i. Mean +/- SEM. Data analysed by 2-way ANOVA.

3.5. RESULTS CHAPTER 1: CONCLUSIONS

Memory inflation is a phenomena observed in CMV infected animals. Both aging and HCMV infection cause an expansion of oligoclonal T-cells in the peripheral blood. The HCMV-specific $CD8^+$ T-cell surface phenotype is primarily highly differentiated ($CD45RO^-$ $CD57^+$ $CCR7^-$ $CD27^-$ $CD28^-$ $CD95^+$ $CTLA4^+$) [156, 342] likewise the cells that accumulate during MCMV infection are also highly differentiated ($CD44^+$ $CD27^-$ $CD62L^-$ $CD122^-$ $CD127^-$ $KLRG1^+$ $NKG2D^+$) [165]. Here, in the first experiment, MCMV *Smith* infected C57BL/6 mice developed an accumulation of $CD8^+$ $CD44^+$ $CD62L^-$ T-cells (T_{EM}) which were tracked to show the dynamic effect MCMV has upon memory T-cell subsets (Figure 3.2). Primary MCMV inoculation corresponded to the generation of T_{EM} and consequently the proportion of T_N lymphocytes decreased. Coinciding with the resolution of infection (week 5) the T_N population managed to repopulate itself with naïve T-cell output maintained up to 16 weeks after infection. However, between week 16 and 52 the accumulation of T_{EM} lymphocytes occurred at such a rapid rate that there was an inversion between the T_N and T_{EM} populations. Crucially others have shown that murine naïve $CD8^+$ T-cells ($CD38^+$ $TREC^+$) are maintained through thymic output and not through peripheral T-cell division [328] therefore the reduced frequency of naïve T-cells observed can be attributed to underlying MCMV infection. At 52 weeks p.i. the MCMV untreated mice had 50% fewer T_N than uninfected mice (Figure 3.3) and therefore would be expected to have a reduced capacity to respond to other infections.

The expansion of virus specific ($CD8^+$ $IFN\gamma^+$) T-cells was then determined in a separate experiment (Figure 3.5). *Ex vivo* peptide stimulation and the synthesis of proinflammatory cytokines by the CTLs enabled the immune response to be monitored during primary

infection and the latent/chronic phase of infection where memory inflation occurs for known specific viral epitopes. The ICS protocol proved to be highly successful with virus specific immune responses detected towards immunodominant epitopes of M38, M45, M57, m139 and IE3 throughout the course of infection. Peak primary immune responses were measured at days seven and 14, for the five antigens, with contraction of the immune response between day 14 and 36 p.i. Memory inflation of epitope-specific $CD8^+$ $IFN\gamma^+$ T-cells occurred between day 36 and day 116. The accumulation of M45 and M57 specific cells is in contrast to what is observed in other previously published models of MCMV also induced memory inflation [165, 196]. The most likely mechanism that explains the high frequency of M45 and M57 virus-specific T-cells is because of strain variations or via cross-presentation of microbial/dietary antigens which are likely to vary between institutions and are known to modulate $CD8^+$ T-cell immunity to MCMV [178, 343].

I was unable to quantify viral reactivation as the MCMV genome was undetectable from 16 weeks p.i. in the salivary gland (Figure 3.4) and were unfortunate that the reaction was not sensitive enough to detect latent MCMV in other tissues.

The acycloguanosine class of antivirals have a broad spectrum of activity. To initiate activity acycloguanosines require phosphorylation first mediated by a viral TK and then by two cellular kinase enzymes. MCMV does not encode a typical TK yet is remains sensitive to acycloguanosine via M97 mediated phosphorylation of the antiviral [194, 344]. The efficacy of aciclovir and valaciclovir towards MCMV strain *Smith* was assessed *in vitro* using the µPRA. Lytic replication and plaque formation was completely inhibited with both antivirals at

concentrations exceeding 1.25 µM (Figure 3.7). The EC_{50} of aciclovir and valaciclovir towards the *Smith* strain of MCMV was calculated to be approximately 0.5 µM (Figure 3.8), demonstrating MCMV to have an equivalent level of sensitivity to acycloguanosines as both HSV-I and HSV-2 [345]. Due to this similarity in antiviral efficacy valaciclovir was selected as the optimal candidate to suppress MCMV replication *in vivo* due to improved bioavailability [346]. Oral valaciclovir has an *in vivo* half-life of approximately two hours [346] therefore to constantly suppress lytic MCMV infection a 1 mg/ml valaciclovir hydrochloride suspension was available *ad libitum* in the animal's drinking water to ensure a sustained dose. Due to the stability of valaciclovir in solution the antiviral containing drinking water was changed up to twice weekly [347]. On average the 30 g mice consumed approximately 4 mg of antiviral per day which equates to an almost equivalent dose of 10 g/day for a 75 kg adult (Figure 3.9) and is therefore comparable to the high doses administered to suppress HCMV reaction post-transplantation [339].

An improvement to these studies would be to quantify the *in vivo* dose of valaciclovir or its metabolites in the serum. Following oral acycloguanosine treatment a valaciclovirase, e.g. biphenyl hydrolase-like protein, cleaves the ester bond from valaciclovir to convert the drug into aciclovir [121-124]. During the first-round of metabolism aciclovir is converted into 9-[(carboxymethoxy) methyl]guanine (CMMG) by an alcohol dehydrogenase and aldehyde dehydrogenase with CMMG converted into 8-hydroxy-aciclovir (8-OH-ACV) by a further oxidation mediated by an aldehyde oxidase enzyme [348-350]. Aciclovir and its metabolites CMMG and 8-OH-ACV can be accurately measured using liquid chromatography/mass

spectrometry and this data would be useful in conjunction with accurate viral load data to assess at what *in vivo* concentration lytic MCMV reactivation can be completely suppressed.

Having shown C57BL/6 mice infected with MCMV *Smith* developed memory inflation (T_{EM} or $CD8^+$ $IFN\gamma^+$ T-cells) and that valaciclovir inhibited lytic MCMV replication *in vitro* the antiviral treatment was given to suppress sporadic MCMV reactivation *in vivo*. Aciclovir has previously been used to suppress MCMV titres in Swiss-Webster mice [344] where the drug was shown to have a high affinity for the MCMV DNA-polymerase and lead to ablation of MCMV titres in all tissues (except the salivary gland) [344]. Rarely is the MCMV-specific immune response monitored for more than 12 months due to the costs associated with keeping the animals. Consequently, this model is amongst the first to mimic the early acquisition of CMV, to assess the how the T-cell response to the virus changes into aged population of animals and to compare the effect of valaciclovir treatment on the CTL response. The old age of these animals is unlikely to be achieved by wild mice due to predation, disease, consequently the 18-month-old mice in this experiment can be considered elderly, and the memory inflation observed in the mice could serve as an indication of treating HCMV clonal expansions in elderly humans.

Initially, three months of valaciclovir treatment proved to be an insufficient period to affect the frequency of virus-specific $CD8^+$ T-cells (Figure 3.10 A-E) which was similar to the findings of Snyder *et al* (2011) [193]. When treatment was given for a total of six months the frequency of $CD8^+$ $IFN\gamma^+$ T-cells were partially reduced in the region of 10-30% (depending on the epitope) in in the MCMV treated mice compared with the untreated mice (Figure 3.10 A-

E). Yet when the antiviral was administered for 12 months highly significant reductions were observed for three of the five $CD8^+$ $IFN\gamma^+$ T-cell responses recorded (with the M57 and m139-specific measurements thought to have failed due to a technical matter). The M38, M45 and IE3 CTL response were all 80% or more greater in the untreated mice compared with the mice that received that antiviral treatment (Figure 3.3 C). This effect was not due to a reduction in absolute lymphocyte numbers (Figure 3.13 B). It appears likely that almost all MCMV $CD8^+$ T-cell responses are sensitive to antiviral treatment.

It was suggested that memory inflation is not dependent on the source of antigen and the kinetics in which it they are expressed, however it is interesting to discuss the source of the three immunodominant $CD8^+$ T-cell responses. One year post MCMV infection the most frequent $CD8^+$ T-cell response was directed was towards the IE3 epitope. Almost 9% of the entire $CD8^+$ T-cell population was specific for this immediate early protein antigen. IE3 is homologous to IE1 that encodes for an inflationary epitope in HCMV HLA-A2 individuals [147]. IE3 is a transactivator of subsequent gene synthesis and critical in the reactivation of latent MCMV. Therefore, it is unsurprising that an IE3 gene product is a target of such large MCMV-specific immune responses. The second most immunodominant immune response was directed towards the m139 epitope (6%). The m139 gene is a member of the US22 family, which is well conserved in HCMV strains. The m139 protein forms part of complex with m140 and m141 proteins [337] and co-localises in the cis-Golgi within the infected cell cytoplasm. The US22 complex is an early gene product and is essential for viral replication in macrophages [338]. m139 is required for lytic replication within macrophages therefore it is an ideal target for $CD8^+$ T-cells. The M38 epitope did not inflate to the same extremes as has

been observed in other studies (>3.5% rather than 10%) [165]. M38 and its family member m38.5 are believed to be viral immune evasion genes. The m38.5 protein is expressed as an early gene product and prevents Bax-mediated apoptosis, however the evasion molecule does not protect against Bak-induced cell death [351]. M38 is a likely candidate for an inflationary immune response because MCMV infected leukocytes that express M38 evade intrinsic cell death mechanisms which results in increased viral dissemination [352].

4. RESULTS 2: ANTIVIRAL TREATMENT REJUVENATES THE IMMUNE SYSTEM OF MCMV INFECTED MICE AND LEADS TO IMPROVED IMMUNITY TO INFLUENZA CHALLENGE

4.1. DOES PRIOR MCMV INFECTION +/- ANTIVIRAL TREATMENT AFFECT *DE NOVO* IMMUNE RESPONSES TO INFLUENZA IN ELDERLY MICE?

The presence of highly differentiated HCMV-specific $CD8^+$ T-cells are implicated as accelerators of immune senescence [146, 308] and the magnitude of the HCMV immune response is correlated to reduced effectiveness of influenza vaccination [353]. In the previous chapter, it was shown that the high frequencies of MCMV-specific $CD8^+$ $IFN\gamma^+$ T-cells could be significantly reduced following 12 months antiviral treatment. Therefore, to assess if the reduction in MCMV-specific lymphocytes led to an improvement in immune function an experiment was designed to determine how prior MCMV infection with and without antiviral treatment affected an elderly animal's primary immune response to IAV challenge. To test this groups of six-eight week old female C57BL/6 mice were inoculated by i.p. injection with $1x10^6$ PFU of *Smith* MCMV. Memory inflation was allowed to develop for six months, subsequently the MCMV infected animals either remained untreated or received 12 months of oral valaciclovir treatment (1 mg/ml). After 18 months of experimental conditions, both the MCMV untreated (MCMV–AV) and antiviral treated mice (MCMV+AV) were challenged with a single i.n. inoculation of $1x10^6$ EID_{50} of clone 7a. Aged matched litter mates, which were MCMV seronegative (MCMV–neg) were also infected with clone 7a after 18 months to provide a control group to compare the IAV immune response in a previously SPF animal (Figure 4.1).

Mice were sacrificed 10 days post clone 7a challenge. The MCMV specific immune response was measured by ICS and tetramer staining to determine the effect of 12 months valaciclovir treatment. The primary clone 7a-specific immune response was also determined by measuring the frequency of NP-specific $CD8^+$ T-cells in the bronchoalveolar lavage (BAL) fluid, caudal mediastinal lymph node (CMLN) and the spleen. Non-immunological parameters such as mortality and weight loss were also recorded for the 10 days of the IAV infection.

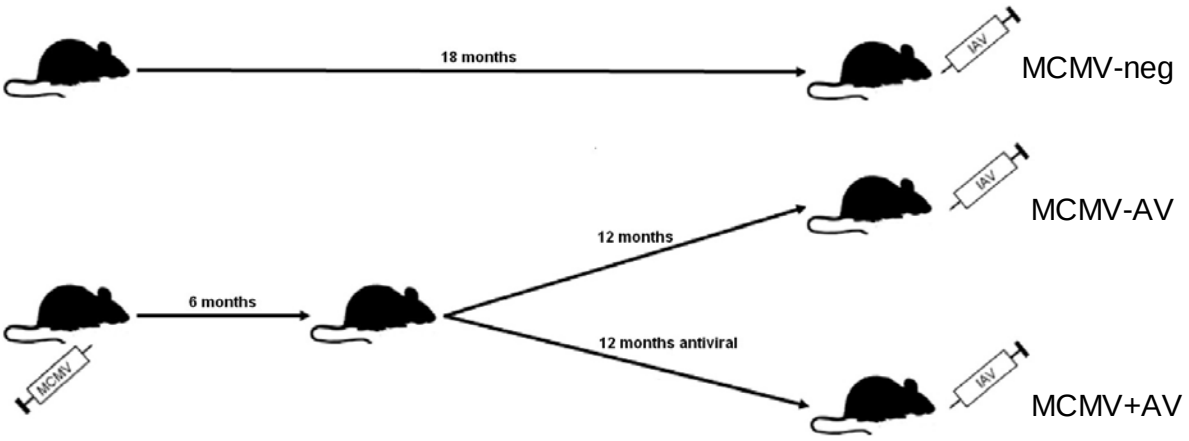

Figure 4.1 Experiment design: Does prior MCMV infection impair immunity to IAV? Mice were either MCMV seronegative and challenged with clone 7a (MCMV-neg n=5) at 18 months p.i.; MCMV seropositive, not administered antiviral and challenged with clone 7a (MCMV-AV n=8) or MCMV seropositive, antiviral treated (1 mg/ml for 12 months) and challenged with clone 7a (MCMV+AV n=4).

4.2. THE FREQUENCY OF MCMV-SPECIFIC $CD8^+$ T-CELLS IS SIGNIFICANTLY REDUCED WITH 12 MONTHS OF ANTIVIRAL TREATMENT

The MCMV-specific immune response to the five immunodominant $CD8^+$ T-cell epitopes (M38, M45, M57, m139 and IE3) were measured in the spleens of the elderly MCMV infected mice by ICS (IFNγ and TNFα) 18 months post-MCMV and 10 days after the IAV infection.

The data from previous chapter showed the prolonged course of antiviral treatment could cause over 80% attrition in the MCMV-specific $CD8^+$ T-cell response. Therefore, 12 months of antiviral treatment was again administered to MCMV infected animals (Figure 4.1). The proportion of MCMV-specific $CD8^+$ T-lymphocytes responding to peptide stimulation was again consistently lower in the valaciclovir treated group (MCMV+AV) compared with the untreated mice (MCMV-AV). For example, the frequency of $CD8^+$ $IFN\gamma^+$ T-cells maintained in MCMV-AV mice to the inflationary epitopes M38 and m139 exceeded 5% and 7% of the $CD8^+$ T-cells but was reduced to 1.5% and 2% following sustained valaciclovir treatment. The MCMV-specific $CD8^+$ T-cells whose population was most significantly reduced in frequency were those cells with specificity for the IE3 immunodominant epitope that has constantly elicited the largest immune response in the chronically infected mice. Here, in MCMV-AV mice over 12% of $CD8^+$ T-cells produced IFNγ in response to IE3-stimuli compared to less than 1% in those mice which received antiviral treatment (**$p<0.01$) (Figure 4.2 B). This is a

relative decrease of 95% in the frequency of IE3-specific $CD8^+$ T-cells and shows that pre-existing memory inflation of IE3-specific $CD8^+$ T-cells is sensitive to blocking viral replication.

Furthermore, immune responses directed against the "non-inflationary" antigens from the M45 and M57 proteins also to rely on MCMV reactivation to maintain their relative frequency in the memory pool. For example, 3% and 5% of $CD8^+$ T-cells in the MCMV-AV mice produced IFNγ in response to M45 and M57 peptide stimulation respectively. However, this frequency was reduced to below 2% for both epitopes in the MCMV+AV group of mice (Figure 4.2 B, Table 4.1). Snyder *et al* (2008) showed, via adoptive transfer of M45 and M57 antigen specific cells, that they had a longer life-span than the short-lived effectors [165] and here the antiviral seems to have been given for a sufficient length of time to suppress the M45 and M57 antigen-specific T-cells much lower dependence on antigen stimulation.

The MCMV-specific $CD8^+$ T-cells associated with memory inflation are polyfunctional and produce IFNγ, TNFα, IL-2, and visible CD107a degranulation [161, 196]. Here, the untreated MCMV-AV mice showed a very strong a positive correlation (R^2>0.98) between those virus-specific cells which produced both IFNγ and TNFα whereas the CTL response in the antiviral treated mice had a similar albeit slightly less strong correlation (R^2>0.82) (Figure 4.3, Table 4.1).

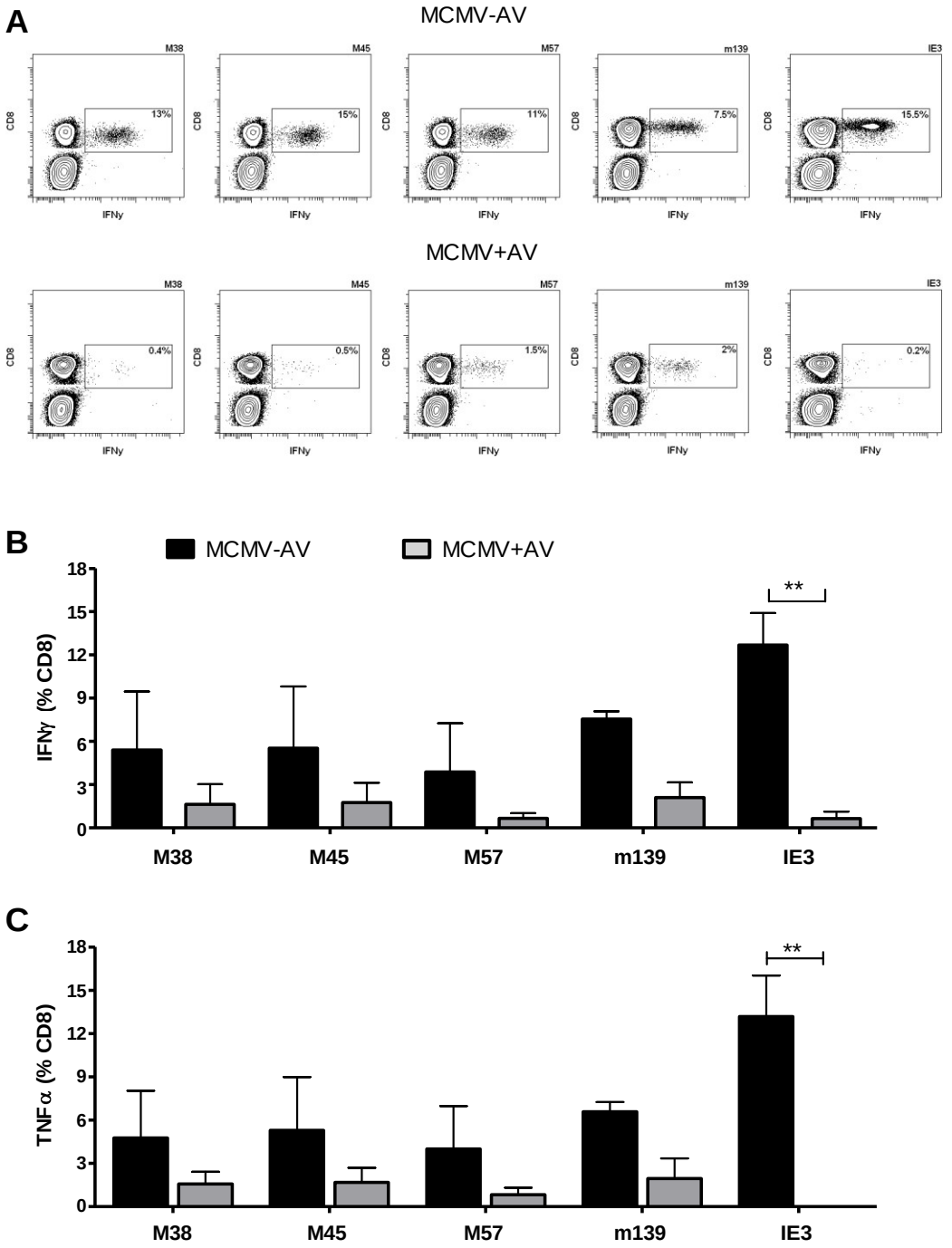

Figure 4.2. Valaciclovir treated mice have significantly reduced frequencies of MCMV-specific CD8$^+$ T-cells. A) Representative ICS FACS plots. Frequency of IFNγ (B) and TNFα (C) specific CD8$^+$ T-cells 18 months p.i. +/- 12 months antiviral treatment. Mean +/- SEM (n=3). Data analysed by 2-way ANOVA plus Bonferroni post-test (p<0.01).**

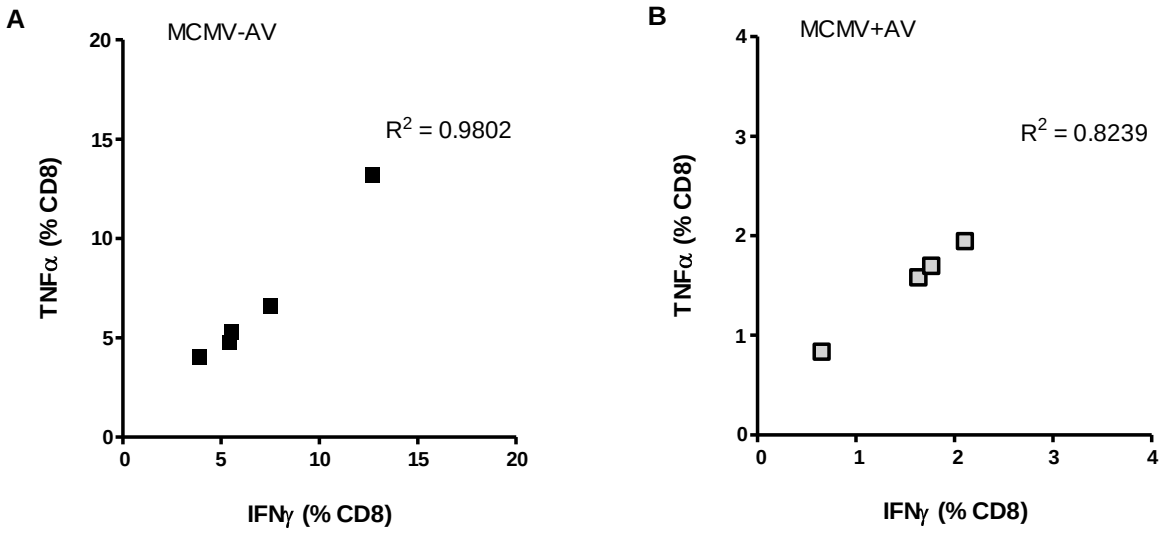

Figure 4.3. MCMV-specific CD8$^+$ T-cells remain polyfunctional. The mean frequency of the M38, M45, M57, m139 and IE3 specific CD8$^+$ T-cells producing IFNγ and TNFα following *ex vivo* peptide stimulation in MCMV-AV (A) and MCMV+AV (B) mice 18 months post-MCMV infection.

Table 4.1. Frequency of IFNγ and TNFα MCMV-specific CD8$^+$ T-cells 18 months post-MCMV infection +/- six months valaciclovir treatment. Mean +/- SEM.

	MCMV-AV (n=3)		MCMV+AV (n=3)	
	I FNγ (% CD8)	T NFα (% CD8)	I FNγ (% CD8)	T NFα (% CD8)
M38	5.40 +/- 4.06	4.77 +/- 3.29	1.63 +/- 1.39	1.58 +/- 0.85
M45	5.53 0+/- 7.29	5.29 +/- 3.70	1.76 +/- 1.37	1.70 +/- 1.00
M57	3.88 +/- 3.36	4.01 +/- 2.98	0.65 +/- 0.37	0.84 +/- 0.48
m139	7.53 +/- 0.55	6.59 +/- 0.66	2.11 +/- 1.05	1.99 +/- 1.41
IE3	12.68 +/ 2.23	13.18 +/- 2.84	0.64 +/- 0.48	-0.19+/- 0.50

4.3. THE IE3-SPECIFIC CD8$^+$ T-CELL POPULATION IS MOST AFFECTED BY ANTIVIRAL TREATMENT AND SHOWS UNUSUAL KINETICS IN RATE OF DECAY

Long-term antiviral-treatment of the latent MCMV-infection successfully reduced the frequency of in IFNγ/TNFα-producing MCMV-specific cells CD8$^+$ T-cells as detected by *ex vivo* peptide stimulation. To confirm that the observed decrease in functional response corresponded to an actual decrease in virus specific cells, IE3 and m139-specific MHC-I tetramers were used (Figure 4.4). The IE3-specific CTLs were the best candidates for tetramer staining due to the 95% reduction in IFNγ-producing cells observed in the spleens in those MCMV infected mice that received the high dose antiviral for 12 months (Figure 4.2).

Memory inflation of IE3-specific cells was evident as 14% of the entire splenic CD8$^+$ T-cell pool stained positive for the MHC-I tetramer in MCMV-AV mice (Figure 4.4 A+B). In comparison the frequency of IE3-specific cells in MCMV+AV group was below 1% of CD8$^+$ T-cell pool (Figure 4.4 A + B). Again, this equates to a relative reduction of IE3-specific CTLs of approximately 90% thus confirming the previous ICS data (Figure 4.2) showing valaciclovir treatment to be effective treatment of memory inflation.

Furthermore, analysis was continued to compare the phenotype of IE3-tetramer specific CD8$^+$ T-cells from the spleens of MCMV infected and those with antiviral treatment. Overall the phenotype of the IE3-tetramer specific CD8$^+$ T-cells detected in the spleens from the

MCMV+AV group was less differentiated than those mice which were untreated (Figure 4.4 C). MCMV-AV mice tended to have a reduced proportion of IE3-specific cells that expressed CD27, CD62L, CD122 and CD127. Significant differences were determined in the level of CD62L between the two groups. For example, expression of CD62L was approximately twenty-times less common on the IE3-specific T-cells from the MCMV-AV than the MCMV+AV group (Figure 4.4 C *$p<0.05$). The reduced CD62L expression observed on the IE3-specific cells and high expression of CD44 show that these cells are almost entirely of an T_{EM} subset in the MCMV-AV groups whereas an elevated proportion of IE3-specific T-cells in MCMV+AV also held a T_{CM} phenotype. The mean percentage expression of CD122 was also elevated in MCMV+AV treated mice (4.8%) in comparison to the untreated mice where expression of CD122 was almost absent (0.2%) (*$p<0.05$). The CD122 antibody labels the gamma-chain of the IL-15Rβ, its ligand (IL-15) provides a proliferative signal to the lymphocyte [354].

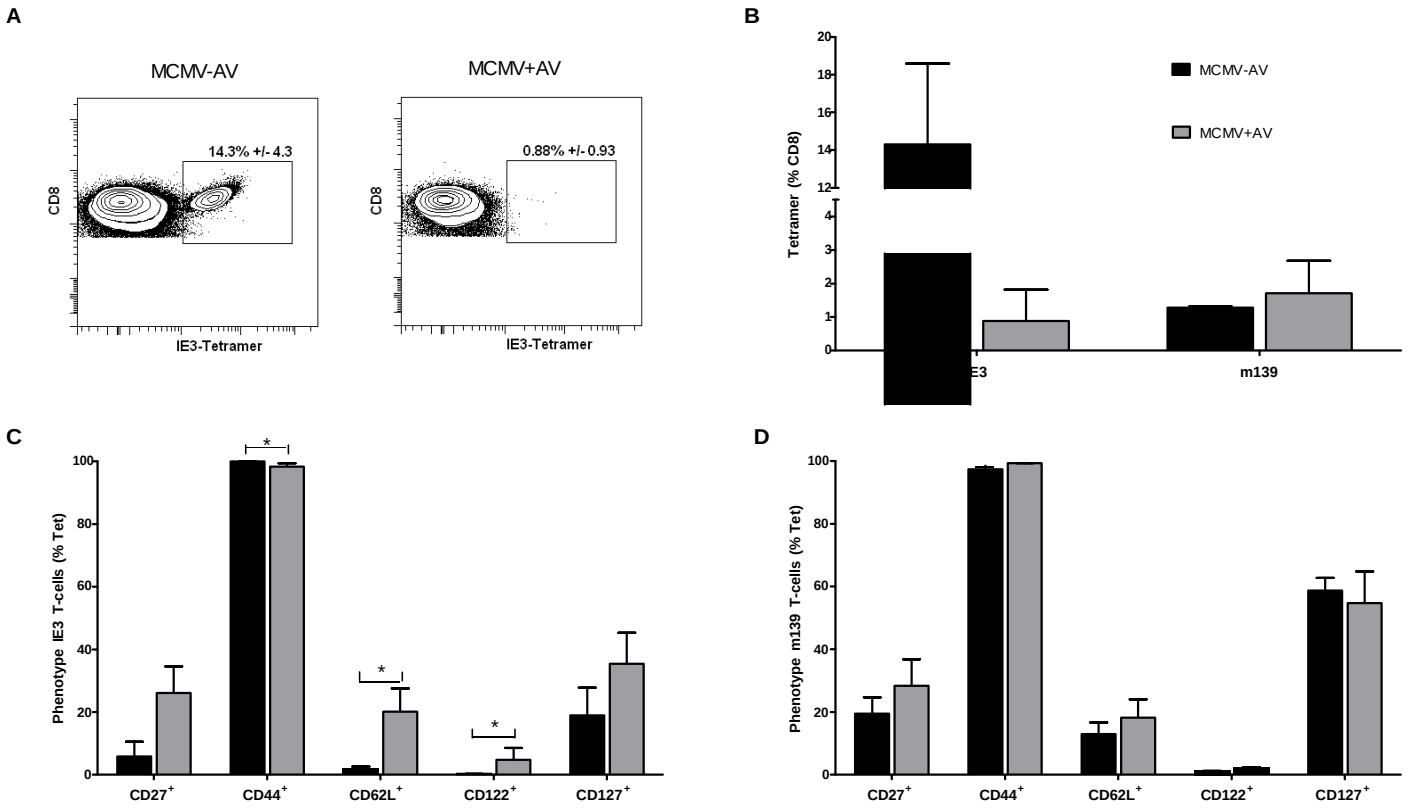

Figure 4.4. Valaciclovir inhibits memory inflation of IE3-tetramer specific CD8$^+$ T-cells. A) Representative FACS plot of the IE3-tetramer specific CD8$^+$ T-cells in the MCMV-AV and MCMV+AV treated mice. B) Frequency of IE3 and 139-tetramer specific CD8$^+$ T-lymphocytes in the 18 months post-MCMV challenge. C) Expression of CD27, CD44, CD62L, CD122 and CD127 on the IE3-tetramer specific CD8$^+$ T-cells. Mean +/- SEM Data analysed by 2-way ANOVA plus Bonferroni post-test (*p<0.05).

Figure 3.11 C showed MCMV untreated mice have an increased proportion of activated $CD8^+$ $CD62L^-$ T-lymphocytes in comparison to mice treated with valaciclovir for six months. 12 month antiviral treatment redistributed the overall memory status of the $CD8^+$ T-lymphocytes in valaciclovir treated mice to resemble an uninfected animal (Figure 4.5 A).

MCMV-AV mice displayed significantly reduced frequencies of T_N (15% *$p<0.05$) and elevated frequencies of T_{EM} $CD8^+$ T-cells (68.2% **$p<0.01$) 18 months p.i. which could be due to uncontrolled viral reactivation and T-lymphocyte priming. In stark comparison the $CD8^+$ T-cells from the MCMV+AV group was much less differentiated with approximately 40% of cells having a T_N phenotype and 35% with a T_{EM} phenotype. The antiviral treatment rejuvenated the distribution of memory subsets making it impossible to distinguish between the MCMV+AV and the MCMV-neg mice (Figure 4.5 B, Table 4.2). Furthermore, the T_{CM} population consisted of 20% of $CD8^+$ T-cells in the MCMV+AV and MCMV-neg mice but only 12% in the MCMV-AV group and although this was not a significant decrease it partially supports the hypothesis that frequent reactivation periods skew the T-cell pool via a transition from least differentiated into highest differentiated T-cells.

MCMV infection also generates a diverse and polyfunctional $CD4^+$ T-cell response [213]. Using the same co-expression of CD44 and CD62L on the $CD4^+$ T-cell pool the MCMV-AV mice were observed to have the lowest frequency of naïve $CD4^+$ T-cells (4%) and the highest frequency of effector $CD4^+$ T-cells (83%). The proportion of T_N $CD4^+$ T-cells did not significantly vary between the three groups of mice, however, the frequency of T_{EM} was significantly reduced to 57% of $CD4^+$ T-cells in the MCMV+AV treated group compared with

the MCMV-AV animals (***p<0.001) (Figure 4.5 C, Table 4.2). These observations suggest that the antiviral does not retain all lymphocytes in a naïve state but does prevent the an accumulation of the MCMV-specific $CD4^+$ T-cells.

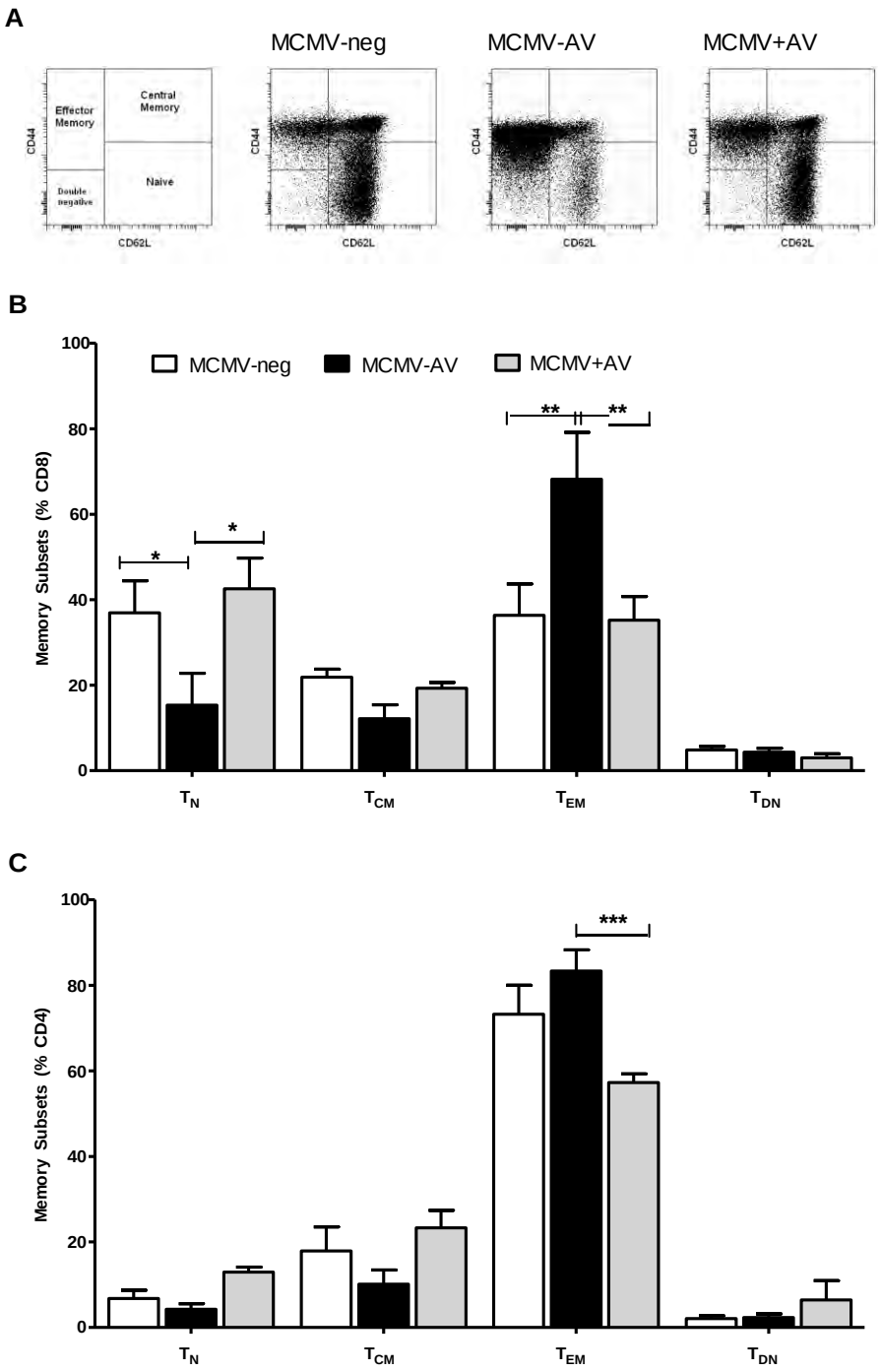

Figure 4.5. Valaciclovir restores the memory status of splenic T-cells. A) Representative gating and T-cell memory subsets. Percentage memory subset of $CD8^+$ (B) and $CD4^+$ (C) T-cells from the spleens of elderly mice 18 months post-MCMV. Mean +/- SEM (n=3-4). Data analysed by 2-way ANOVA plus Bonferroni post-test (*p<0.05, **p<0.01 and ***p<0.001).

Table 4.2. Frequency of $CD8^+$ and $CD4^+$ memory T-cells from the spleen of 18 month old MCMV-neg, MCMV-AV and MCMV+AV treated mice. Mean +/- SEM.

		% $CD8^+$ T-cells	
	MCMV– neg (n=4)	**MCMV-AV (n=3)**	**MCMV+AV (n=3)**
T_N	36.93 +/- 7.511	15.29 +/- 7.50	42.53 +/- 7.18
T_{CM}	21.87 +/- 1.856	12.19 +/- 3.26	19.28 +/- 1.34
T_{EM}	36.34 +/- 7.397	68.19 +/- 11.00	35.19 +/- 5.51
T_{DN}	4.86 +/- 0.827	4.34 +/- 0.93	3.00 +/- 0.97
		% $CD4^+$ T-cells	
T_N	6.80 +/- 2.14	4.23 +/- 1.82	12.92 +/- 1.37
T_{CM}	17.90 +/- 6.27	10.14 +/- 4.65	23.32 +/- 4.68
T_{EM}	73.23 +/- 7.60	83.34 +/- 7.01	57.32 +/- 2.29
T_{DN}	2.07 +/- 0.73	2.29 +/- 1.28	6.44 +/- 5.18

4.4. SURVIVAL AND WEIGHT LOSS ARE NON-IMMUNOLOGICAL PARAMETERS AFFECTED BY A HISTORY OF MCMV-INFECTION AND TREATMENT

Both elderly humans and mice are often more susceptible to IAV infection therefore the history of MCMV infection (+/-treatment) was examined in the context of the subsequent generation of an immune response to IAV.

The IAV clone 7a used to challenge the mice is a combination of two IAVs rearranged to form a less virulent virus suitable for non-lethal infection in mice. However, due the old age of these mice all animals demonstrated adverse side effects to the procedure such as inactivity and a hunched posture. In two of the eight MCMV-AV mice, acute infection was so severe it was lethal. No mice that were MCMV–neg or MCMV+AV treated died upon exposure to IAV. Moreover, the MCMV-AV mice displayed the worst clinical symptoms with one mouse developing severe ataxia prior to its death on day four. Comparison of the Kaplan-Meier curves by log rank test show this difference in survival between the three groups of mice to be insignificant ($p=0.135$), however, this study was not powered sufficiently to determine if prior MCMV infection contributes to an increased risk of death to IAV (Figure 4.6 A).

Experiments which have compared weight loss differences between adult and aged mice in response to IAV infection (A/PuertoRico/8/34) showed elderly mice to be more sensitive to rapid weight loss [355]. During the 10 day period post-IAV challenge, all mice lost a large proportion of their body mass and no animals fully regained the mass lost during the acute

infection. The MCMV-AV group lost the greatest percentage of their original body mass during acute IAV infection. The average body mass of these MCMV-AV mice decreased from 30.3 g to 23.2 g, equivalent to 23.3% reduction of their initial body mass (Figure 4.6 B). Surprisingly, the MCMV-neg group also lost body mass with similar kinetics to the MCMV-AV group, i.e. a decrease from 31.7 g to 25.0 g (21.2%). In contrast, the MCMV+AV treated mice displayed biphasic kinetics. During the first five days, post-challenge, the MCMV+AV treated group lost mass with the same kinetics as the mice in the other two groups. Yet, between days five and 10 a plateau phase was achieved where no further body mass was lost in the MCMV+AV group of animals. Therefore, over the entire 10 day period the MCMV+AV treated mice saw only a modest decline of 14.30% from their original body mass (Figure 4.6 B). The maintenance of body mass between day five and day 10 in the MCMV+AV mice would coincide with the induction of an IAV-specific adaptive immune response.

.

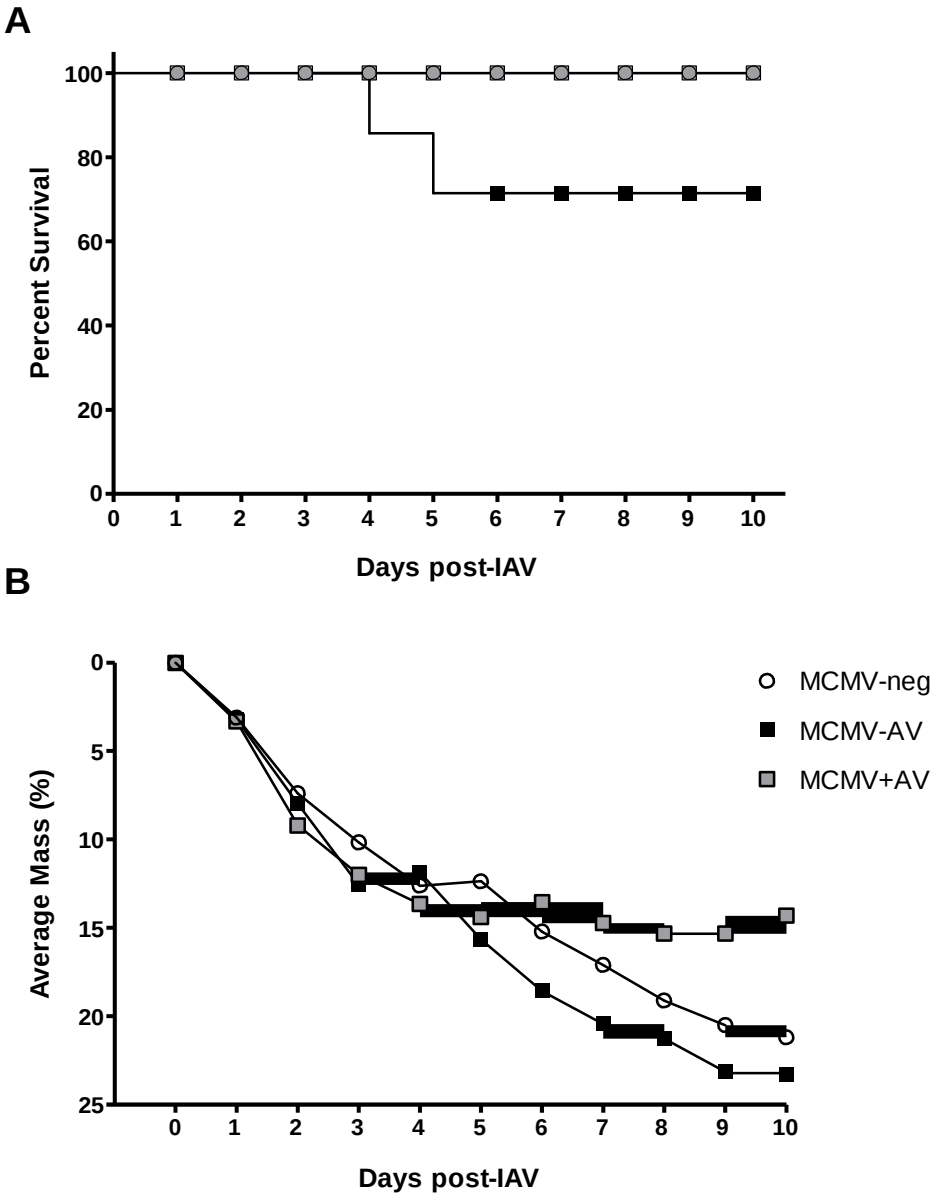

Figure 4.6. Antiviral treatment provides protection to IAV challenge. A) Kaplan-Meier survival curves following acute IAV infection in MCMV-neg (open circle), MCMV-AV (black square) and MCMV+AV (grey square) treated mice. B) The mean percentage decrease in animal body mass measured during IAV infection.

4.5. THE MAGNITUDE OF NP-SPECIFIC $CD8^+$ T-CELL RESPONSES WERE COMPARABLE IN BAL, CMLN AND SPLEEN DESPITE MCMV INFECTION OR TREATMENT

In view of the relative clinical protection against IAV challenge that was afforded by long term antiviral therapy the magnitude and quality of the IAV-specific immune response was determined using the $NP_{366-374}$ MHC-I tetramer. The frequency of tetramer-binding cells was measured in the bronchoalveolar lavage fluid (BAL), the caudal mediastinal lymph node (CMLN) and the spleen in order to study the adaptive immunity in local tissue, the draining lymph node and systemic tissue.

The magnitude of the NP-specific immune response was greatest in BAL fluid where it represented on average 6% of the $CD8^+$ T-cell pool and this relative frequency was comparable between all groups. In addition, NP-specific tetramer staining was seen on 1-2% of $CD8^+$ T-cells in both the CMLN and spleen and this value was again similar in all groups (Figure 4.7 A+B). Additionally, the number of NP-specific CTLs in the BAL and CMLN were obtained from the flow-cytometer and there were no significant difference in the absolute size of the response in the three groups of mice (Figure 4.8 A + B, Table 4.3). This is in contrast to the recent data presented by Cicin-Sain *et a*l (2012) who noted much reduced frequencies of influenza NP-specific cells in the blood of eight month old BALB/c which were administered MCMV five months previously and then challenged with a low dose (EID_{50} 300) of IAV [356].

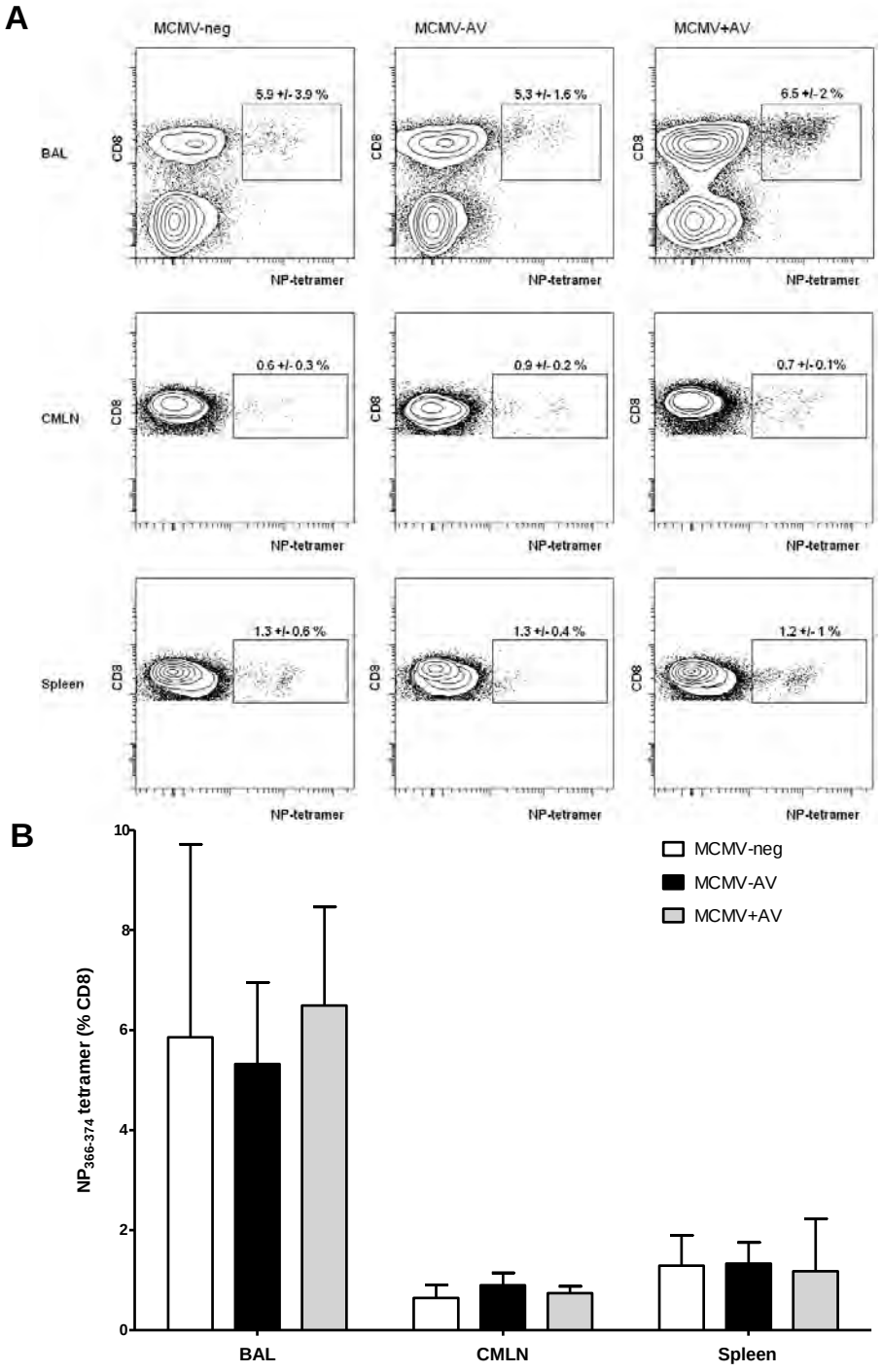

Figure 4.7. NP-tetramer specific CD8$^+$ T-cells in BAL, CMLN and spleen. A) Representative NP-tetramer staining in the BAL fluid, CMLN and spleen 10 days post-clone 7a infection. B) Frequency of NP-specific CD8$^+$ T-cells. Mean +/- SEM (n=4-6).

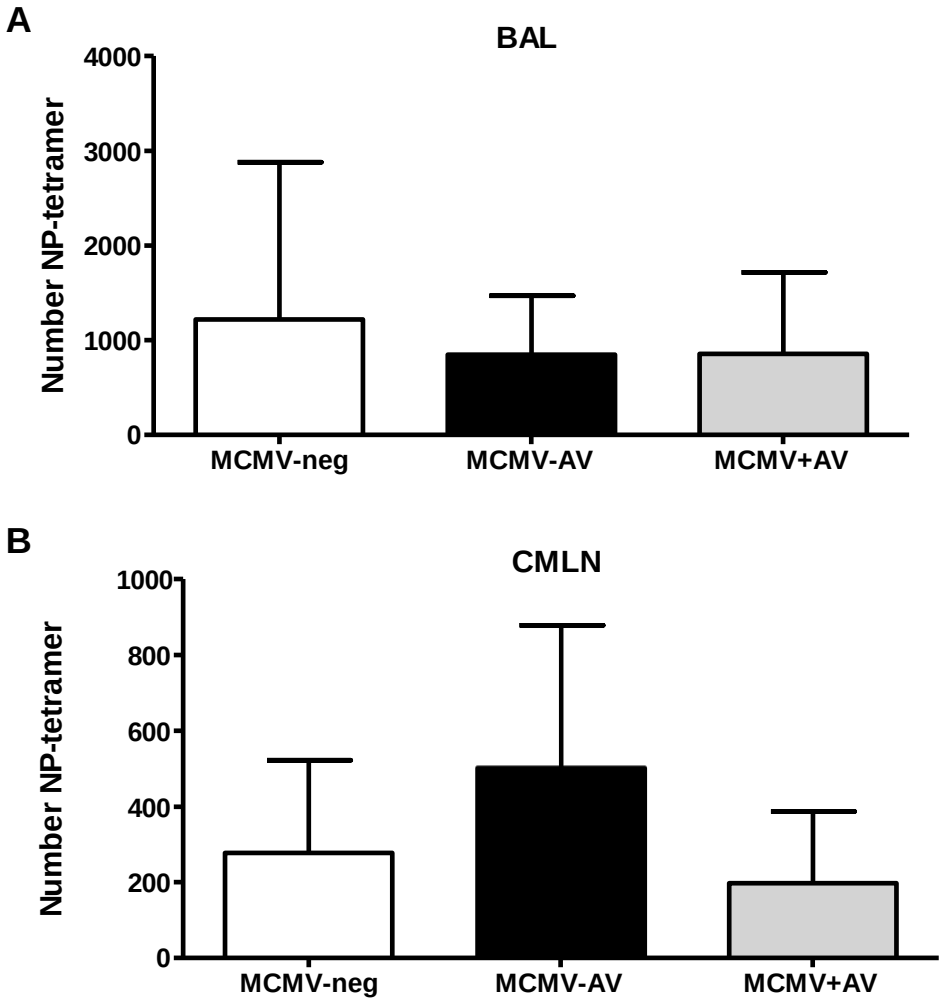

Figure 4.8. Numbers of NP-specific CTLS are not significantly altered by MCMV or treatment. Number of lymphocytes in BAL (A) and CMLN (B). Mean +/- SEM (n=3-6).

Table 4.3. Number of NP T-cells in BAL and CMLN. Mean +/- SEM.

	Number NP-tetramer positive cells	
	BAL	**CMLN**
MCMV-neg (n=5)	1220.6 +/- 1659.3	277.8 +/- 244.7
MCMV-AV (n=6)	847.0 +/- 622.7	503.8 +/- 374.3
MCMV+AV (n=3-4)	856.7 +/- 862.2	197.3 +/- 190.1

4.6. THE NP-SPECIFIC $CD8^+$ T-CELL IMMUNE RESPONSE WAS MOST ALTERED IN THE CMLN IN THE MCMV+AV GROUP

The memory status and phenotype of NP-tetramer positive cells was determined in the BAL, CMLN and spleen (Figure 4.9). In all three groups of mice the NP-tetramer positive lymphocytes from the BAL almost exclusively displayed a T_{EM} phenotype (>90%) (Figure 4.9 A). To ensure that these cells are retained within the bronchoalveolar airspace, over 93% of all the NP-specific cells up-regulated expression of the CD44 adhesion molecule and down-regulated CD62L on their cell surface (Figure 4.10 B). Overall, the phenotype of the antigen-specific T-cells in the BAL appeared independent of MCMV seropositivity and antiviral treatment with exception of CD127 expression. CD127 was expressed significantly higher by the NP-specific cells in the BAL from MCMV-neg (29%) mice compared with MCMV-AV (19%, *$p<0.05$) and the MCMV + antiviral (11%, *$p<0.001$) treated mice. It has been shown experimentally that CD127 is down-regulated as a result of IL-7 and also IL-4 stimuli [357] and in the context of HIV infection CD127 loss is associated with T-cell activation which is partially restored by HAART [358]. Furthermore, loss of CD127 results in impaired $CD8^+$ T-cell proliferation [357], therefore it is possible that MCMV exposed mice may have had impaired proliferative responses to IAV on an individual cell basis that was not detected by measuring cell frequencies.

There were multiple phenotypic differences in the NP-response from the CMLN in the MCV+AV group of animals. The NP-memory subsets in the CMLN have a similar distribution, approximately 20% T_{CM} and 75% T_{EM} $CD8^+$ T-cells, amongst the untreated MCMV-AV and

MCMV-neg mice (Figure 4.10 C). In contrast, the MCMV+AV treated mice displayed significantly reduced frequencies of T_{EM} NP-specific $CD8^+$ T-cells (55%) in comparison with the MCMV-neg (*p<0.05) and MCMV-AV (**p<0.01) mice. The decrease in T_{EM} was offset by an increased frequency of T_{CM} NP-specific cells in the CMLN of MCMV+AV treated mice. This finding indicates that the less differentiated NP-specific cells are retained preferentially within CMLN. Further to the increase in T_{CM} NP-response those tetramer specific cells also displayed significantly elevated levels of CD127 on their surface in MCMV+AV than the MCMV-AV group of mice (*p<0.01) (Figure 4.9 D).

Previously Figure 4.8 A+B showed that the NP-specific cells within the spleen did not vary in frequency between the three groups and here the memory status of NP-tetramer specific $CD8^+$ T-lymphocytes was consistent between groups (Figure 4.10 E). The NP-response in the spleen most closely resembled that in the BAL fluid with the predominant subset being the T_{EM} population (80%) (Figure 4.10 E). The T_{CM} NP-tetramer specific response in the spleen ranged from 8% to 11%, which was higher than what was observed in the BAL but lower than that was detected in the CMLN (Figure 4.9 E). There were no significant alterations to the percentage expression of CD27, CD44, CD62L, CD122 or CD127 on the NP-tetramer positive cells. The NP-tetramer specific response from the spleen was judged as highly differentiated and independent of MCMV seropositivity and antiviral treatment.

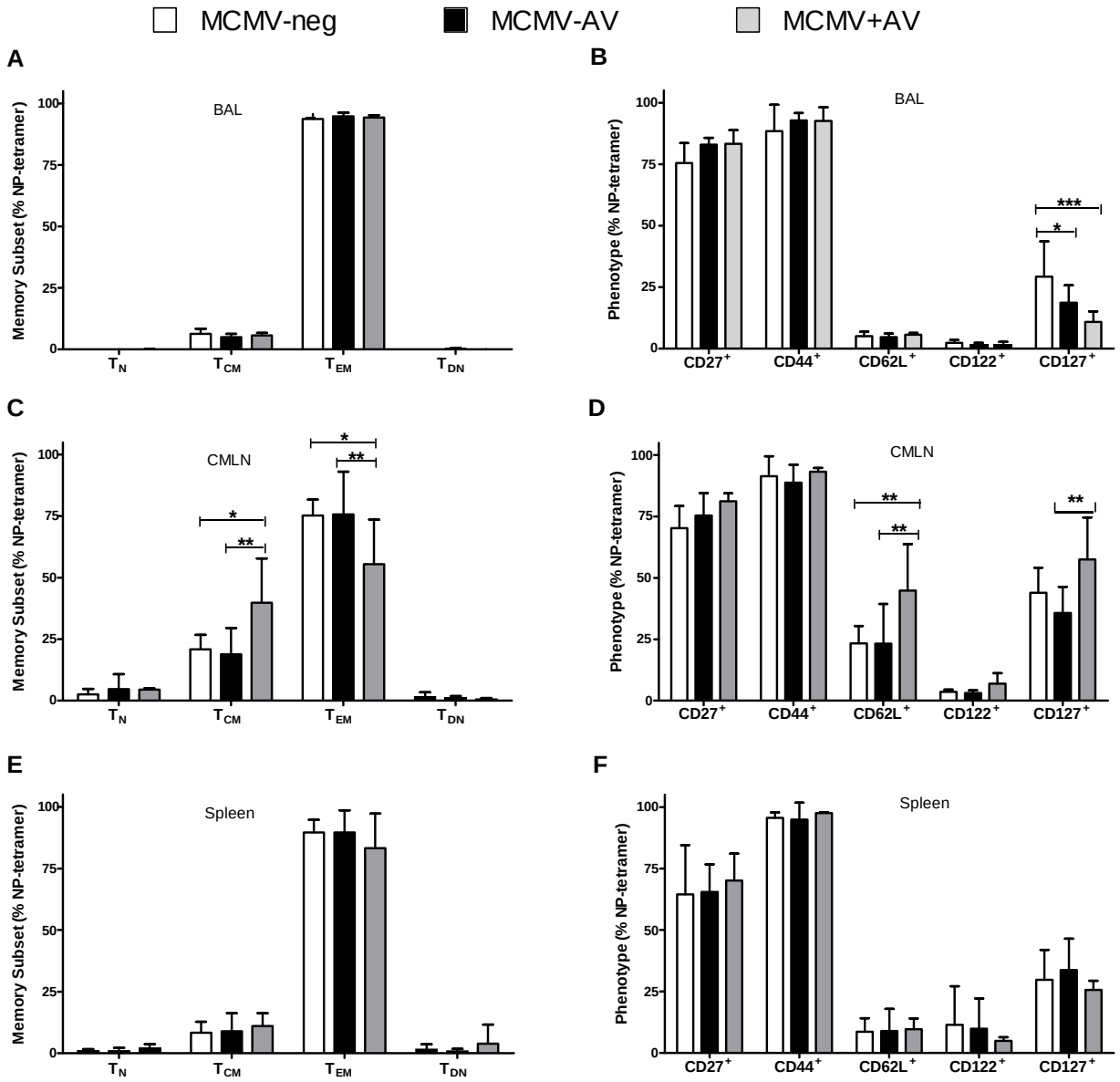

Figure 4.9. Altered NP-specific $CD8^+$ T-cell immunity in the BAL, CMLN and spleen 10 days post-IAV challenge. Memory-subsets of NP-specific $CD8^+$ T-cells in BAL (A), CMLN (C) and spleen (E). Percentage expression of CD27, CD44, CD62L, CD122 and CD127 on the NP-specific $CD8^+$ T-cells in the BAL fluid (B), CMLN (D) and spleen (F). Mean +/- SEM (n=4-6). Data analysed by 2way-ANOVA plus Bonferroni post-test (*p<0.05, **p<0.01 and ***p<0.001).

4.7. THE $CD4^+$ T-CELL IMMUNE RESPONSE WAS LEAST DIFFERENTIATED IN THE CMLN OF VALACICLOVIR TREATED MICE 10 DAYS POST-IAV CHALLENGE

Because of the observation that the CTL response sampled from the CMLN was most different between the three groups of mice, the memory and phenotypic status of the $CD4^+$ T-cells from the CMLN was also examined for phenotypic changes. It was surprising to see how similar the MCMV-AV and MCMV-neg mice were concerning their $CD4^+$ T-cell response within the CMLN compared to the MCMV+AV group of mice. Both the MCMV-neg and MCMV-AV mice $CD4^+$ T-cell response was primarily of a T_{EM} phenotype (57-58%) which was significantly higher than that detected from the treated MCMV+AV group (43%) (*$p<0.05$) (Figure 4.10 A). The reduced frequency of T_{EM} $CD4^+$ T-cells in the valaciclovir treated mice was due to a slight increase in less differentiated T_N and T_{CM} subsets of $CD4^+$ T-cells. To coincide with the reduced T_{EM} population it was confirmed that the percentage expression of CD44 was significantly reduced (*$p<0.05$) and CD62L significantly elevated (*$p<0.05$) on the $CD4^+$ T-cell populations from the CMLN of the MCMV+AV animals (Figure 4.11 A). No differences were observed in the levels of CD27, CD122 or CD127. Overall, the $CD4^+$ T-cell phenotype would best be described as $CD44^+$ $CD62L^{int}$ $CD27^{int}$ $CD122^-$ and $CD127^{int}$ (where intermediate [^{int}] is between 40-60%) in all groups independent of MCMV infection or treatment.

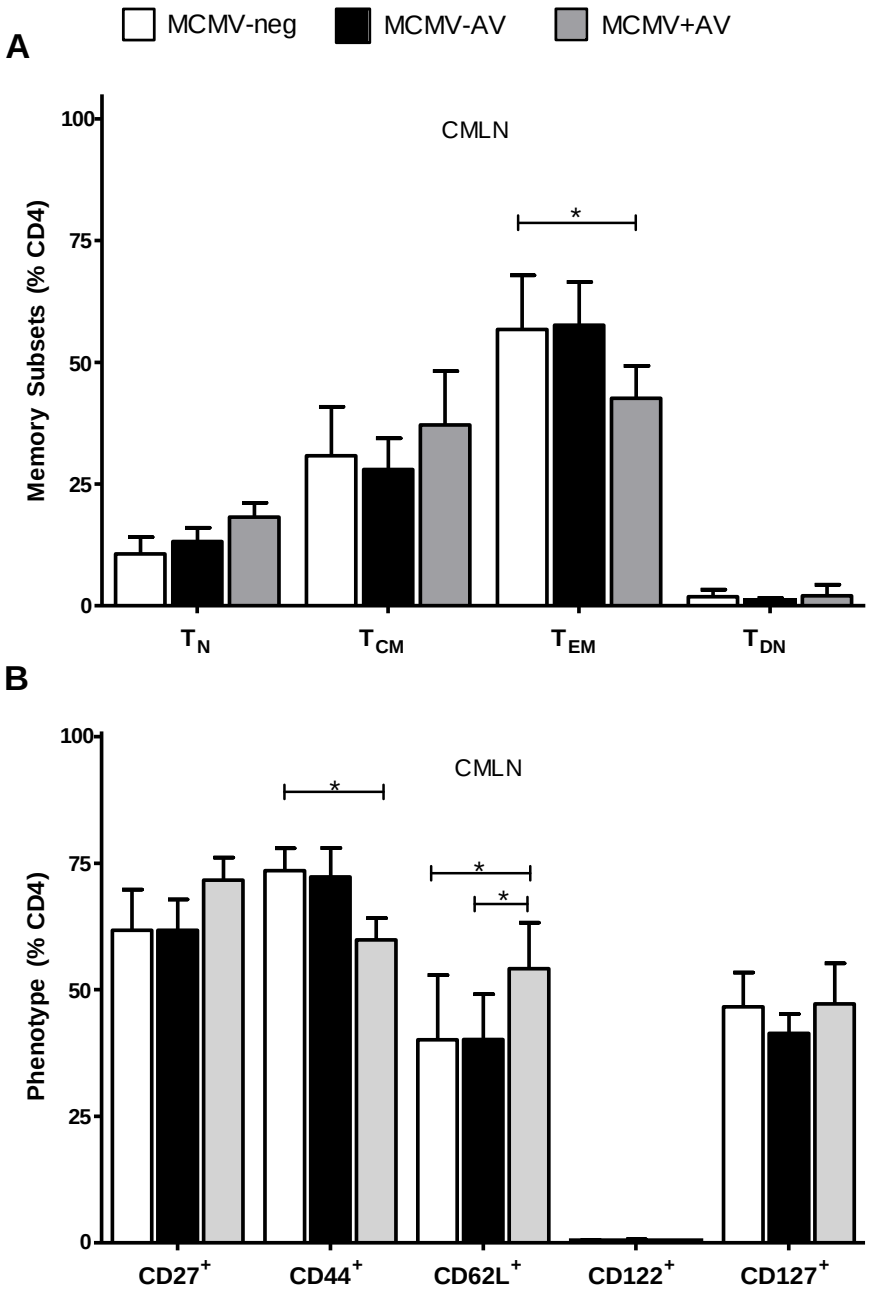

Figure 4.10. The $CD4^+$ T-cells in response from the CMLN is least differentiated in MCMV+AV treated group of animals. The frequency of each memory subset (A) and phenotype (B) of $CD4^+$ T-cells from the CMLN 10 days post IAV-challenge. Mean+/- SEM (n=4-6). Data analysed by 2way ANOVA plus Bonferroni post-test (*p<0.05).

4.8. ANTIVIRAL TREATMENT OF MCMV CAN RESTORE CD4:CD8 T-CELL RATIOS TO THAT OF MCMV NEGATIVE ANIMALS

The IRP states a CD4:CD8 T-cell ratio below one (in the peripheral blood) is a predictor of poor immune function in the elderly. Therefore, as an aside to the factors which directly contribute to the control of IAV, the ratio of $CD4^+$ to $CD8^+$ T-cells was determined in the BAL fluid, CMLN and spleen to re-examine if the expansion of $CD8^+$ T-cells is reversed with valaciclovir treatment.

The BAL fluid contained large proportions of infiltrating lymphocytes of which the majority were $CD8^+$ (47-61%) rather than $CD4^+$ T-cells (14-19%) in all three groups of clone 7a infected animals. The presence of high frequencies of $CD8^+$ T-cells in this localised tissue is most likely a direct response to the IAV burden and a requirement therefore for cytotoxic lymphocytes. The MCMV-AV mice had the lowest average CD4:CD8 ratio (0.23) compared to both the MCMV-neg (0.36) and MCMV+AV (0.35) treated mice (Figure 4.11 A). If were are to assume that the optimum ratio of $CD4^+$ to $CD8^+$ T-cells would occur in uninfected MCMV-neg mice then the valaciclovir treatment appeared to have rejuvenated the accumulation of MCMV-specific $CD8^+$ T-cells restoring the CD4:CD8 ratio in the BAL.

Within the CMLN of the untreated MCMV-AV group only 13% were $CD8^+$ and 20% $CD4^+$ T-lymphocytes, therefore the remaining lymphocytes are most probably B-cells. In comparison, the MCMV+AV group had elevated frequencies of both $CD8^+$ (31%) and $CD4^+$ T-lymphocytes (30%). The MCMV-neg CD4:CD8 ratio equalled 1.14 which suggests that for

normal immunological control of IAV infection alone an equal ratio of $CD4^+$ and $CD8^+$ T-cells are required in the CMLN. This ratio was most closely upheld within the lymph node of the MCMV+AV group (0.97) whereas the untreated MCMV-AV mice had a CD4:CD8 ratio of 1.51 (*$p<0.05$) approximately 50% more $CD4^+$ T-cells than $CD8^+$ T-cells (Figure 4.11 B).

The spleens are a site of large populations of circulating lymphocytes in young mice, however in the 18-month-old mice the number of viable lymphocytes was markedly reduced due to hyposplenism; therefore, memory inflation should further skew the T-cell ratio. Additionally, at day 10 post-clone 7a challenge, one mouse from the MCMV-neg group had severe splenomegaly although the CD4:CD8 ratio was comparable to the other members of the group and a second animal from the same group was excluded due to insufficient cells to test the CD4:CD8 ratio. Unsurprisingly, the untreated MCMV-AV mice had the highest proportion of $CD8^+$ T-cells (17%) in the spleen due to the expansion of MCMV-specific inflationary T-cells. However, the untreated MCMV-AV group also had the highest frequency of $CD4^+$ T-cell (36%) resulting in the largest CD4:CD8 ratio (2.20). In contrast, the MCMV+AV treated mice had a much lower frequency of $CD4^+$ T-cells which resulted in that group having the lowest CD4:CD8 ratio (1.54) which was most similar to the MCMV-neg group (1.87) (Figure 4.11. C). These findings are contrary to what is observed in the peripheral blood of HCMV-seropositive humans and indicate that this parameter o the IRP is not directly transferable to lymphocytes populations from mice.

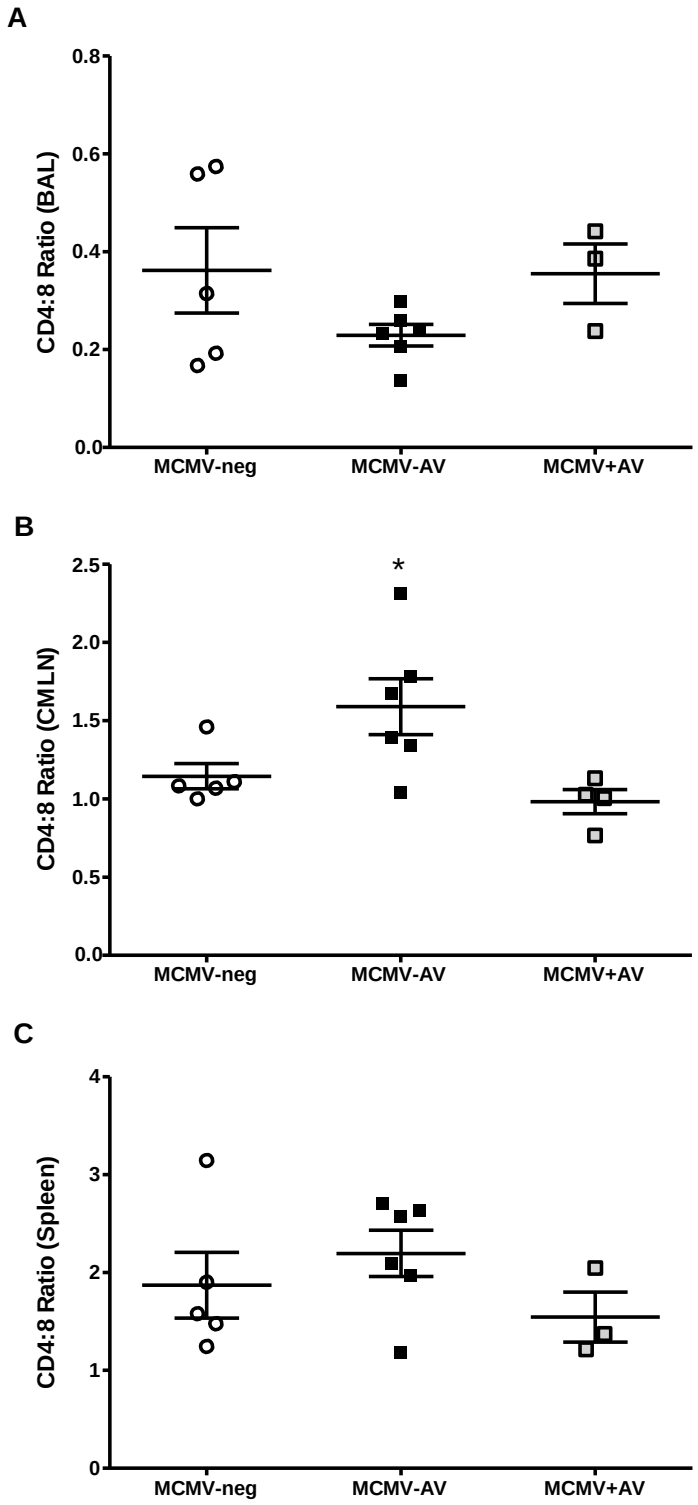

Figure 4.11. Antiviral treatment restores the CD4:CD8 T-cell ratio to resemble an uninfected animal. The CD4:CD8 T-cell ratios determined in the BAL (A), CMLN (B) and spleen (C). Mean +/- SEM (n=4-6). Data analysed by Kruskal Wallis (*p<0.05).

4.9. UNTREATED MCMV INFECTION LEAD TO SIGNIFICANTLY ELEVATED INFLUENZA VIRUS TITRES IN THE LUNG

The lungs are the primary site of IAV replication; therefore, clone 7a viral titres were determined by plaque assay 10 days p.i. (Figure 4.12. Table 4.4) and were comparable to the day 10 titres observed by Toapanta *et al* (2009) following similar infection models in elderly mice (up to 10^4 PFU/lung) [359].

The untreated MCMV-AV group of animals had the highest IAV titre of approximately 5500 PFU/lung which was significantly higher than the 1216 PFU/lung detected in MCMV-neg mice (*$p<0.05$). Treatment with valaciclovir reduced the IAV titre of the MCMV+AV mice to just below 2000 PFU/lung. This is a relative reduction of approximately 70% when compared with the MCMV-AV group (*$p<0.05$). These findings suggest that the elevated titres are due to a lack of immune control of the clone 7a infection some of which is mediated by the $CD8^+$ T-cell response.

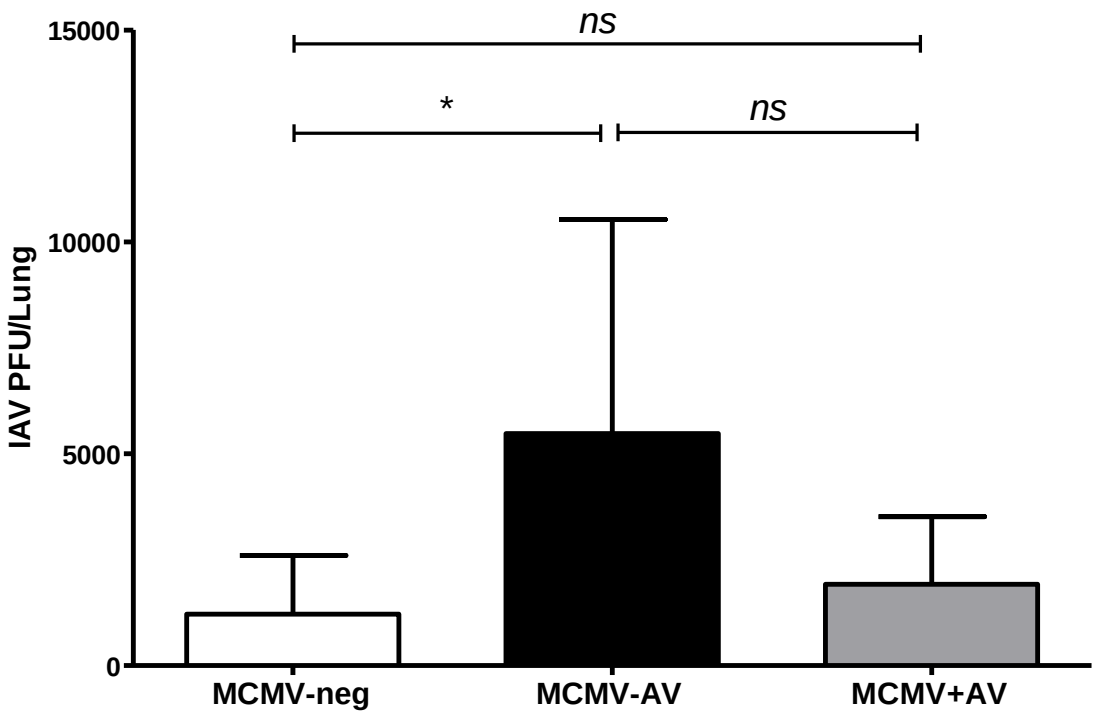

Figure 4.12. Untreated MCMV infection leads to elevated IAV titres. The IAV titres were determined 10 days post-IAV challenge in the lung by plaque assay. Mean +/- SEM (n=4-6). Data analysed by 2way-ANOVA plus Bonferroni post-test (*p<0.05).

Table 4.4. IAV titres in the lung 10 days post-IAV challenge. Mean +/- SEM.

	MCMV-neg (n=5)	MCMV-AV (n=6)	MCMV+AV (n=4)
PFU/Lung	1216 +/- 620	5478 +/- 2258	1920 +/- 797

4.10. RESULTS CHAPTER 2: CONCLUSIONS

Antigen is essential for priming cytotoxic $CD8^+$ T-cell proliferation during primary infection and pathogen re-exposure. In cases of high antigenaemia, e.g. LCMV infection (in mice) [360] or untreated HIV infection (in humans) there is an associated high frequency of antigen-specific $CD8^+$ T-cells detected in the circulation [361, 362]. The experiments in this chapter sought to determine whether MCMV reactivation - and therefore the availability of antigen - is responsible for generating memory inflation in elderly mice with chronic/latent MCMV infection. To block MCMV-reactivation mice were administered valaciclovir hydrochloride (1 mg/ml) in their drinking water for up to 12 months.

This study is not the first to demonstrate that blocking viral-replication/reactivation will lead to a reduction in the corresponding $CD8^+$ T-cell response. Both Gray *et al* (1999) and Weekes *et al* (2006) documented an attrition in the frequency/number of HIV-specific $CD8^+$ T-cells in patients undergoing HAART [361, 362]. HAART medications typically include ziovudine (nucleoside analogue of thymidine) and lamvudine (nucleoside analogue reverse-transcriptase inhibitor) which in combination can ablate HIV-1 RNA levels and in those studies the absence of viral-RNA correlated with significant reductions in the circulating HIV-specific CTL response. A murine model of memory inflation utilising systemic HSV-1 infection generates high frequencies of circulating gB-specific $CD8^+$ T-cells that are similar in phenotype to those associated with MCMV infection (i.e. $CD8^+$ $CD62L^-$ $CD127^{int}$ $CD27^-$) [363, 364]. The transfer of gB-specific $CD8^+$ T-cells into SPF mice showed these cells to rely on the presence of latent virus to maintain cell number. Furthermore, Lang *et al* (2009) demonstrated that memory inflation of gB-specific $CD8^+$ T-cells can be reduced by 75% if the

systemic HSV-1 infection was treated with famciclovir (2 mg/ml) for one month [363]. Famciclovir treatment was most effective if administered prophylactically (seven days before infection) and in addition, treatment resulted in a less differentiated gB T-cell surface phenotype ($CD8^+$ $CD62L^{int}$ $CD127^+$ $CD27^+$). The authors remarked that the population of HSV-1 specific T-cells is maintained by periodic yet subclinical reactivation of the latent persistent virus. Unfortunately, it is impossible to pre-empt herpesvirus infection therefore prophylactic treatment may not always be an option even though antiviral treatment has the potential to modulate T-cell frequency and diversity.

Here, MCMV infected mice were left to develop memory inflation of the $CD8^+$ T-lymphocyte for six months before antiviral treatment was administered for 12 months. In doing so, the study aimed to replicate the clonal expansions of HCMV-specific $CD8^+$ T-cells seen in the elderly population. A limitation of studying the immune response in an aged population of mice (>18 months) is that fewer lymphocytes can be obtained from the spleen in comparison to those experiments where younger animals were sampled. The spleen is a secondary lymphoid organ and like the thymus undergoes atrophy [365]. Here there was not observe an obvious decrease in size of the spleen size however there was an age associated decline in the number of lymphocytes isolated from the spleen of older mice. This form of hyposplenism occurred in 50% of MCMV-AV mice whereas treatment with valaciclovir resulted in hyposplenism in only 25% of cases; however, the sample size was insufficient to prove that untreated MCMV accelerated hyposplenism.

Valaciclovir treatment was provided for 12 months which is four times greater than the longest estimated half-life of the inflationary MCMV-specific T-cell response [165]. During this time MCMV would be expected to reactivate an unknown number times in the untreated mice but the administration of valaciclovir would supress viral DNA-replication. It is a limitation of this study that both lytic MCMV and viral genomes were not detected after the resolution of acute infection. Therefore, there is uncertainty that antiviral treatment successfully suppressed MCMV reactivation entirely as the process may have been partially incomplete with virus replicating in niche cells/organs partially explaining why the CTL response was not ablated.

These are the first series of experiments to investigate the effect of long-term antiviral suppression of a non-modified MCMV in C57BL/6 mice. Previously Snyder *et al* (2011) showed that prophylactic famciclovir treatment of mutant MCMV infection (MCMV-TK) resulted in approximately 50% reduction in the frequency of M38 and m139 specific CTLs. Furthermore, the frequency of IE3-specific CTLs was significantly reduced by almost 90% (from >8% in untreated mice compared to <1%) because of prophylactic antiviral treatment [193]. The data presented within this chapter also demonstrated that memory inflation is also sensitive to the effects of 12 months of valaciclovir treatment. The IFNγ response to the five immunodominant peptides totalled approximately 35% of $CD8^+$ T-cells in the MCMV-AV mice compared to less than 10% in the MCMV+AV group. Reductions were observed towards all five epitopes assayed, however the effect of treatment was most pronounced towards the IE3-epitope. The frequency of cytotoxic $CD8^+$ $IFN\gamma^+$ IE3-specific cells was 95% higher in the untreated mice compared to the antiviral treated group 18 months after

MCMV infection. The frequencies of MCMV-specific cells reported by Snyder *et al* (2011) following prophylactic treatment and here after 12 months of treatment are very similar and prove that antigen partially maintains memory inflation and the sensitivity of each individual immune response varies to treatment.

Immunity to a variety of pathogens is known to wane in old age as leukocytes lose function and the capacity to control infections [331, 364, 366-369]. For example, studies of pp65-specific $CD8^+$ T-cells in the very old were shown to be dysfunctional as on a per cell basis the cells produced less IFNγ and IL-10 upon stimulation [370]. Here there was no functional impairment (IFNγ or TNFα production) of the inflationary lymphocytes in response to *ex vivo* peptide stimulation in the MCMV-AV and MCMV+AV treated mice. However, the surface phenotype of the IE3-specific $CD8^+$ T-cells showed evidence that not treating MCMV infection causes the most highly differentiated phenotype associated with memory inflation. The majority of IE3-tetramer specific lymphocytes from the MCMV-AV mice were $CD8^+$ $CD27^-$ $CD44^+$ $CD62L^-$ $CD122^-$ $CD127^-$ whereas in the MCMV+AV group those same IE3-tetramer specific lymphocytes were $CD8^+$ $CD27^{int}$ $CD44^+$ $CD62L^{int}$ $CD122^-$ $CD127^{int}$, which is representative of less differentiation.

The reduced frequencies of T_{EM} $CD8^+$ T-cells seen in the antiviral treated mice seemed to rejuvenate the CTL pool to that of MCMV-neg mice. There was a concern that the antiviral was having an immunosuppressive effect on lymphocyte output from the bone marrow [371, 372]. However, the reduced MCMV-specific immune response and decline in T_{EM} in $CD8^+$ T-cells was not a global effect on all other lymphocyte subset/phenotypes. For

example, in the spleen and BAL the distribution of $CD4^+$ T-cell memory subsets was not significantly altered between MCMV+AV and the MCMV-neg control mice. The antiviral treatment only reduced the proportion of T_{EM} $CD4^+$ T-cells in the CMLN, which may be attributable to the IAV infection. Additionally, if valaciclovir were immunosuppressive the *de novo* NP-specific T-cell response the memory subsets and NP-specific T-cell phenotypes should have been affected in all three sites and not only the CMLN.

The elderly are at the greatest risk of non-pandemic IAV infection [373-375] and numerous publications have shown an age associated immune senescence of antigen-presenting cells, innate immunity and adaptive immune response towards influenza in mice [359, 376, 377]. Here, it was intriguing and somewhat illogical to see that the MCMV+AV animals had abrogated clinical effects during the IAV-infection and generated perhaps the most proficient NP T-cell response in the CMLN. It would be expected that the MCMV-neg mice to maintain their body weight best of the three groups due to these animals never having generated an MCMV response and therefore should be most capable of generating an effective cytotoxic IAV-specific immune response. The accumulation of MCMV-specific T-cells and the corresponding memory inflation in the MCMV-AV mice would be predicted to cause senescence towards IAV similar to that observed in elderly HCMV seropositive humans [353]. However, antiviral treatment may unmask a potential benefit and perhaps symbiotic effect of underlying MCMV infection. CMV are highly immunogenic and here may have generated a pro-inflammatory environment within the lung with elevated levels of lymphocytic cytokines such as interleukins, IFNγ and TNFα which are normally impaired in aged mice during IAV infection [359]. The underlying MCMV infection could help prime the

APCs for cross-presentation of IAV epitopes or via bystander activation of innate or cross-reactive leukocytes [378] which may have resulted in reduced IAV viral titres.

Post-IAV inoculation there was no significant differences in the average frequency of NP-tetramer specific lymphocytes (% $CD8^+$ T-cells) in the BAL, CMLN and spleen. However, the IAV response in the CMLN was unique and it is known that antigen presentation within the CMLN is critical for the control of influenza [379]. The CMLN is a large unpaired node located behind the heart and is a reservoir of lung associated T-lymphocytes. Here the MCMV-AV mice had the largest number of lymphocytes in the CMLN but the lowest percentage of $CD8^+$ and $CD4^+$ T-cells. The lack of T-lymphocytes in the CMLN suggests MCMV-AV have impaired T-cell recruitment to the lymph node therefore future experiments should consider chemokine receptor levels, e.g. CCR7. The remaining lymphocytes in the node are likely to be B-cells that are probably required to compensate for the impaired T-cell recruitment. It would be interesting to compare the ability of the animal's serum to inhibit haemagglutination of erythrocytes as an additional determinant of immune senescence.

Valaciclovir is an inhibitor of the herpes-virus DNA-polymerase (M54) and therefore should not affect the IAV which are RNA viruses and do not contain an ortholog of the M54 gene. However, future experiments should include a further control group that received the same dose of antiviral treatment as the MCMV+AV group but were themselves not infected with MCMV. The additional group would help to prove that the low IAV titres in MCMV+AV mice were not a result of antiviral treatment but was due to immunological factors. There is no

evidence of aciclovir(s) having anti-IAV properties in the literature however a including valaciclovir to an *in vitro* plaque assay type experiment could show that the antiviral is highly specific and not a confounding factor of these experiments.

5. RESULTS 3: *tsm5* DOES NOT GENERATE MEMORY INFLATION AND THEREFORE LYTIC REPLICATION IS KEY TO $CD8^+$ T-CELL MEMORY INFLATION

5.1. ATTENUATION OF MCMV REPLICATION AND ITS IMPACT UPON MEMORY INFLATION OF CD8$^+$ T-LYMPHOCYTES

In the previous two chapters, administration of the prolonged course of 12 months continuous valaciclovir treatment to latently MCMV infected mice significantly reduced the frequency of MCMV-specific CD8$^+$ T-cells. The antiviral blocks progress of the viral DNA-polymerase and prevents herpesvirus replication (Chapter 1 Figure 1.4). Therefore, the question was raised whether an attenuated virus could maintain the high frequencies of virus-specific T-cells.

There have been previous attempts to investigate the immune responses to an attenuated MCMV strain [193, 380]. For example, Snyder *et al* (2010, 2011) generated an attenuated viral strain by deletion of the entire gene that encodes for an essential surface glycoprotein (ΔgL-MCMV) [193, 380]. The ΔgL-MCMV remains infective, however, upon the first round of viral replication virions were incapable of spreading to neighbouring cells and therefore the virus is unable to fully disseminate and establish a genuine latent infection [380]. It was reported that following systemic administration of the ΔgL-MCMV into either BALB/c or C57BL/6 mice that memory inflation still occurred but at a lower magnitude to that observed with infection with a non-attenuated MCMV [193].

The temperature-sensitive mutant 5 (*tsm5*) is a live-attenuated, replication defective MCMV strain generated by chemical mutagenesis of the *K181-Birmingham* variant of MCMV [315]. The stock of *tsm5* contains multiple viruses with a number of non-synonymous mutations

including five in essential viral genes: M27, M36, M98, M56 and M70. The M70 ORF encodes for the MCMV DNA-primase and a truncating mutation (C890Y) alone sufficiently impedes the DNA primase-helicase complex and prevents DNA-synthesis [381, 382]. Although *tsm5* is attenuated, it was previously uncovered that inoculation of BALB/c mice with *tsm5* can induce primary immune responses. In fact, inoculation with a dose of as few 40 PFU of *tsm5* induced protective immunity to subsequent challenge towards salivary gland passaged *K181* [383]. The *tsm5* virus is capable of establishing a latent infection as viral DNA has been detected in multiple organs (salivary glands, lung, spleen, liver, kidney, and heart) during latency, however, viral RNA transcripts have never been detected [383, 384].

To test whether the replication defective *tsm5* virus would cause memory inflation a group of C57BL/6 mice were inoculated i.p. with *tsm5*. The frequency of MCMV-specific CTLs was measured in the spleen at one, seven, 14 and 52 weeks p.i. (Figure 5.1). Detection of lytic viral replication within the salivary glands, liver, lungs, kidneys and heart were assessed by plaque assay.

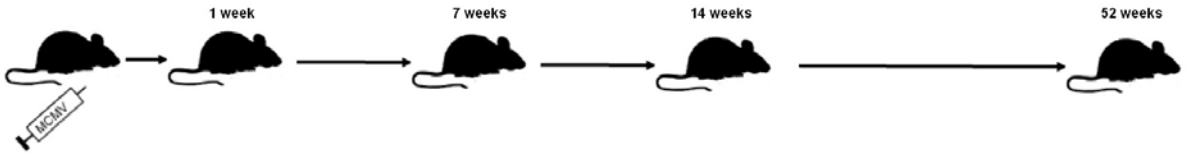

Figure 5.1. Experiment design: six to eight week old C57BL/6 mice were inoculated i.p. with 1x10^4 PFU of *tsm5* virus. The MCMV-specific immune response was subsequently measured in the spleen at one (n=4), seven (n=4), 14 (n=4) and 52 (n=4) weeks p.i. by ICS. Tetramer staining for m139 and IE3-tetramer specific cells was performed 52 weeks p.i. The salivary glands, liver, lungs, kidneys and heart from each animal were used to detect the presence of lytic *tsm5* virus.

5.2. LYTIC *tsm5* IS UNDETECTABLE IN C57BL/6 INFECTED MICE

The *tsm5* virus is replication defective because of a switch from cysteine to tyrosine at position 890 of the M70 ORF resulting in a truncated DNA-helicase/primase complex. However, the *tsm5* viral stock is impure and contains an unknown number of other mutant viruses, many but not all of which contain the M70 mutation. *tsm5* replication is partially under immune control as replicates with delayed kinetics infection in immunodeficient SCID [381, 383]. To determine if *tsm5* replicated to detectable levels within C57BL/6 mice the lytic viral titres were assessed by explant culture of tissue homogenate onto MEFs. Normally, MCMV titres are highest in the salivary gland during acute infection, here at one-week p.i. there was no evidence of CPE of the MEF monolayer (Figure 5.2). If lytic replication did occur, it was below the limit of detection by conventional plaque assay. In addition, lytic *tsm5* virus was not found in the kidneys, liver, lungs or heart at one-week p.i. The plaque assay method was performed at all subsequent time points and lytic virus was always below the limit of detection in C57BL/6 mice.

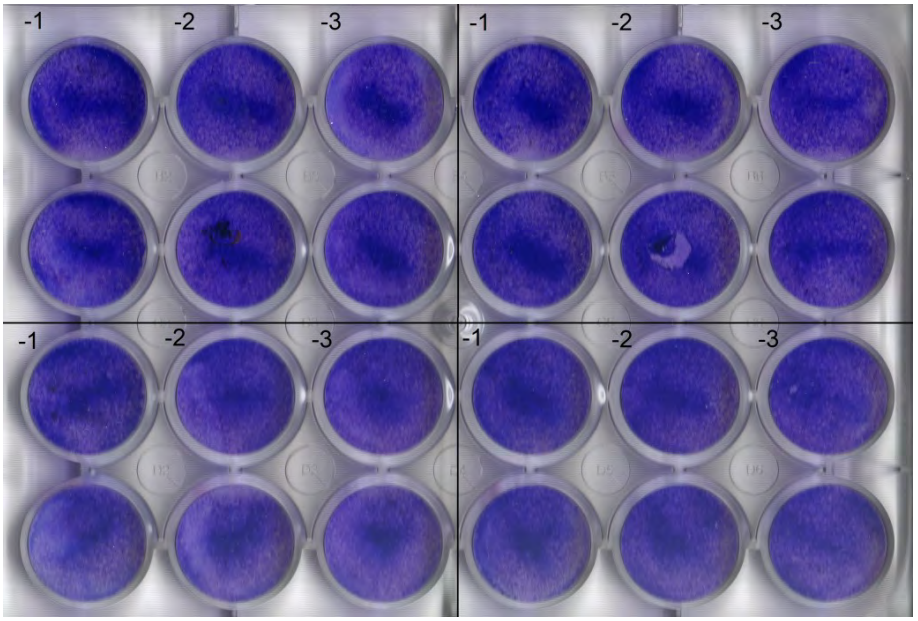

Figure 5.2. Lytic *tsm5* is undetectable in C57BL/6 infected mice. *tsm5* plaque assay. Briefly, salivary glands from four C57BL/6 mice, one week post-*tsm5* inoculation, were removed and homogenised in 1 ml of RPMI, then the supernatant was serially diluted ($1x10^{-1}$, $1x10^{-2}$ and $1x10^{-3}$) and added to confluent MEFs in 24 well plates (in duplicate). Plates were returned to the incubator for one week after which the homogenate was removed and the MEF stained with crystal violet, visible plaques were counted at x10 magnification.

5.3. INFECTION WITH *tsm5* DOES NOT ELICIT MEMORY INFLATION

The *tsm5* virus has previously been demonstrated to be immunogenic, promoting normal humoral immune responses with immunoglobulin titres comparable between *tsm5* and *K181* infected mice and acute cytotoxic $CD8^+$ T-cell responses to m04 (YGPSLYRRF) and M84 (AYAGLFTPL) peptides in BALB/c mice [383, 385]. However, it was uncertain whether *tsm5* would promote a cytotoxic $CD8^+$ T-cell response during infection in C57BL/6 mice due to the different MHC-I antigens and the interaction between Ly49h receptor in the mouse and the viral protein m157.

Firstly, i.p. inoculation of the *tsm5* virus did elicit a detectable primary $CD8^+$ T-cell response in C57BL/6 mice. CTL specific for the same five immunodominant MCMV-specific $CD8^+$ T-cell epitopes used throughout this study (M38, M45, M57, m139 and IE3) were evident by ICS for IFNγ (Figure 5.3, Table 5.1). However, the primary MCMV-specific immune response to this replication defective strain was not as robust as the proliferation of virus-specific $CD8^+$ T-cells seen one week post-inoculation if *K181* or *Smith* strains of MCMV were used [165]. The frequencies of the $CD8^+$ T-cell responses were highest towards the M57 epitope (1.46%) and lowest towards the IE3 epitope (1.01%). However, the range of CTL frequencies, of the five epitopes, was narrower and could coincide with a lower initial antigen burden. The frequency of MCMV-specific CTLs ranged from approximately 1-2% of $CD8^+$ T-cells per epitope (Figure 5.3, Table 5.1), which is very similar to the MCMV acute response observed

in the peripheral blood by Snyder *et al* (2010) when they infected C57BL/6 with their attenuated ΔgL-MCMV [380].

I then sought to determine whether the replication defective *tsm5* virus could promote memory inflation over the course of 52 weeks of *tsm5* infection. It is important to note that lytic replication was never evident by explant culture in those infected mice. Seven weeks p.i. the immune response to *tsm5* showed a small contraction in the frequency of M38, M45, M57 and m139 specific $CD8^+$ T-cells in the spleen from day seven. This is likely a reflection of the resolution of acute infection and the lymphocytes undergoing programmed cell death and natural decay in the absence of antigen [165]. The frequency of M38, M45, M57 and m139-specific CTLs declined from approximately 1.3-1.5% at one week p.i. to below 1% of the $CD8^+$ T-cell pool by week seven (Figure 5.3, Table 5.1). The IE3-specific immune response was the only one measured not to undergo a phase of contraction remaining stable at approximately 1.1% of $CD8^+$ T-cells at week seven (Figure 5.3, Table 5.1). Again it is important to note that these changes are only small fluctuations in the frequency of virus specific CTLs and are not statistically significant between week one and seven.

Memory inflation tends to coincide with the induction of latent infection therefore the frequency of the *tsm5*-specific $CD8^+$ T-cells was measured at the later time points of 14 and 52 weeks p.i. Here the most apparent finding is that the frequency of MCMV-specific $CD8^+$ T-cells did not undergo memory inflation. Critically, the frequency of IFNγ-specific CTLs in the spleen remained below 1.5% of the total $CD8^+$ T-cell pool for each individual MCMV epitope (Figure 5.3). There had been a change in the immunodominance hierarchy with the m139

and IE3 specific immune response becoming the most abundant, however this pattern of immune response is entirely different to the memory inflation seen with *Smith* infected C57BL/6 mice.

To prove that the failure to detect memory inflation is not due to a loss of IFNγ synthesis which would not be accurately determined by ICS, the frequency of *tsm5*-specific $CD8^+$ T-cells was determined using MHC-I tetramer reagents specific for the inflationary m139 and IE3 $CD8^+$ T-cells (Figure 5.4 A). Here, 52 weeks post-*tsm5* infection, the frequency of m139-specific CTLs was approximately 0.5% of the entire splenic $CD8^+$ T-cell population (Figure 5.4 B). Likewise, the frequency of IE3-specific cells was also very low with approximately 0.1% of the $CD8^+$ T-cell pool being tetramer specific (Figure 5.4 B). The evidence presented in Figure 5.3 and 5.4 clearly show that memory inflation does not occur with *tsm5* infection. Therefore, the M70 mutation, which attenuates the virus, is likely to prevent sporadic viral lytic reactivation and T-cell proliferation.

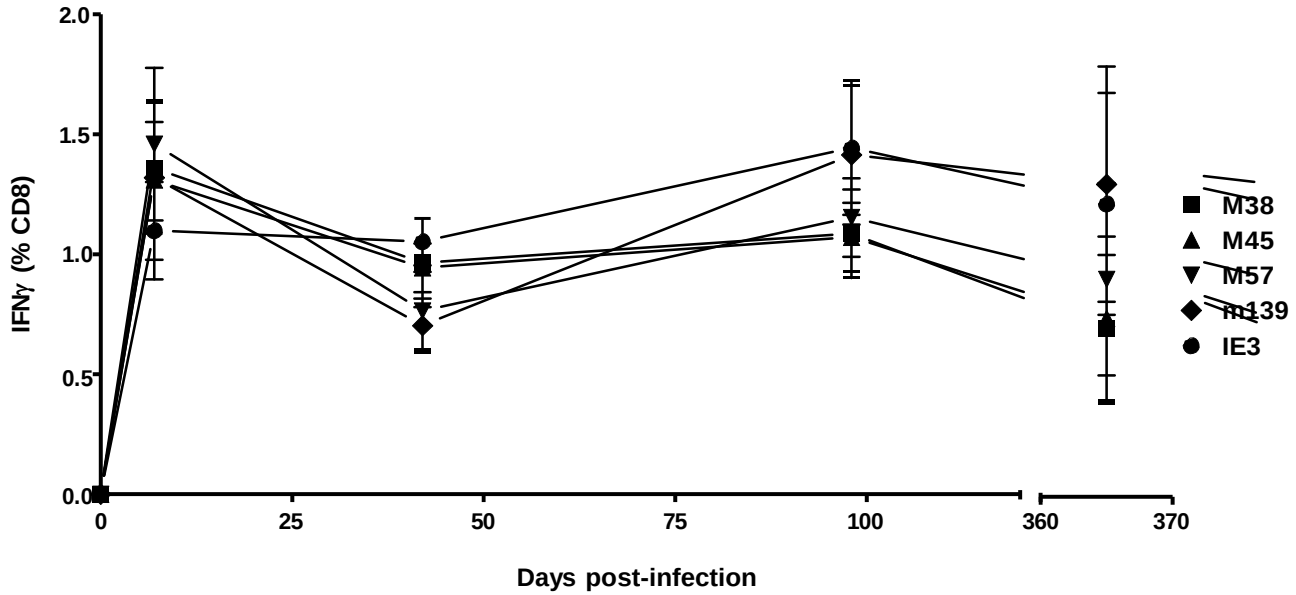

Figure 5.3. *tsm5* does not promote MCMV-specific T-cell accumulation (ICS). Frequency of IFNγ-producing CD8$^+$ T-cells following peptide stimulation of splenocytes at weeks one, seven, 14 and 52 post-*tsm5* infection. Mean +/- SEM (n=4 per time point).

Table 5.1. Frequency of *tsm5*-specific CD8$^+$ T-lymphocytes detected within the spleen, using ICS for IFNγ, expressed as a percentage of CD8$^+$ T-cells. Mean +/- SEM.

	I FNγ CD8 $^+$ T-cell (% CD8) (n=4)			
Epitope	**Week 1**	**Week 7**	**Week 14**	**Week 52**
M38	1.36 +\- 0.27	0.96 +\- 0.19	1.09 +\- 0.19	0.69 +\- 0.31
M45	1.31 +\- 0.33	0.94 +\- 0.10	1.07 +\- 0.14	0.73 +\- 0.34
M57	1.46 +\- 0.32	0.77 +\- 0.16	1.15 +\- 0.16	0.90 +\- 0.40
M139	1.32 +\- 0.23	0.70 +\- 0.11	1.42 +\- 0.29	1.29 +\- 0.49
IE3	1.10 +\- 0.20	1.05 +\- 0.10	1.44 +\- 0.28	1.21 +\- 0.46

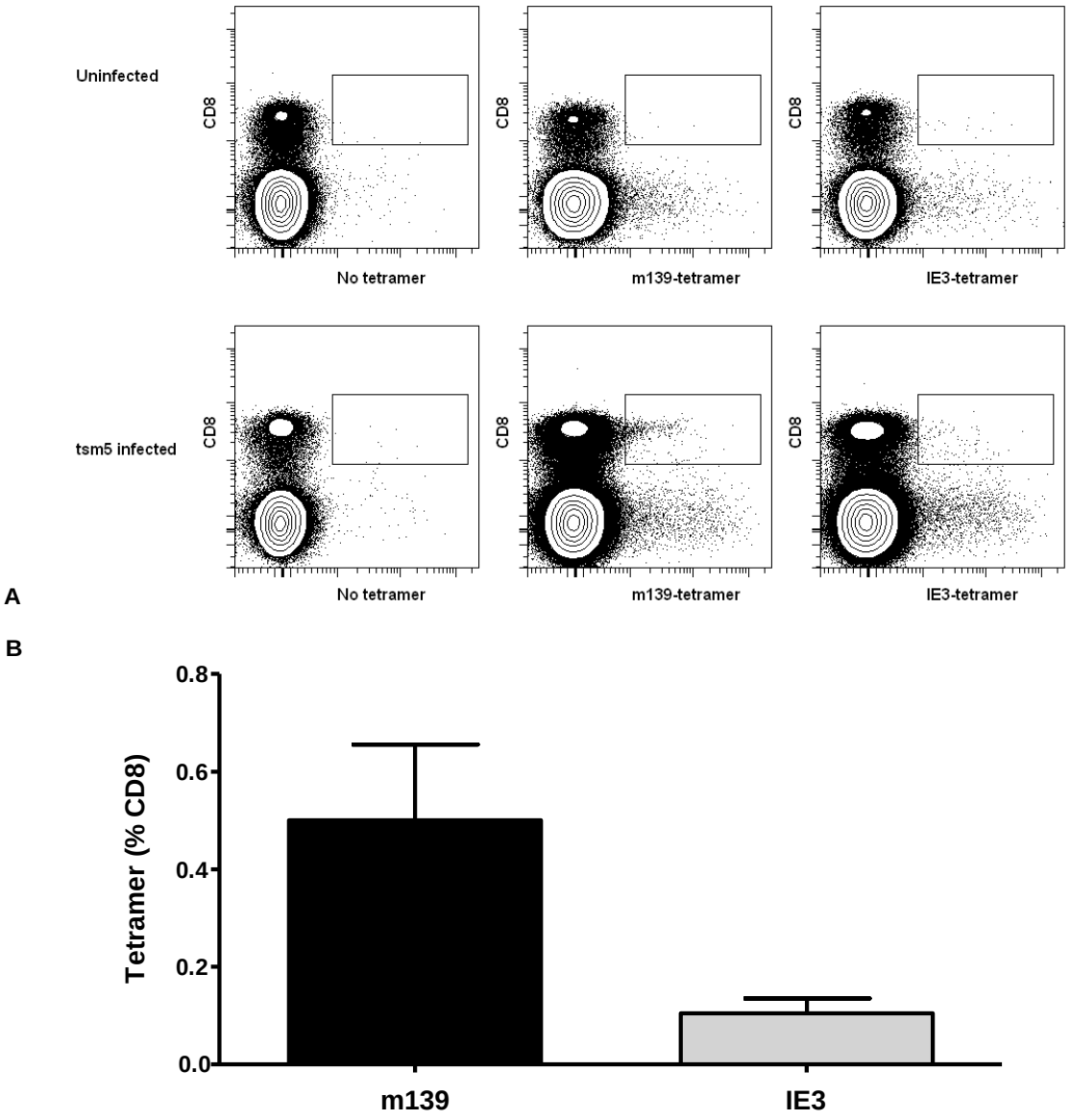

Figure 5.4. *tsm5* does not promote MCMV-specific T-cell accumulation (tetramer). A) Representative m139 and IE3-tetramer staining in uninfected and *tsm5* infected mice 52 weeks p.i. B) Frequency of m139 and IE3-tetramer specific $CD8^+$ T-cells splenocytes 52 weeks post tsm5 infection. Mean +/- SEM (n=4).

5.4. *tsm5* DOES NOT DRIVE THE VIRUS SPECIFIC CD8 T-CELLS TO A HIGHLY DIFFERENTIATED T_{EM} PHENOTYPE

A hallmark of HCMV infection is the accumulation of highly differentiated, TEMRA HCMV-specific $CD8^+$ T-cells [145, 386, 387]. Similarly *wt* MCMV infection of C57BL/6 mice generates an accumulation of highly differentiated lymphocytes ($CD8^+$ $CD44^+$ $CD62L^-$) indicative of repeated antigen exposure [165]. Having previously shown that *tsm5* infection does not cause an accumulation of virus specific $CD8^+$ T-cells (Figure 5.3 + 5.4) the level of differentiation of the virus-specific and wider $CD8^+$ T-cell pool was assessed.

Following infection with MCMV *Smith*, C57BL/6 mice showed an accumulation of T_{EM} $CD8^+$ T-lymphocytes which includes high frequencies of m139 and IE3-tetramer specific lymphocytes; in contrast *tsm5* infected mice do not develop the same accumulation of highly differentiated T-cells. The phenotype of the m139-specific CTLs, 52 weeks post-*tsm5* infection, was a more even distribution of T_{CM} (40%) and T_{EM} T-cells (55%) (Figure 5.5 A). Likewise, the IE3-tetramer specific cells were more equally distributed between T_{CM} (43%) and T_{EM} (42%) T-cells (Figure 5.5 A). It was proposed that the inflationary subset associated with *Smith* infection is replenished through the repopulation of less differentiated cells (T_N and T_{CM}) [45] and the data supports this hypothesis because attenuation of viral replication has blocked both the accumulation of and high differentiation status of MCMV-specific T-cells.

The mean fluorescence intensity (MFI) of CD27, CD44, CD62L, CD122 and CD127 were recorded on the m139 and IE3-tetramer labelled cells and compared to the T_{EM} $CD8^+$ T-cells from *tsm5*-infected mice 52 weeks p.i. (Figure 5.5 B). MFI rather frequencies were used for this analysis, as there was no direct group to compare the expression of the phenotypic markers. It was observed that there was a significant decline in the fluorescence intensity of CD44 on the m139 (***$p<0.001$) and the IE3-tetramer (*$p<0.05$) cells compared with the overall T_{EM} $CD8^+$ T-cells. This shift in CD44 florescence is likely to be a reflection of the high proportion of tetramer specific cells that are less differentiated belonging to the T_{CM} population (Figure 5.5 A). In addition, the MFI of CD127 was elevated on the m139-specific cells in comparison to the effector memory $CD8^+$ T-cells ($p>0.05$). Expression of CD122 (***$p<0.001$) and CD127 (**$p<0.01$) were statistically elevated on the IE3-tetramer specific cells compared with the overall effector memory population. The higher expression of these cytokine receptors, 52 weeks p.i., suggests the cells have retained the molecules needed for homeostatic proliferation. In addition, CD27 and CD62L were expressed at a greater intensity on the tetramer specific cells (Figure 5.5 B). These findings further suggest that lytic replication is responsible for heightened T-cell differentiation associated with MCMV infection.

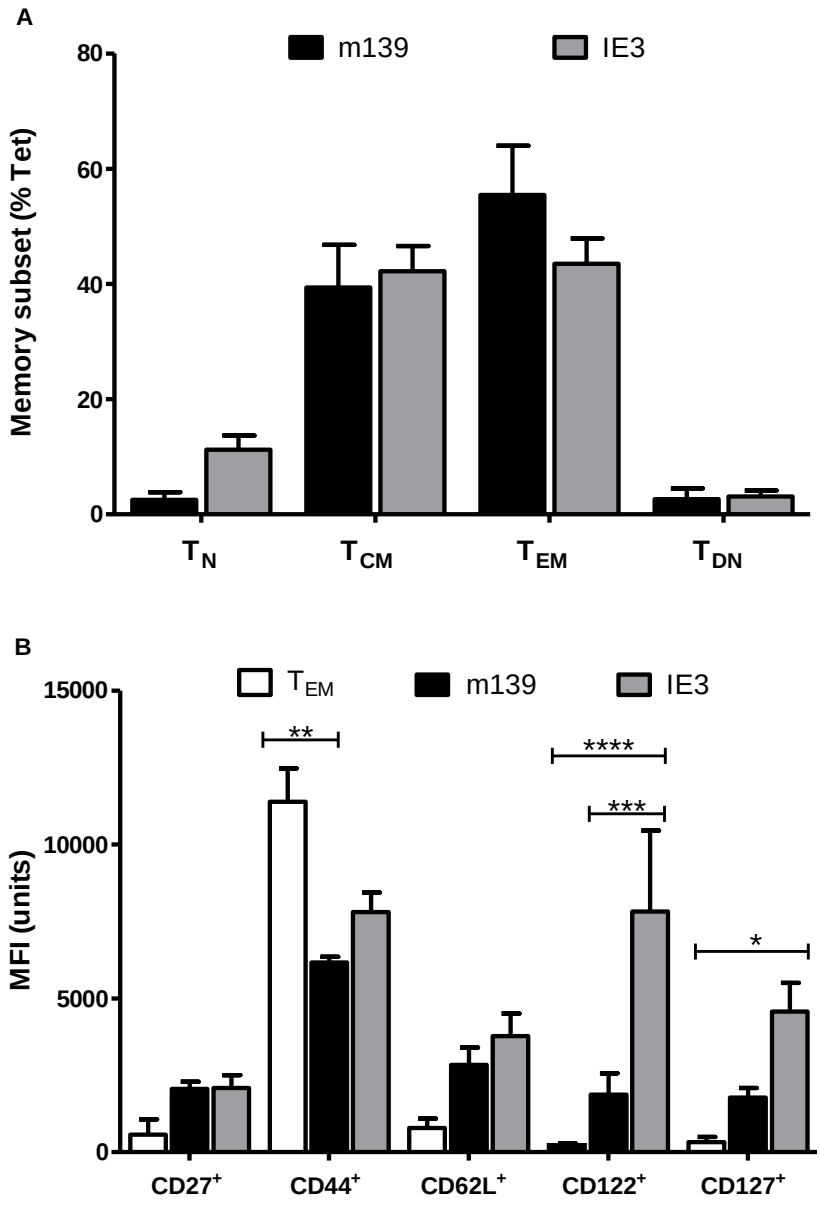

Figure 5.5. The *tsm5*-tetramer specific CD8$^+$ T-cell response is less differentiated. A) Memory status of m139 and IE3-tetramer specific CD8$^+$ T-cells, detected in the spleen, 52 weeks post *tsm5* infection. Mean +/- SEM (n=4). B) MFI of CD27, CD44, CD62L, CD122 and CD127 on the T_{EM} CD8$^+$ T-cell population and the m139 and IE3-tetramer specific CD8$^+$ T-cells. Mean +/- SEM (n=4). Data analysed by 2-way ANOVA plus Bonferroni post-test (*p<0.05, *p<0.01, ***p<0.001 and ****p<0.0001).

5.5. INOCULATION WITH *tsm5* GENERATES A CTL RESPONSE BUT DOES NOT EXPAND THE T_{EM} $CD8^+$ T-CELL POOL

In the previous chapters, *Smith* infection was shown to expand the T_{EM} pool at the expense of the naïve T-cell pool. The low frequency of naïve $CD8^+$ T-cells was linked to these mice responding less well to IAV challenge than MCMV seronegative animals. The frequency of each memory subset of the $CD8^+$ T-lymphocyte pool was determined using a combination of CD44 and CD62L labelling 52 weeks p.i.

Overall the distribution of $CD8^+$ T-cell memory subsets in *tsm5* infected animals was less differentiated than that observed in mice infected with MCMV *Smith* and was more similar to an MCMV negative animal (**NB** *the uninfected SPF animals were not litter mates but were aged matched*) (Figure 5.6 A+B). For example, the most predominant subset of $CD8^+$ T-cells in *tsm5* infected animals was the T_N subset with over 65% of $CD8^+$ T-cells expressing the combination of $CD44^-$ and $CD62L^+$ (Figure 5. 6 B). Only 10% of MCMV-specific $CD8^+$ T-cells displayed the T_{EM} phenotypic combination. The frequency of non-inflationary T_{CM} $CD8^+$ T-cells was similar for *tsm5* and MCMV negative animals. Inoculation with *tsm5* did not expand the T_{EM} pool and naïve lymphocytes remained the most abundant cell type 52 weeks after the initial viral challenge.

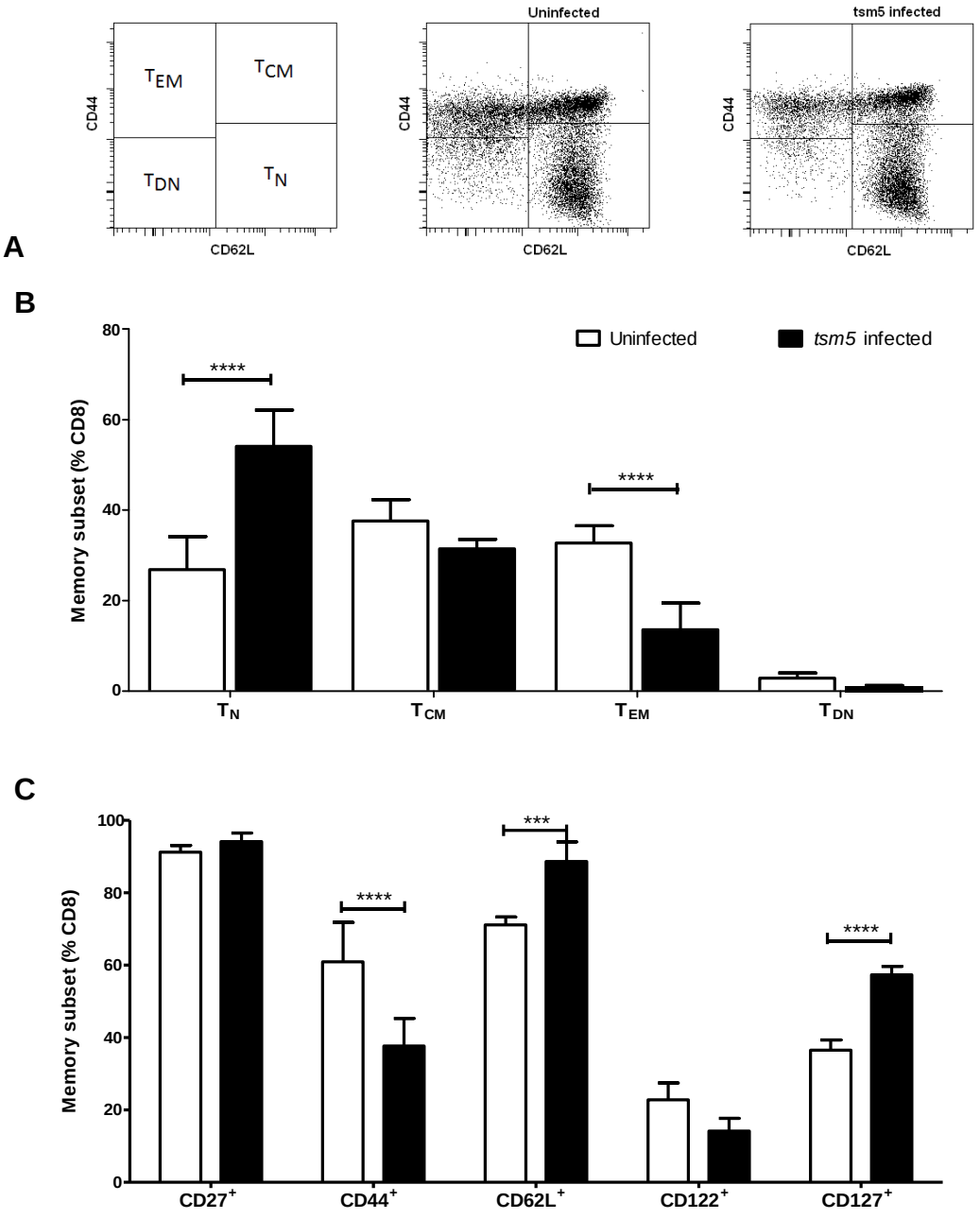

Figure 5.6. Inoculation of *tsm5* does not expand the T_{EM} T-cell pool, 52 weeks p.i. A) FACS plots showing $CD8^+$ T-cell memory subsets in uninfected and *tsm*5-infected mice. B) Frequency of T_N, T_{CM}, T_{EM} and T_{DN} $CD8^+$ T-cells. C) Phenotype of splenic $CD8^+$ T-cells. Mean +/- SEM (n=4). Data analysed by 2way-ANOVA plus Bonferroni post-test (**p<0.0001, ***p<0.001). N.B uninfected mice are aged matched but not litter mates.**

5.6. RESULTS CHAPTER 3: CONCLUSIONS

In older individuals, HCMV seropositivity dramatically skews the constitution of the immune system towards an IRP. Oligoclonal HCMV-specific $CD8^+$ T-lymphocyte expansions, specific for a number of immunodominant epitopes, are readily detectable in the peripheral blood and accumulate to a large frequency with an increase in age [147]. Likewise, large $CD8^+$ T-cell expansions can be detected in latently MCMV infected mice [165]. Both the inflationary HCMV [312] and MCMV [165] subsets of virus-specific $CD8^+$ T-cells are relatively short-lived (compared to other memory subsets) and their accumulation is paradoxical. Having previously shown that administration of long-term valaciclovir therapy can significantly reduce the MCMV-specific $CD8^+$ T-cell response. The valaciclovir treated mice retained a greater proportion of naïve $CD8^+$ T-cells that also corresponded with improved control of IAV infection.

To prove that lytic MCMV reactivation was the event that drives memory inflation the immune response to the MCMV live-attenuated virus *tsm5* was tested. During latent HCMV/MCMV infection there is potentially sufficient viral reactivation to provide a frequent source of stimuli to replenish the virus-specific $CD8^+$ T-cell pool. This hypothesis is difficult to prove, as latent HCMV/MCMV is notoriously difficult to detect in explant cultures due to the low number of latently infected cells and even fewer lytic reactivation events.

The *tsm5* virus provides a unique opportunity to study memory inflation with a replication defective MCMV strain. The *tsm5* virus is a live-attenuated virus generated by chemical mutagenesis (N-methyl-N'-nitro-N-nitrosoguanidine) [315]. Non-synonymous mutations

were mapped to genes essential for viral pathogenesis including mutations in immune evasion genes, DNA encapsulation genes and the DNA-primase ORF (M70) [381]. The M70 mutation alone (or in combination with the M56 and/or M98 mutations) renders the virus replication defective in DNA synthesis [382] and restricts growth at normal murine body temperature [313-315].

Previously the immune response to the attenuated ΔgL-MCMV was declared to cause an accumulation of MCMV-specific $CD8^+$ T-cells albeit at a much lower frequency than infection with the non-mutant virus [193]. The ΔgL-MCMV is able to undergo one round of replication and therefore there is small chance of the virus recovering gL-expression, through homologous recombination, that could serve to provide the antigen for memory inflation. In contrast, the *tsm5* virus is replication defective due to mutated DNA-helicase/primase complex therefore homologous recombination is theoretically impossible. However, the *tsm5* viral stock is impure and contains contaminating viruses that do not contain the M70 mutation. It was previously shown that *tsm5* is capable of replicating although with delayed kinetics following inoculation in SCID mice [381], however, here lytic *tsm5* was not detected at any phase of infection in immunocompetent C57BL/6 mice. The lack of lytic virus during the acute infection would suggest that immunological control is sufficient to control aberrant replication of non-M70 mutants without initiating memory inflation.

Snyder *et al* (2011) had stated that the attenuated ΔgL-MCMV is not eradicated from the host and drives memory inflation through repeatedly generating viral antigens [193]. Here memory inflation was not observed at any phase of *tsm5* infection. The frequency of *tsm5*-

specific $CD8^+$ $IFN\gamma^+$ T-cells never exceeded 1.5% of $CD8^+$ T-cell pool for each of the five immunodominant peptides used *for ex vivo* stimulation (Figure 5.3). The absence of lytic virus (Figure 5.2) and the low frequencies of MCMV-specific T-cells generated by *tsm5* infection again indicate that viral replication is somewhat responsible for memory inflation. This finding is contrary to the conclusions of Snyder *et al* (2011) when they infected animals with their attenuated ΔgL-MCMV [193]. The difference in immune response between these two viruses is likely due to the mechanism through which they are attenuated. The ΔgL-MCMV virus is infective however virions are incapable of spreading to neighbouring cells, transcription remains possible and could therefore could serve to generate the viral antigens that elicit memory inflation [193]. Similarly, the establishment of a systemic latent infection may be crucial to the subsequent T-cell response. The route of HSV-1 infection was shown to be critical for the generation of high-frequencies of gB-specific $CD8^+$ T-cells [363] and correspondingly footpad inoculation of ΔgL-MCMV does not elicit the characteristic memory inflation [193].

At one year post-*tsm5* infection there was not the typical accumulation of T_{EM} T-cells as seen following *Smith* infection. Within the spleen of *tsm5* infected mice, approximately 70% of $CD8^+$ T-cells have the T_N phenotype, 20% were T_{CM} and only 10% were the most differentiated T_{EM} populations (Figure 5.6 B). HCMV is associated with the accumulation of the most differentiated $CD8^+$ and $CD4^+$ T-cells therefore it is attractive property of the attenuated *tsm5* that inoculation does not cause the memory inflation.

In spite of lytic reactivation not being detected, the *tsm5* virus is likely to establish latent infection in C57BL/6 mice as it has previously been noted in BALB/c and SCID mice [381, 383]. It is unknown if *tsm5* reactivation occurs naturally and here the lack of memory inflation suggests that *tsm5* does not undergo lytic replication. However, the viral stock contains variants that lack the M70 mutation. These non-attenuated variants could be responsible for most differentiated antigen-specific lymphocytes observed in Figure 5.5.

The term "latency" is sometimes loosely to describe the absence of lytic replication; however, post-inoculation each virus particle would operate independently and be in different stage of its lifecycle. Therefore, although the virus is not detectable by conventional techniques there maybe virus within specific cell types or ecological niches that is either truly latent, undergoing sporadic lytic replication or subverting the immune system. The process of abortive reactivation could serve as a method of priming memory inflation whilst evading the brunt of the immune response. "Normal" T-cell memory development requires endogenous peptide to be processed by the immunoproteasome and presented via MHC-I interacting with the cognate TCR [189] or the cross-presentation of exogenous proteins from professional and non-professional antigen presenting cells [388]. However, the controlled process of abortive reactivation sees the virus utilising the activation of T-cells to impair NK-cell mediated cytotoxicity at the expense of sensitising CTLs. Stimulation of $CD8^+$ T-cells is less significant to MCMV survival as deletion of MHC-I presentation evasins does not alter the magnitude of the $CD8^+$ T-cell response [380].

The *tsm5* virus would serve to be an excellent model for designing a vaccine for use in human trials. Firstly, the virus generates protective immunity at very low doses, as inoculation 40 PFU of *tsm5* induced protective immunity to subsequent challenge with salivary gland passaged *K181* MCMV [383]. Secondly, the virus does elicit $CD8^+$ T-cell responses without the deleterious accumulation of highly differentiated virus-specific T-cells and the naïve T-cell pool remains more akin to an uninfected animal. Thirdly, *tsm5* also contributes to normal immunoglobulin titres which are comparable to infection with non-replication defective MCMV [383]. Therefore, if a live attenuated HCMV vaccine is generated with a similar mutation in the DNA-primase, and is proved replication defective, it has the potential provide additional immunity that could have large implications for health.

6. DISCUSSION: *ANTIVIRAL THERAPY CAN REVERSE THE DEVELOPMENT OF IMMUNE SENESCENCE IN ELDERLY MICE WITH LATENT CYTOMEGALOVIRUS INFECTION*

6.1. CMV AND IMMUNE SENESCENCE

In 1998, a Swedish longitudinal study examined a series of immune parameters including T-cell frequencies and related those findings to the age of donor. It was concluded that a high number of $CD8^+$ T-lymphocytes and low number of $CD4^+$ T-cell in the peripheral blood were associated with a significant increase in two-year mortality in individuals over 80 years old [148]. These findings were confirmed in samples taken from octogenarians in the Swedish longitudinal OCTO immune study. The observed expansion of $CD8^+$ T-cells in the peripheral blood caused an inversion of the CD4:CD8 T-cell ratio in almost a third of donors [216]. Furthermore, the accumulation of differentiated $CD8^+$ $CD28^-$ $CD57^+$ T-cells was specifically associated with increased mortality [216]. In the following Swedish NONA-Immune study, the elevated risk of mortality was analysed in greater detail and the expansion of the highly differentiated $CD8^+$ $CD27^-$ $CD28^-$ $CD56^+$ $CD57^+$ $CD45RA^+$ T-cells occurred most commonly within those individuals who were HCMV-seropositive [217]. Subsequently, HCMV seropositivity was confirmed as an indicator of poor health outcomes in the elderly. The acquisition of HCMV early in life and having expansions of virus specific CTL was estimated to alter the $CD8^+$ T-cell compartment with an equivalent 'ageing effect' of the $CD8^+$ T-cells by 35 years [308]. Importantly HCMV is often acquired at an early age and is highly prevalent, through an annual rate of HCMV seroconversion in adults (18-60 years) of 0.55% [91, 389]; therefore immune senescence associated with HCMV is an issue that will continue to develop unless therapeutic intervention is successfully made.

The precise mechanism(s) through which HCMV infection causes senescence of the immune system is not known. Both epidemiological and laboratory based evidence has illustrated

that individuals with the highest anti-HCMV IgG titres are at the highest risk of failing to developing sufficient antibody titres towards a trivalent Influenza vaccine [353]. Likewise, the oligoclonal expansion of highly differentiated $CD8^+$ T-lymphocytes are more common in HCMV-seropositive individuals and their presence is implicated in a six-fold reduction in EBV-specific $CD8^+$ T-cells [146] which could be due adaptive immunity being a finite system. The process of thymic atrophy results in the naïve T-cell pool having a more limited TCR diversity in old age and as a consequence *de novo* immune responses are weakened in the elderly. As the magnitude of the CMV-immune response also increases with advancing age, it raises the question whether the accumulation of CMV-specific immunity is an additional cause or an indicator of immune senescence.

Previous adoptive transfer studies of MCMV-specific T-cells into naïve and infected mice have estimated that the half-life of the inflationary MCMV-specific T-cells is up to 60 days [165]. However, in a separate study in thymectomised mice, 100 days post MCMV-infection, there was a relative expansion of memory $CD8^+$ T-cells ($CD8^+$ $CD44^{hi}$) which included M38 and m139 peptide-specific T-cells but not IE3-specific $CD8^+$ T-cells [390]. These conflicting reports show that the relative T-cell half-live does vary between institutional MCMV models. When prolonged valaciclovir treatment was administered, equivalent to four times the half-live of MCMV-specific $CD8^+$ T-cells there was almost an 80% reduction in the combined $CD8^+$ T-cell response to the five immunogenic peptides (m38, M45, M57, m139 and IE3). The mice in these experiments had been infected for at least 6 months prior to starting antiviral therapy and therefore this model parallels the acquisition of HCMV at an early age, many years prior to potential consideration of antiviral therapy.

Measuring the rate of decay of the MCMV-specific T-cells, the half-life for the five-immunodominant CTL populations (relative difference in frequency to the untreated controls) was between 200-250 days when taken over a 12-month period of treatment (Figure 6.1). This estimated half-life is considerably longer than has previously been measured in the adoptive transfer of MCMV-specific CTLs [165]. The difference between these two measurements again may similarly be due to differences within the institutional models or could relate to the completeness of the antiviral treatment. In the setting of adoptive transfer into SPF animals the transferred CTLs are entering an environment completely devoid of viral replication and transcription whereas the treatment was given to virally infected mice to prevent viral replication but not transcription of genes prior to DNA-synthesis. Consequently, it would be expected that the presence of MCMV transcripts produced during latency provide additional stimuli to the immune system and continue to repopulate the CTL response to the virus. In addition to the longer half-life the kinetics of T-cell decline were not linear. There was a tendency for the $t_{1/2}$ of decay to become more rapid with time and the IE3-specific response was the most marked in this regard, as IE3 CTLS declined at a $t_{1/2}$ rate of only 40 days in the last six months of treatment that could suggest as near complete absence of viral antigen. Studies of HCMV-specific T-cells, utilising deuterated glucose, had shown that although the pp65-specific T-cells remain clonal (stable Vβ TCR chain usage) and at a high frequency, although individually the cells are disappearing at a rate 1-2% per day [312]. Therefore, the rate of decay of MCMV and HCMV inflationary CTLs are both estimated to be measured in months rather than years which is different to virus-specific immune responses to most other pathogens [391].

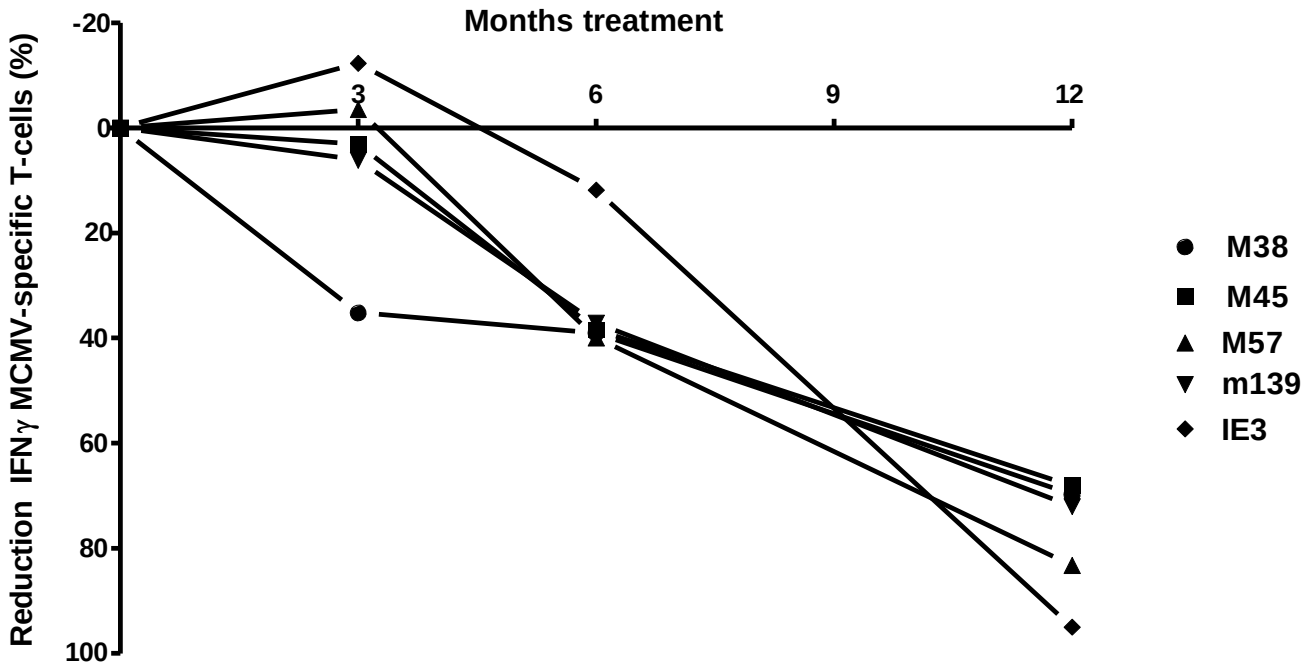

Figure 6.1. The estimated rate of decay of the MCMV-specific CD8$^+$ T-cells. The data is obtained from the independent experiments that show the effects of three and six months antiviral treatment (Figure 3.10, Table 3.3) and 12 months of treatment (Figure 4.3, Table 4.1) relative to the frequency of MCMV-specific CD8$^+$ T-cells in untreated animals.

Carries of HCMV have markedly increased numbers of memory cells in the peripheral blood and reduced numbers of naïve T-cells [386] which is mirrored in our MCMV models. Importantly, in the MCMV model, valaciclovir treatment reversed the skewing of the CD8$^+$ T-cell phenotype. In MCMV-neg mice, the naïve T-cells compartment comprised 37% of CD8$^+$ T-cells at age 18 months (Figure 4.5 B). Compare this with the MCMV-AV group of mice in which only 15% of CD8$^+$ T-cells had a naïve phenotype. Remarkably, valaciclovir treatment completely restored the frequency of naïve CD8$^+$ T-cell pool to 42% of CD8$^+$ T-cells. Additionally, the effector memory CD8$^+$ T-cell pool almost doubled in the MCMV-AV group to almost 80% of CD8$^+$ T-cells compared to MCMV-neg mice and following 12 months of

antiviral treatment suppressed the T_{EM} population to a more normal frequency of 40% (Figure 4.5 B). Furthermore, *tsm5* infected mice do not develop high frequencies of T_{EM} at the expense of T_N $CD8^+$ T-cells (Figure 5.5 A) showing that viral replication is critical to the accumulation of virus-specific T_{EM} CTLs. It is tempting to hypothesise that the data presented throughout this thesis is directly applicable to the treatment of HCMV; however, there are differences in how humans and mice maintain the peripheral naïve T-lymphocyte pool in old age. The human $CD8^+$ T-cell pool is repopulated primarily by homeostatic divisions of naïve lymphocytes following atrophy and involution of the thymus whereas in aged mice the naïve T-cell pool is sustained by greater thymopoiesis than in humans [392]. Consequently antiviral treatment of HCMV would be needed prior to the exhaustion of thymopoiesis and is only of value if treatment was shown to improve the functional immune capacity of the host.

To assess whether treatment was successfully improved immune function in the elderly mice the animals were also challenged with influenza. This is a relevant model as influenza infection remains a major cause of infectious death, and HCMV-specific immunity has been shown to be an important determinant of vaccine-dependent immunity in some, but not all, studies [353, 393]. It was of interest that the most severe clinical features, e.g. shaking, ataxia and rapid breathing only occurred in the MCMV-AV group following IAV challenge. These symptoms were observed within the first few days of infection and therefore MCMV infection seemed to impair elements of the innate response. Valaciclovir therapy did prevent the most significant clinical features of the infection and prevented the death of the mice (Figure 4.7 A). Weight loss was also measured as a non-immunological parameter during the period of IAV challenge. Somewhat mysteriously, the MCMV+AV mice lost the least weight

of all groups with a plateau phase reached and maintained between day five and 10 p.i. (Figure 4.6 B). It was expected that the MCMV+AV mice would have the largest IAV specific immune response and lowest viral titres. Here, the MCMV+AV treated mice did not generate the largest NP-specific $CD8^+$ T-cell response in the BAL, CMLN or spleen (Figure 4.7-4.8) yet antiviral treatment did seem to reduce IAV titres to an equivalent levels to MCMV-neg mice (Figure 4.12). Unfortunately samples were not taken before day 10 (post-Influenza challenge) and therefore the immediate mechanism was not elucidated but is likely include a number of other immune cells such as pulmonary $CD103^+$ dendritic cells that transport IAV antigens from the lung to the CMLN and present processed antigens via MHC-I [379]. MCMV infection of mice that lack $CD103^+$ dendritic cells ($Batf3^{-/-}$) do not generate memory inflation therefore the suppression of the MCMV replication with valaciclovir may partially activate and licence a greater number/frequency of DCs to present IAV antigens which consequently improved the IAV response in the antiviral treated mice.

In addition to memory inflation of the virus-specific $CD8^+$ T-cell pool there is a high incidence of elevated immunoglobulin titres in the serum of elderly individuals. Studies have shown that elderly individuals (>60 years) with the highest quartile of anti-HCMV IgG compared with lower quartiles, were at an elevated (1.43 times) risk of all-cause mortality and cardio vascular disease mortality [218]. In addition, a high anti-HCMV specific IgG titre (>50 UA/ml) was shown to be linked to the proportion of non-responders to a tri-valent anti-influenza vaccine (A/Beijing/262/95 (H1N1), A/Sydney/5/97 (H3N2) and B/Beijing/184/93) [353] with HCMV was accepted as an accelerator of immune senescence of the B-cell response towards unfamiliar pathogens. More recently conflicting evidence obtained from elderly residents of

long-term care facilities which concluded HCMV seropositivity did not affected the generation of a protective immune response to influenza vaccination (A/Nanchang/933/95 (H3N2), A/Johannesburg/82/96 (H1N1) and B/Harbin/7/94) [393]. A limitation of these studies is that only humoral parameters were measured and the cytotoxic T-lymphocyte response was not assessed. Here, in the animal model, neither three nor six months of antiviral treatment reduced the titres of anti-MCMV-specific IgG compared to untreated mice (Figure 3.12 B) whereas longer periods of treatment did help to reduce the MCMV specific CTL response (Figure 3.13 C – 4.2).

Acycloguanosine antivirals are highly specific as the drug are selectively incorporated into the replicating viral genome; however, prolonged periods such as those used here have been associated with neurotoxicity and nephrotoxicity. However, during the experimental procedure, there was no increased risk of death associated with valaciclovir treatment. In addition, the valaciclovir treated mice displayed no aversion to prolonged periods of treatment and necropsy did not reveal any notable alterations to organ pathology. Herpes infections are often successfully treated for long periods with acycloguanosine antivirals without serious side effects. Aciclovir is one of the least toxic and has a safety index of approximately 3,000 (concentration associated with toxicity divided by therapeutic concentration) [394]. In addition, aciclovir and its metabolites are generated within virally infected cells meaning that any toxicity should be localised. With this in mind, aciclovir has been proposed to have direct immunosuppressive effect upon T-lymphocytes through inhibiting the actions of cellular purine nucleoside phosphorylase (PNP) enzymes. PNP are involved in guanine base synthesis and inhibition of PNP results in selective deficiency of T-

cell proliferation [395]. Aciclovir and its metabolites have been shown to have *in vitro* and *in vivo* immunotoxicity primarily towards $CD8^+$ T-cells in mice [195]. *In vitro* measures of both murine and human T-cell proliferation to mitogen/antigen stimuli seems to be inhibited at aciclovir concentrations in excess of 100 µM [195, 394, 396]. It is estimated that although the antiviral treated mice received high doses of antiviral the actual *in vivo* concentrations were below this threshold as 3.8 mg/day of treatment equates to 117 µM of which only 55% is bioavailable after the first round of metabolism. Furthermore, if the valaciclovir treatment suppressed $CD8^+$ T-cell proliferation the antiviral treated mice would have been more lymphopenic that the other mice, however this was not the case as hyposplenism was most common in MCMV infected mice and cellularity of the spleen was not affected by 12 months of treatment. Additionally, preventing $CD8^+$ T-cell proliferation would result in elevated CD4:CD8 T-cell ratios and this did not occur. Antiviral treatment actually restored the CD4:CD8 T-cell ratio to that of MCMV naïve mouse in the BAL, CMLN and spleen (Figure 4.11). Consequently, we would suggest that prolonged valaciclovir is safe for trial in humans.

HCMV is a highly prevalent virus and often contracted in the first few years, consequently individuals are likely to carry and potentially shed HCMV for the majority of their life. It is possible that as human and herpesvirus evolution occurred in parallel that acquiring HCMV could have beneficial/symbiotic effects. A high profile study into herpes virus co-infection in mice concluded that the presence of herpes viruses is beneficial under specific experimental circumstances. The study concluded that acute infection with either MCMV (or γHV68) provided a degree of short-term protection against *Listeria monocytogenes* and/or *Yersinia pestis* challenge [378, 397]. The acute herpes viral infection induced a transient

proinflammatory environment that activated macrophages and led to reduced bacterial loads. The same symbiotic effect was not apparent when testing later time-points (28 days p.i.) which the authors remarked corresponded to the latent phase of infection.

6.2. SUMMARY

The data presented throughout this thesis could have important implications for the potential treatment of patients with high levels of HCMV-specific immunity – i.e. display an IRP – and are therefore at the greatest risk of immune senescence [398]. Using the MCMV model it was shown that memory inflation is reversible with prolonged treatment. Unfortunately, it was not possible to prove that antiviral treatment did lead to a reduction in lytic reactivation events, as MCMV was undetectable so far out from the initial infection. However, treatment of latent infection lead to a partial rejuvenation of the $CD8^+$ T-cell pool as increased frequencies of naïve $CD8^+$ T-cells were detected in the spleen, and valaciclovir treated mice did appear to have superior control during acute influenza challenge. Valaciclovir is routinely administered for many years in order to suppress reactivation of genital herpesvirus and is well tolerated. Viral resistance to valaciclovir is rare and is most commonly during immune suppression. The amount of valaciclovir used in our study was equivalent to the dose administered for treatment of acute VZV infection or control of HCMV replication in patients undergoing immune suppression. However, the dose of valaciclovir that would be required to suppress HCMV replication in immunocompetent subjects and reduce the magnitude of the HCMV immune response may be much less than this and will be the subject of future investigations. In addition, it may now also be appropriate to consider the use of an attenuated HCMV vaccine to provide additional immunity without the side-effects of memory inflation with the aim to provide successful anti-HCMV therapeutic intervention and improve health other outcomes such as IAV vaccinations success.

REFERENCES

1. Beswick, M., et al., Antiviral therapy can reverse the development of immune senescence in elderly mice with latent cytomegalovirus infection. J Virol, 2012.

2. Solana, R., et al., CMV and Immunosenescence: from basics to clinics. Immun Ageing, 2012. 9(1): p. 23.

3. Davison, A.J., Herpesvirus systematics. Vet Microbiol, 2010. 143(1): p. 52-69.

4. Davison, A.J., et al., The order Herpesvirales. Arch Virol, 2009. 154(1): p. 171-7.

5. Schelhaas, M., et al., Herpes simplex virus type 1 exhibits a tropism for basal entry in polarized epithelial cells. J Gen Virol, 2003. 84(Pt 9): p. 2473-84.

6. Ongradi, J., V. Kovesdi, and G.P. Medveczky, [Human herpesvirus 6]. Orv Hetil, 2010. 151(13): p. 523-32.

7. Ongradi, J., V. Kovesdi, and E. Kovats, [Human herpesvirus 7]. Orv Hetil, 2010. 151(16): p. 645-51.

8. Klenovsek, K., et al., Protection from CMV infection in immunodeficient hosts by adoptive transfer of memory B cells. Blood, 2007. 110(9): p. 3472-9.

9. Pedron, B., et al., Development of cytomegalovirus and adenovirus-specific memory CD4 T-cell functions from birth to adulthood. Pediatr Res. 69(2): p. 106-11.

10. Andrews, D.M., et al., Innate immunity defines the capacity of antiviral T cells to limit persistent infection. J Exp Med, 2010. 207(6): p. 1333-43.

11. Sinclair, J., Human cytomegalovirus: Latency and reactivation in the myeloid lineage. J Clin Virol, 2008. 41(3): p. 180-5.

12. Yamanishi, K., et al., Identification of human herpesvirus-6 as a causal agent for exanthem subitum. Lancet, 1988. 1(8594): p. 1065-7.

13. Lepone, L., et al., Monofunctional and polyfunctional CD8+ T cell responses to human herpesvirus 8 lytic and latency proteins. Clin Vaccine Immunol. 17(10): p. 1507-16.

14. Chilet, M., et al., Virological and immunological features of active cytomegalovirus infection in nonimmunosuppressed patients in a surgical and trauma intensive care unit. J Med Virol, 2010. 82(8): p. 1384-91.

15. Weller, T.H., J.B. Hanshaw, and D.E. Scott, Serologic differentiation of viruses responsible for cytomegalic inclusion disease. Virology, 1960. 12: p. 130-2.

16. Bate, S.L., S.C. Dollard, and M.J. Cannon, Cytomegalovirus seroprevalence in the United States: the national health and nutrition examination surveys, 1988-2004. Clin Infect Dis. 50(11): p. 1439-47.

17. He, R., et al., Sequence variability of human cytomegalovirus UL143 in low-passage clinical isolates. Chin Med J (Engl), 2006. 119(5): p. 397-402.

18. Pignatelli, S., et al., Genetic polymorphisms among human cytomegalovirus (HCMV) wild-type strains. Rev Med Virol, 2004. 14(6): p. 383-410.

19. Cunningham, C., et al., Sequences of complete human cytomegalovirus genomes from infected cell cultures and clinical specimens. J Gen Virol, 2010. 91(Pt 3): p. 605-15.

20. Dargan, D.J., et al., Sequential mutations associated with adaptation of human cytomegalovirus to growth in cell culture. J Gen Virol. 91(Pt 6): p. 1535-46.

21. Bradley, A.J., et al., High-throughput sequence analysis of variants of human cytomegalovirus strains Towne and AD169. J Gen Virol, 2009. 90(Pt 10): p. 2375-80.

22. Akter, P., et al., Two novel spliced genes in human cytomegalovirus. J Gen Virol, 2003. 84(Pt 5): p. 1117-22.

23. Davison, A.J., et al., Homology between the human cytomegalovirus RL11 gene family and human adenovirus E3 genes. J Gen Virol, 2003. 84(Pt 3): p. 657-63.

24. Yu, D., et al., Construction of a self-excisable bacterial artificial chromosome containing the human cytomegalovirus genome and mutagenesis of the diploid TRL/IRL13 gene. J Virol, 2002. 76(5): p. 2316-28.

25. Smith, L.M., et al., Laboratory strains of murine cytomegalovirus are genetically similar to but phenotypically distinct from wild strains of virus. J Virol, 2008. 82(13): p. 6689-96.

26. Cheng, T.P., et al., Stability of murine cytomegalovirus genome after in vitro and in vivo passage. J Virol, 2010. 84(5): p. 2623-8.

27. Chee, M.S., et al., Analysis of the protein-coding content of the sequence of human cytomegalovirus strain AD169. Curr Top Microbiol Immunol, 1990. 154: p. 125-69.

28. Murphy, E., et al., Coding potential of laboratory and clinical strains of human cytomegalovirus. Proc Natl Acad Sci U S A, 2003. 100(25): p. 14976-81.

29. Rawlinson, W.D., H.E. Farrell, and B.G. Barrell, Analysis of the complete DNA sequence of murine cytomegalovirus. J Virol, 1996. 70(12): p. 8833-49.

30. Hamprecht, K., et al., Epidemiology of transmission of cytomegalovirus from mother to preterm infant by breastfeeding. Lancet, 2001. 357(9255): p. 513-8.

31. Kurz, S.K., et al., Focal transcriptional activity of murine cytomegalovirus during latency in the lungs. J Virol, 1999. 73(1): p. 482-94.

32. Bergallo, M., et al., Human cytomegalovirus glycoprotein B genotyping from bronchoalveolar lavage specimens. Can J Microbiol. 57(4): p. 273-7.

33. Bohm, V., et al., Immune evasion proteins enhance cytomegalovirus latency in the lungs. J Virol, 2009. 83(19): p. 10293-8.

34. Balthesen, M., M. Messerle, and M.J. Reddehase, Lungs are a major organ site of cytomegalovirus latency and recurrence. J Virol, 1993. 67(9): p. 5360-6.

35. Seckert, C.K., et al., Liver sinusoidal endothelial cells are a site of murine cytomegalovirus latency and reactivation. J Virol, 2009. 83(17): p. 8869-84.

36. Sinzger, C., et al., Hepatocytes are permissive for human cytomegalovirus infection in human liver cell culture and In vivo. J Infect Dis, 1999. 180(4): p. 976-86.

37. Zhou, W., et al., Impact of donor CMV status on viral infection and reconstitution of multifunction CMV-specific T cells in CMV-positive transplant recipients. Blood, 2009. 113(25): p. 6465-76.

38. Kahl, M., et al., Efficient lytic infection of human arterial endothelial cells by human cytomegalovirus strains. J Virol, 2000. 74(16): p. 7628-35.

39. Streblow, D.N., et al., Mechanisms of cytomegalovirus-accelerated vascular disease: induction of paracrine factors that promote angiogenesis and wound healing. Curr Top Microbiol Immunol, 2008. 325: p. 397-415.

40. Riegler, S., et al., Monocyte-derived dendritic cells are permissive to the complete replicative cycle of human cytomegalovirus. J Gen Virol, 2000. 81(Pt 2): p. 393-9.

41. Sinzger, C., et al., Macrophage cultures are susceptible to lytic productive infection by endothelial-cell-propagated human cytomegalovirus strains and present viral IE1 protein to CD4+ T cells despite late downregulation of MHC class II molecules. J Gen Virol, 2006. 87(Pt 7): p. 1853-62.

42. Hahn, G., R. Jores, and E.S. Mocarski, Cytomegalovirus remains latent in a common precursor of dendritic and myeloid cells. Proc Natl Acad Sci U S A, 1998. 95(7): p. 3937-42.

43. Hsu, K.M., et al., Murine cytomegalovirus displays selective infection of cells within hours after systemic administration. J Gen Virol, 2009. 90(Pt 1): p. 33-43.

44. Kern, M., et al., Virally infected mouse liver endothelial cells trigger CD8+ T-cell immunity. Gastroenterology, 2010. 138(1): p. 336-46.

45. Torti, N., et al., Non-Hematopoietic Cells in Lymph Nodes Drive Memory CD8 T Cell Inflation during Murine Cytomegalovirus Infection. PLoS Pathog, 2011. 7(10): p. e1002313.

46. Nowlin, D.M., N.R. Cooper, and T. Compton, Expression of a human cytomegalovirus receptor correlates with infectibility of cells. J Virol, 1991. 65(6): p. 3114-21.

47. Compton, T., D.M. Nowlin, and N.R. Cooper, Initiation of human cytomegalovirus infection requires initial interaction with cell surface heparan sulfate. Virology, 1993. 193(2): p. 834-41.

48. Kari, B. and R. Gehrz, A human cytomegalovirus glycoprotein complex designated gC-II is a major heparin-binding component of the envelope. J Virol, 1992. 66(3): p. 1761-4.

49. Kari, B. and R. Gehrz, Structure, composition and heparin binding properties of a human cytomegalovirus glycoprotein complex designated gC-II. J Gen Virol, 1993. 74 (Pt 2): p. 255-64.

50. Feire, A.L., H. Koss, and T. Compton, Cellular integrins function as entry receptors for human cytomegalovirus via a highly conserved disintegrin-like domain. Proc Natl Acad Sci U S A, 2004. 101(43): p. 15470-5.

51. Feire, A.L., et al., The glycoprotein B disintegrin-like domain binds beta 1 integrin to mediate cytomegalovirus entry. J Virol. 84(19): p. 10026-37.

52. Wang, X., et al., Integrin alphavbeta3 is a coreceptor for human cytomegalovirus. Nat Med, 2005. 11(5): p. 515-21.

53. Wang, X., et al., Epidermal growth factor receptor is a cellular receptor for human cytomegalovirus. Nature, 2003. 424(6947): p. 456-61.

54. Chan, G., M.T. Nogalski, and A.D. Yurochko, Activation of EGFR on monocytes is required for human cytomegalovirus entry and mediates cellular motility. Proc Natl Acad Sci U S A, 2009. 106(52): p. 22369-74.

55. Fairley, J.A., et al., Human cytomegalovirus infection inhibits epidermal growth factor (EGF) signalling by targeting EGF receptors. J Gen Virol, 2002. 83(Pt 11): p. 2803-10.

56. Melnick, M., et al., Small molecule inhibitors of the host cell COX/AREG/EGFR/ERK pathway attenuate cytomegalovirus-induced pathogenesis. Exp Mol Pathol. 91(1): p. 400-410.

57. Compton, T., R.R. Nepomuceno, and D.M. Nowlin, Human cytomegalovirus penetrates host cells by pH-independent fusion at the cell surface. Virology, 1992. 191(1): p. 387-95.

58. Bodaghi, B., et al., Entry of human cytomegalovirus into retinal pigment epithelial and endothelial cells by endocytosis. Invest Ophthalmol Vis Sci, 1999. 40(11): p. 2598-607.

59. Saffert, R.T., R.R. Penkert, and R.F. Kalejta, Cellular and viral control over the initial events of human cytomegalovirus experimental latency in CD34+ cells. J Virol. 84(11): p. 5594-604.

60. Saffert, R.T. and R.F. Kalejta, Human cytomegalovirus gene expression is silenced by Daxx-mediated intrinsic immune defense in model latent infections established in vitro. J Virol, 2007. 81(17): p. 9109-20.

61. Hwang, J. and R.F. Kalejta, Human cytomegalovirus protein pp71 induces Daxx SUMOylation. J Virol, 2009. 83(13): p. 6591-8.

62. Saffert, R.T. and R.F. Kalejta, Inactivating a cellular intrinsic immune defense mediated by Daxx is the mechanism through which the human cytomegalovirus pp71 protein stimulates viral immediate-early gene expression. J Virol, 2006. 80(8): p. 3863-71.

63. Penkert, R.R. and R.F. Kalejta, Nuclear localization of tegument-delivered pp71 in human cytomegalovirus-infected cells is facilitated by one or more factors present in terminally differentiated fibroblasts. J Virol. 84(19): p. 9853-63.

64. Shirakata, M., et al., Novel immediate-early protein IE19 of human cytomegalovirus activates the origin recognition complex I promoter in a cooperative manner with IE72. J Virol, 2002. 76(7): p. 3158-67.

65. Spengler, M.L., et al., SUMO-1 modification of human cytomegalovirus IE1/IE72. J Virol, 2002. 76(6): p. 2990-6.

66. Murphy, E.A., et al., The human cytomegalovirus IE86 protein can block cell cycle progression after inducing transition into the S phase of permissive cells. J Virol, 2000. 74(15): p. 7108-18.

67. Murphy, E., et al., Reevaluation of human cytomegalovirus coding potential. Proc Natl Acad Sci U S A, 2003. 100(23): p. 13585-90.

68. Davison, A.J., et al., The human cytomegalovirus genome revisited: comparison with the chimpanzee cytomegalovirus genome. J Gen Virol, 2003. 84(Pt 1): p. 17-28.

69. Castillo, J.P. and T.F. Kowalik, Human cytomegalovirus immediate early proteins and cell growth control. Gene, 2002. 290(1-2): p. 19-34.

70. Kalejta, R.F. and T. Shenk, Manipulation of the cell cycle by human cytomegalovirus. Front Biosci, 2002. 7: p. d295-306.

71. Pari, G.S. and D.G. Anders, Eleven loci encoding trans-acting factors are required for transient complementation of human cytomegalovirus oriLyt-dependent DNA replication. J Virol, 1993. 67(12): p. 6979-88.

72. Pari, G.S., Nuts and bolts of human cytomegalovirus lytic DNA replication. Curr Top Microbiol Immunol, 2008. 325: p. 153-66.

73. McMahon, T.P. and D.G. Anders, Interactions between human cytomegalovirus helicase-primase proteins. Virus Res, 2002. 86(1-2): p. 39-52.

74. Fortunato, E.A. and D.H. Spector, Regulation of human cytomegalovirus gene expression. Adv Virus Res, 1999. 54: p. 61-128.

75. Gibson, W., M.K. Baxter, and K.S. Clopper, Cytomegalovirus "missing" capsid protein identified as heat-aggregable product of human cytomegalovirus UL46. J Virol, 1996. 70(11): p. 7454-61.

76. Butcher, S.J., et al., Structure of the human cytomegalovirus B capsid by electron cryomicroscopy and image reconstruction. J Struct Biol, 1998. 124(1): p. 70-6.

77. Varnum, S.M., et al., Identification of proteins in human cytomegalovirus (HCMV) particles: the HCMV proteome. J Virol, 2004. 78(20): p. 10960-6.

78. Sanchez, V., et al., Localization of human cytomegalovirus structural proteins to the nuclear matrix of infected human fibroblasts. J Virol, 1998. 72(4): p. 3321-9.

79. Yao, Z.Q., et al., Site-directed mutation in a conserved kinase domain of human cytomegalovirus-pp65 with preservation of cytotoxic T lymphocyte targeting. Vaccine, 2001. 19(13-14): p. 1628-35.

80. Becke, S., et al., Modification of the major tegument protein pp65 of human cytomegalovirus inhibits virus growth and leads to the enhancement of a protein complex with pUL69 and pUL97 in infected cells. J Gen Virol, 2010. 91(Pt 10): p. 2531-41.

81. Kamil, J.P. and D.M. Coen, Human cytomegalovirus protein kinase UL97 forms a complex with the tegument phosphoprotein pp65. J Virol, 2007. 81(19): p. 10659-68.

82. Cepeda, V., M. Esteban, and A. Fraile-Ramos, Human cytomegalovirus final envelopment on membranes containing both trans-Golgi network and endosomal markers. Cell Microbiol. 12(3): p. 386-404.

83. Irmiere, A. and W. Gibson, Isolation and characterization of a noninfectious virion-like particle released from cells infected with human strains of cytomegalovirus. Virology, 1983. 130(1): p. 118-33.

84. Irmiere, A. and W. Gibson, Isolation of human cytomegalovirus intranuclear capsids, characterization of their protein constituents, and demonstration that the B-capsid assembly protein is also abundant in noninfectious enveloped particles. J Virol, 1985. 56(1): p. 277-83.

85. Gibson, W., Structure and assembly of the virion. Intervirology, 1996. 39(5-6): p. 389-400.

86. Chan, G., M.T. Nogalski, and A.D. Yurochko, Human Cytomegalovirus Stimulates Monocyte-to-Macrophage Differentiation via the Temporal Regulation of Caspase 3. J Virol, 2012.

87. Reeves, M.B., et al., Latency, chromatin remodeling, and reactivation of human cytomegalovirus in the dendritic cells of healthy carriers. Proc Natl Acad Sci U S A, 2005. 102(11): p. 4140-5.

88. Reeves, M.B., et al., An in vitro model for the regulation of human cytomegalovirus latency and reactivation in dendritic cells by chromatin remodelling. J Gen Virol, 2005. 86(Pt 11): p. 2949-54.

89. Robain, M., et al., Incidence and sexual risk factors of cytomegalovirus seroconversion in HIV-infected subjects. The SEROCO Study Group. Sex Transm Dis, 1998. 25(9): p. 476-80.

90. The, T.H., et al., The cytomegalovirus antigenemia assay: a plea for standardization. Scand J Infect Dis Suppl, 1995. 99: p. 25-9.

91. Staras, S.A., et al., Seroprevalence of cytomegalovirus infection in the United States, 1988-1994. Clin Infect Dis, 2006. 43(9): p. 1143-51.

92. Cannon, M.J., D.S. Schmid, and T.B. Hyde, Review of cytomegalovirus seroprevalence and demographic characteristics associated with infection. Rev Med Virol, 2010. 20(4): p. 202-13.

93. Becker, S.D., et al., Serological survey of virus infection among wild house mice (Mus domesticus) in the UK. Lab Anim, 2007. 41(2): p. 229-38.

94. Parker, S.E., et al., Infectious diseases in wild mice (Mus musculus) collected on and around the University of Pennsylvania (Philadelphia) Campus. Comp Med, 2009. 59(5): p. 424-30.

95. Pereira, L., et al., Insights into viral transmission at the uterine-placental interface. Trends Microbiol, 2005. 13(4): p. 164-74.

96. Bia, F.J., et al., Vaccination for the prevention of maternal and fetal infection with guinea pig cytomegalovirus. J Infect Dis, 1980. 142(5): p. 732-8.

97. Bia, F.J., S.A. Miller, and K.H. Davidson, The guinea pig cytomegalovirus model of congenital human cytomegalovirus infection. Birth Defects Orig Artic Ser, 1984. 20(1): p. 233-41.

98. Schleiss, M.R., et al., Protection against congenital cytomegalovirus infection and disease in guinea pigs, conferred by a purified recombinant glycoprotein B vaccine. J Infect Dis, 2004. 189(8): p. 1374-81.

99. Kimberlin, D.W., et al., Effect of ganciclovir therapy on hearing in symptomatic congenital cytomegalovirus disease involving the central nervous system: a randomized, controlled trial. J Pediatr, 2003. 143(1): p. 16-25.

100. Fowler, K.B., et al., The outcome of congenital cytomegalovirus infection in relation to maternal antibody status. N Engl J Med, 1992. 326(10): p. 663-7.

101. Stegmann, B.J. and J.C. Carey, TORCH Infections. Toxoplasmosis, Other (syphilis, varicella-zoster, parvovirus B19), Rubella, Cytomegalovirus (CMV), and Herpes infections. Curr Womens Health Rep, 2002. 2(4): p. 253-8.

102. Hamprecht, K., R. Goelz, and J. Maschmann, Breast milk and cytomegalovirus infection in preterm infants. Early Hum Dev, 2005. 81(12): p. 989-96.

103. Hamprecht, K., et al., Cytomegalovirus transmission to preterm infants during lactation. J Clin Virol, 2008. 41(3): p. 198-205.

104. Hamprecht, K., et al., Detection of cytomegaloviral DNA in human milk cells and cell free milk whey by nested PCR. J Virol Methods, 1998. 70(2): p. 167-76.

105. Hamprecht, K., et al., Transmission of cytomegalovirus infection through breast milk in term and preterm infants. The role of cell free milk whey and milk cells. Adv Exp Med Biol, 2000. 478: p. 231-9.

106. Maschmann, J., et al., Cytomegalovirus infection of extremely low-birth weight infants via breast milk. Clin Infect Dis, 2001. 33(12): p. 1998-2003.

107. van der Strate, B.W., et al., Viral load in breast milk correlates with transmission of human cytomegalovirus to preterm neonates, but lactoferrin concentrations do not. Clin Diagn Lab Immunol, 2001. 8(4): p. 818-21.

108. Vochem, M., et al., Transmission of cytomegalovirus to preterm infants through breast milk. Pediatr Infect Dis J, 1998. 17(1): p. 53-8.

109. Vollmer, B., et al., Postnatally acquired cytomegalovirus infection via breast milk: effects on hearing and development in preterm infants. Pediatr Infect Dis J, 2004. 23(4): p. 322-7.

110. Gautheret-Dejean, A., et al., Detection of human Betaherpesvirinae in saliva and urine from immunocompromised and immunocompetent subjects. J Clin Microbiol, 1997. 35(6): p. 1600-3.

111. Gerberding, J.L., et al., Risk of transmitting the human immunodeficiency virus, cytomegalovirus, and hepatitis B virus to health care workers exposed to patients with AIDS and AIDS-related conditions. J Infect Dis, 1987. 156(1): p. 1-8.

112. Fernandez-Ruiz, M., et al., Cytomegalovirus myopericarditis and hepatitis in an immunocompetent adult: successful treatment with oral valganciclovir. Intern Med, 2008. 47(22): p. 1963-6.

113. Yonezawa, A., T. Onaka, and K. Imada, [Cytomegalovirus-associated infectious mononucleosis-like syndrome accompanied by transient monoclonal expansion of CD8+ T-cells]. Rinsho Ketsueki, 2009. 50(8): p. 652-7.

114. Nishikawa, J., et al., Infectious mononucleosis with atypical manifestations accompanied by transient IgM antibody response for cytomegalovirus. J Infect Chemother.

115. Page, M.J., et al., Cytomegalovirus enteritis: a highly lethal condition requiring early detection and intervention. Dis Colon Rectum, 1998. 41(5): p. 619-23.

116. Musani, M.A., et al., Association of herpes simplex virus infection and Bell's palsy. J Pak Med Assoc, 2009. 59(12): p. 823-5.

117. Shirts, B.H., et al., Antibodies to cytomegalovirus and Herpes Simplex Virus 1 associated with cognitive function in schizophrenia. Schizophr Res, 2008. 106(2-3): p. 268-74.

118. Lingappa, J.R., et al., Daily acyclovir for HIV-1 disease progression in people dually infected with HIV-1 and herpes simplex virus type 2: a randomised placebo-controlled trial. Lancet. 375(9717): p. 824-33.

119. Michel, D. and T. Mertens, The UL97 protein kinase of human cytomegalovirus and homologues in other herpesviruses: impact on virus and host. Biochim Biophys Acta, 2004. 1697(1-2): p. 169-80.

120. Kim, S.T., et al., A randomized trial of preemptive therapy for prevention of cytomegalovirus disease after allogeneic hematopoietic stem cell transplantation. Int J Hematol. 91(5): p. 886-91.

121. Kim, I., et al., Identification of a human valacyclovirase: biphenyl hydrolase-like protein as valacyclovir hydrolase. J Biol Chem, 2003. 278(28): p. 25348-56.

122. Kim, I., G.M. Crippen, and G.L. Amidon, Structure and specificity of a human valacyclovir activating enzyme: a homology model of BPHL. Mol Pharm, 2004. 1(6): p. 434-46.

123. Kim, I., et al., A novel nucleoside prodrug-activating enzyme: substrate specificity of biphenyl hydrolase-like protein. Mol Pharm, 2004. 1(2): p. 117-27.

124. Lai, L., et al., Molecular basis of prodrug activation by human valacyclovirase, an alpha-amino acid ester hydrolase. J Biol Chem, 2008. 283(14): p. 9318-27.

125. Biron, K.K., Antiviral drugs for cytomegalovirus diseases. Antiviral Res, 2006. 71(2-3): p. 154-63.

126. Emery, V.C. and A.F. Hassan-Walker, Focus on new drugs in development against human cytomegalovirus. Drugs, 2002. 62(13): p. 1853-8.

127. Winston, D.J., et al., Maribavir prophylaxis for prevention of cytomegalovirus infection in allogeneic stem cell transplant recipients: a multicenter, randomized, double-blind, placebo-controlled, dose-ranging study. Blood, 2008. 111(11): p. 5403-10.

128. Gilbert, C. and G. Boivin, New reporter cell line to evaluate the sequential emergence of multiple human cytomegalovirus mutations during in vitro drug exposure. Antimicrob Agents Chemother, 2005. 49(12): p. 4860-6.

129. Baldanti, F., N. Lurain, and G. Gerna, Clinical and biologic aspects of human cytomegalovirus resistance to antiviral drugs. Hum Immunol, 2004. 65(5): p. 403-9.

130. Limaye, A.P., et al., Emergence of ganciclovir-resistant cytomegalovirus disease among recipients of solid-organ transplants. Lancet, 2000. 356(9230): p. 645-9.

131. Drew, W.L., et al., Prevalence of resistance in patients receiving ganciclovir for serious cytomegalovirus infection. J Infect Dis, 1991. 163(4): p. 716-9.

132. Jabs, D.A., et al., Cytomegalovirus retinitis and viral resistance: ganciclovir resistance. CMV Retinitis and Viral Resistance Study Group. J Infect Dis, 1998. 177(3): p. 770-3.

133. Chou, S., et al., Cytomegalovirus UL97 phosphotransferase mutations that affect susceptibility to ganciclovir. J Infect Dis, 2002. 185(2): p. 162-9.

134. Chou, S., Cytomegalovirus UL97 mutations in the era of ganciclovir and maribavir. Rev Med Virol, 2008. 18(4): p. 233-46.

135. Weber, O., et al., Inhibition of murine cytomegalovirus and human cytomegalovirus by a novel non-nucleosidic compound in vivo. Antiviral Res, 2001. 49(3): p. 179-89.

136. Bernstein, D.I., et al., Randomized, double-blind, Phase 1 trial of an alphavirus replicon vaccine for cytomegalovirus in CMV seronegative adult volunteers. Vaccine, 2009. 28(2): p. 484-93.

137. Pass, R.F., Development and evidence for efficacy of CMV glycoprotein B vaccine with MF59 adjuvant. J Clin Virol, 2009. 46 Suppl 4: p. S73-6.

138. Mitchell, D.K., et al., Immunogenicity of a recombinant human cytomegalovirus gB vaccine in seronegative toddlers. Pediatr Infect Dis J, 2002. 21(2): p. 133-8.

139. Griffiths, P.D., et al., Cytomegalovirus glycoprotein-B vaccine with MF59 adjuvant in transplant recipients: a phase 2 randomised placebo-controlled trial. Lancet. 377(9773): p. 1256-63.

140. Hansen, S.G., et al., Evasion of CD8+ T cells is critical for superinfection by cytomegalovirus. Science, 2010. 328(5974): p. 102-6.

141. Biron, C.A., K.S. Byron, and J.L. Sullivan, Severe herpesvirus infections in an adolescent without natural killer cells. N Engl J Med, 1989. 320(26): p. 1731-5.

142. Robain, M., et al., [Prevalence and incidence of cytomegalovirus infection in patients infected with HIV-1. SEROCO group]. Presse Med, 1998. 27(20): p. 949-53.

143. Sinclair, J., Manipulation of dendritic cell functions by human cytomegalovirus. Expert Rev Mol Med, 2008. 10: p. e35.

144. Verhoeven, D., J.R. Teijaro, and D.L. Farber, Heterogeneous memory T cells in antiviral immunity and immunopathology. Viral Immunol, 2008. 21(2): p. 99-113.

145. Khan, N., et al., Comparative analysis of CD8+ T cell responses against human cytomegalovirus proteins pp65 and immediate early 1 shows similarities in precursor frequency, oligoclonality, and phenotype. J Infect Dis, 2002. 185(8): p. 1025-34.

146. Khan, N., et al., Herpesvirus-specific CD8 T cell immunity in old age: cytomegalovirus impairs the response to a coresident EBV infection. J Immunol, 2004. 173(12): p. 7481-9.

147. Khan, N., et al., Cytomegalovirus seropositivity drives the CD8 T cell repertoire toward greater clonality in healthy elderly individuals. J Immunol, 2002. 169(4): p. 1984-92.

148. Wikby, A., et al., Changes in CD8 and CD4 lymphocyte subsets, T cell proliferation responses and non-survival in the very old: the Swedish longitudinal OCTO-immune study. Mech Ageing Dev, 1998. 102(2-3): p. 187-98.

149. Wikby, A., et al., An immune risk phenotype, cognitive impairment, and survival in very late life: impact of allostatic load in Swedish octogenarian and nonagenarian humans. J Gerontol A Biol Sci Med Sci, 2005. 60(5): p. 556-65.

150. Schlub, T.E., et al., Comparing the Kinetics of NK Cells, CD4, and CD8 T Cells in Murine Cytomegalovirus Infection. J Immunol, 2011.

151. Salmond, R.J., et al., T-cell receptor proximal signaling via the Src-family kinases, Lck and Fyn, influences T-cell activation, differentiation, and tolerance. Immunol Rev, 2009. 228(1): p. 9-22.

152. Dustin, M.L. and D. Depoil, New insights into the T cell synapse from single molecule techniques. Nat Rev Immunol, 2011. 11(10): p. 672-84.

153. Sharpe, A.H. and G.J. Freeman, The B7-CD28 superfamily. Nat Rev Immunol, 2002. 2(2): p. 116-26.

154. Reddehase, M.J., Antigens and immunoevasins: opponents in cytomegalovirus immune surveillance. Nat Rev Immunol, 2002. 2(11): p. 831-44.

155. Wills, M.R., et al., Human cytomegalovirus encodes an MHC class I-like molecule (UL142) that functions to inhibit NK cell lysis. J Immunol, 2005. 175(11): p. 7457-65.

156. Wills, M.R., et al., The human cytotoxic T-lymphocyte (CTL) response to cytomegalovirus is dominated by structural protein pp65: frequency, specificity, and T-cell receptor usage of pp65-specific CTL. J Virol, 1996. 70(11): p. 7569-79.

157. Babel, N., et al., Clonotype analysis of cytomegalovirus-specific cytotoxic T lymphocytes. J Am Soc Nephrol, 2009. 20(2): p. 344-52.

158. Posnett, D.N., et al., Oligoclonal expansions of antigen-specific CD8+ T cells in aged mice. Ann N Y Acad Sci, 2003. 987: p. 274-9.

159. Waller, E.C., et al., Differential costimulation through CD137 (4-1BB) restores proliferation of human virus-specific "effector memory" (CD28(-) CD45RA(HI)) CD8(+) T cells. Blood, 2007. 110(13): p. 4360-6.

160. Wang, G.C., et al., Cytomegalovirus infection and the risk of mortality and frailty in older women: a prospective observational cohort study. Am J Epidemiol, 2010. 171(10): p. 1144-52.

161. Sierro, S., R. Rothkopf, and P. Klenerman, Evolution of diverse antiviral CD8+ T cell populations after murine cytomegalovirus infection. Eur J Immunol, 2005. 35(4): p. 1113-23.

162. Pollock, J.L. and H.W.t. Virgin, Latency, without persistence, of murine cytomegalovirus in the spleen and kidney. J Virol, 1995. 69(3): p. 1762-8.

163. Cheung, K.S. and D.J. Lang, Detection of latent cytomegalovirus in murine salivary and prostate explant cultures and cells. Infect Immun, 1977. 15(2): p. 568-75.

164. Munks, M.W., et al., Four distinct patterns of memory CD8 T cell responses to chronic murine cytomegalovirus infection. J Immunol, 2006. 177(1): p. 450-8.

165. Snyder, C.M., et al., Memory inflation during chronic viral infection is maintained by continuous production of short-lived, functional T cells. Immunity, 2008. 29(4): p. 650-9.

166. Wherry, E.J., et al., Lineage relationship and protective immunity of memory CD8 T cell subsets. Nat Immunol, 2003. 4(3): p. 225-34.

167. Li, J., G. Huston, and S.L. Swain, IL-7 promotes the transition of CD4 effectors to persistent memory cells. J Exp Med, 2003. 198(12): p. 1807-15.

168. Kaech, S.M., et al., Selective expression of the interleukin 7 receptor identifies effector CD8 T cells that give rise to long-lived memory cells. Nat Immunol, 2003. 4(12): p. 1191-8.

169. Zuo, J., et al., IL-15 independent maintenance of virus-specific CD8(+) T cells in the CNS during chronic infection. J Neuroimmunol, 2009. 207(1-2): p. 32-8.

170. Dubois, S., T.A. Waldmann, and J.R. Muller, ITK and IL-15 support two distinct subsets of CD8+ T cells. Proc Natl Acad Sci U S A, 2006. 103(32): p. 12075-80.

171. Hintzen, R.Q., et al., Regulation of CD27 expression on subsets of mature T-lymphocytes. J Immunol, 1993. 151(5): p. 2426-35.

172. Penaloza-MacMaster, P., et al., Opposing effects of CD70 costimulation during acute and chronic lymphocytic choriomeningitis virus infection of mice. J Virol, 2011. 85(13): p. 6168-74.

173. Green, J.M., et al., Absence of B7-dependent responses in CD28-deficient mice. Immunity, 1994. 1(6): p. 501-8.

174. Ouyang, Q., et al., Age-associated accumulation of CMV-specific CD8+ T cells expressing the inhibitory killer cell lectin-like receptor G1 (KLRG1). Exp Gerontol, 2003. 38(8): p. 911-20.

175. Henson, S.M., et al., KLRG1 signaling induces defective Akt (ser473) phosphorylation and proliferative dysfunction of highly differentiated CD8+ T cells. Blood, 2009. 113(26): p. 6619-28.

176. Thimme, R., et al., Increased expression of the NK cell receptor KLRG1 by virus-specific CD8 T cells during persistent antigen stimulation. J Virol, 2005. 79(18): p. 12112-6.

177. Kao, C., et al., Transcription factor T-bet represses expression of the inhibitory receptor PD-1 and sustains virus-specific CD8+ T cell responses during chronic infection. Nat Immunol, 2011. 12(7): p. 663-71.

178. Tanaka, K., et al., Role of the indigenous microbiota in maintaining the virus-specific CD8 memory T cells in the lung of mice infected with murine cytomegalovirus. J Immunol, 2007. 178(8): p. 5209-16.

179. Jonjic, S., et al., Site-restricted persistent cytomegalovirus infection after selective long-term depletion of CD4+ T lymphocytes. J Exp Med, 1989. 169(4): p. 1199-212.

180. Ridge, J.P., F. Di Rosa, and P. Matzinger, A conditioned dendritic cell can be a temporal bridge between a CD4+ T-helper and a T-killer cell. Nature, 1998. 393(6684): p. 474-8.

181. Bennett, S.R., et al., Help for cytotoxic-T-cell responses is mediated by CD40 signalling. Nature, 1998. 393(6684): p. 478-80.

182. Snyder, C.M., et al., CD4+ T cell help has an epitope-dependent impact on CD8+ T cell memory inflation during murine cytomegalovirus infection. J Immunol, 2009. 183(6): p. 3932-41.

183. Walton, S.M., et al., T-cell help permits memory CD8(+) T-cell inflation during cytomegalovirus latency. Eur J Immunol, 2011. 41(8): p. 2248-59.

184. Hildner, K., et al., Batf3 deficiency reveals a critical role for CD8alpha+ dendritic cells in cytotoxic T cell immunity. Science, 2008. 322(5904): p. 1097-100.

185. Torti, N., et al., Batf3 transcription factor-dependent DC subsets in murine CMV infection: differential impact on T-cell priming and memory inflation. Eur J Immunol, 2011. 41(9): p. 2612-8.

186. Macagno, A., et al., Dendritic cells up-regulate immunoproteasomes and the proteasome regulator PA28 during maturation. Eur J Immunol, 1999. 29(12): p. 4037-42.

187. Khan, S., et al., A cytomegalovirus inhibitor of gamma interferon signaling controls immunoproteasome induction. J Virol, 2004. 78(4): p. 1831-42.

188. Zimmermann, A., et al., A cytomegaloviral protein reveals a dual role for STAT2 in IFN-{gamma} signaling and antiviral responses. J Exp Med, 2005. 201(10): p. 1543-53.

189. Hutchinson, S., et al., A dominant role for the immunoproteasome in CD8+ T cell responses to murine cytomegalovirus. PLoS One, 2011. 6(2): p. e14646.

190. Walton, S.M., et al., Absence of cross-presenting cells in the salivary gland and viral immune evasion confine cytomegalovirus immune control to effector CD4 T cells. PLoS Pathog, 2011. 7(8): p. e1002214.

191. Seckert, C.K., et al., Antigen-presenting cells of hematopoietic origin prime cytomegalovirus-specific CD8 T cells but are not sufficient for driving memory inflation during viral latency. J Gen Virol, 2011.

192. Mitrovic, M., et al., The NK Cell Response to Mouse Cytomegalovirus Infection Affects the Level and Kinetics of the Early CD8+ T-Cell Response. J Virol, 2012. 86(4): p. 2165-75.

193. Snyder, C.M., et al., Sustained CD8+ T Cell Memory Inflation after Infection with a Single-Cycle Cytomegalovirus. PLoS Pathog, 2011. 7(10): p. e1002295.

194. Burns, W.H., et al., Thymidine kinase not required for antiviral activity of acyclovir against mouse cytomegalovirus. J Virol, 1981. 39(3): p. 889-93.

195. Poluektova, L., et al., In vitro lymphotoxicity and selective T cell immunotoxicity of high doses of acyclovir and its derivatives in mice. Int J Immunopharmacol, 1996. 18(6-7): p. 429-38.

196. Jones, M., et al., IL-10 restricts memory T cell inflation during cytomegalovirus infection. J Immunol, 2010. 185(6): p. 3583-92.

197. Humphreys, I.R., et al., Biphasic role of 4-1BB in the regulation of mouse cytomegalovirus-specific CD8(+) T cells. Eur J Immunol, 2010. 40(10): p. 2762-8.

198. Humphreys, I.R., et al., OX40 costimulation promotes persistence of cytomegalovirus-specific CD8 T Cells: A CD4-dependent mechanism. J Immunol, 2007. 179(4): p. 2195-202.

199. Arens, R., et al., Differential B7-CD28 Costimulatory Requirements for Stable and Inflationary Mouse Cytomegalovirus-Specific Memory CD8 T Cell Populations. J Immunol, 2011. 186(7): p. 3874-81.

200. Selin, L.K., et al., Reduction of otherwise remarkably stable virus-specific cytotoxic T lymphocyte memory by heterologous viral infections. J Exp Med, 1996. 183(6): p. 2489-99.

201. Selin, L.K., et al., Attrition of T cell memory: selective loss of LCMV epitope-specific memory CD8 T cells following infections with heterologous viruses. Immunity, 1999. 11(6): p. 733-42.

202. McNally, J.M., et al., Attrition of bystander CD8 T cells during virus-induced T-cell and interferon responses. J Virol, 2001. 75(13): p. 5965-76.

203. Bahl, K., et al., IFN-induced attrition of CD8 T cells in the presence or absence of cognate antigen during the early stages of viral infections. J Immunol, 2006. 176(7): p. 4284-95.

204. Jiang, J., et al., Depletion of T cells by type I interferon: differences between young and aged mice. J Immunol, 2005. 175(3): p. 1820-6.

205. Libri, V., et al., Cytomegalovirus infection induces the accumulation of short-lived, multifunctional CD4+ CD45RA+ CD27 T cells: the potential involvement of interleukin-7 in this process. Immunology, 2011. 132(3): p. 326-39.

206. Litjens, N.H., E.A. de Wit, and M.G. Betjes, Differential effects of age, cytomegalovirus-seropositivity and end-stage renal disease (ESRD) on circulating T lymphocyte subsets. Immun Ageing, 2011. 8(1): p. 2.

207. Pourgheysari, B., et al., The cytomegalovirus-specific CD4+ T-cell response expands with age and markedly alters the CD4+ T-cell repertoire. J Virol, 2007. 81(14): p. 7759-65.

208. Sylwester, A.W., et al., Broadly targeted human cytomegalovirus-specific CD4+ and CD8+ T cells dominate the memory compartments of exposed subjects. J Exp Med, 2005. 202(5): p. 673-85.

209. Bitmansour, A.D., et al., Clonotypic structure of the human CD4+ memory T cell response to cytomegalovirus. J Immunol, 2001. 167(3): p. 1151-63.

210. Price, D.A., et al., Induction and evolution of cytomegalovirus-specific CD4+ T cell clonotypes in rhesus macaques. J Immunol, 2008. 180(1): p. 269-80.

211. Dunn, H.S., et al., Dynamics of CD4 and CD8 T cell responses to cytomegalovirus in healthy human donors. J Infect Dis, 2002. 186(1): p. 15-22.

212. Alonso-Arias, R., et al., IL-15 preferentially enhances functional properties and antigen-specific responses of CD4+CD28(null) compared to CD4+CD28+ T cells. Aging Cell, 2011.

213. Arens, R., et al., Cutting edge: murine cytomegalovirus induces a polyfunctional CD4 T cell response. J Immunol, 2008. 180(10): p. 6472-6.

214. Walton, S.M., et al., The dynamics of mouse cytomegalovirus-specific CD4 T cell responses during acute and latent infection. J Immunol, 2008. 181(2): p. 1128-34.

215. Arens, R., et al., B7-mediated costimulation of CD4 T cells constrains cytomegalovirus persistence. J Virol, 2010. 85(1): p. 390-6.

216. Olsson, J., et al., Age-related change in peripheral blood T-lymphocyte subpopulations and cytomegalovirus infection in the very old: the Swedish longitudinal OCTO immune study. Mech Ageing Dev, 2000. 121(1-3): p. 187-201.

217. Wikby, A., et al., Expansions of peripheral blood CD8 T-lymphocyte subpopulations and an association with cytomegalovirus seropositivity in the elderly: the Swedish NONA immune study. Exp Gerontol, 2002. 37(2-3): p. 445-53.

218. Roberts, E.T., et al., Cytomegalovirus antibody levels, inflammation, and mortality among elderly Latinos over 9 years of follow-up. Am J Epidemiol, 2010. 172(4): p. 363-71.

219. Aiello, A.E., et al., The influence of latent viral infection on rate of cognitive decline over 4 years. J Am Geriatr Soc, 2006. 54(7): p. 1046-54.

220. Waldmann, T.A. and W. Strober, Metabolism of immunoglobulins. Prog Allergy, 1969. 13: p. 1-110.

221. Bonilla, F.A., Pharmacokinetics of immunoglobulin administered via intravenous or subcutaneous routes. Immunol Allergy Clin North Am, 2008. 28(4): p. 803-19, ix.

222. Chidrawar, S., et al., Cytomegalovirus-seropositivity has a profound influence on the magnitude of major lymphoid subsets within healthy individuals. Clin Exp Immunol, 2009. 155(3): p. 423-32.

223. Shanley, J.D., M.C. Jordan, and J.G. Stevens, Modification by adoptive humoral immunity of murine cytomegalovirus infection. J Infect Dis, 1981. 143(2): p. 231-7.

224. Cekinovic, D., et al., Passive immunization reduces murine cytomegalovirus-induced brain pathology in newborn mice. J Virol, 2008. 82(24): p. 12172-80.

225. Reddehase, M.J., et al., The conditions of primary infection define the load of latent viral genome in organs and the risk of recurrent cytomegalovirus disease. J Exp Med, 1994. 179(1): p. 185-93.

226. Jonjic, S., et al., Antibodies are not essential for the resolution of primary cytomegalovirus infection but limit dissemination of recurrent virus. J Exp Med, 1994. 179(5): p. 1713-7.

227. Farrell, H.E. and G.R. Shellam, Protection against murine cytomegalovirus infection by passive transfer of neutralizing and non-neutralizing monoclonal antibodies. J Gen Virol, 1991. 72 (Pt 1): p. 149-56.

228. Orange, J.S. and Z.K. Ballas, Natural killer cells in human health and disease. Clin Immunol, 2006. 118(1): p. 1-10.

229. Pahwa, S., et al., Persistent cytomegalovirus infection: association with profound immunodeficiency and treatment with interferon. Clin Immunol Immunopathol, 1983. 28(1): p. 77-89.

230. Rook, A.H., et al., Interleukin-2 enhances the depressed natural killer and cytomegalovirus-specific cytotoxic activities of lymphocytes from patients with the acquired immune deficiency syndrome. J Clin Invest, 1983. 72(1): p. 398-403.

231. Bancroft, G.J., G.R. Shellam, and J.E. Chalmer, Genetic influences on the augmentation of natural killer (NK) cells during murine cytomegalovirus infection: correlation with patterns of resistance. J Immunol, 1981. 126(3): p. 988-94.

232. Shellam, G.R., et al., Increased susceptibility to cytomegalovirus infection in beige mutant mice. Proc Natl Acad Sci U S A, 1981. 78(8): p. 5104-8.

233. Scalzo, A.A., et al., Cmv-1, a genetic locus that controls murine cytomegalovirus replication in the spleen. J Exp Med, 1990. 171(5): p. 1469-83.

234. Scalzo, A.A., et al., The effect of the Cmv-1 resistance gene, which is linked to the natural killer cell gene complex, is mediated by natural killer cells. J Immunol, 1992. 149(2): p. 581-9.

235. Adams, E.J., et al., Structural elucidation of the m157 mouse cytomegalovirus ligand for Ly49 natural killer cell receptors. Proc Natl Acad Sci U S A, 2007. 104(24): p. 10128-33.

236. Dimasi, N. and R. Biassoni, Structural and functional aspects of the Ly49 natural killer cell receptors. Immunol Cell Biol, 2005. 83(1): p. 1-8.

237. Orr, M.T., et al., Ly49H signaling through DAP10 is essential for optimal natural killer cell responses to mouse cytomegalovirus infection. J Exp Med, 2009. 206(4): p. 807-17.

238. Huard, B. and K. Fruh, A role for MHC class I down-regulation in NK cell lysis of herpes virus-infected cells. Eur J Immunol, 2000. 30(2): p. 509-15.

239. Corbett, A.J., et al., Functional Consequences of Natural Sequence Variation of Murine Cytomegalovirus m157 for Ly49 Receptor Specificity and NK Cell Activation. J Immunol.

240. Corbett, A.J., et al., Functional consequences of natural sequence variation of murine cytomegalovirus m157 for Ly49 receptor specificity and NK cell activation. J Immunol. 186(3): p. 1713-22.

241. Lanier, L.L., Evolutionary struggles between NK cells and viruses. Nat Rev Immunol, 2008. 8(4): p. 259-68.

242. Yewdell, J.W. and A.B. Hill, Viral interference with antigen presentation. Nat Immunol, 2002. 3(11): p. 1019-25.

243. Holtappels, R., et al., Cytomegalovirus encodes a positive regulator of antigen presentation. J Virol, 2006. 80(15): p. 7613-24.

244. Andrews, D.M., et al., Infection of dendritic cells by murine cytomegalovirus induces functional paralysis. Nat Immunol, 2001. 2(11): p. 1077-84.

245. Rolle, A. and J. Olweus, Dendritic cells in cytomegalovirus infection: viral evasion and host countermeasures. APMIS, 2009. 117(5-6): p. 413-26.

246. LoPiccolo, D.M., et al., Effective inhibition of K(b)- and D(b)-restricted antigen presentation in primary macrophages by murine cytomegalovirus. J Virol, 2003. 77(1): p. 301-8.

247. Lemmermann, N.A., et al., In vivo impact of cytomegalovirus evasion of CD8 T-cell immunity: facts and thoughts based on murine models. Virus Res, 2011. 157(2): p. 161-74.

248. Kleijnen, M.F., et al., A mouse cytomegalovirus glycoprotein, gp34, forms a complex with folded class I MHC molecules in the ER which is not retained but is transported to the cell surface. EMBO J, 1997. 16(4): p. 685-94.

249. Lu, X., D.G. Kavanagh, and A.B. Hill, Cellular and molecular requirements for association of the murine cytomegalovirus protein m4/gp34 with major histocompatibility complex class I molecules. J Virol, 2006. 80(12): p. 6048-55.

250. Reusch, U., et al., AP-1A and AP-3A lysosomal sorting functions. Traffic, 2002. 3(10): p. 752-61.

251. Gold, M.C., et al., The murine cytomegalovirus immunomodulatory gene m152 prevents recognition of infected cells by M45-specific CTL but does not alter the immunodominance of the M45-specific CD8 T cell response in vivo. J Immunol, 2002. 169(1): p. 359-65.

252. Zhi, L., et al., Direct interaction of the mouse cytomegalovirus m152/gp40 immunoevasin with RAE-1 isoforms. Biochemistry, 2010. 49(11): p. 2443-53.

253. Park, B., et al., Human cytomegalovirus inhibits tapasin-dependent peptide loading and optimization of the MHC class I peptide cargo for immune evasion. Immunity, 2004. 20(1): p. 71-85.

254. Hewitt, E.W., S.S. Gupta, and P.J. Lehner, The human cytomegalovirus gene product US6 inhibits ATP binding by TAP. EMBO J, 2001. 20(3): p. 387-96.

255. Hengel, H., et al., A viral ER-resident glycoprotein inactivates the MHC-encoded peptide transporter. Immunity, 1997. 6(5): p. 623-32.

256. Ahn, K., et al., The ER-luminal domain of the HCMV glycoprotein US6 inhibits peptide translocation by TAP. Immunity, 1997. 6(5): p. 613-21.

257. Trgovcich, J., et al., Human cytomegalovirus protein pp71 disrupts major histocompatibility complex class I cell surface expression. J Virol, 2006. 80(2): p. 951-63.

258. Wang, X., et al., The viral E3 ubiquitin ligase mK3 uses the Derlin/p97 endoplasmic reticulum-associated degradation pathway to mediate down-regulation of major histocompatibility complex class I proteins. J Biol Chem, 2006. 281(13): p. 8636-44.

259. Oresic, K., C.L. Ng, and D. Tortorella, TRAM1 participates in human cytomegalovirus US2- and US11-mediated dislocation of an endoplasmic reticulum membrane glycoprotein. J Biol Chem, 2009. 284(9): p. 5905-14.

260. Park, B., et al., The HCMV membrane glycoprotein US10 selectively targets HLA-G for degradation. J Exp Med, 2010. 207(9): p. 2033-41.

261. Loewendorf, A.I., et al., The mouse cytomegalovirus glycoprotein m155 inhibits CD40 expression and restricts CD4 T cell responses. J Virol, 2011. 85(10): p. 5208-12.

262. Yang, Z. and P.J. Bjorkman, Structure of UL18, a peptide-binding viral MHC mimic, bound to a host inhibitory receptor. Proc Natl Acad Sci U S A, 2008. 105(29): p. 10095-100.

263. Kim, Y., et al., Human cytomegalovirus UL18 utilizes US6 for evading the NK and T-cell responses. PLoS Pathog, 2008. 4(8): p. e1000123.

264. Park, B., et al., The MHC class I homolog of human cytomegalovirus is resistant to down-regulation mediated by the unique short region protein (US)2, US3, US6, and US11 gene products. J Immunol, 2002. 168(7): p. 3464-9.

265. Leong, C.C., et al., Modulation of natural killer cell cytotoxicity in human cytomegalovirus infection: the role of endogenous class I major histocompatibility complex and a viral class I homolog. J Exp Med, 1998. 187(10): p. 1681-7.

266. Browne, H., M. Churcher, and T. Minson, Construction and characterization of a human cytomegalovirus mutant with the UL18 (class I homolog) gene deleted. J Virol, 1992. 66(11): p. 6784-7.

267. Ashiru, O., et al., NKG2D ligand MICA is retained in the cis-Golgi apparatus by human cytomegalovirus protein UL142. J Virol, 2009. 83(23): p. 12345-54.

268. Wilkinson, G.W., et al., Modulation of natural killer cells by human cytomegalovirus. J Clin Virol, 2008. 41(3): p. 206-12.

269. Chalupny, N.J., et al., Down-regulation of the NKG2D ligand MICA by the human cytomegalovirus glycoprotein UL142. Biochem Biophys Res Commun, 2006. 346(1): p. 175-81.

270. Tobita, K., [Classification and nomenclature of influenza viruses]. Nihon Rinsho, 1997. 55(10): p. 2512-4.

271. Kuiken, T., et al., Host species barriers to influenza virus infections. Science, 2006. 312(5772): p. 394-7.

272. Hirst, G.K., The Agglutination of Red Cells by Allantoic Fluid of Chick Embryos Infected with Influenza Virus. Science, 1941. 94(2427): p. 22-3.

273. Fazekas De St Groth, S., Viropexis, the mechanism of influenza virus infection. Nature, 1948. 162(4112): p. 294.

274. Varki, A., Glycan-based interactions involving vertebrate sialic-acid-recognizing proteins. Nature, 2007. 446(7139): p. 1023-9.

275. Weis, W., et al., Structure of the influenza virus haemagglutinin complexed with its receptor, sialic acid. Nature, 1988. 333(6172): p. 426-31.

276. Stevens, J., et al., Structure and receptor specificity of the hemagglutinin from an H5N1 influenza virus. Science, 2006. 312(5772): p. 404-10.

277. Kida, H., et al., Potential for transmission of avian influenza viruses to pigs. J Gen Virol, 1994. 75 (Pt 9): p. 2183-8.

278. Ito, T., et al., Continued circulation of reassortant H1N2 influenza viruses in pigs in Japan. Arch Virol, 1998. 143(9): p. 1773-82.

279. Campbell, D., et al., Genetic composition and virulence of influenza virus: differences in facets of virulence in ferrets between two pairs of recombinants with RNA segments of the same parental origin. J Gen Virol, 1982. 58(Pt 2): p. 387-98.

280. Campbell, D., C. Sweet, and H. Smith, Comparisons of virulence of influenza virus recombinants in ferrets in relation to their behaviour in man and their genetic constitution. J Gen Virol, 1979. 44(1): p. 37-44.

281. Toms, G.L., et al., The relation of pyrexia and nasal inflammatory response to virus levels in nasal washings of ferrets infected with influenza viruses of differing virulence. Br J Exp Pathol, 1977. 58(4): p. 444-58.

282. Barnard, D.L., Animal models for the study of influenza pathogenesis and therapy. Antiviral Res, 2009. 82(2): p. A110-22.

283. Rigoni, M., et al., The mouse model is suitable for the study of viral factors governing transmission and pathogenesis of highly pathogenic avian influenza (HPAI) viruses in mammals. Vet Res, 2010. 41(5): p. 66.

284. Ning, Z.Y., et al., Detection of expression of influenza virus receptors in tissues of BALB/c mice by histochemistry. Vet Res Commun, 2009. 33(8): p. 895-903.

285. Deckhut, A.M., et al., Prominent usage of V beta 8.3 T cells in the H-2Db-restricted response to an influenza A virus nucleoprotein epitope. J Immunol, 1993. 151(5): p. 2658-66.

286. Buchweitz, J.P., et al., Modulation of airway responses to influenza A/PR/8/34 by Delta9-tetrahydrocannabinol in C57BL/6 mice. J Pharmacol Exp Ther, 2007. 323(2): p. 675-83.

287. Valkenburg, S.A., et al., Immunity to seasonal and pandemic influenza A viruses. Microbes Infect. 13(5): p. 489-501.

288. Johnson, N.P. and J. Mueller, Updating the accounts: global mortality of the 1918-1920 "Spanish" influenza pandemic. Bull Hist Med, 2002. 76(1): p. 105-15.

289. Khandaker, G., et al., Systematic review of clinical and epidemiological features of the pandemic influenza A (H1N1) 2009. Influenza Other Respi Viruses. 5(3): p. 148-56.

290. Fujisawa, H., Neutrophils play an essential role in cooperation with antibody in both protection against and recovery from pulmonary infection with influenza virus in mice. J Virol, 2008. 82(6): p. 2772-83.

291. Cheung, C.Y., et al., Induction of proinflammatory cytokines in human macrophages by influenza A (H5N1) viruses: a mechanism for the unusual severity of human disease? Lancet, 2002. 360(9348): p. 1831-7.

292. McGill, J., J.W. Heusel, and K.L. Legge, Innate immune control and regulation of influenza virus infections. J Leukoc Biol, 2009. 86(4): p. 803-12.

293. Paget, C., et al., Potential role of invariant NKT cells in the control of pulmonary inflammation and CD8+ T cell response during acute influenza A virus H3N2 pneumonia. J Immunol, 2011. 186(10): p. 5590-602.

294. Chen, W., et al., Mice deficient in perforin, CD4+ T cells, or CD28-mediated signaling maintain the typical immunodominance hierarchies of CD8+ T-cell responses to influenza virus. J Virol, 2002. 76(20): p. 10332-7.

295. Belz, G.T., et al., A previously unrecognized H-2D(b)-restricted peptide prominent in the primary influenza A virus-specific CD8(+) T-cell response is much less apparent following secondary challenge. J Virol, 2000. 74(8): p. 3486-93.

296. Belz, G.T., W. Xie, and P.C. Doherty, Diversity of epitope and cytokine profiles for primary and secondary influenza a virus-specific CD8+ T cell responses. J Immunol, 2001. 166(7): p. 4627-33.

297. Falk, K., et al., Allele-specific motifs revealed by sequencing of self-peptides eluted from MHC molecules. 1991. J Immunol, 2006. 177(5): p. 2741-7.

298. Townsend, A.R., et al., The epitopes of influenza nucleoprotein recognized by cytotoxic T lymphocytes can be defined with short synthetic peptides. Cell, 1986. 44(6): p. 959-68.

299. Khatri, M., et al., Swine influenza H1N1 virus induces acute inflammatory immune responses in pig lungs: a potential animal model for human H1N1 influenza virus. J Virol, 2010. 84(21): p. 11210-8.

300. Palladino, G., P.A. Scherle, and W. Gerhard, Activity of CD4+ T-cell clones of type 1 and type 2 in generation of influenza virus-specific cytotoxic responses in vitro. J Virol, 1991. 65(11): p. 6071-6.

301. Sarawar, S.R. and P.C. Doherty, Concurrent production of interleukin-2, interleukin-10, and gamma interferon in the regional lymph nodes of mice with influenza pneumonia. J Virol, 1994. 68(5): p. 3112-9.

302. S, F.d.S.G. and M. Donnelley, Studies in experimental immunology of influenza. IV. The protective value of active immunization. Aust J Exp Biol Med Sci, 1950. 28(1): p. 61-75.

303. Dong, L., et al., The senescence-accelerated mouse shows aging-related defects in cellular but not humoral immunity against influenza virus infection. J Infect Dis, 2000. 182(2): p. 391-6.

304. Price, P., et al., Characterization of thymic involution induced by murine cytomegalovirus infection. Immunol Cell Biol, 1993. 71 (Pt 3): p. 155-65.

305. Wallace, D.L., et al., Direct measurement of T cell subset kinetics in vivo in elderly men and women. J Immunol, 2004. 173(3): p. 1787-94.

306. Goodwin, K., C. Viboud, and L. Simonsen, Antibody response to influenza vaccination in the elderly: a quantitative review. Vaccine, 2006. 24(8): p. 1159-69.

307. Holland, A.M. and M.R. van den Brink, Rejuvenation of the aging T cell compartment. Curr Opin Immunol, 2009. 21(4): p. 454-9.

308. Northfield, J., et al., Does memory improve with age? CD85j (ILT-2/LIR-1) expression on CD8 T cells correlates with 'memory inflation' in human cytomegalovirus infection. Immunol Cell Biol, 2005. 83(2): p. 182-8.

309. Welsh, R.M. and L.K. Selin, Attrition of memory CD8 T cells. Nature, 2009. 459(7247): p. E3-4; discussion E4.

310. Vezys, V., et al., Memory CD8 T-cell compartment grows in size with immunological experience. Nature, 2009. 457(7226): p. 196-9.

311. Nikolich-Zugich, J., Ageing and life-long maintenance of T-cell subsets in the face of latent persistent infections. Nat Rev Immunol, 2008. 8(7): p. 512-22.

312. Wallace, D.L., et al., Human cytomegalovirus-specific CD8(+) T-cell expansions contain long-lived cells that retain functional capacity in both young and elderly subjects. Immunology, 2011. 132(1): p. 27-38.

313. Akel, H.M., A.M. Furarah, and C. Sweet, Further studies of 31 temperature-sensitive mutants of mouse cytomegalovirus: thermal stability, replication and analysis of temperature-sensitive functions by temperature shift. FEMS Microbiol Lett, 1993. 114(3): p. 311-6.

314. Akel, H.M. and C. Sweet, Isolation and preliminary characterisation of twenty-five temperature-sensitive mutants of mouse cytomegalovirus. FEMS Microbiol Lett, 1993. 113(3): p. 253-60.

315. Sammons, C.C. and C. Sweet, Isolation and preliminary characterization of temperature-sensitive mutants of mouse cytomegalovirus of differing virulence for 1-week-old mice. J Gen Virol, 1989. 70 (Pt 9): p. 2373-81.

316. Pavic, I., et al., Flow cytometric analysis of herpes simplex virus type 1 susceptibility to acyclovir, ganciclovir, and foscarnet. Antimicrob Agents Chemother, 1997. 41(12): p. 2686-92.

317. Weyand, C.M., et al., Lymphoid microstructures in rheumatoid synovitis. Curr Dir Autoimmun, 2001. 3: p. 168-87.

318. Gallatin, M., et al., Lymphocyte homing receptors. Cell, 1986. 44(5): p. 673-80.

319. Aruffo, A., et al., CD44 is the principal cell surface receptor for hyaluronate. Cell, 1990. 61(7): p. 1303-13.

320. Tedder, T.F., D.A. Steeber, and P. Pizcueta, L-selectin-deficient mice have impaired leukocyte recruitment into inflammatory sites. J Exp Med, 1995. 181(6): p. 2259-64.

321. Arbones, M.L., et al., Lymphocyte homing and leukocyte rolling and migration are impaired in L-selectin-deficient mice. Immunity, 1994. 1(4): p. 247-60.

322. Ley, K. and G.S. Kansas, Selectins in T-cell recruitment to non-lymphoid tissues and sites of inflammation. Nat Rev Immunol, 2004. 4(5): p. 325-35.

323. DeGrendele, H.C., P. Estess, and M.H. Siegelman, Requirement for CD44 in activated T cell extravasation into an inflammatory site. Science, 1997. 278(5338): p. 672-5.

324. Pure, E. and C.A. Cuff, A crucial role for CD44 in inflammation. Trends Mol Med, 2001. 7(5): p. 213-21.

325. Stoop, R., et al., Trafficking of CD44-deficient murine lymphocytes under normal and inflammatory conditions. Eur J Immunol, 2002. 32(9): p. 2532-42.

326. McKallip, R.J., et al., Role of CD44 in activation-induced cell death: CD44-deficient mice exhibit enhanced T cell response to conventional and superantigens. Int Immunol, 2002. 14(9): p. 1015-26.

327. Mekker, A., et al., Immune senescence: relative contributions of age and cytomegalovirus infection. PLoS Pathog, 2012. 8(8): p. e1002850.

328. den Braber, I., et al., Maintenance of Peripheral Naive T Cells Is Sustained by Thymus Output in Mice but Not Humans. Immunity, 2012. 36(2): p. 288-297.

329. Cicin-Sain, L., et al., Loss of naive T cells and repertoire constriction predict poor response to vaccination in old primates. J Immunol, 2010. 184(12): p. 6739-45.

330. Mosley, R.L., M.M. Koker, and R.A. Miller, Idiosyncratic alterations of TCR size distributions affecting both CD4 and CD8 T cell subsets in aging mice. Cell Immunol, 1998. 189(1): p. 10-8.

331. Messaoudi, I., et al., Age-related CD8 T cell clonal expansions constrict CD8 T cell repertoire and have the potential to impair immune defense. J Exp Med, 2004. 200(10): p. 1347-58.

332. Ku, C.C., et al., CD8+ T-cell clones in old mice. Immunol Rev, 1997. 160: p. 139-44.

333. Ahmed, M., et al., Clonal expansions and loss of receptor diversity in the naive CD8 T cell repertoire of aged mice. J Immunol, 2009. 182(2): p. 784-92.

334. Ahasan, M.M. and C. Sweet, Murine cytomegalovirus open reading frame m29.1 augments virus replication both in vitro and in vivo. J Gen Virol, 2007. 88(Pt 11): p. 2941-51.

335. Schlub, T.E., et al., Comparing the kinetics of NK cells, CD4, and CD8 T cells in murine cytomegalovirus infection. J Immunol, 2011. 187(3): p. 1385-92.

336. Seckert, C.K., et al., Antigen-presenting cells of haematopoietic origin prime cytomegalovirus-specific CD8 T-cells but are not sufficient for driving memory inflation during viral latency. J Gen Virol, 2011. 92(Pt 9): p. 1994-2005.

337. Karabekian, Z., et al., Complex formation among murine cytomegalovirus US22 proteins encoded by genes M139, M140, and M141. J Virol, 2005. 79(6): p. 3525-35.

338. Menard, C., et al., Role of murine cytomegalovirus US22 gene family members in replication in macrophages. J Virol, 2003. 77(10): p. 5557-70.

339. Winston, D.J., et al., Randomized comparison of oral valacyclovir and intravenous ganciclovir for prevention of cytomegalovirus disease after allogeneic bone marrow transplantation. Clin Infect Dis, 2003. 36(6): p. 749-58.

340. Kline, J., et al., Pre-transplant ganciclovir and post transplant high-dose valacyclovir reduce CMV infections after alemtuzumab-based conditioning. Bone Marrow Transplant, 2006. 37(3): p. 307-10.

341. Klenerman, P. and P.R. Dunbar, CMV and the art of memory maintenance. Immunity, 2008. 29(4): p. 520-2.

342. Weekes, M.P., et al., Large clonal expansions of human virus-specific memory cytotoxic T lymphocytes within the CD57+ CD28- CD8+ T-cell population. Immunology, 1999. 98(3): p. 443-9.

343. Casey, K.A., et al., Antigen-Independent Differentiation and Maintenance of Effector-like Resident Memory T Cells in Tissues. J Immunol, 2012.

344. Glasgow, L.A., J.T. Richards, and E.R. Kern, Effect of acyclovir treatment on acute and chronic murine cytomegalovirus infection. Am J Med, 1982. 73(1A): p. 132-7.

345. Kern, E.R., et al., In vitro activity and mechanism of action of methylenecyclopropane analogs of nucleosides against herpesvirus replication. Antimicrob Agents Chemother, 2005. 49(3): p. 1039-45.

346. de Miranda, P. and T.C. Burnette, Metabolic fate and pharmacokinetics of the acyclovir prodrug valaciclovir in cynomolgus monkeys. Drug Metab Dispos, 1994. 22(1): p. 55-9.

347. Granero, G.E. and G.L. Amidon, Stability of valacyclovir: implications for its oral bioavailability. Int J Pharm, 2006. 317(1): p. 14-8.

348. Landowski, C.P., et al., Gene expression in the human intestine and correlation with oral valacyclovir pharmacokinetic parameters. J Pharmacol Exp Ther, 2003. 306(2): p. 778-86.

349. Soul-Lawton, J., et al., Absolute bioavailability and metabolic disposition of valaciclovir, the L-valyl ester of acyclovir, following oral administration to humans. Antimicrob Agents Chemother, 1995. 39(12): p. 2759-64.

350. Hellden, A., et al., The aciclovir metabolite CMMG is detectable in the CSF of subjects with neuropsychiatric symptoms during aciclovir and valaciclovir treatment. J Antimicrob Chemother, 2006. 57(5): p. 945-9.

351. Jurak, I., et al., Murine cytomegalovirus m38.5 protein inhibits Bax-mediated cell death. J Virol, 2008. 82(10): p. 4812-22.

352. Manzur, M., et al., Virally mediated inhibition of Bax in leukocytes promotes dissemination of murine cytomegalovirus. Cell Death Differ, 2009. 16(2): p. 312-20.

353. Trzonkowski, P., et al., Association between cytomegalovirus infection, enhanced proinflammatory response and low level of anti-hemagglutinins during the anti-influenza vaccination--an impact of immunosenescence. Vaccine, 2003. 21(25-26): p. 3826-36.

354. Messaoudi, I., J. Warner, and J. Nikolich-Zugich, Age-related CD8+ T cell clonal expansions express elevated levels of CD122 and CD127 and display defects in perceiving homeostatic signals. J Immunol, 2006. 177(5): p. 2784-92.

355. Sun, J., et al., Altered influenza virus haemagglutinin (HA)-derived peptide is potent therapy for CIA by inducing Th1 to Th2 shift. Cell Mol Immunol, 2011. 8(4): p. 348-58.

356. Cicin-Sain, L., et al., Cytomegalovirus infection impairs immune responses and accentuates T-cell pool changes observed in mice with aging. PLoS Pathog, 2012. 8(8): p. e1002849.

357. Crawley, A.M., et al., Interleukin-4 downregulates CD127 expression and activity on human thymocytes and mature CD8+ T cells. Eur J Immunol, 2010. 40(5): p. 1396-407.

358. Benito, J.M., et al., Down-regulation of interleukin-7 receptor (CD127) in HIV infection is associated with T cell activation and is a main factor influencing restoration of CD4(+) cells after antiretroviral therapy. J Infect Dis, 2008. 198(10): p. 1466-73.

359. Toapanta, F.R. and T.M. Ross, Impaired immune responses in the lungs of aged mice following influenza infection. Respir Res, 2009. 10: p. 112.

360. Moskophidis, D., et al., Virus persistence in acutely infected immunocompetent mice by exhaustion of antiviral cytotoxic effector T cells. Nature, 1993. 362(6422): p. 758-61.

361. Weekes, M.P., et al., Large HIV-specific CD8 cytotoxic T-lymphocyte (CTL) clones reduce their overall size but maintain high frequencies of memory CTL following highly active antiretroviral therapy. Immunology, 2006. 118(1): p. 25-38.

362. Gray, C.M., et al., Frequency of class I HLA-restricted anti-HIV CD8+ T cells in individuals receiving highly active antiretroviral therapy (HAART). J Immunol, 1999. 162(3): p. 1780-8.

363. Lang, A., J.D. Brien, and J. Nikolich-Zugich, Inflation and long-term maintenance of CD8 T cells responding to a latent herpesvirus depend upon establishment of latency and presence of viral antigens. J Immunol, 2009. 183(12): p. 8077-87.

364. Lang, A., et al., Age-related dysregulation of CD8+ T cell memory specific for a persistent virus is independent of viral replication. J Immunol, 2008. 180(7): p. 4848-57.

365. Ravaglia, G., et al., Splenic function in old age. Gerontology, 1998. 44(2): p. 91-4.

366. Duah, N.O., et al., Acquisition of antibody isotypes against Plasmodium falciparum blood stage antigens in a birth cohort. Parasite Immunol, 2010. 32(2): p. 125-34.

367. LeMaoult, J., et al., Age-related dysregulation in CD8 T cell homeostasis: kinetics of a diversity loss. J Immunol, 2000. 165(5): p. 2367-73.

368. Deng, Y., et al., Age-related impaired type 1 T cell responses to influenza: reduced activation ex vivo, decreased expansion in CTL culture in vitro, and blunted response to influenza vaccination in vivo in the elderly. J Immunol, 2004. 172(6): p. 3437-46.

369. Yajima, N., K. Sakamaki, and S. Yonehara, Age-related thymic involution is mediated by Fas on thymic epithelial cells. Int Immunol, 2004. 16(7): p. 1027-35.

370. Ouyang, Q., et al., Dysfunctional CMV-specific CD8(+) T cells accumulate in the elderly. Exp Gerontol, 2004. 39(4): p. 607-13.

371. Wingard, J.R., et al., Effect of several antiviral agents on human lymphocyte functions and marrow progenitor cell proliferation. Antimicrob Agents Chemother, 1983. 23(4): p. 593-7.

372. Szczech, G.M., Preclinical development of antiviral drugs. Clin Infect Dis, 1996. 22(2): p. 355-60.

373. Thompson, W.W., et al., Mortality associated with influenza and respiratory syncytial virus in the United States. JAMA, 2003. 289(2): p. 179-86.

374. Mullooly, J.P., et al., Influenza- and RSV-associated hospitalizations among adults. Vaccine, 2007. 25(5): p. 846-55.

375. Thompson, W.W., et al., Influenza-associated hospitalizations in the United States. JAMA, 2004. 292(11): p. 1333-40.

376. Jiang, J., E.M. Fisher, and D.M. Murasko, CD8 T cell responses to influenza virus infection in aged mice. Ageing Res Rev, 2011. 10(4): p. 422-7.

377. Jiang, J., et al., Limited expansion of virus-specific CD8 T cells in the aged environment. Mech Ageing Dev, 2009. 130(11-12): p. 713-21.

378. Barton, E.S., et al., Herpesvirus latency confers symbiotic protection from bacterial infection. Nature, 2007. 447(7142): p. 326-9.

379. Ho, A.W., et al., Lung CD103+ dendritic cells efficiently transport influenza virus to the lymph node and load viral antigen onto MHC class I for presentation to CD8 T cells. J Immunol, 2011. 187(11): p. 6011-21.

380. Snyder, C.M., et al., Cross-presentation of a spread-defective MCMV is sufficient to prime the majority of virus-specific CD8+ T cells. PLoS One, 2010. 5(3): p. e9681.

381. Sweet, C., et al., Mutations in the temperature-sensitive murine cytomegalovirus (MCMV) mutants tsm5 and tsm30: a study of genes involved in immune evasion, DNA packaging and processing, and DNA replication. J Med Virol, 2007. 79(3): p. 285-99.

382. Timoshenko, O., et al., Role of mutations identified in ORFs M56 (terminase), M70 (primase) and M98 (endonuclease) in the temperature-sensitive phenotype of murine cytomegalovirus mutant tsm5. Virology, 2009. 392(1): p. 114-22.

383. Morley, P.J., P. Ertl, and C. Sweet, Immunisation of Balb/c mice with severely attenuated murine cytomegalovirus mutants induces protective cellular and humoral immunity. J Med Virol, 2002. 67(2): p. 187-99.

384. Bevan, I.S., C.C. Sammons, and C. Sweet, Investigation of murine cytomegalovirus latency and reactivation in mice using viral mutants and the polymerase chain reaction. J Med Virol, 1996. 48(4): p. 308-20.

385. Morley, P.J., P.F. Ertl, and C. Sweet, High-frequency interferon-gamma-secreting splenocytes specific for murine cytomegalovirus immediate-early-1 (IE-1) peptide 168YPHFMPTNL176 are insufficient to provide complete protection from viral challenge. J Med Virol, 2003. 69(2): p. 240-50.

386. Derhovanessian, E., et al., Infection with cytomegalovirus but not herpes simplex virus induces the accumulation of late differentiated CD4+ and CD8+ T-cells in humans. J Gen Virol, 2011.

387. Wills, M.R., et al., Human virus-specific CD8+ CTL clones revert from CD45ROhigh to CD45RAhigh in vivo: CD45RAhighCD8+ T cells comprise both naive and memory cells. J Immunol, 1999. 162(12): p. 7080-7.

388. Ackerman, A.L., et al., Early phagosomes in dendritic cells form a cellular compartment sufficient for cross presentation of exogenous antigens. Proc Natl Acad Sci U S A, 2003. 100(22): p. 12889-94.

389. Hecker, M., et al., Continuous cytomegalovirus seroconversion in a large group of healthy blood donors. Vox Sang, 2004. 86(1): p. 41-4.

390. Loewendorf, A.I., et al., Dissecting the requirements for maintenance of the CMV-specific memory T-cell pool. Viral Immunol, 2011. 24(4): p. 351-5.

391. Hammarlund, E., et al., Duration of antiviral immunity after smallpox vaccination. Nat Med, 2003. 9(9): p. 1131-7.

392. Fagnoni, F.F., et al., Shortage of circulating naive CD8(+) T cells provides new insights on immunodeficiency in aging. Blood, 2000. 95(9): p. 2860-8.

393. den Elzen, W.P., et al., Cytomegalovirus infection and responsiveness to influenza vaccination in elderly residents of long-term care facilities. Vaccine, 2011. 29(29-30): p. 4869-74.

394. Steele, R.W., D.J. Marmer, and R.E. Keeney, Comparative in vitro imunotoxicology of acyclovir and other antiviral agents. Infect Immun, 1980. 28(3): p. 957-62.

395. Boehncke, W.H., et al., Evidence for a pathway independent from 2'-deoxyguanosine and reversible by IL-2 by which purine nucleoside phosphorylase inhibitors block T-cell proliferation. Scand J Immunol, 1994. 39(3): p. 327-32.

396. Levin, M.J., P.L. Leary, and R.D. Arbeit, Effect of acyclovir on the proliferation of human fibroblasts and peripheral blood mononuclear cells. Antimicrob Agents Chemother, 1980. 17(6): p. 947-53.

397. Barton, E.S., D.W. White, and H.W. Virgin, Herpesvirus latency and symbiotic protection from bacterial infection. Viral Immunol, 2009. 22(1): p. 3-4; author reply 5-6.

398. Wills, M., et al., Report from the Second Cytomegalovirus and Immunosenescence Workshop. Immun Ageing, 2011. 8(1): p. 10.